

***IN VITRO* TRANSFORMATION OF
CAPSICUM FRUTESCENS
FOR THE PRODUCTION OF VANILLIN**

CHEE JENN YANG, BSc.

Thesis submitted to the University of Nottingham for
the degree of Doctor of Philosophy

School of Biosciences

ABSTRACT

The need for an alternative approach to the production of vanillin that is generally regarded as safe and “natural” is receiving much attention in the current market trend. This is due to the high market price of natural vanilla extract compared to cheap synthetic vanillin (a major flavouring compound in vanilla extract). Hence, this research was aimed at producing vanillin by the *in vitro* transformation of *Capsicum frutescens* (chilli plant), an alternative to the current production systems using a plant-based approach. Plant tissues which are transformed with genes of feruloyl-CoA synthetase (*fcs*) and enoyl-CoA hydratase (*ech*) from bacterium *Amycolatopsis* sp. ATCC 39116 or the gene of vanillin synthase (*VpVAN*) from *Vanilla planifolia* were expected to biosynthesize vanillin using ferulic acid as the precursor. An optimisation study of plant tissue culture conditions for the chilli plant was first conducted to regenerate chilli explants into callus for the prospective production of target phenolics, particularly vanillin. Sterile cultures were established from the seeds of *C. frutescens* after a surface sterilisation with 70% (v/v) ethanol for 5 min, followed by 15–20% (v/v) commercial bleach for 20 min. MS media supplemented with 0.5 mg/l kinetin and 2.0 mg/l 2,4-D induced callusing from cotyledon, hypocotyl and root explants, with the highest amount of biomass being produced from the hypocotyl explants. High performance liquid chromatography (HPLC) analyses of cultured plant tissues of *C. frutescens* revealed only trace amounts of vanillin and ferulic acid in the analysed tissues. Ferulic acid (the precursor) feeding of callus cultures for one-month period revealed no significant elicitation of vanillin production. Subsequently, the *fcs*, *ech* and *VpVAN* genes have been codon optimised

and cloned separately into transformation vectors via Gateway Cloning, Golden Gate Cloning or double restriction-ligation cloning, with the cauliflower mosaic virus 35S promoter or nopaline synthase promoter upstream of the genes. The constructed expression vectors were delivered into hypocotyl explants of *C. frutescens* through microprojectile bombardment using the optimised parameters of 1.6 µm gold particle size, 1350 psi He pressure and 6 cm target distance. Calli that were transformed with both *fcs* and *ech* genes or the *VpVAN* gene showed significant gene expression levels of the transgenes (up to 131.3-fold, 0.4-fold and 8.4-fold high for *fcs*, *ech* and *VpVAN*, respectively) compared to no detectable expression levels in untransformed calli and remarkable increases in vanillin (up to 1231.7 µg per gram tissue), vanillin-β-D-glucoside (up to 340.5 µg per gram tissue) and vanillic acid (up to 604.6 µg per gram tissue) contents. These findings have laid a foundation for future improvements in the use of genetic manipulation approaches in chilli plants as an alternative to the production of vanillin.

PUBLICATIONS

Chee, MJY, Lycett, GW, Khoo, Teng-Jin & Chin, CF (2016) Bioengineering of the plant culture of *Capsicum frutescens* with vanillin synthase gene for the production of vanillin. *Molecular Biotechnology*, 59(1): 1–8.

Chee, JY & Chin, CF (2015) Gateway Cloning Technology: Advantages and drawbacks. *Journal of Cloning and Transgenesis*, 4: 138.

Dedicated to my wife and family

ACKNOWLEDGEMENT

First of all, I would like to thank my principal supervisor, Dr Chin Chiew Foan, for providing guidance through this project. Heartfelt appreciation to Dr Grantley Lycett from the Division of Plant and Crop Sciences and Dr Khoo Teng-Jin from the School of Pharmacy for co-supervising this work. Also thanks to Dr Ajit Singh for his helpful suggestions along the way. My appreciation to the assessors of this work, especially Prof Sandy Loh, for providing advice to improve my work. Not to be missed, many thanks to the lab technicians, Norasyikin, Siti Lin, Shankari, Linda, Asma and Yun, who provided assistance during the conduct of my laboratory experiments.

Sincere gratitude to friends and colleagues around me, particularly Li Chin, Xiao Ying, Ee Leen, Eu Sheng, Johnathan Foong, Hooi Sin and Sin Ling who have given me a lot of support.

My biggest love goes to my wife, my wonderful family, and my loving relatives, for the warmth and love, and for being the biggest pillar of support in my life.

Last but not least, my acknowledgement to the Ministry of Science, Technology and Innovation (MOSTI) Malaysia for providing funding to support this research through e-Science Grant (02-02-12-SF0130) and the Ministry of Education for supporting my studies through the MyBrain15 PhD Scholarship programme. Appreciation to Raymond Leong, who customised the HBT vector that was used in my studies. Special thanks to Dr Stuart Wilkinson and Dr Robert Linforth for their useful advice in my HPLC work. Appreciation to Dr Eunice Ngai and Dr Wong Hann Ling for their advice in my cloning works.

TABLE OF CONTENTS

ABSTRACT	i
PUBLICATIONS	iii
ACKNOWLEDGEMENT	v
TABLE OF CONTENTS	vi
LIST OF ABBREVIATIONS.....	xiv
LIST OF FIGURES.....	xx
LIST OF TABLES	xxviii
CHAPTER 1: INTRODUCTION	1
1.1 BACKGROUND, PROJECT OVERVIEW AND OBJECTIVES OF STUDY.....	1
1.2 THESIS OUTLINE	5
1.3 LITERATURE REVIEW	6
1.3.1 Vanilla planifolia	6
1.3.1.1 Agronomic Traits	6
1.3.1.2 Vanillin.....	9
1.3.2 Amycolatopsis sp.....	14
1.3.2.1 Genome of Amycolatopsis sp. Strain ATCC 39116.....	14
1.3.2.2 Genes of Feruloyl-CoA Synthetase and Enoyl-CoA Hydratase/Aldolase	15
1.3.3 C. frutescens.....	17
1.3.3.1 Agronomic Traits	17
1.3.3.2 Capsaicin Biosynthetic Pathway.....	18
1.3.3.3 Transformation and Regeneration of Capsicum spp.	21
1.3.4 Alternative Means of Vanillin Production	22
1.3.4.1 Synthetic Vanillin by Chemical Synthesis	23
1.3.4.2 Biosynthesis by Microorganisms	24
1.3.4.3 Biotransformation in Plant Cell Cultures.....	26

1.3.5	Plant Regeneration by Tissue Culture	27
1.3.5.1	<i>Dedifferentiation</i>	30
1.3.5.2	<i>Organogenesis</i>	33
1.3.6	Biolistic-mediated Plant Transformation Approach.....	38
1.3.6.1	<i>Types of Explants</i>	38
1.3.6.2	<i>Components and Procedures</i>	39
1.3.6.3	<i>Advantages</i>	44
1.3.6.4	<i>Limitations</i>	46
CHAPTER 2: GENERAL MATERIALS AND METHODS.....		48
2.1	STANDARD REAGENTS	50
2.2	PLANT TISSUE CULTURE.....	53
2.2.1	Plant Materials	53
2.2.2	Tissue Culture Media	53
2.2.3	Plant Growth Regulators / Hormones	53
2.2.4	Antibiotics	54
2.2.5	Plant Culture Incubation Conditions	54
2.3	BACTERIAL CULTURE	55
2.3.1	Bacterial Strains and Plasmids.....	55
2.3.2	Bacterial Culture Media	57
2.3.3	Antibiotics	58
2.3.4	Bacterial Culture Incubation Conditions	58
2.4	POLYMERASE CHAIN REACTION (PCR).....	59
2.4.1	PCR Reagents	59
2.4.2	Thermal Cycling Programme	59
2.5	AGAROSE GEL ELECTROPHORESIS.....	60
2.6	QUANTIFICATION OF NUCLEIC ACIDS	61
2.7	STATISTICAL ANALYSIS.....	62
CHAPTER 3: PLANT TISSUE CULTURE FOR THE CALLUS REGENERATION OF <i>CAPSICUM FRUTESCENS</i> L.		63
3.1	INTRODUCTION.....	63

3.1.1	Callus Regeneration in Chilli	64
3.1.2	Specific Objectives.....	65
3.2	MATERIALS AND METHODS	65
3.2.1	Surface Sterilisation of Seeds of <i>C. frutescens</i>	65
3.2.2	Callus Regeneration	68
3.2.3	Statistical Analysis.....	69
3.3	RESULTS	69
3.3.1	Establishment of Sterile Cultures	69
3.3.1.1	<i>Germination and Infection Frequencies from Different Concentrations of Sterilising Agent</i>	69
3.3.1.2	<i>Germination and Infection Rates of Different Cultivars</i>	72
3.3.2	Callus Regeneration	75
3.3.2.1	<i>Effects of 2,4-D and Kinetin</i>	75
3.3.2.2	<i>Effects of BAP and NAA/IAA</i>	79
3.4	DISCUSSION.....	81
3.4.1	Establishment of Sterile Cultures	81
3.4.1.1	<i>Seed Viability and Seed Germination</i>	81
3.4.1.2	<i>Genotype Dependency in Seed Germination</i>	84
3.4.1.3	<i>Seed Infection</i>	85
3.4.2	Callus Regeneration with 2,4-D and Kinetin	87
3.4.3	High BAP to NAA/IAA Ratios Stimulated Direct Organ Regeneration	88
3.5	CONCLUSION	90
CHAPTER 4: CONSTRUCTION OF EXPRESSION VECTORS FOR THE NUCLEAR TRANSFORMATION OF <i>CAPSICUM FRUTESCENS</i> L.....		91
4.1	INTRODUCTION.....	91
4.1.1	The pcDNA™6.2 Transformation Vector	92
4.1.2	The pHBT12K Transformation Vector.....	93
4.1.3	Specific Objectives.....	94
4.2	MATERIALS AND METHODS.....	95

4.2.1	Propagation and Isolation of Plasmids from <i>E. coli</i>	97
4.2.1.1	<i>Transformation of E. coli</i>	97
4.2.1.2	<i>Propagation of Plasmid</i>	98
4.2.1.3	<i>Isolation of Plasmids Using GeneAll® Hybrid-Q™ Plasmid Rapidprep Kit</i>	98
4.2.1.4	<i>Isolation of Plasmids Using Alkaline Lysis Method</i>	99
4.2.2	Purification of DNA Fragments during the Construction of Vectors	101
4.2.2.1	<i>Purification of DNA Fragments Using GeneAll® Expin™ PCR SV and Gel SV Kits</i>	101
4.2.2.2	<i>Purification of DNA Fragments Using PEG Method</i>	102
4.2.3	Polymerase Chain Reactions (PCRs)	103
4.2.4	Restriction Endonuclease (RE) Digestions	103
4.2.5	Ligation of DNA	104
4.2.6	Codon Optimisation and Gene Synthesis	104
4.2.7	Gateway® Cloning	105
4.2.7.1	<i>BP Reaction</i>	107
4.2.7.2	<i>LR Reaction</i>	108
4.2.8	Golden Gate Cloning	109
4.2.9	Double Restriction and Ligation for the Construction of <i>pcDNA6.2::35Sp-sgfp</i>	110
4.2.10	Gateway® Cloning for the Construction of <i>pcDNA6.2::35Sp- fcs-NOSp-ech</i> Expression Vector	112
4.2.10.1	<i>BP Reactions to Create pENTR L1-35Sp-R5, pENTR L5- fcs-L4, pENTR R4-NOSp-R3 and pENTR L3-ech-L2</i> ...	113
4.2.10.2	<i>LR Reaction to Create pcDNA6.2::35Sp-fcs-NOSp-ech</i>	114
4.2.11	Gateway® Cloning for the Construction of <i>pcDNA6.2::35Sp- fcs</i> Expression Vector	115
4.2.11.1	<i>BP Reaction to Create pENTR L5-fcs-L2</i>	116
4.2.11.2	<i>LR Reaction to Create pcDNA6.2::35Sp-fcs</i>	116

4.2.12	Golden Gate Cloning for the Construction of pcDNA6.2::NOSp- <i>ech</i> Expression Vector.....	117
4.2.13	Double Restriction and Ligation for the Construction of pcDNA6.2::35Sp- <i>VpVAN</i> Expression Vector.....	119
4.2.14	Golden Gate Cloning for the Construction of pHBT12K::35Sp- <i>VpVAN</i> Expression Vector.....	120
4.3	RESULTS	121
4.3.1	Construction of pcDNA6.2::35Sp- <i>sgfp</i>	121
4.3.2	Construction of pcDNA6.2::35Sp- <i>fcs</i> -NOSp- <i>ech</i>	124
4.3.3	Construction of pcDNA6.2::35Sp- <i>fcs</i>	127
4.3.4	Construction of pcDNA6.2::NOSp- <i>ech</i>	130
4.3.5	Construction of pcDNA6.2::35Sp- <i>VpVAN</i>	133
4.3.6	Construction of pHBT12K::35Sp- <i>VpVAN</i>	136
4.4	DISCUSSION.....	138
4.4.1	Restriction-Ligation, Gateway [®] , and Golden Gate Cloning Systems	138
4.4.2	Construction of Expression Vectors	141
4.5	CONCLUSION	145
CHAPTER 5: MICROPROJECTILE BOMBARDMENT AND ANTIBIOTIC SELECTION OF <i>CAPSICUM FRUTESCENS</i> L.		146
5.1	INTRODUCTION.....	146
5.1.1	Transformation of <i>C. frutescens</i> by Biolistics	147
5.1.2	Blasticidin S Antibiotic as a Selective Agent.....	148
5.1.3	Specific Objectives.....	149
5.2	MATERIALS AND METHODS.....	150
5.2.1	Minimal Inhibitory Concentration of Blasticidin S.....	150
5.2.2	Optimisation of Biolistic Parameters	151
5.2.2.1	<i>Preparation of Explants</i>	151
5.2.2.2	<i>Preparation of Microcarriers</i>	151
5.2.2.3	<i>Coating DNA on Microcarriers</i>	152
5.2.2.4	<i>Microprojectile Bombardment</i>	152

5.2.2.5	<i>Selection and Regeneration of Plant Transformants</i>	155
5.2.2.6	<i>Screening of Plant Transformants</i>	155
5.2.2.7	<i>Purification of Plant Genomic DNA</i>	158
5.2.2.8	<i>Confirmation by PCR to Detect sgfp Gene</i>	159
5.2.3	Statistical Analysis	159
5.2.4	Transformation of <i>C. frutescens</i> with Vanillin Biosynthetic Genes	160
5.3	RESULTS	161
5.3.1	Minimal Inhibitory Concentration of Blastidicin S	161
5.3.2	Effects of Microparticle Size, Target Distance and Bombardment He Pressure on Transformation	162
5.3.3	Intensity of sGFP Over Time and Distribution in Transformants	165
5.3.4	Verification of Gene Integration in Calli Transformed with Vanillin Biosynthetic Genes	167
5.4	DISCUSSION	170
5.4.1	Inhibitory Effects of Blastidicin S	170
5.4.2	Optimisation of Biolistic Parameters	171
5.4.3	Expression Pattern of GFP	173
5.4.4	Genomic Integration of Vanilin Biosynthetic Genes	178
5.5	CONCLUSION	179
CHAPTER 6: EVALUATION OF GENE EXPRESSION LEVELS AND PHENOLIC CONTENTS IN CALLUS CULTURES OF <i>CAPSICUM FRUTESCENS</i> L.		180
6.1	INTRODUCTION	180
6.1.1	RT-qPCR for the Quantification of Gene Expression Levels	181
6.1.2	HPLC for the Quantification of Plant Metabolites	183
6.1.3	Specific Objectives	185
6.2	MATERIALS AND METHODS	186
6.2.1	Analysis of RNA Levels by RT-qPCR	186
6.2.1.1	<i>Purification of RNA Using TRIzol[®] Reagent</i>	187

6.2.1.2	<i>Quantification of RNA</i>	188
6.2.1.3	<i>Design and Synthesis of Primers</i>	188
6.2.1.4	<i>Synthesis of cDNA by Reverse Transcription</i>	189
6.2.1.5	<i>qPCR Analysis</i>	189
6.2.1.6	<i>Validation of qPCR Amplification Efficiency</i>	191
6.2.1.7	<i>Analysis of Relative RNA Levels</i>	191
6.2.2	<i>Analysis of Plant Phenolic Contents by Reverse-Phase HPLC</i>	192
6.2.2.1	<i>Preparation of Standards</i>	193
6.2.2.2	<i>Preparation of Mobile Phase Eluents</i>	193
6.2.2.3	<i>HPLC Specifications and Settings</i>	194
6.2.2.4	<i>Optimisation of Mobile Phase Composition</i>	195
6.2.2.5	<i>Concentration Curve of Standards</i>	197
6.2.2.6	<i>Extraction of Phenolic Compounds</i>	197
6.2.2.7	<i>HPLC Analysis of Phenolic Compounds</i>	198
6.3	RESULTS	201
6.3.1	Reverse Transcription-Quantitative PCR	201
6.3.1.1	<i>RNA Quality</i>	201
6.3.1.2	<i>Validation of Primers</i>	203
6.3.1.3	<i>Analysis of Reference Genes</i>	206
6.3.1.4	<i>qPCR Amplification Efficiency of Target Genes</i>	209
6.3.1.5	<i>Melt Curve Analysis</i>	211
6.3.1.6	<i>Expression Levels in Transformed and Untransformed Calli</i>	213
6.3.2	Reverse-Phase HPLC	214
6.3.2.1	<i>Mobile Phase Compositions</i>	214
6.3.2.2	<i>UV Wavelengths for Compound Detection</i>	217
6.3.2.3	<i>Concentration Curve of Standards</i>	219
6.3.2.4	<i>Accuracy, Precision, Limit of Detection and Limit of Quantitation</i>	220

6.3.2.5	<i>Native Phenolic Contents in Various Tissues of C. frutescens</i>	222
6.3.2.6	<i>Phenolic Contents in Callus Cultures Fed with Ferulic Acid</i>	223
6.3.2.7	<i>Phenolic Contents in Transformed and Untransformed Callus Cultures</i>	225
6.4	DISCUSSION	230
6.4.1	Native Phenolic Contents and Ferulic Acid Feeding of <i>C. frutescens</i>	230
6.4.2	The Expression Levels of Vanillin Biosynthetic Genes and the Phenolic Contents	232
6.4.3	Comparison of pcDNA6.2 and pHBT12K Vectors for Vanillin Production	236
6.4.4	Limitations in qPCR Analysis	236
6.4.5	Limitations in HPLC Analysis.....	238
6.5	CONCLUSION	241
CHAPTER 7: GENERAL DISCUSSION AND FUTURE PERSPECTIVES		243
7.1	PROS AND CONS OF PLANT SYSTEMS AS BIOFACTORIES FOR METABOLITE PRODUCTION THROUGH TRANSGENESIS	244
7.2	CHALLENGES IN NUCLEAR TRANSFORMATION	247
7.3	MODIFICATIONS TO THE PHENYLPROPANOID PATHWAY FOR VANILLIN BIOSYNTHESIS	250
7.4	RECOMMENDATIONS AND FUTURE PERSPECTIVES.....	251
APPENDIX		255
REFERENCES		270

LIST OF ABBREVIATIONS

1O ₂	Singlet oxygen
2,4-D	2,4-Dichlorophenoxyacetic acid
35Sp	35S promoter from cauliflower mosaic virus
ACT	Actin
AU	Arbitrary unit
ABA	Abscisic acid
AFB	AUXIN F-BOX PROTEIN
AgNO ₃	Silver nitrate
ANOVA	Analysis of variance
ARF	AUXIN RESPONSE FACTOR
ARR	<i>ARABIDOPSIS</i> RESPONSE REGULATOR
ATCC	American Type Culture Collection
ATP	Adenosine triphosphate
β-TUB	β-tubulin
BA	6-Benzylaminopurine
BD	Becton Dickinson
Bla	Beta-lactamase (gene abbreviation, <i>bla</i>)
bp	Base pair(s)
BS	Blasticidin S
BSA	Bovine serum albumin
BSD	Blasticidin S deaminase (gene abbreviation, <i>bsd</i>)
Ca(ClO) ₂	Calcium hypochlorite

CA3H	<i>p</i> -coumaric acid-3-hydroxylase
CA4H	Cinnamic acid-4-hydroxylase
CaCl ₂	Calcium carbonate
CAD	Cinnamyl alcohol dehydrogenase
CaMV	Cauliflower mosaic virus
CAOMT	Caffeic acid-O-methyltransferase
Cat	Chloramphenicol acyltransferase (gene abbreviation, <i>cat</i>)
CCoAMT	Caffeoyl-CoA-O-methyltransferase
CCR	Cinnamoyl CoA reductase
CDK	Cyclin-dependent kinase
cDNA	Copy DNA
CIM	Callus induction media
CLV3	CLAVATA3
CoCl ₂	Cobalt chloride
Cq	Cycle of quantification
CS	Capsaicinoid synthetase
CV	Coefficient of variance
CVG	Coefficient of velocity of germination
CYC	Cyclin
DEPC	Diethyl pyrocarbonate
DMSO	Dimethyl sulfoxide
DNA	Deoxyribonucleic acid
dNTPs	Deoxynucleotides
DP	DIMERIZATION PARTNER
E2Fa	E2 PROMOTER BINDING FACTOR a

Ech	Enoyl-CoA hydratase / aldolase (gene abbreviation, <i>ech</i>)
EDTA	Ethylenediaminetetraacetic acid
EMBL-EBI	European Molecular Biology Laboratory-European Biotechnology Institute
ESR	ENHANCED SHOOT REGENERATION
Fcs	Feruloyl-CoA synthetase (gene abbreviation, <i>fcs</i>)
GA	Gibberellic acid
GAPDH	Glyceraldehyde-3-phosphate dehydrogenase
GFP	Green fluorescent protein
GUS	β -glucuronidase
G+C	Guanine and cytosine
H ₂ O	Water
H ₂ O ₂	Hydrogen peroxide
HBT	HBT-sGFP(S65T)-NOS transformation vector
HCHL	4-hydroxy-3-methoxyphenyl-hydroxypropanoyl-CoA hydrolyase (feruloyl-CoA-forming) or 3-hydroxy-3-(4-hydroxyl-3-methoxyphenyl) propanoyl-CoA vanillin-lyase (acetyl-CoA-forming)
HCl	Hydrochloric acid
HC-Pro	Helper component-proteinase
He	Helium
HgCl ₂	Mercury(II) chloride or mercuric chloride
HPLC	High performance liquid chromatography
IAA	Indole-3-acetic acid
IBA	Indole-3-butyric acid

ICH	International Conference on <i>Harmonisation</i> of Technical Requirements for Registration of Pharmaceuticals for Human Use
IUPAC	International Union of Pure and Applied Chemistry
KCl	Potassium chloride
KMnO ₄	Potassium permanganate
KNOX	KNOTTED-like homeobox
KOAc	Potassium acetate
LAX	LIKE AUX1
LB	Lysogeny broth
LBD	LATERAL ORGAN BOUNDARIES DOMAIN
LOB	Limit of blank
LOD	Limit of detection
LOQ	Limit of quantitation
LSD	Least significant difference
MgCl ₂	Magnesium chloride
MGR	Mean germination rate
MgSO ₄	Magnesium sulphate
MGT	Mean germination time
MIR	Mean infection rate
MIT	Mean infection time
mRNA	Messenger RNA
MS	Murashige and Skoog
NAA	1-Naphthaleneacetic acid
NaCl	Sodium chloride
NaOAc	Sodium acetate

NaOCl	Sodium hypochlorite
NaOH	Sodium hydroxide
NCBI	National Center for Biotechnology Information
NOS	Nopaline synthase
NOSp	Nopaline synthase promoter
NOS _t	Nopaline synthase terminator
NPA	Naphthylphthalamic acid
NRT	No reverse transcriptase (control)
ORF	Open reading frame
PAL	Phenylalanine ammonia-lyase
pAMT	Vanillin aminotransferase
pcDNA6.2	pcDNA TM 6.2/V5-pL-DEST transformation vector
PCR	Polymerase chain reaction
PDA	Photodiode array
PDS	PDS-1000/He TM Particle Delivery System
PEG	Polyethylene glycol
PIG	Particle inflow gun
PIN	PINFORMED
PLT	PLETHORA
<i>pmi</i>	Phosphomannose-isomerase gene
Ppm	Parts per million
PPS1	Plasmid purification solution 1
PPS2	Plasmid purification solution 2
PPS3	Plasmid purification solution 3
Ori	Origin of replication

QC	Quiescent centre
qPCR	Quantitative polymerase chain reaction
RE	Restriction endonuclease
RIN	RNA integrity number
RNA	Ribonucleic acid
rRNA	Ribosomal RNA
RSD	Relative standard deviation
RT	Reverse transcription
SD	Standard deviation
SDS	Sodium dodecyl sulphate
SEM	Scanning electron microscopy
SHY2	SHORT HYPOCOTYL 2
STM	SHOOTSTEMLESS
UBI-1	Ubiquitin-conjugating enzyme
TAE	Tris-acetate-EDTA
TE	Tris-EDTA
TIR1	TRANSPORT INHIBITOR RESPONSE 1
TK pA	Herpes Simplex Virus Thymidine Kinase polyadenylation signal
Tris-Cl	Tris-chloride
UHPLC	Ultra-high performance liquid chromatography
VpVAN	Vanillin synthase identified from <i>Vanilla planifolia</i> (gene abbreviation, VpVAN)
WUS	WUSCHEL

LIST OF FIGURES

Figure 1.1 An overall flow chart of the research methodology	5
Figure 1.2 A two-dimensional chemical structure and a three-dimensional conformer of vanillin, C ₈ H ₈ O ₃	9
Figure 1.3 Possible pathways from ferulic acid to vanillin	12
Figure 1.4 Possible conversion route from ferulic acid to vanillin, which is catalysed by <i>VpVAN</i>	13
Figure 1.5. Pathways showing the conversion of ferulic acid into vanillin and subsequently, vanillic acid and protocatechuic acid by <i>Amycolatopsis</i> sp. ATCC 39116.....	16
Figure 1.6 Fruiting 4-month old plants of <i>C. frutescens</i> L. cv. Hot Lava in the shadehouse.....	18
Figure 1.7 The capsaicin biosynthetic pathway.....	20
Figure 1.8 Chemical synthesis of vanillin from eugenol by alkaline hydrolysis using potassium hydroxide (KOH) followed by oxidation	23
Figure 1.9 Synthesis of vanillin from coniferin through the intermediate, glucovanillin.....	24
Figure 1.10 Outline of production of vanillin, starting from benzene (1). (2) guaiacol	24
Figure 1.11 Callus regenerated from a hypocotyl explant of <i>C. frutescens</i>	29
Figure 1.12 The structures of leaf primordia and shoot apical meristem from direct organogenesis of a cotyledon explant of <i>C. frutescens</i>	29
Figure 1.13 Illustration of different types of callus.....	31
Figure 1.14 The Helios [®] Gene Gun System.....	40

Figure 1.15 Schematic diagram of the components of a biolistic apparatus for the direct delivery of foreign DNA into target sample	41
Figure 1.16 Schematic diagram of the particle inflow gun and connections from the copper helium line to the syringe filter in the bombardment chamber	43
Figure 3.1 Illustration of various colony morphologies of bacteria or fungi	67
Figure 3.2 Illustration of colony density	67
Figure 3.3 Bar charts showing the percentage of seeds of Skyrocket, Full Sky and Hot Lava that germinated and were infected after surface sterilisation with 5%, 10%, 15% and 20% bleach concentrations	71
Figure 3.4 Microbial growth on culture plates	72
Figure 3.5 Germination rates of surface sterilised seeds of <i>C. frutescens</i> cv. Skyrocket, cv. Full Sky and cv. Hot Lava over 25 days	73
Figure 3.6 Infection rates of surface sterilised seeds of <i>C. frutescens</i> cv. Skyrocket, cv. Full Sky and cv. Hot Lava over 25 days	74
Figure 3.7 Calli induced on MS media supplemented with 0.5 mg/l 2,4-D + 0.5 mg/l kinetin, 1.0 mg/l 2,4-D + 0.5 mg/l kinetin, 1.5 mg/l 2,4-D + 0.5 mg/l kinetin, 2.0 mg/l 2,4-D + 0.5 mg/l kinetin, 2.5 mg/l 2,4-D + 0.5 mg/l kinetin, 3.0 mg/l 2,4-D + 0.5 mg/l kinetin, 0.5 mg/l kinetin, and no plant growth regulator.....	77
Figure 3.8 Hypocotyl explants on standard MS with 5.0 mg/l BAP and 0.1 mg/l NAA. Both ends of explant formed primordial structures after 10 days; shoot apex at one end of the explant after 20 days; root at another end of the explant after 20 days; newly developed whole plant after 40 days, sub-cultured; grown whole plant after 2 months, sub-cultured into tall culture jar; and after 3 months, transplanted into soil ...	81
Figure 4.1 Illustration showing the origins of the target genes, <i>sgfp</i> , <i>fcs</i> , <i>ech</i> and <i>VpVAN</i> , and the promoters, 35Sp and NOSp, which were used for the construction of the respective target cassettes that were cloned into pcDNA6.2 or pHBT12K to produce the final expression vectors	96

Figure 4.2 The general workflow of Gateway® Cloning of four DNA elements into a destination vector through BP and LR reactions to produce a final expression vector	106
Figure 4.3 The general workflow of Golden Gate Cloning	110
Figure 4.4 Illustration of the cloning process for pcDNA6.2::35Sp- <i>sgfp</i> expression vector	112
Figure 4.5 Illustration of the cloning process for BP recombination reactions between PCR amplified attB1-35Sp-attB5r PCR product, pUCIDT- <i>fcs</i> , pUCIDT-NOSp and pUCIDT- <i>ech</i> , and their respective donor vectors, pDONR™ P1-P5r, pDONR™ P5-P4, pDONR™ P4r-P3r and pDONR™ P3-P2, to produce entry clones, pENTR L1-35Sp-R5, pENTR L5- <i>fcs</i> -L4, pENTR R4-NOSp-R3 and pENTR L3- <i>ech</i> -L2.....	114
Figure 4.6 Illustration of the cloning process for LR recombination reaction to produce the final expression vector, pcDNA6.2::35Sp- <i>fcs</i> -NOSp- <i>ech</i>	115
Figure 4.7 Illustration of the cloning process for BP recombination reaction to produce entry clone, pENTR L5- <i>fcs</i> -L2	116
Figure 4.8 Illustration of the cloning process for LR recombination reaction to produce the final expression vector, pcDNA6.2::35Sp- <i>fcs</i>	117
Figure 4.9 Illustration of Golden Gate Cloning to produce pcDNA6.2::NOSp- <i>ech</i> expression vector	118
Figure 4.10 Illustration of the cloning process for pcDNA6.2::35Sp- <i>VpVAN</i> expression vector	120
Figure 4.11 Illustration of Golden Gate Cloning to produce pHBT12K::35Sp- <i>VpVAN</i> expression vector	121
Figure 4.12 PCR profile of the 35Sp- <i>sgfp</i> cassette (1303 bp) amplified from plasmid, HBT	122
Figure 4.13 RE digestion profile of pcDNA6.2 using REs, <i>Pst</i> I and <i>Age</i> I, resulting in two fragments, the pcDNA6.2 backbone (4879 bp) and the <i>Pst</i> I- <i>Age</i> I region (1814 bp)	122

Figure 4.14 PCR profile of the 35Sp- <i>sgfp</i> cassette (1303 bp) amplified from the expression vector, pcDNA6.2::35Sp- <i>sgfp</i>	123
Figure 4.15 Schematic diagram for the resulting 35Sp- <i>sgfp</i> cassette in the construction of pcDNA6.2::35Sp- <i>sgfp</i>	123
Figure 4.16 PCR profile of the attB1-35Sp-attB5r fragment (407 bp) amplified from HBT plasmid	125
Figure 4.17 RE digestion profiles of pENTR L1-35Sp-R5 (2958 bp), pENTR L5- <i>fcs</i> -L4 (4050 bp), pENTR R4-NOSp-R3 (2906 bp) and pENTR L3- <i>ech</i> -L2 (3418 bp) using RE, <i>PvuI</i>	125
Figure 4.18 PCR profiles of 35Sp (407 bp), <i>fcs</i> (1534 bp), NOSp (233 bp) and <i>ech</i> (922 bp) from the expression vector, pcDNA6.2::35Sp- <i>fcs</i> -NOSp- <i>ech</i>	126
Figure 4.19 Schematic diagram for the resulting 35Sp- <i>fcs</i> -NOSp- <i>ech</i> cassette in the construction of pcDNA6.2::35Sp- <i>fcs</i> -NOSp- <i>ech</i>	127
Figure 4.20 PCR profile of the attB5- <i>fcs</i> -attB2 fragment (1576 bp) amplified from holding vector, pUCIDT- <i>fcs</i>	128
Figure 4.21 RE digestion profile of pENTR L5- <i>fcs</i> -L2 (4075 bp) using RE, <i>PvuI</i>	128
Figure 4.22 PCR profile of the 35Sp fragment (407 bp) and the <i>fcs</i> fragment (1576 bp), which were amplified from pcDNA6.2::35Sp- <i>fcs</i> expression vector	129
Figure 4.23 Schematic diagram for the resulting 35Sp- <i>fcs</i> cassette in the construction of pcDNA6.2::35Sp- <i>fcs</i>	130
Figure 4.24 PCR profile of the NOSp fragment (273 bp) amplified from holding vector, pUCIDT-NOSp	131
Figure 4.25 PCR profile of the <i>ech</i> fragment (922 bp) amplified from holding vector, pUCIDT- <i>ech</i>	131
Figure 4.26 PCR profile of the NOSp fragment (273 bp) and the <i>ech</i> fragment (922 bp), which were amplified from pcDNA6.2::NOSp- <i>ech</i> expression vector	132

Figure 4.27 Schematic diagram for the resulting NOSp- <i>ech</i> cassette in the construction of pcDNA6.2::NOSp- <i>ech</i>	133
Figure 4.28 RE digestion profile of pUCIDT-35Sp- <i>VpVAN</i> using REs, <i>Pst</i> I and <i>Bam</i> HI	134
Figure 4.29 RE digestion profile of pcDNA6.2 using REs, <i>Pst</i> I and <i>Bam</i> HI.....	134
Figure 4.30 RE digestion profile of pcDNA6.2::35Sp- <i>VpVAN</i> using REs, <i>Pst</i> I and <i>Bam</i> HI	135
Figure 4.31 Schematic diagram for the resulting 35Sp- <i>VpVAN</i> cassette in the construction of pcDNA6.2::35Sp- <i>VpVAN</i>	135
Figure 4.32 PCR profile of the 35Sp- <i>VpVAN</i> cassette (1505 bp) amplified from holding vector, pUCIDT-35Sp- <i>VpVAN</i>	136
Figure 4.33 RE digestion profile of pHBT12K::35Sp- <i>VpVAN</i> using RE, <i>Bbs</i> I	137
Figure 4.34 Schematic diagram for the resulting 35Sp- <i>VpVAN</i> cassette in the construction of pHBT12K::35Sp- <i>VpVAN</i>	137
Figure 5.1 Illustration of the He-driven PDS system and its components	154
Figure 5.2 The process of microprojectile bombardment before and after the rupture disk burst	155
Figure 5.3 Microscopic diagram showing the measurement of GFP intensity across an explant	157
Figure 5.4 An example of microscopic photograph of a callus expressing GFP before and after analysis using Corel® PHOTO-PAINT®	158
Figure 5.5 One-month culture of cotyledon, hypocotyl and root explants on MS media with 0.25 mg/l BS turned brown and without BS	162
Figure 5.6 Bar chart representing the mean percentage of transformants achieved under different microparticle sizes, target distances and He pressures	164

Figure 5.7 PCR of <i>sgfp</i> gene (720 bp) from the genomic DNA of transformed calli	165
Figure 5.8 The transient expression of GFP at the wounded part of a hypocotyl explant	166
Figure 5.9 Plot of the highest mean intensities (background-subtracted) of purportedly stable GFP fluorescence over 60 days after bombardment	166
Figure 5.10 Regenerated tissues of calli expressing GFP at different intensities after bombardment	167
Figure 5.11 Genomic DNA profiles of transformed calli	168
Figure 5.12 PCR of <i>fcs</i> and <i>ech</i> genes (1473 and 861 bp, respectively) from the genomic DNA of calli transformed with pcDNA6.2::35Sp- <i>fcs</i> -NOSp- <i>ech</i>	168
Figure 5.13 PCR of <i>fcs</i> gene (1473 bp) from the genomic DNA of calli transformed with pcDNA6.2::35Sp- <i>fcs</i>	168
Figure 5.14 PCR of <i>ech</i> gene (861 bp) from the genomic DNA of calli transformed with pcDNA6.2::NOSp- <i>ech</i>	169
Figure 5.15 PCR of <i>VpVAN</i> gene (1068 bp) from the genomic DNA of calli transformed with pcDNA6.2::35Sp- <i>VpVAN</i>	169
Figure 5.16 PCR of 35Sp- <i>VpVAN</i> cassette (1505 bp) from the genomic DNA of calli transformed with pHBT12K::35Sp- <i>VpVAN</i>	169
Figure 6.1 Illustration of a vacuum filtration unit.....	194
Figure 6.2 The RNA profiles after agarose gel electrophoresis and Agilent 2100 Bioanalyzer analysis	203
Figure 6.3 PCR profiles of reference genes, UBI-1, GAPDH, β -TUB and ACT, at gradient annealing temperatures	204
Figure 6.4 PCR profiles of target genes, <i>fcs</i> , <i>ech</i> and <i>VpVAN</i> , at gradient annealing temperatures	205
Figure 6.5 Amplification of reference genes and target genes with NRT	205

Figure 6.6 An example of the amplification curve showing baseline correction in the determination of Cq values	206
Figure 6.7 The summary of preliminary geNorm analysis indicating the M values for the expression stability of <i>ACT</i> (0.091), <i>UBI-1</i> (0.091), <i>GAPDH</i> (0.108), and β - <i>TUB</i> (0.107)	207
Figure 6.8 Box plot graph of Cq values of <i>ACT</i> and <i>UBI-1</i> in transformed calli (Ech, Fcs, FcsEch, pcVAN and pHVAN) and untransformed control (Neg)	208
Figure 6.9 The summary of post-experimental geNorm analysis indicating the M values for <i>ACT</i> (0.030) and <i>UBI-1</i> (0.030)	208
Figure 6.10 Concentration curves of <i>fcs</i> , <i>ech</i> , and <i>VpVAN</i> plotted with Cq values against log starting quantities, and R ² values of 0.997, 0.992 and 0.994, respectively	210
Figure 6.11 Melt peaks for individual reactions indicating single amplification products of target genes, <i>fcs</i> , <i>ech</i> , and <i>VpVAN</i> , and the accompanying reference genes (<i>ACT</i> and <i>UBI-1</i>) included for normalisation	212
Figure 6.12 Bar chart showing the relative expression levels (fold-change) of <i>fcs</i> gene in FcsEch and Fcs samples, <i>ech</i> gene in FcsEch and Ech samples, and <i>VpVAN</i> gene in pcVAN and pHVAN samples	214
Figure 6.13 A HPLC chromatogram showing the peaks and retention times of vanillin glucoside (5.12 min), vanillic acid (8.25 min), vanillin (9.61 min) and ferulic acid (11.88 min) at 280 nm wavelength	216
Figure 6.14 A HPLC chromatogram showing the peak and retention time of capsaicin (4.85 min) at 222 nm wavelength	216
Figure 6.15 Isoabsorbance plots showing the intensities of absorbance signals (from blue, very low or nothing, to red, very high) over a range of wavelengths	218
Figure 6.16 Concentration curves of analytical standards	219
Figure 6.17 An example of performance and noise report from the chromatography of a plant extract containing vanillin	222

Figure 6.18 Native contents of vanillin and ferulic acid, which were the product and the precursor in the vanillin biosynthetic pathway, respectively, in different tissue types of <i>C. frutescens</i> with the extract from vanilla pod as a reference	223
Figure 6.19 Analysed contents of vanillin, vanillic acid, vanillin glucoside and ferulic acid in callus cultures of <i>C. frutescens</i> after feeding with 0.0, 0.2, 0.4, 0.6, 0.8 and 1.0 mM ferulic acid. Calli fed with 0.6 mM ferulic acid were analysed at 5 time points (0, 7, 14, 21 and 28 days)	225
Figure 6.20 Analysed (A) vanillin, (B) vanillin glucoside, (C) vanillic acid and (D) ferulic acid contents of transformed calli (pcVAN, pHVAN, Ech, Fcs and FcsEch) and untransformed calli (Neg) and their corresponding growth media	227
Figure 6.21 HPLC chromatograms of phenolic compounds extracted from a transformed callus of <i>C. frutescens</i>	229
Figure 6.22 HPLC chromatograms of phenolic compounds extracted from a transformed callus of <i>C. frutescens</i> and a chilli fruit	230
Figure 7.1 The model of capsaicin biosynthetic pathway in a cell.....	250
Figure 7.2 The metabolic pathway showing the purported focusing of vanillin biosynthesis from ferulic acid with the overexpression of <i>fcs</i> and <i>ech</i> or <i>VpVAN</i> in the transformed callus cells of <i>C. frutescens</i>	251

LIST OF TABLES

Table 1.1 The frequency of open pollination of the <i>Vanilla</i> genus in the natural setting.....	8
Table 2.1 The list of materials used and their respective producers	48
Table 2.2 The list of <i>E. coli</i> strains used and their respective genotypes ..	55
Table 2.3 The list of plasmids used and their components	55
Table 2.4 A general PCR thermal cycling programme	60
Table 3.1 Effect of various concentrations of 2,4-D on the period and the mean number of callus induced from cotyledon, hypocotyl and root explants	77
Table 3.2. Effect of different 2,4-D concentrations on the fresh weight and area of callus induced from cotyledon, hypocotyl and root explants...	78
Table 3.3 Comparison on the number of cotyledon and hypocotyl explants forming shoot and root between the different combinations of BAP and NAA or IAA in the regeneration media.....	80
Table 4.1 The selection and justification of the cloning methods used for the construction of target DNA into pcDNA6.2 and pHBT12K to produce the final expression vectors	140
Table 5.1 The parameters that affect transformation using PDS	148
Table 5.2 The average number of explants callusing from the cotyledon, hypocotyl and root explants of <i>C. frutescens</i> L. cv. Hot Lava across different concentrations of BS	161
Table 5.3 The transformation frequency of hypocotyl explants bombarded using the optimum parameters	163
Table 6.1 The components in a genomic DNA elimination reaction.....	189
Table 6.2 The components in a reverse transcription reaction.....	189

Table 6.3 The components in a qPCR reaction	190
Table 6.4 The HPLC programme for the optimisation of mobile phase composition and for the analysis of phenolic compounds extracted from plant tissues	196
Table 6.5 The measured concentrations, 260 nm/280 nm ratios and RINs of the RNA samples analysed	202
Table 6.6 The starting mobile phase compositions of x:y methanol–1% acetic acid and their corresponding retention times, peak widths at the base and R_s values for the separation of vanillin and ferulic acid	215
Table 6.7 The optimised gradient HPLC programme for the analysis of vanillin, vanillic acid, vanillin glucoside and ferulic acid	216
Table 6.8 The accuracy for each target compound that was estimated using spike recovery method	220
Table 6.9 The precision of retention time for each target compound as estimated from the coefficient of variance.....	220
Table 6.10 The precision of peak area for each target compound as estimated from the coefficient of variance.....	221

CHAPTER 1

INTRODUCTION

1.1 BACKGROUND, PROJECT OVERVIEW AND OBJECTIVES OF STUDY

Vanilla is one of the most important flavours in the food and beverage industries, and it is also used in perfumery and pharmaceutical products. Natural vanilla extract from *Vanilla planifolia* (*V. planifolia*) or *Vanilla tahitensis* is made up of over 200 components, the major compound being vanillin (4-hydroxy-3-methoxybenzaldehyde). Other compounds include vanillic acid, p-hydroxybenzaldehyde, p-hydroxybenzoic acid, sugars and lipids (Ramachandra and Ravishankar, 2000b). Medically, vanillin was reported to be able to suppress the proliferation of cancer cells and prevent chemically and physically induced mutagenesis (Cheng *et al.*, 2007). It was also reported that vanillin exhibits antimicrobial properties (Cerrutti *et al.*, 1997).

Despite the usefulness of vanilla or more specifically, vanillin, natural vanillin is very expensive to produce. This is largely attributed to the laborious and time-consuming process to extract vanillin from vanilla beans (Sinha *et al.*, 2008). Besides that, only a small portion of vanilla-flavoured products in the market are derived from natural vanilla beans because ~500 kg of vanilla beans (from ~40,000 pollinated flowers of

Vanilla orchids) is needed to produce 1 kg of vanillin, causing a limited supply of vanilla beans and hence, extensive fluctuations in the market price (Gallage and Møller, 2015). The market price of natural vanilla has soared to USD 400–500 per kg in 2016, which is more than a ten times increase from its lowest price at just USD 20 per kg ten years ago (ITC Market Insider, 2016). Only 2000 tons out of more than 15,000 tons of the global demand is provided by vanilla beans (Rana *et al.*, 2013). The rest is supplied by synthetic vanillin produced from lignin and eugenol. Nevertheless, the market share of natural vanilla is not affected by their artificial counterparts due to the shift in demand towards food regarded as natural and organic. US and EU labeling regulations allow only goods produced using natural vanilla to be labeled “vanilla” (de Melo *et al.*, 2015; Sabisch and Smith, 2014). In addition, bioengineered vanillin from plant tissues and microorganisms is still of low success because of the high cost incurred in culture fermentation and the requirement to optimize various culture conditions (Converti *et al.*, 2010; Longo and Sanromán, 2006).

Recently, the vanillin biosynthetic pathway in *V. planifolia* has been explored by Gallage and co-workers (Gallage *et al.*, 2014). An enzyme named vanillin synthase (*VpVAN*) was found to directly convert ferulic acid and its glucoside to vanillin and its glucoside (see **Figure 1.3, subchapter 1.3.1.2**), respectively, based on transient expression in tobacco and stable expression in barley. *VpVAN* is a type of hydratase or lyase that shows high sequence similarity to that of cysteine proteinases. Before its discovery in *V. planifolia*, vanillin synthase-like enzymes in bacteria had been reported by Pometto and Crawford (1983), and by Narbad and Garsson (1998). Similar enzymes in fungi have also been reported by Hansen and co-workers (2009). The enzymes were generally referred to as aldehyde oxidase, CoA ligase, dehydrogenase, hydratase or reductase. Therefore, *VpVAN* was

seen as a potentially useful enzyme that could be employed for the heterologous production of vanillin in biological systems other than *V. planifolia*.

Apart from *VpVAN*, two other enzymes, feruloyl-CoA synthetase (Fcs) and enoyl-CoA hydratase/aldolase (Ech), which was identified in *Amycolatopsis* sp., has been identified to bioconvert ferulic acid to vanillin (see **Figure 1.5, subchapter 1.3.2.2**) (Achterholt *et al.*, 2000). Subsequent to the discovery of Fcs and Ech, bioengineered *Escherichia coli* (*E. coli*) with the expression of *fcs* and *ech* under an isopropyl β -D-1-thiogalactopyranoside (IPTG)-inducible promoter has successfully produced vanillin (Yoon *et al.*, 2005). More recently, constitutive expression of *fcs* and *ech* in bioengineered *Amycolatopsis* sp. ATCC 39116, which is used for vanillin production at an industrial scale, has seen remarkable increase in vanillin concentrations in the fermentation process (Fleige and Meyer, 2016). As such, Fcs and Ech were purportedly effective enzymes for the heterologous production of vanillin in biological systems other than *Amycolatopsis* sp.

This research explores a plant-based alternative to the current vanillin production systems, as the heterologous expression of *VpVAN*, *fcs* and *ech* genes in callus cultures of *Capsicum frutescens* (*C. frutescens*) L. var. Hot Lava (chilli) could hypothetically lead to the elevated production of vanillin in the chilli callus. Ferulic acid (4-hydroxy-3-methoxycinnamic acid) and vanillin were found to be the precursors for the biosynthesis of capsaicin in chilli (see **Figure 1.7, subchapter 1.3.3.2**) (Sukrasno and Yeoman, 1993). Thus, the constitutive expression of *VpVAN*, *fcs* and/or *ech* could potentially enable the bioconversion of endogenous ferulic acid to vanillin in the transformed callus cultures of *C. frutescens* at higher levels than the untransformed callus. This could potentially lead to the production

of “natural,” pure vanillin using an alternative bioengineered plant-based system in another food crop by the gene expression of exogenous vanillin biosynthetic genes, which is the first study of its kind to date.

The overall aim of this project was to genetically modify the genomic DNA of the *in vitro* cultures of a chilli plant species, *Capsicum frutescens*, to produce vanillin at a level that was significantly higher than the untransformed cultures. This could be achieved by accomplishing the following specific objectives:

- (i) establishing the optimum plant tissue culture media for the regeneration of *C. frutescens*;
- (ii) molecular cloning of the genes of synthetic green fluorescent protein (*sgfp*), vanillin synthase (*VpVAN*), feruloyl-CoA synthetase (*fcs*) and enoyl-CoA hydratase (*ech*) into the respective expression vectors
- (iii) determining the working concentration of blasticidin S (BS) antibiotic in the selective media for plant transformation and optimising the microprojectile bombardment (biolistic) parameters for *C. frutescens* using GFP assay followed by the delivery of transgenes (*fcs*, *ech* and *VpVAN*) using biolistics;
- (iv) analysing the expression levels of *fcs*, *ech* and *VpVAN* in transformed plant cultures using reverse transcription-quantitative polymerase chain reaction (RT-qPCR) and analysing the levels of phenolic compounds (vanillin, vanillic acid, vanillin- β -D-glucoside and ferulic acid) using high performance liquid chromatography (HPLC)

The research methodology of this project is outlined in **figure 1.1**.

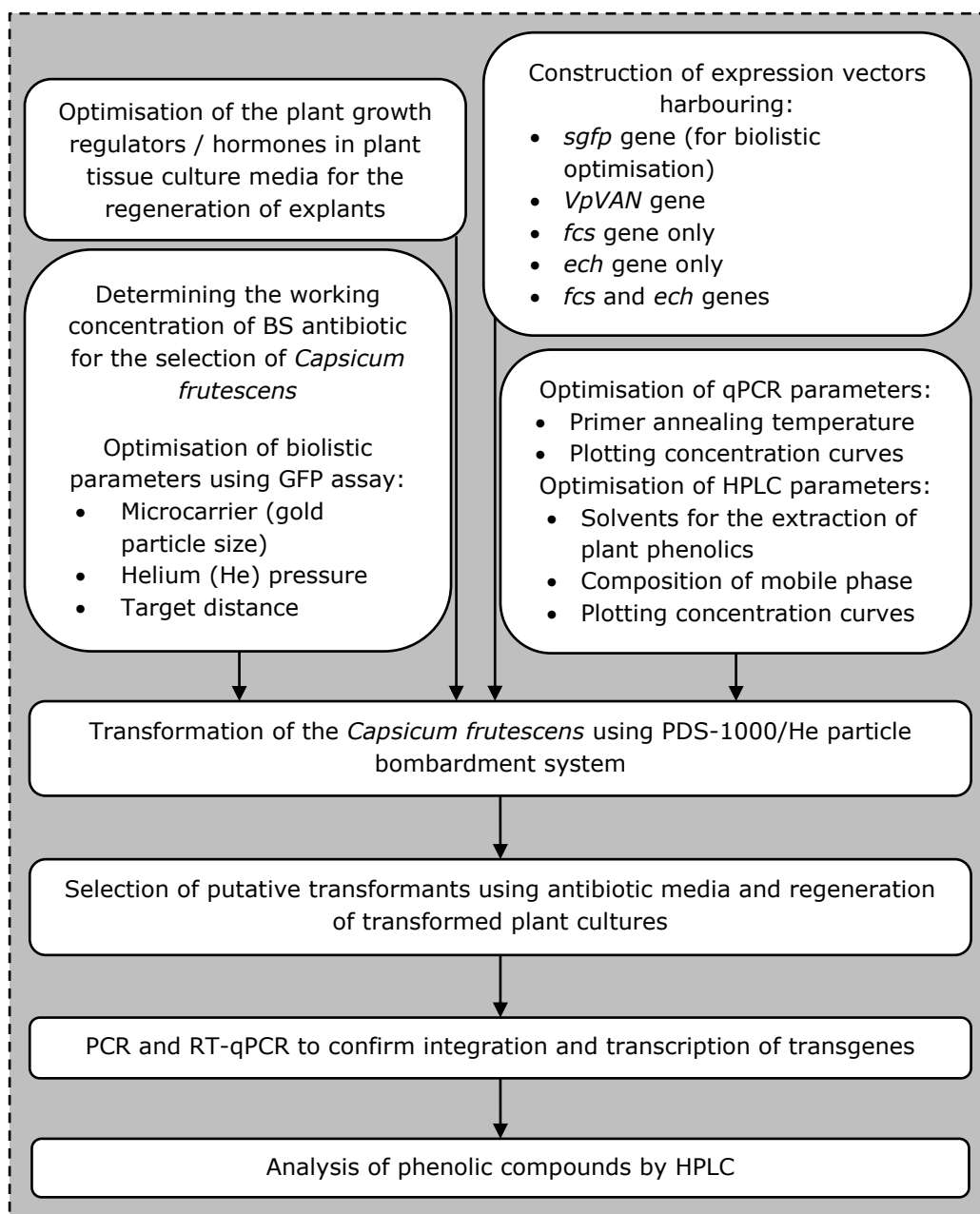


Figure 1.1 An overall flow chart of the research methodology.

1.2 THESIS OUTLINE

Several objectives were to be achieved during the course of this study, as described in **subchapter 1.1**. This thesis provides a review of literature in **chapter 1**, followed by the general materials and methods used throughout the project in **chapter 2**. Subsequently, **chapter 3** describes the manipulation of plant tissue culture media with different combinations

of auxin and cytokinin for the regeneration of *C. frutescens*. **Chapter 4** describes the construction of five expression vectors, which harboured the *sgfp*, *VpVAN*, *fcs* and *ech* transgenes and the combined *fcs-ech* cassette respectively. **Chapter 5** describes the determination of the minimal inhibitory concentration of BS antibiotic in the selective media for plant transformants and the optimisation of biolistic parameters for *C. frutescens* using GFP assay, followed by the delivery of the constructed expression vectors into the explants of *C. frutescens*. Confirmation of transgene integration into the genomic DNA of plant cultures by PCR is reported. **Chapter 6** describes the optimisation of qPCR annealing temperature and validation of the qPCR methods, followed by RT-qPCR analysis of gene expression in the transformed and untransformed plant cultures. In addition, the optimisation and validation of HPLC parameters for the analysis of vanillin, vanillic acid, vanillin- β -D-glucoside and ferulic acid is reported. This is followed by a description on the quantification of the phenolic compounds in the transformed and untransformed plant cultures. Finally, **chapter 7** provides a general discussion and the future perspectives that is derived from this project.

1.3 LITERATURE REVIEW

1.3.1 Vanilla planifolia

1.3.1.1 Agronomic Traits

Vanilla is a famous flavouring agent used in many industries, predominantly food and perfumery. Natural vanilla is extracted from the pods of a type of perennial orchid plant called *Vanilla planifolia* (or *V. planifolia*) Jacks ex. Andrews, commonly known as the vanilla plant. Out of

the 110 species classified under the *Vanilla* genus, *V. planifolia* is the only crop with economic significance (Fouché and Jouve, 1999). The other *Vanilla* species recognized for the making of vanilla products, as defined by the USA Food and Drug Administration, is *V. tahitiensis* Moore (Azeez, 2008). *V. tahitiensis* and another less significant source, *Vanilla pompona*, are grown in Tahiti (Azeez, 2008).

Conventionally propagated from stem cuttings, a vanilla plant produces greenish yellow flowers of about 2 inches long after two years of growth (in the third year). It can take from two years to five years to fully mature and produce vanilla pods. The flowers are hermaphroditic (with both male and female parts); they are self-fertile, but are not capable of effective self-pollination naturally (Fouché and Jouve, 1999; Hernandez-Hernandez, 2010; Lubinsky *et al.*, 2008). Many species of *Vanilla* have very low incidence of successful open pollination (statistics in **table 1.1**). As such, vanilla flowers need to be hand pollinated in farms. The flower is open for 24 hours, but it must be pollinated within eight to twelve hours. In their native regions, vanilla flowers are pollinated by *Melipona* bees (*Melipona beechii*), hummingbirds (*Cynnis* sp.) and bats that approach the flowers for their nectar. In Mexico, *Eulaema* sp. bees were found to contribute to the pollination of 5% of *V. pompona* flowers (Azeez, 2008; Hernandez-Hernandez and Lubinsky, 2010; Hernandez-Hernandez, 2010). The geographical origin of vanilla was south east Mexico and Guatemala. Now the vanilla producers are—by production ranking from the highest to the lowest—Indonesia, Madagascar, Mexico, Papua New Guinea, China, Turkey, Tonga, Uganda, French Polynesia, Comoros, Malawi, Kenya, Zimbabwe, Guadeloupe, and Réunion (Food and Agriculture Organization of the United Nations, 2013).

Table 1.1 The frequency of open pollination of the *Vanilla* genus in the natural setting. Adapted from Rodolphe *et al.* (2011).

Species	Natural fruit set (open pollination)
<i>V. barbellata</i>	18.2%
<i>V. chamissonis</i>	15%
<i>V. claviculata</i>	17.9
<i>V. crenulata</i>	0%
<i>V. cristato-callosa</i>	6.6%
<i>V. dilloniana</i>	14.5%
<i>V. planifolia</i>	1%
<i>V. poitaei</i>	6.4%
<i>V. pompona subsp. grandiflora</i>	0.9%
<i>V. riberoi</i>	1.1%

Vanilla plants should be cultivated at tropical climates, where temperatures are in the range of 20–30°C with a minimum rainfall of 2,000 mm a year. Nevertheless, the plants can typically tolerate temperatures as low as 10°C or up to 33°C (Fouché and Jouve, 1999). The plants grow well in well-drained and generally neutral to slightly acidic (pH 6.0–7.5) soil, such as loam, volcanic soil or laterite, with rich humus (Fouché and Jouve, 1999; Weiss, 2002).

As an epiphytic vine plant, vanilla grows by attaching and climbing onto a phorophyte (a plant on which epiphyte grows) up to 15–20 m high under natural conditions. Their stem diameter increases with plant length and the stem diameter is smaller under the shade than under the sunlight (Fouché and Jouve, 1999). However, the plant grows most vigorously under 50% shade (Hernandez-Hernandez and Lubinsky, 2010). Nevertheless, the vanilla plant only flowers when the diameter of the stem is 0.6 cm or more. As such, decapitation of the plant apex causes branching, which in turn gives rise to nodes with bigger diameter (Fouché and Jouve, 1999).

1.3.1.2 Vanillin

Vanillin is a phenolic aldehyde, an organic compound with the International Union of Pure and Applied Chemistry (IUPAC) nomenclature "4-hydroxy-3-methoxybenzaldehyde." The chemical formula for vanillin is $C_8H_8O_3$ (see **figure 1.2** for chemical structures). Vanillin is toxic to cells at high concentration. Therefore it is present in the form of vanillin- β -D-glucoside, also known as glucovanillin, a vanillin derivative, in mature green pods of the vanilla plant (Gallage *et al.*, 2014). It is through the curing process that the hydrolysis of vanillin- β -D-glucoside releases vanillin. Natural vanilla extract consists of about 250 other aromatic compounds. Vanillin is present at levels about 2% (20,000 parts per million, ppm) in cured vanilla pods, while 30 other identified compounds are present at levels of more than 1 ppm (Reineccius, 1994). The other major compounds identified are *p*-hydroxybenzaldehyde, *p*-hydroxybenzoic acid, vanillic acid and vanillyl alcohol (Azeez, 2008; Ranadive, 2010; Peter, 2004).

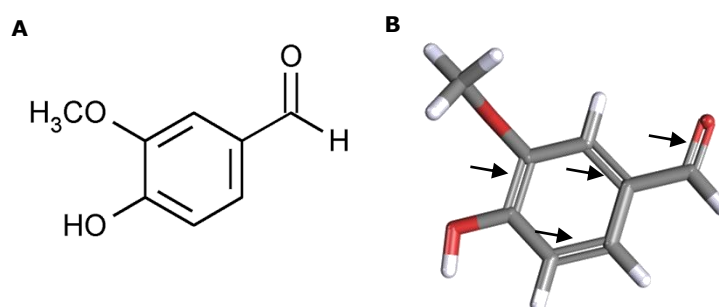


Figure 1.2 (A) A two-dimensional chemical structure¹ and (B) a three-dimensional conformer² of vanillin, $C_8H_8O_3$. In (B), grey arms represent the carbon atoms, white arms represent the hydrogen atoms, and red arms represent the oxygen atoms. Double bonds are pointed by arrows.

¹Adapted from U.S. Pharmacopeia USP29-NF24, http://www.pharmacopeia.cn/v29240/usp29nf24s0_m87890.html. Accessed 4 January 2015.

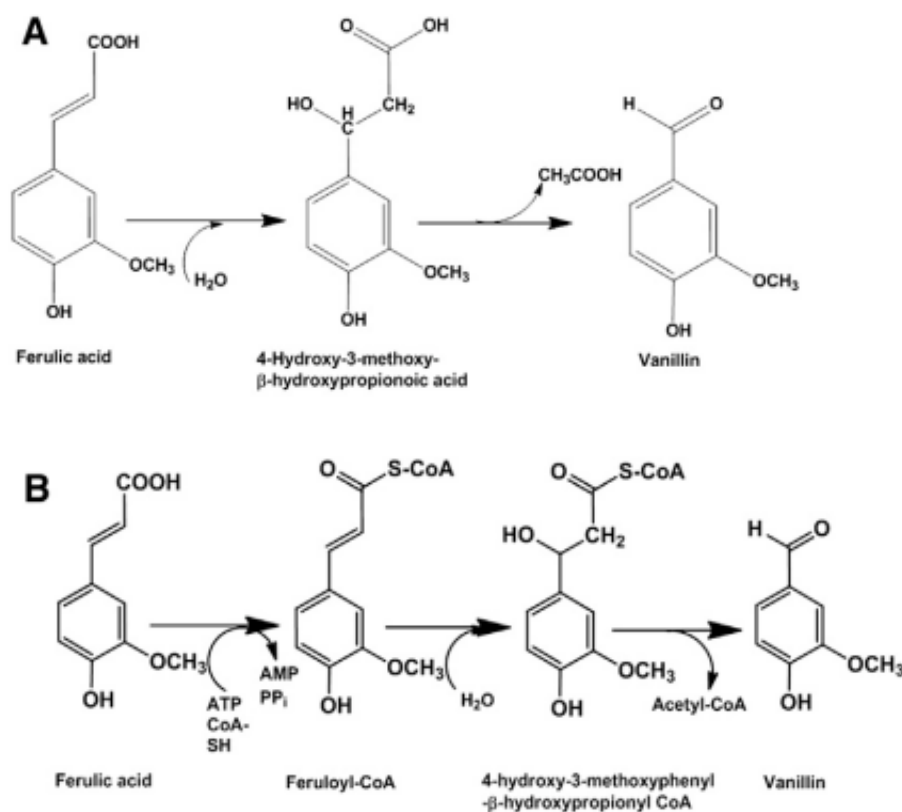
²Adapted from PubChem Open Chemistry Database, <http://pubchem.ncbi.nlm.nih.gov/vw3d/vw3d.cgi?cmd=img&reqid=1447315710945797682>. Accessed 5 January 2015.

Vanillin is famous for its fragrance and is commonly recognised as “vanilla.” It is not only being used as a flavouring agent for foods such as ice cream, chocolate, baked food and pudding; it can also act as taste enhancer for some dairy products and beverages. Thus it is one of the most popular flavouring agents—approximately 60% of vanillin is used in food and beverages, 33% in cosmetics and perfumes and 7% in pharmaceuticals (Korthou and Verpoorte, 2004; Kumar *et al.*, 2012; Priefert *et al.*, 2001). Apart from that, there has been a shift in uses of vanillin, from flavouring to chemical intermediate in the syntheses of compounds, such as papaverine (for treating heart problem), hydrazones (herbicides), antifoaming agents (additives in lubricants) and trimethoprim (antibacterial compound) (Hocking, 1997).

Vanillin has pharmaceutical application because of its antioxidant (Burri *et al.*, 1989) and antimicrobial properties (Cerruti and Alzamora, 1996; Lopez-Malo *et al.*, 1995). A study using a combination of 3,000 ppm vanillin and 500 ppm ascorbic acid in addition to blanching successfully extended the shelf life of strawberry puree over 60 days at room temperature (Cerrutti *et al.*, 1997). More recently, natural vanillin had been found to inhibit the activator protein 1 (AP-1) activity and down-regulate most of the genes associated with cancer progression. This finding suggested that vanillin may exhibit the anticancer potential in human hepatocarcinoma cells (Cheng *et al.*, 2007). Apart from that, vanillin has been identified as a potentially useful substance for treating sickle cell anemia due to its covalent reaction with sickle haemoglobin (Abraham *et al.*, 1991).

Over the decades, the exact routes and enzymes involved in the vanillin biosynthetic pathway remained unclear. Recently, the biosynthesis of vanillin in *V. planifolia* was found to be catalysed by a single enzyme,

vanillin synthase (*VpVAN*) (Gallage *et al.*, 2014). Free and bound ferulic acid, one of the most abundant phenylpropanoids in plants, has been the most explored substrate in vanillin production (Gallage and Møller, 2015). Ferulic acid is found naturally in the forms of free homodimers, and dehydromers and dehydrotrimers esterified with proteins and sugars bound to cell walls (Dobberstein and Bunzel, 2010; Matthew and Abraham, 2004). In microorganisms, five possible pathways for the bioconversion of ferulic acid to vanillin have been proposed, that is (i) CoA-independent retro-aldol reaction, (ii) CoA-dependent retro-aldol reaction, (iii) CoA-dependent β -oxidation, (iv) non-oxidative decarboxylation, and (v) via a reducing pathway (**Figure 1.3**). Although microorganisms are not known to synthesise ferulic acid natively, many of them are known to utilise ferulic acid as their carbon source (Gallage and Møller, 2015). *VpVAN* converts ferulic acid and ferulic acid glucoside directly to vanillin and vanillin glucoside, respectively, via a CoA-independent retro-aldol reaction (**Figure 1.4**) (Gallage *et al.*, 2014).



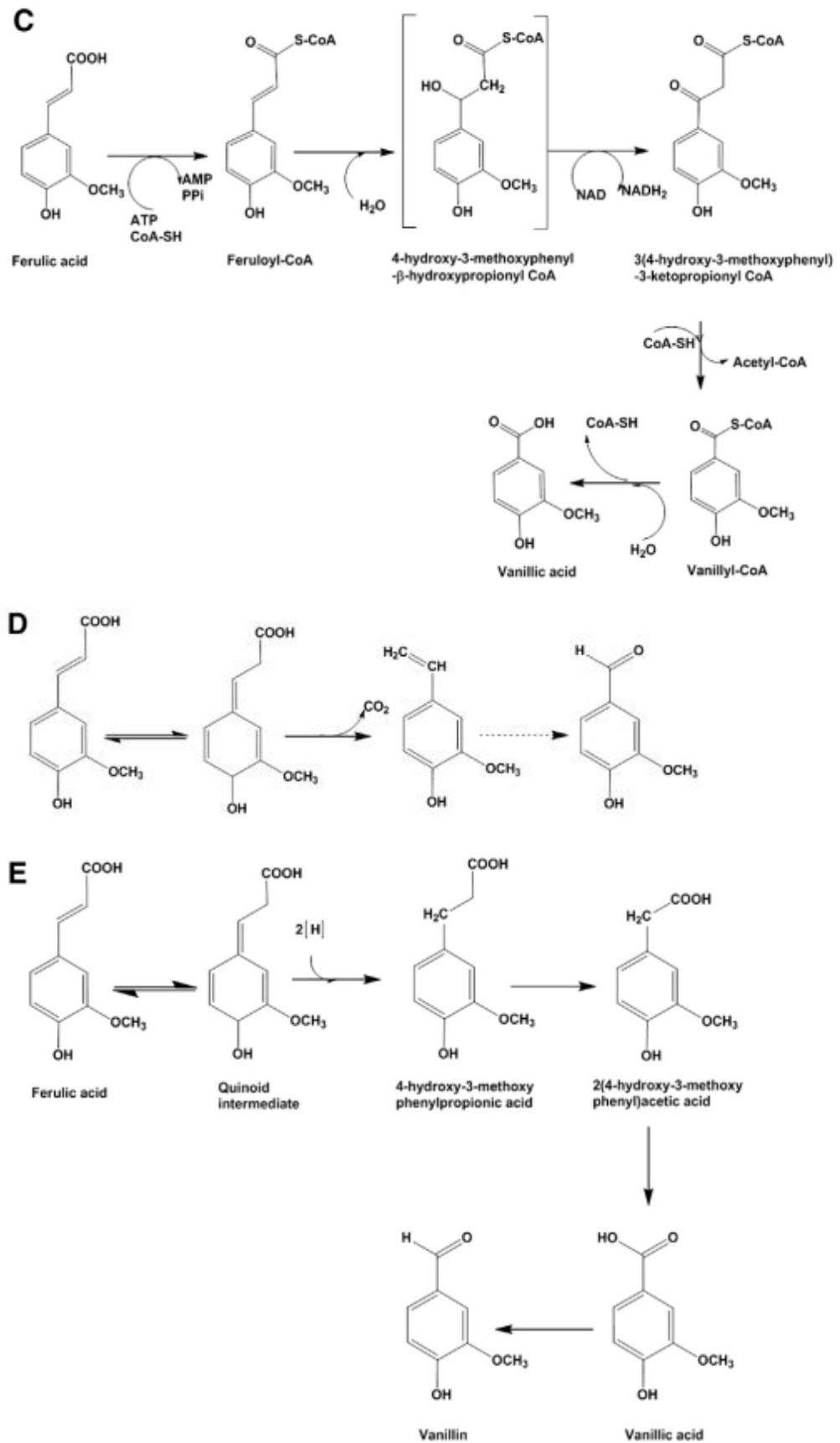


Figure 1.3 Possible pathways from ferulic acid to vanillin. (A) CoA-independent retro-aldol reaction, (B) CoA-dependent retro-aldol reaction, (C) CoA-dependent β -oxidation, (D) non-oxidative decarboxylation, and (E) via a reducing step. Adapted from (Gallage and Møller, 2015).

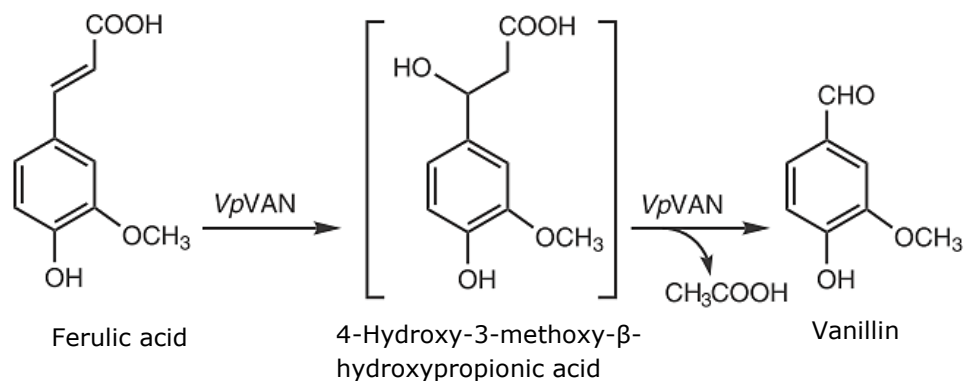


Figure 1.4 Possible conversion route from ferulic acid to vanillin, which is catalysed by *VpVAN*, through two-step reactions initially taking place with hydration addition reaction and subsequently followed by retro-aldol elimination reaction. Adapted from Gallage *et al.* (2014).

VpVAN has high sequence identity to cysteine proteinases, the catalytic enzymes that degrade proteins. In cysteine proteinases, there is a pro-peptide domain consisting of 130–160 amino acid residues with endoplasmic reticulum-targeting signal peptide at the N-terminus. The pro-peptide is removed by the help of another processing enzyme to produce a mature protein (Gallage *et al.*, 2014). It has also been inferred that the presence of a conserved sumoylation site in *VpVAN* as in the tomato cysteine proteinase suggests the involvement of *VpVAN* in vanilla pod senescence because sumoylation of the cysteinase targets the cysteinase to the cell nucleus to activate ethylene biosynthesis (Gallage *et al.*, 2014). Homologues of the vanillin synthase, which were generally referred as aldehyde oxidase, CoA ligase, dehydrogenase, hydratase or reductase, have been reported in bacteria, such as *Bacillus subtilis*, *Pseudomonas fluorescens* and *Streptomyces viridosporus* (Narbad and Gasson, 1998; Pometto and Crawford, 1983). Similar enzymes have also been discovered in fungi, such as fission yeast (*Saccharomyces pombe*) and baker's yeast (*Saccharomyces cerevisiae*) (Hansen *et al.*, 2009). The molecular weight of *VpVAN* is 39.15 kDa, whereas the molecular weight of

vanillin synthase homologues in the microorganisms is 31 kDa (Schomburg *et al.*, 2010). The catalytic activity of VpVAN is optimum at pH 6, with an acceptable range of pH 5.4–8 (Schomburg *et al.*, 2010).

1.3.2 *Amycolatopsis* sp.

The actinomycete *Amycolatopsis* sp. strain ATCC 39116 (previously known as *Streptomyces griseus*) was first isolated from soil in Idaho and was deposited at the American Type Culture Collection (ATCC) as *Streptomyces setonii* (*S. setonii*) (Millard and Burr) Waksman (American Type Culture Collection [ATCC], 2012). It is a soil bacterium, which has the ability to catabolise lignin deposits of plant biomass into benzoate, catechol, gentisate, guaiacol, p-coumarate, protocatechuate, ferulate and vanillin (Sutherland, 1986; Davis *et al.*, 2012). Studies on *S. setonii* that was grown on lignocelluloses of softwood, hardwood and grass revealed the decomposition of lignocelluloses, causing a loss of lignin and carbohydrate in the plant materials (Antai *et al.*, 1981). Greater decomposition was observed on grass compared to softwood and hardwood. The degradation process occurred with the oxidation of the lignin aromatic ring and propane side chain carbons to carbon dioxide. In addition, *Streptomyces* strains are able to degrade both lignified and non-lignified plant cell walls (Antai *et al.*, 1981). Therefore, such bioconversion capability of *Amycolatopsis* sp. has led to growing interest in the bacterium for biotechnological applications to produce useful organic compounds, such as vanillin.

1.3.2.1 *Genome of Amycolatopsis* sp. Strain ATCC 39116

The genome size of *Amycolatopsis* sp. ATCC 39116 is 8,442,518 bp with

71.9% guanine and cytosine (G+C) content (Davis *et al.*, 2012). A number of 8,264 candidate genes encoding proteins were identified. The master record for the whole genome shotgun sequencing project was deposited at GenBank (AFWY00000000), while the contig sequence data was deposited as 119 scaffolds from AFWY03000001-AFWY03000119.

In accordance with the lignin-breakdown characteristic of *Amycolatopsis* sp. ATCC 39116, genes of putative lignin-depolymerizing enzymes, such as haem peroxidases, laccases, catalases and oxidases have been identified. Similarly, genes encoding canonical pathways for catabolism of catechol, benzoate, protocatechuate, phenylacetate, and methylated aromatic compounds were also discovered. On the contrary, the bacterium lacks genes encoding cellulases but genes encoding other carbohydrate-degrading enzymes were present (Davis *et al.*, 2012).

1.3.2.2 Genes of Feruloyl-CoA Synthetase and Enoyl-CoA Hydratase/Aldolase

Among the genes involved in the catabolism of lignin, genes of feruloyl-CoA synthetase (*fcs*) and enoyl-CoA hydratase/aldolase (*ech*) have been found to be involved in the conversion of ferulic acid (a hydroxycinnamic acid, plant cell wall component) into vanillin (**Figure 1.5**) (Fleige *et al.* 2013; Achterholt *et al.* 2000; Lee *et al.* 2009; Priefert *et al.* 2001; Torre *et al.* 2004; Yoon *et al.* 2007; Yoon *et al.* 2005). *Fcs* converts ferulic acid into feruloyl-CoA, while *Ech* converts the latter into 4-hydroxy-3-methoxyphenyl- β -hydroxypropionyl-CoA and subsequently, vanillin. The initial step involves catalysis by decarboxylase. A second mechanism involves the shortening of the ferulic acid side chain by deacetylation. However, vanillin is susceptible to further degradation into vanillic acid by

vanillin dehydrogenase before being converted into guaiacol and protocatechuic acid by vanillate demethylase; both enzymes are also present in *Amycolatopsis* sp. (Achterholt *et al.*, 2000).

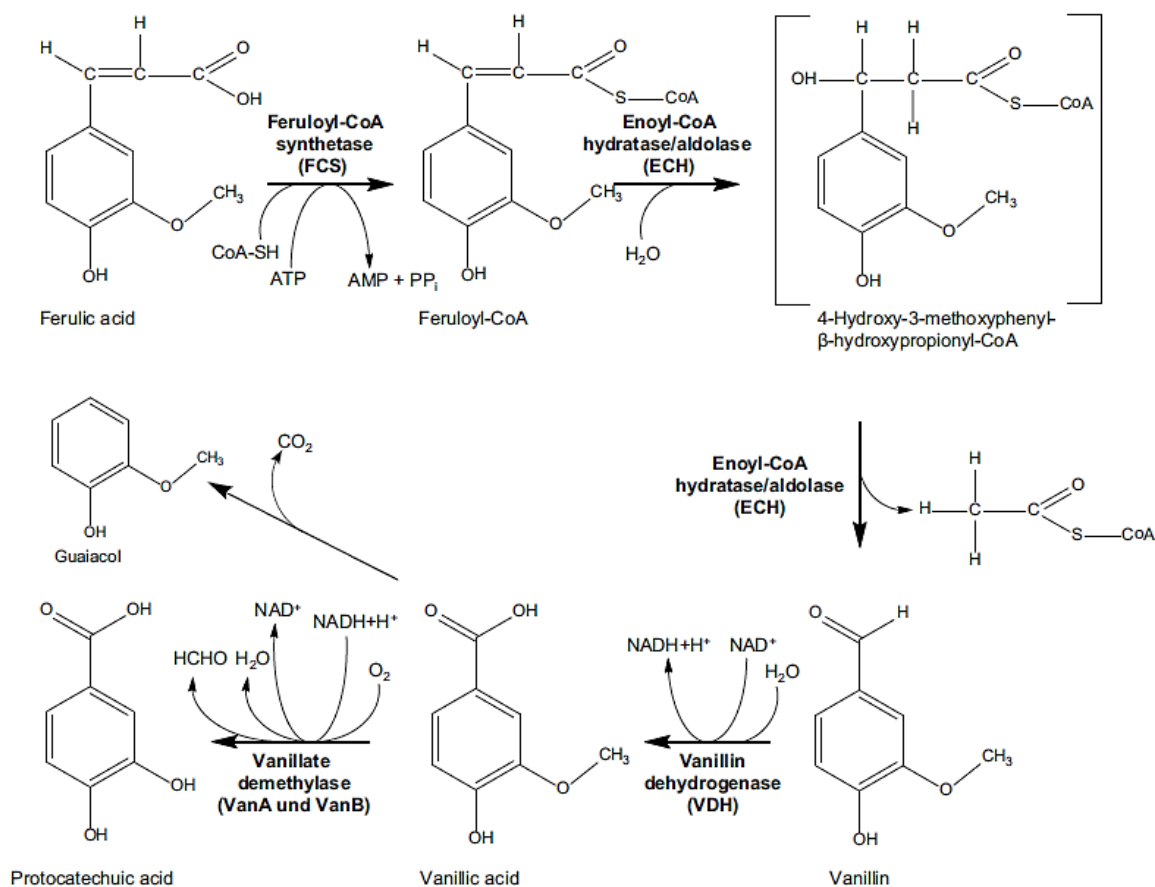


Figure 1.5 Pathways showing the conversion of ferulic acid into vanillin and subsequently, vanillic acid and protocatechuic acid by *Amycolatopsis* sp. ATCC 39116. Adapted from Fleige *et al.* (2013).

The gene sequence of *fcs* and *ech* are 1,476 bp and 864 bp, respectively (Achterholt *et al.*, 2000). An alignment of the *fcs* and *ech* sequence data of *Amycolatopsis* sp. ATCC 39116 using Basic Local Alignment Search Tool (BLAST) showed 100% similarity with those of *Amycolatopsis* sp. HR167, suggesting high sequence homology among the two strains. The molecular weight of Fcs and Ech were 51.9 kDa and 31.9 kDa, respectively (Yang *et al.*, 2013). The derived amino acid sequence of Fcs of *Amycolatopsis* sp. strain HR167 displayed 37% amino acid similarity

to those of the fatty acid coenzyme A ligases, but no significant similarity to the Fcs of *Pseudomonas* sp. strain HR199. On the other hand, the derived amino acid sequence of Ech showed 62% similarity to those of the Ech of *Pseudomonas* sp. strain HR199 (Achterholt *et al.*, 2000). However, sequence analysis of the *fcs* and *ech* genes of *Streptomyces* sp. strain V-1 showed exact similarity with those of *Amycolatopsis* sp. strain HR167, and the translational start codon GTG of *fcs* overlapped with the stop codon TAG of *ech* in the same way, suggesting translational coupling of the two genes (Yang *et al.*, 2013).

1.3.3 *C. frutescens*

1.3.3.1 Agronomic Traits

C. frutescens, like other *Capsicum* species, is an annual or short-lived perennial plant (**Figure 1.6**). *Capsicum* in general is believed to have originated from tropical or subtropical America (Wang and Bosland, 2006). The optimum growing conditions for the chilli plants are sunny with temperatures ranging from 15°C to 30°C (Burt, 2005). However, this species is frost-sensitive. Chilli plants can thrive in various soil textures that are moist and well-drained from pH 5.5 to 6.5 with low salinity (Burt, 2005). Under favourable conditions, chillies can live for 2 years—rapid growth during the first year, followed by much slower growth and finally wilt. Flowering, which does not require photoperiod, occurs after 3 months of growth. However, there have been reported differences between *C. frutescens* and *Capsicum annuum* (*C. annuum*) as well as between two genotypes of *C. frutescens* in the effect of photoperiod on flowering. It was found that long-day photoperiods (more than 14–15 h) generally inhibit flowering in *C. frutescens* more strongly than in *C. annuum* and that a

given genotype of *C. frutescens* may take longer time to flower or may not flower at all under long-day photoperiods (Yamamoto *et al.*, 2007). The flowers are capable of self-pollination.



Figure 1.6 Fruiting 4-month old plants of *C. frutescens* L. cv. Hot Lava in the shadehouse. Ripened chilli fruits may appear red or green in colour (Original).

Out of about 30 species of *Capsicum*, five species are being domesticated—*Capsicum annuum* L., *Capsicum chinense* Jacq., *Capsicum frutescens* L., *Capsicum pubescens* Ruiz and Pavon, and *Capsicum baccatum* L. (Wang and Bosland, 2006).

1.3.3.2 Capsaicin Biosynthetic Pathway

Ferulic acid and vanillin are known to be contributing intermediates in the capsaicin biosynthetic pathway, which is unique to *Capsicum* (Sukrasno and Yeoman, 1993). The elucidation of enzymatic pathways leading to the production of capsaicin in chillies has come a long way. The pathway of capsaicin biosynthesis from phenylpropanoids is illustrated in **figure 1.7**. Phenylalanine ammonia-lyase (PAL), cinnamic acid-4-hydroxylase (CA4H),

p-coumaric acid-3-hydroxylase (CA3H), caffeic acid-O-methyltransferase (CAOMT), caffeoyl-CoA-O-methyltransferase (CCoAOMT), 4-hydroxy-3-methoxyphenyl-hydroxypropanoyl-CoA hydrolase (feruloyl-CoA-forming, HCHL), 3-hydroxy-3-(4-hydroxy-3-methoxyphenyl) propanoyl-CoA vanillin-lyase (acetyl-CoA-forming, HCHL), vanillin aminotransferase (pAMT) and capsaicinoid synthetase (CS) are the key enzymes involved in the conversion of phenylalanine through to feruloyl-CoA, vanillin, vanillylamine and finally, capsaicin (Chee *et al.*, 2017; Ochoa-Alejo and Gómez-Peralta, 1993). Vanillylamine, the downstream intermediate after vanillin, and 8-methyl nonenoic acid is condensed to produce capsaicin by CS. Therefore, CS is suggested as the key enzyme responsible for pungency in *Capsicum* spp. In the callus of *C. annuum* L., the activities of PAL, CA4H and CA3H were similar to those in the chilli fruit, but the activity of CAOMT and CS were six times lower in callus than in fruit (Ochoa-Alejo and Gómez-Peralta, 1993). This suggests that capsaicin biosynthetic activity is not only present in chilli fruits, but it is also present in the callus at lower levels.

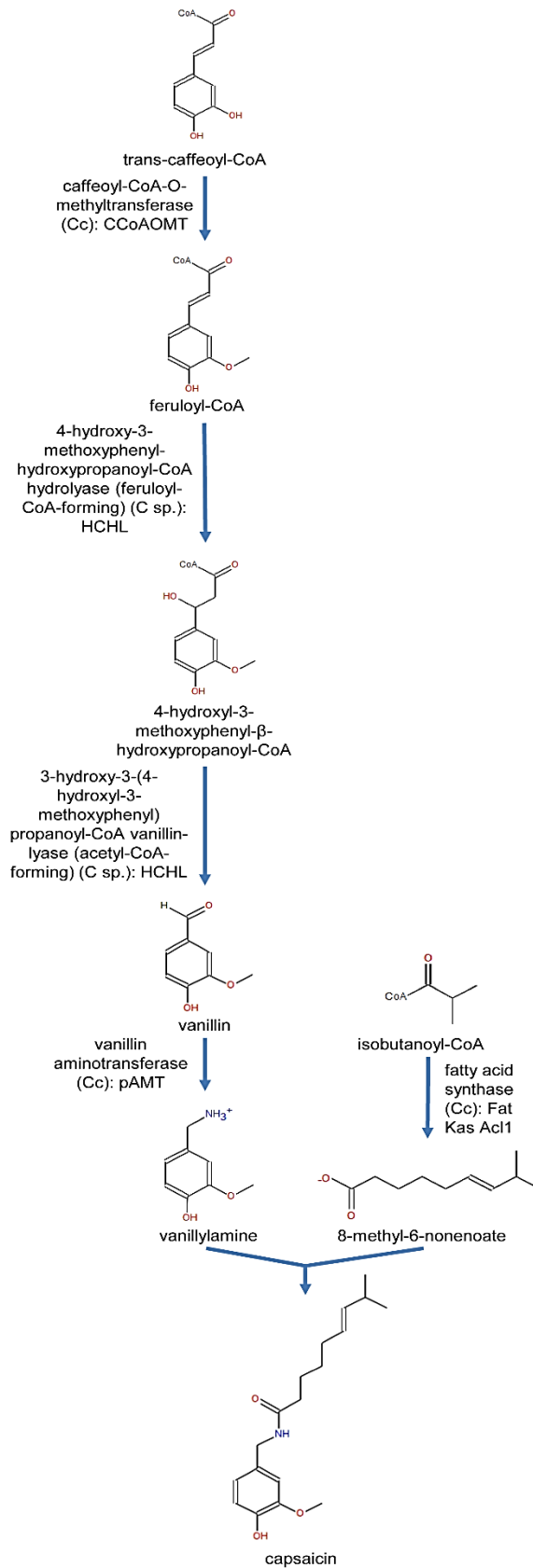


Figure 1.7 The capsaicin biosynthetic pathway via (i) CoA derivatives of amino acid, such as valine (right pathway); and (ii) phenylpropanoid biosynthesis (left pathway), subsequently from ferulate to vanillylamine and finally capsaicin, which is unique to *Capsicum*. Published in Chee *et al.* (2016).

1.3.3.3 Transformation and Regeneration of *Capsicum* spp.

Plant regeneration and transformation studies on *Capsicum* species have been focused mainly on *C. annuum* co-cultivated with *Agrobacterium tumefaciens* (*A. tumefaciens*) strains (Kothari *et al.*, 2010). Highly efficient transformation with neomycin phosphotransferase II gene (*nptII* for kanamycin resistance) using vector *A. tumefaciens* was achieved by Li and co-workers (2003). Cotyledon explants were preconditioned on Murashige and Skoog (MS) medium supplemented with 1.0 mg/l indole-3-acetic acid (IAA) and 5.0 mg/l benzylaminopurine (BAP). After co-cultivation with *A. tumefaciens*, the explants were regenerated on the same medium, but with the addition of 10 mg/l silver nitrate (AgNO_3), 50 mg/l kanamycin sulphate and 500 mg/l carbenicillin. Explants with shoot buds were then transferred to MS supplemented with 10 mg/l AgNO_3 , 1.0 mg/l IAA, 3.0 mg/l BAP and 2.0 mg/l gibberellic acid (GA). Rooting medium was MS with 0.2 mg/l NAA and 0.1 mg/l IAA. Shoot buds were induced at a frequency of 81.3%; shoot elongation at 61.5%; rooting at 89.5%; and 40.8% transgenic plants were obtained. In another study, hypocotyl explants that were co-cultivated with *A. tumefaciens* carrying *nptII* gene and *uidA* (β -glucuronidase, GUS) gene developed adventitious primordial buds on MS containing 5 mg/l BAP and 1 mg/l IAA at 58.4% frequency (Delis *et al.*, 2005). Zhu and co-workers (1996) reported a high regeneration rate of *C. annuum* after transformation by *A. tumefaciens* harbouring a plasmid with the cucumber mosaic virus coat protein (CMV-CP) gene. After co-cultivation, shoot buds were induced on MS supplemented with 8 mg/l BAP, 2 mg/l IA and 500 mg/l carbenicillin. Shoot elongation was achieved on MS with 2 mg/l BAP and 2 mg/l GA. Individual buds were transferred to MS containing 2 mg/l BAP, 2 mg/l GA and 0.5 mg/l abscisic acid (ABA). Finally, shoots longer than 2 cm were rooted on MS with 0.1 mg/l NAA, 50 mg/l kanamycin and

500 mg/l carbenicillin. Besides that, using MS with 1.7 μ M IAA and 22.2 μ M BAP, shoot regeneration efficiency of 14.6 shoots per explant were achieved from the hypocotyl of Habanero chilli (*Capsicum chinense*) (Valadez-Bustos *et al.*, 2009).

Specifically, for the species of *C. frutescens*, a few reports on the regeneration protocols have also been published. Wang and co-workers (1991) reported that shoot induction was the most optimal on MS medium containing 4–6 mg/l BAP and 0.5 mg/l IAA. Shoot elongation took place in MS with 2 mg/l zeatin or 2 mg/l BAP and 1–3 mg/l GA, while rooting was induced in MS supplemented with 0.1–0.5 mg/l 1-naphthaleneacetic acid (NAA). Transformation of the plant with *A. tumefaciens* using the leaf disc method successfully produced plant transformants expressing *gus* gene. An efficient protocol had been developed by Hasnat and co-workers (2008) for two varieties of *C. frutescens*, Nepali and NARC-IV, where hypocotyl explants were inoculated with different dilutions of *A. tumefaciens*. The increased ability of explants to regenerate was achieved with lower bacterial density as compared to high density. Besides that, the effects of AgNO₃ and CoCl₂ on shoot multiplication and *in vitro* flowering of *C. frutescens* Mill had been studied (Sharma *et al.* 2008). External supply of AgNO₃ and CoCl₂ at 30 μ M concentration showed maximum shoot length and induction frequency while *in vitro* flowering was achieved with 40 μ M AgNO₃ and 30 μ M CoCl₂. Pollen from the *in vitro* flowers were also successfully transformed.

1.3.4 Alternative Means of Vanillin Production

Only 0.2% of vanillin used in the market is sourced from plant, where *Vanilla* is the main source. Most of the vanillin is synthetically made, while

several tons are derived from microbial processes (Korthou and Verpoorte, 2004).

1.3.4.1 Synthetic Vanillin by Chemical Synthesis

Synthetic vanillin, which cannot be labelled as natural flavouring, is produced from various starting materials. These include eugenol, lignin, coniferin and guaiacol (Korthou and Verpoorte, 2004). After the first isolation of vanillin from vanilla beans in 1858, from around 1874 until the 1920s, eugenol from clove oil was used to synthesise vanillin (**Figure 1.8**). In 1875, the smell of vanillin was detected from spent sulphite liquor, a byproduct from the sulphite process to make wood pulp. The compound was detected after the pyrolysis of dried waste sulphite liquor. Further research confirmed the use of the lignin fraction of the liquor and subsequently paved the way for large-scale production in 1936 (Hocking, 1997). Another little-used method from 1874 is the oxidation of coniferin, a glucoside from the sap of fir trees, into vanillin (**Figure 1.9**) (Baumann and Pigman, 1957; Havkin-Frenkel and Belanger, 2008). Today, most of the synthetic vanillin is produced using guaiacol from petrochemical sources as starting material (**Figure 1.10**) (Esposito *et al.*, 1997).

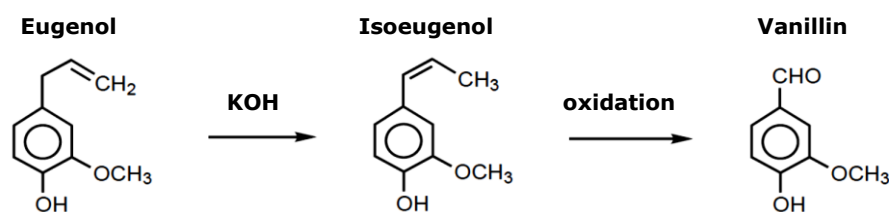


Figure 1.8 Chemical synthesis of vanillin from eugenol by alkaline hydrolysis using potassium hydroxide (KOH) followed by oxidation. Adapted from Hocking (1997).

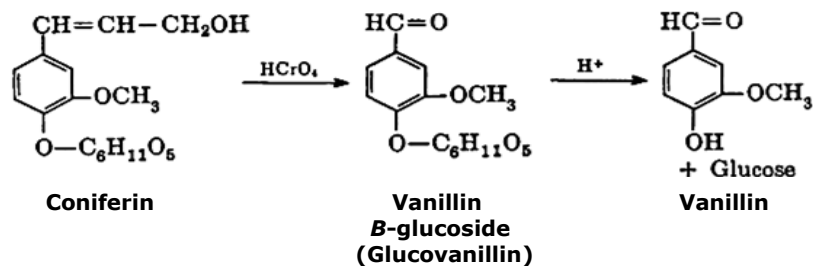


Figure 1.9 Synthesis of vanillin from coniferin through the intermediate, glucovanillin. Adapted from Baumann and Pigman (1957).

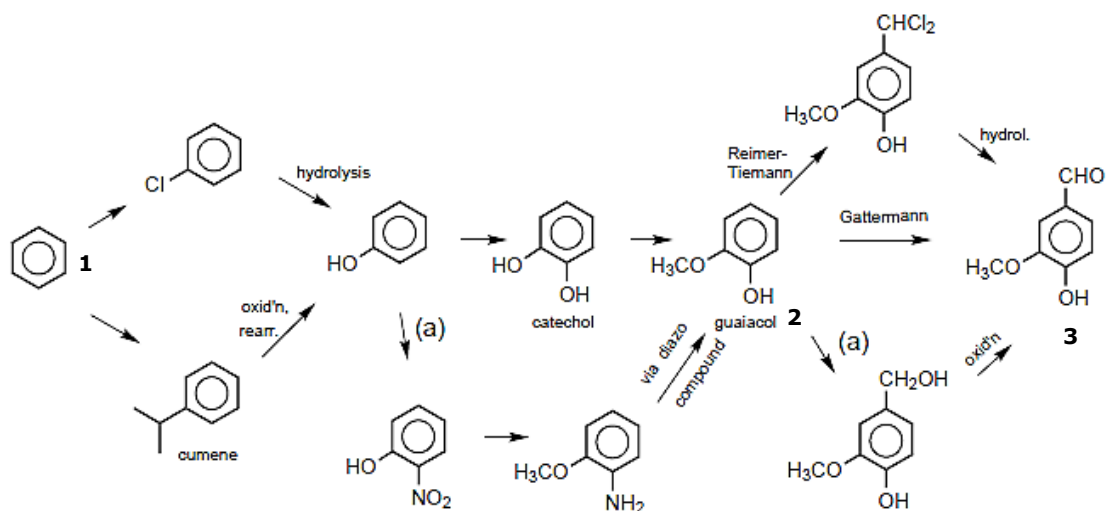


Figure 1.10 Outline of production of vanillin (3), starting from benzene (1). (2) guaiacol. Adapted from Hocking (1997).

1.3.4.2 Biosynthesis by Microorganisms

The use of microorganisms as the biological hosts to produce vanillin has been studied for quite some time. For example, vanillyl alcohol oxidase extracted from *Penicillium simplicissimum* was used to convert creosol and vanillylamine into vanillin at high yield in alkaline conditions at 25°C (van den Heuvel *et al.*, 2001). In another study, up to 65 mg/l of vanillin was produced from glucose in *Schizosaccharomyces pombe* (fission yeast) and *S. cerevisiae* (baker's yeast) through metabolic engineering of 3-dehydroshikimate dehydratase from dung mould (*Podospira pauciseta*),

aromatic carboxylic acid reductase from a *Nocardia* bacterium, and O-methyltransferase from *Homo sapiens* into the yeasts (Hansen et al. 2009). A mutant strain of *Rhodococcus jostii* RHA1, which lacked the vanillin dehydrogenase gene, produced vanillin up to 96 mg/l by breaking down lignin (Sainsbury et al., 2013).

Degradation of ferulic acid into vanillin has been elucidated for *Comamonas acidovorans*, *Bacillus subtilis*, *Burkholderia cepacia* and *Streptomyces setonii*, as well as for *Amycolatopsis* sp. strain HR167 with the identification of enzymes feruloyl-CoA synthetase and enoyl-CoA hydratase/aldolase (Achterholt et al., 2000). Feruloyl-CoA synthetase and feruloyl hydratase/aldolase from *Pseudomonas fluorescens* BF13 has also been expressed in *E. coli* through metabolic engineering for the bioconversion of ferulic acid into vanillin (Barghini et al., 2007). Similar work using the same enzymes in immobilised cells of *E. coli* strain JM109/pBB1 was done by Torre and co-workers (2004) to demonstrate the production of vanillin from ferulate continuously using resting cell system. Metabolic engineering of *E. coli* with the *fcs* gene encoding feruloyl-CoA synthetase and *ech* gene encoding enoyl-CoA hydratase/aldolase from *Amycolatopsis* sp. strain HR104 produced up to 1.1 g/l vanillin from 0.2% (w/v) ferulic acid (Yoon et al. 2005). However, in the same research, it was reported that vanillin production decreased with the addition of glucose, fructose, arabinose, galactose or glycerol. As high vanillin concentration in the culture causes toxicity to the microorganisms, vanillin production could be increased with the employment of NTG mutagenesis (in "NTG" nucleic acid sequence) to generate vanillin-resistant mutants (Yoon et al. 2007) and with the addition of XAD-2 resin into the medium to reduce the concentration of vanillin (Stentelaire et al., 2000; Yoon et al., 2007). Besides that, *Pseudomonas putida* KT2440 has been genetically engineered

with *fcs* and *ech* genes to produce vanillin up to 8.6 mM (Graf and Altenbuchner, 2014). *E. coli* has also been engineered to produce vanillin from L-tyrosine, glucose, xylose and glycerol (Ni *et al.*, 2015)

Bioreactors for the production of vanillin from vanillic acid by *Pycnoporus cinnabarinus* have also been studied. A concentration of up to 1575 mg/l vanillin with a significant level of methoxyhydroquinone was produced (Stentelaire *et al.*, 2000). An IE27 strain of *Pseudomonas putida* was able to produce vanillin from isoeugenol, but not from vanillin or eugenol, to a concentration of 16.1 g/l after incubation with 10% (v/v) dimethyl sulfoxide (Yamada *et al.*, 2007).

1.3.4.3 Biotransformation in Plant Cell Cultures

Much research has been done in order to increase the production of natural vanillin from *V. planifolia*. A few of the methods to achieve that include supplying phytohormones and elicitors to the *V. planifolia* culture (Funk and Brodelius, 1990), feeding the precursor of vanillin (Westcott *et al.*, 1994), immobilizing cell cultures (Ramachandra and Ravishankar, 2000a; Westcott *et al.*, 1994), using charcoal as absorbent (Westcott *et al.*, 1994), and inhibiting the competing pathway (Funk and Brodelius, 1990).

In another study, immobilised cell cultures of *Capsicum frutescens* Mill were able to biotransform up to 315 µg vanillin/culture in medium treated with ferulic acid and up to 190 µg capsaicin/culture in medium treated with vanillylamine (Johnson *et al.*, 1996). Freely suspended cells and immobilised cell cultures of the same plant were also able to biotransform externally supplied protocatechuic aldehyde and caffeic acid into vanillin and capsaicin (Rao & Ravishankar 2000). These studies

indicate that *Capsicum* plants have the vanillin biosynthesis capability. This is because vanillin appears to be the intermediate in the production of capsaicin (see **Figure 1.7, subchapter 1.3.3.2**), the compound responsible for pungency in chilli fruit placentas (Chapa-Oliver and Mejía-Teniente, 2016; Gururaj *et al.*, 2012; Mazourek *et al.*, 2009).

1.3.5 Plant Regeneration by Tissue Culture

Plant tissue culture techniques are used to maintain plant cells, tissues or organs or to produce multiple clonal plant materials from a stock material under sterile conditions *in vitro* (Thorpe, 2013). This method enables plant propagation in a relatively shorter time than conventional plant propagation methods by sexual or asexual means. Conventionally, plants were propagated sexually through flowering, pollination, fertilisation and seed formation, after which new plants develop from germinated seeds. On the other hand, asexual methods include cutting and planting of vegetative plant parts, grafting and budding (Borlaug, 1983). Since the discovery of callus formation during the observation of wound healing in plants by Henri-Loius Duhumel du Monceau in 1756, the concept and techniques of plant tissue culture has been studied (Thorpe, 2013). A large-scale culture of plant suspension cells was first described by Tulecke and Nickell (1959). Extensive use of plant tissue culture techniques has been observed from the mid-1960s after various discoveries, such as the development of nutrient media (Nitsch and Nitsch, 1956; Murashige and Skoog, 1962; White, 1963; Gamborg *et al.*, 1976), shoot tip culture (Ball, 1946; Morel, 1960), ovary culture (LaRue, 1942) and *in vitro* fertilisation (Kanta *et al.*, 1962), and the isolation of protoplast using fungal cellulase (Cocking, 1960). Plant tissue culture techniques are now often employed to multiply

plants that have been genetically modified or bred through other breeding methods. These are possible owing to the unique capacity of plant cells to regenerate regardless of their ploidy level or their form of specialisation (Bhojwani and Razdan, 1983).

Plant tissue culture approaches could be categorised into three broad categories: indirect organogenesis, direct organogenesis and somatic embryogenesis. Indirect organogenesis begins with the dedifferentiation of explant tissues into callus (**Figure 1.11**). Meristemoid cells then develop and are succeeded with the development of primordia and the initiation of adventitious organs, such as shoots (caulogenesis) or roots (rhizogenesis) (Ziv, 1999). In many plants, regeneration through callus results in higher chances of undesired variation between clones, a phenomenon that is known as somaclonal variation. Therefore, direct regeneration could be attempted. Direct organogenesis bypasses the callus stage and typically takes place either by caulogenesis or by rhizogenesis directly from the explant through the development of meristems and primordia (**Figure 1.12**) (Dhaliwal *et al.*, 2003). Somatic embryogenesis is the development of a bipolar structure similar to a zygotic embryo from a haploid or diploid somatic cell that has no vascular connection with the parental tissue (von Arnold *et al.*, 2002). In monocotyledonous plants, cells undergoing somatic embryogenesis generally display the development of globular tissue, followed by scutellar and then coleoptile embryo before emerging as a new plantlet (Krishnaraj and Vasil, 1995). In dicotyledonous plants, cells develop into early pro-embryo, globular and heart-shaped tissue, which then becomes torpedo-shaped and finally bipolar cotyledonary embryo before emerging as a new plantlet (Brown *et al.*, 1995).



Figure 1.11 Callus regenerated from a hypocotyl explant of *C. frutescens* (Original).

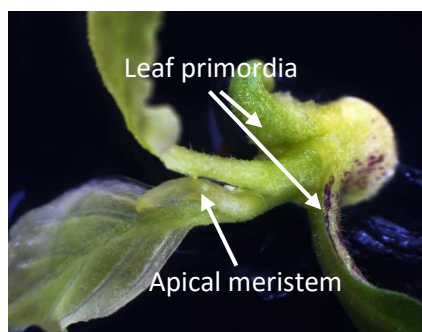


Figure 1.12 The structures of leaf primordia and shoot apical meristem from direct organogenesis of a cotyledon explant of *C. frutescens* (Original).

The regeneration patterns of plants are generally controlled by the balance of plant growth regulators (hormones), such as auxin and cytokinin, in the growth media. The establishment of regeneration systems for plants is often limited by the lack of information on growth stimulating factors. Based on pioneering studies, the general rule of thumb is that a low ratio of auxin to cytokinin induces caulogenesis, while a high ratio of auxin to cytokinin induces rhizogenesis, directly from an explant (Su *et al.*, 2011). An intermediate auxin to cytokinin ratio induces dedifferentiation and callus formation (Ikeuchi *et al.*, 2013).

1.3.5.1 Dedifferentiation

The formation of callus, a mass of unorganised cells, typically results from the dedifferentiation of plant tissues due to wounding or pathogen infection (Ikeuchi *et al.*, 2013). In the *in vitro* environment, callus regeneration from an explant can be achieved by the exogenous application of auxin and cytokinin in the callus-inducing medium. Although other hormones like abscisic acid can also induce or inhibit callus, auxin and cytokinin have been by far the most studied and used hormones (Peterson and Smith, 1991; Ruduś *et al.*, 2001). The formation of callus could have been caused by disruption of the flow of polar signals, for example, auxin, from young tissues in the shoot to the root. Callus formation in relation to polarity is a complex process that depends on not only the stability of gene expression, but also on the cell type and orientation, cell competence, vascular differentiation and cellular responses linked to the synthesis and transport of such signals (Fukuda *et al.* 1994; Sachs 1991).

Based on the macroscopic observation of different types of calli that have been regenerated, calli that have no apparent organ formation can be friable or compact callus, while calli with some extent of organ regeneration can be classified as shooty, rooty or embryonic callus, depending on the generated organs (**Figure 1.13**) (Ikeuchi *et al.*, 2013). Nevertheless, it should be noted that not all explants can form callus and not all callus cell types are competent to become totipotent and regenerate into differentiated organs (Smith, 2013). As an example, a study by Sugimoto and co-workers (2010) demonstrated that the cotyledon, root and petal explants of *Arabidopsis* mutants that were not capable of lateral root formation could not form callus. This shows the importance of the root development mechanism for callus formation from any parts of a plant, as

opposed to the widely believed simple reprogramming of cells to undifferentiated state.

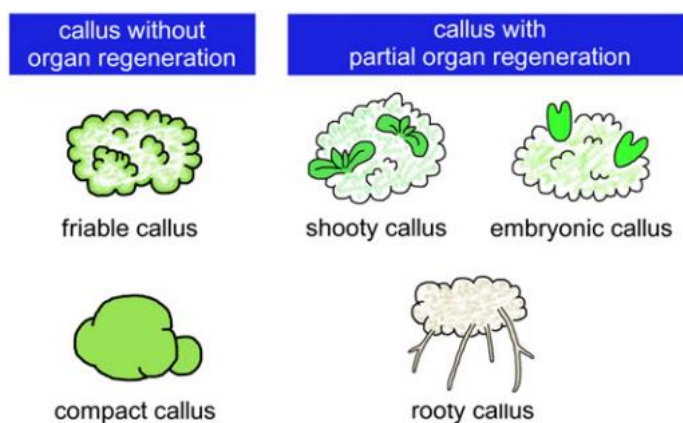


Figure 1.13 Illustration of different types of callus. Adapted from Ikeuchi *et al.* (2013).

The molecular basis of callus formation has been studied through the identification of mutants impaired in callus formation. As terminally differentiated plant cells have suppressed progression into mitosis, the cells need to regain the competence to proliferate into callus. However, the activation of cell cycle regulators alone, such as cyclins (CYCs) and cyclin-dependent kinases (CDKs), is not enough to induce callus (Boudolf *et al.*, 2009; Cockroft *et al.*, 2000; Ikeuchi *et al.*, 2013). In fact, most of the callus induction processes are profoundly correlated to transcriptional or post-transcriptional regulators that affect the expression of genes. For example, auxin is known to induce certain transcription factors of the LATERAL ORGAN BOUNDARIES DOMAIN (LBD) family, which mediate the downstream responses of AUXIN RESPONSE FACTORS (ARFs) (Fan *et al.*, 2012; Huang *et al.*, 2016). It was shown that the callus induction medium upregulated the expression of *LBD16*, *LBD17*, *LBD18* and *LBD29* and the overexpression of either one of the four was able to induce callus (Fan *et al.*, 2012). The LBDs then induce another transcription factor, E2

PROMOTER BINDING FACTOR a (E2Fa), which is crucial for cell cycle re-entry and is involved in the transcription of genes for DNA replication by dimerizing with DIMERIZATION PARTNER (DP) proteins (De Veylder *et al.*, 2007; Inzé and De Veylder, 2006). In short, the auxin signal transduction pathway takes place via ARF transcription factors to activate the expression of LBD transcription factors, which in turn induce E2Fa/DPa to promote cell proliferation.

Besides auxin, cytokinin also plays a role in callus induction. Cytokinin is perceived by histidine (His) kinases at the membrane, which then transfer the signal through a multi-step His-aspartate (Asp) phosphorelay system to the downstream transcription factors (Aoyama and Oka, 2003; Maxwell and Kieber, 2010). The important families of transcription factors in cytokinin signaling are the type A and type B *ARABIDOPSIS* RESPONSE REGULATOR (ARR). The expression of type A ARR can be regulated by cytokinin while those of type B is constitutive (Terouchi *et al.*, 2010; To *et al.*, 2007). In a negative feedback loop, cytokinin-inducible ARR4, RAR5, ARR6 and ARR7 are transcription repressors in cytokinin signalling (Hwang and Sheen, 2001). In addition, the transcription of type A ARRs is induced by type B ARRs (Terouchi *et al.*, 2010). The overexpression of type B ARR1 and ARR21 resulted in callus formation without exogenous cytokinin (Hwang and Sheen, 2001; Ikeuchi *et al.*, 2013). The enhanced expression of ARR10 caused a hypersensitive response to cytokinin, such as greening of callus (Hill and Schaller, 2013). The type B ARRs potentially activate CYCD3 for re-entry into cell cycle as the application of cytokinin upregulated the expression of CYCD3, whereas the overexpression of CYCD3 without exogenous cytokinin promoted callus formation (Ikeuchi *et al.*, 2013). In another cytokinin signal transduction pathway, the ENHANCER OF SHOOT REGENERATION (ESR) transcription

factors are thought to be involved in cytokinin-mediated callus induction. In *Arabidopsis*, the overexpression of *ESR* resulted in an increased response to cytokinin. The overexpression of *ESR1* or *ESR2* without exogenous cytokinin stimulated callus formation (Banno *et al.*, 2001; Ikeda *et al.*, 2006). *ESR2* directly activates *CYCD1;1* and OBF BINDING PROTEIN1 (OBP1) transcription factor, which promotes cell cycle re-entry by binding to the promoter of *CYCD3;1* and an S phase-specific DNA-BINDING ONE ZINC FINGER 2;3 (DOF2;3) transcription factor (Ikeuchi *et al.*, 2013; Skirycz *et al.*, 2008). In summary, cytokinin signal transduction pathway takes place (i) via ARRs, which activates *CYCD3* for cell proliferation, or (ii) via ESRs, where *ESR2* directly activates *CYCD1;1* for cell proliferation or activates OBP1, which in turn activates *CYCD3;1* and DOF2;3 for cell proliferation.

1.3.5.2 Organogenesis

The use of various hormone combinations in the plant growth media has been studied extensively with respect to shoot and root regeneration. With the general knowledge of a high cytokinin to auxin ratio for shoot induction and a high auxin to cytokinin ratio for root induction, different plant materials require different combinations of auxin and cytokinin. For example, five-day old cotyledons of watermelon (*Citrullus vulgaris*) developed shoots with a high frequency (60–92%) after being cultured on MS medium supplemented with 5 mg/l BAP and 0.5 mg/l IAA. The shoots were then rooted on MS medium containing 0.1 mg/l NAA (Dong and Jia, 1991). MS medium with 5 mg/l BAP and 0.3 mg/l IAA was used to induce shoot buds from rooted hypocotyls of *C. annuum* (Valera-Montero and Ochoa-Alejo, 1992). Shoot bud differentiation was observed on the seed

explants of chickpea (*Cicer arietinum*) at 75–100 μM BAP, followed by root induction from the shoots at less than 12.5 μM BAP (Polisetty *et al.*, 1997). Cytokinin was also found to be responsible for the determination of embryo meristematic axes. A study on cotton (*Gossypium hirsutum*) found that a moderate concentration of BAP (3 mg/l) induced an optimum number of shoots per embryogenic axis, but higher or lower BAP concentrations gave fewer shoots per explant (Morre *et al.*, 1998). Multiple shoots could also be induced from the embryo axes with 0.4 μM BAP and 0.1 μM NAA, followed by rooting with 0.5 μM NAA (Banerjee *et al.*, 2003). Besides BAP, the use of other cytokinin and additive has been studied. For example, 10 μM thidiazuron induced shoots from protoplast-derived calli of pea, but subsequent rooting was not possible (Böhmer *et al.*, 1995). Thidiazuron (7 μM) was also added in the MS medium for the induction of shoots from cotyledon explants of mulberry (*Morus alba*), followed by shoot elongation using 5 μM BAP and rooting using 1–7 μM IBA or NAA (Thomas, 2003). Apart from BAP and NAA, the addition of ascorbic acid was found to be crucial to induce axillary shoots in emetic swallow-wort (*Tylophora indica*) (Sharma and Chandel, 1992). Nitrogen compounds, such as allantoin and amides, were also found to stimulate shoot regeneration in the presence of BAP, based on a study of soybean (Shetty *et al.*, 1992).

The interaction between auxin and cytokinin regulates the development of shoot apical meristems. As a higher ratio of cytokinin over auxin promotes shoot development, this suggests that cytokinin positively regulates the activity of shoot apical meristems. Deficiency in cytokinin causes a decrease in the size and activity of shoot meristems (Werner and Schmülling, 2009). The size of shoot apical meristem is maintained by WUSCHEL (WUS) and CLAVATA3 (CLV3) in *Arabidopsis*. Type A ARRs, the main genes in the cytokinin signalling response, activate CLV3, which

down-regulates WUS that down-regulates the ARRs in return in a negative feedback loop (Brand *et al.*, 2002; Su *et al.*, 2011; Yadav *et al.*, 2011). The enhanced expression of *ARR10* caused elevated sensitivity to cytokinin, such as shoot induction (Hill and Schaller, 2013). SHOOTSTEMLESS (STM) maintains the stem cells in the meristem and prevents their differentiation into organ-specific cells and promotes cytokinin biosynthesis (Laxmi *et al.*, 2013). Cytokinin activates KNOTTED-like homeobox (KNOX) transcription factors, which in turn activates cytokinin biosynthesis in a positive feedback loop but represses gibberellic acid, a hormone that stimulates transition from meristem to shoot (Gupta and Chakrabarty, 2013). Auxin accumulates at relatively high levels compared to cytokinin at the peripheral zone of meristem. Auxin inhibits the expression of STM and hence, down-regulates cytokinin biosynthesis in shoots (Su *et al.*, 2011). As STM is the inhibitor of stem cell differentiation, the suppression of STM results in cell differentiation into organs at the peripheral region of meristems. Besides that, other genes of the cytokinin signal transduction pathway are also involved in shoot organogenesis. The overexpression of *ESR1* induced shoot formation from root explants of *Arabidopsis* without exogenous cytokinin and effectively increased shoot regeneration in the presence of cytokinin (Banno *et al.*, 2001). *ESR2* regulates the transcription of *CUP-SHAPED COTYLEDON 1 (CUC1)* for the development of normal cotyledon phenotypes (Ikeda *et al.*, 2006).

Cellular organisation of roots and the central role of auxin in shaping the root architecture has been well-characterised. Cells that are determined as the root meristematic zone undergo division and become gradually displaced from the meristematic zone. Cells in the displaced region, where cell division slows down, begin to elongate and then differentiate to appear as root hairs from epidermal cells (Overvoorde *et al.*,

2010). In short, the axis along the meristematic region through the elongation and differentiation regions constitute a continuously renewing gradient of cell differentiation towards root development. The biosynthesis, transport, distribution and polarisation of auxin have been closely associated with dose-dependent increase in root length, formation of root primordia and gravitropism (Perrot-Rechenmann, 2010). PLETHORA (PLT) proteins of the AP2 class of transcription factors are the main regulators that determine root stem cell niche (Aida *et al.*, 2004; Galinha *et al.*, 2007). PLT responds to the accumulation of auxin and specifies the activity of quiescent centre (QC), a small region that maintains stem cells in the primary root (Aida *et al.*, 2004). The accumulated PLT transcripts interact with the radial domains of SHORT-ROOT and SCARECROW to contribute to positional regulation of the stem cell niche (Aida *et al.*, 2004). As the activity of PLT is dose-dependent, high PLT activity causes specification and maintenance of stem cells, low activity causes mitosis of stem cells and even lower activity causes cell differentiation (Galinha *et al.*, 2007). The elongation of cells during root hair development and the initiation of lateral roots is mediated by AUX1-directed auxin import into epidermis (Jones *et al.*, 2009; Swarup *et al.*, 2001). Auxin transport from the production centre (shoot) to the sink (root) is mediated by auxin efflux facilitators, the PINFORMED (PIN) proteins (Grieneisen *et al.*, 2007). The importance of shoot-to-root transport of auxin in root development was demonstrated when the levels of free IAA in roots and the number of lateral roots decreased after the application of the auxin transport inhibitor, naphthylphthalamic acid (NPA), at the shoot-root junction of *Arabidopsis* (Reed *et al.*, 1998). Besides that, numerous other molecular components have been identified to be involved in auxin signalling and root development. These include TRANSPORT INHIBITOR RESPONSE 1 (TIR1)

protein, AUXIN F-BOX PROTEINS (AFBs), members of the Aux/IAA proteins, and ARF transcription factors (Overvoorde *et al.*, 2010)

The role of auxin in root development is undoubtedly important. However, supplementation of culture medium with different auxins may have different effect on root induction. For example, in a study of purple coneflower (*Echinacea purpurea*), IBA was more effective than IAA, while NAA was not effective for root induction (Choffe *et al.*, 2000). Other plant hormones, such as cytokinins, brassinosteroids, ethylene, ABA, gibberellins, jasmonic acid, polyamines and strigolactones act either synergistically or antagonistically with auxin to induce a series of events that lead to rhizogenesis (Saini *et al.*, 2013). Focusing on cytokinin, a well-known hormone that interacts with auxin across a wide range of plant developmental processes, cytokinin regulates lateral root development through antagonistic interaction with auxin. While auxin is mainly synthesised in shoots, cytokinin is synthesised in root tips. Cytokinin promotes shoot development, but it negatively regulates root development (Aloni *et al.*, 2006). Through a study of *Arabidopsis*, transactivation of the cytokinin-degrading enzyme, cytokinin oxidase 1, promoted the development of lateral roots (Laplaze *et al.*, 2007). Cytokinin stimulates mitosis in the QC of the root apical meristem through the repression of LIKE AUX1 (LAX) 2 (Zhang *et al.*, 2013). The antagonistic effect of auxin and cytokinin has also been shown through SHORT HYPOCOTYL 2 (SHY2). Cytokinin enhances the transcription of *SHY2*, which in turn suppresses *PIN* genes and causes the relocation of auxin for cell differentiation. Auxin regulates the degradation of SHY2 for the expression of *PIN* genes (Su *et al.*, 2011).

1.3.6 Biolistic-mediated Plant Transformation Approach

Biolistics (also known as particle bombardment or microprojectile) is a universal transformation method involving the bombardment of DNA-coated gold or tungsten microcarriers into target tissues at high velocity using helium (He) pressure (Rao *et al.*, 2009). The particle bombardment approach was first reported by Sanford and co-workers (1987), who used macroprojectile and stopping plate and accelerated tungsten particles to 328–656 ms⁻¹ velocities. The particles penetrated cell walls and entered cells without resulting in mortality. This method is advantageous over *Agrobacterium*-mediated transformation as it does not rely on complex and unpredictable interactions between the bacterium and host plant (Newell, 2000). However, to utilise the advantages of both *Agrobacterium*- and biolistic-mediated transformations, there has been a report of *A. tumefaciens* cells being used as the coating of microprojectile particles for the transformation of the leaf explants of strawberry, resulting in transformation frequencies of as high as 20.7% (de Mesa *et al.*, 2000). A number of dicotyledonous and monocotyledonous plant species, for example, tobacco, soybean, cotton, rice and maize, have been transformed for improvements by numerous refinements in the bombardment apparatus used (Newell, 2000).

1.3.6.1 Types of Explants

In biolistic-mediated transformation, cells that are competent for transformation and regeneration should be targeted. These are commonly but not limited to embryogenic tissues, which have a high regenerative capability (Christou, 1991). Subsequent to the first use of microprojectile acceleration by Sanford *et al.* (1987), Klein *et al.* (1987) successfully

introduced genes into the epidermal cells of onion. The leaf explants of tea and *Brassica rapa* were effectively transformed for β -glucuronidase (GUS) expression (Sandal *et al.*, 2015; Young *et al.*, 2008). GUS expression was also recorded with the biolistic-mediated transformation of shoot tip, hypocotyl and cotyledon of tomato (Ruma *et al.*, 2009). Besides intact leaf, shoot tip, hypocotyl and cotyledon, many other types of explants, such as somatic embryos (Pérez-Barranco *et al.*, 2007; Robertson *et al.*, 1992), zygotic embryos (Aulinger *et al.*, 2003; Fitch and Manshardt, 1990; Rochange *et al.*, 1995) and microspores (Carlson *et al.*, 2001; Shim and Kasha, 2003; Yao *et al.*, 1997) were successfully transformed via biolistics.

1.3.6.2 Components and Procedures

The instruments that are commonly used for biolistics is the Bio-Rad Helios[®] Gene Gun System (hereinafter referred as the gene gun), the Bio-Rad PDS-1000/He[™] Particle Delivery System (hereinafter referred as PDS) and the particle inflow gun (PIG).

The gene gun, which is a portable handheld device, allows for *in situ*, *in vitro*, *ex vivo* and *in vivo* experiments (**Figure 1.14**). The system can exert 100–600 psi pressure to propel DNA- or RNA-coated microcarriers to the external or exposed internal area of a target sample (Bio-Rad, n.d.). The components required for the operation of the gene gun are microcarriers, plastic tubing and the Helios unit. To operate the system, the DNA or RNA of interest is coated onto microcarriers, which are then coated along the inner surface of the plastic tubing. The plastic tubing is cut into small cartridges and one of the cartridges is loaded into the gene gun. The gun is fired when the trigger button on the gun is pressed, thereby releasing a helium wave through the gun barrel and brushing the

microcarriers off the inner surface of the cartridge. The microcarriers are propelled at high velocity into the target sample over an area of 2 cm² in diameter. The important parameters that affect the transformation efficiency are He pressure and the amount of gold used as microcarriers (Helenius *et al.*, 2000). Besides the He pressure and the amount of gold, the amount of DNA and the size of gold particle could also affect the level of transgene expression, based on a study of transient expression of synthetic *gfp* in rice callus (Carsono and Yoshida, 2008). Biolistic delivery of plasmid DNA using the gene gun has been used to introduce genes into explants that could not be infiltrated efficiently by *Agrobacterium*, such as the leaf tissue of *Arabidopsis* (Komori *et al.*, 2007).



Figure 1.14 The Helios[®] Gene Gun System. Adapted from Bio-Rad Bulletin 5443 (n.d.).

The PDS is a benchtop instrument, which is suitable for *in vitro*, *ex vivo* and *in vivo* experiments. Apart from the benchtop instrument, the system requires a vacuum pump, He gas, rupture disk, macrocarrier, microcarrier and stopping screen to operate (Bio-Rad, n.d.). **Figure 1.15** illustrates the components of the PDS apparatus. The target sample is first

placed in the bombardment chamber, where the chamber pressure is then reduced using the vacuum pump. When the instrument is fired, the He gas is directed through the gas acceleration tube and is held by the rupture disk until the specific pressure is achieved. Upon bursting, the rupture disk gives way to a sudden wave of He, which drives the macrocarrier that is carrying the DNA-coated microcarriers. The macrocarrier travels a short distance before being retained by the stopping screen, which only allows the microcarriers to pass through at a high velocity to penetrate the target cells up to an area of 40 cm² in diameter.

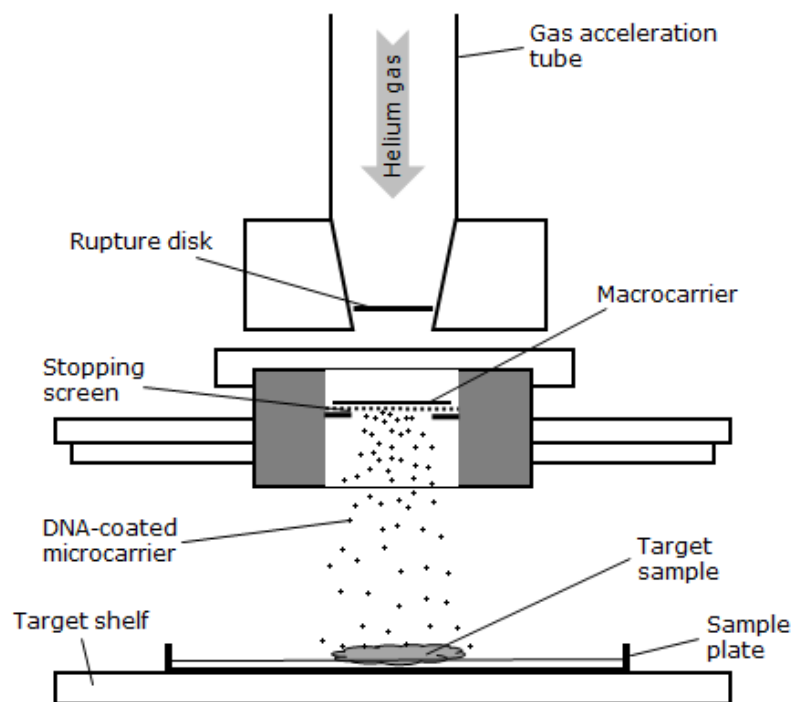


Figure 1.15 Schematic diagram of the components of a biolistic apparatus for the direct delivery of foreign DNA into target sample (Original).

The applications of PDS are strongly influenced not only by biological factors, such as the type of explants or plant species, the state of growth of target tissues, the expression vector and the osmotic condition of the bombardment medium, but also by physical factors, such as the He

pressure, distance between the stopping screen and the explant (target distance), the size of microcarriers, chamber vacuum and the amount of DNA used (Heiser, n.d.; Jain *et al.*, 1996; Sanford *et al.*, 1993). For example, Jain and co-workers (1996) reported improvement in the biolistic procedure in their study of rice embryogenic suspension cells with the use of the strong rice actin 1 gene (Act1) promoter, incubation of cells on medium supplemented with osmoticum (0.25 M mannitol) for 24 h before bombardment and using a high agarose concentration in the regeneration medium. For *Eucalyptus globulus* (a gum tree), six-day old embryos in culture were reported to be the best target material for bombardment (Rochange *et al.*, 1995). The transformation rate of cotyledons, zygotic embryos and meristemic shoot tips of common bean (*Phaseolus vulgaris* L.) was increased when the target tissues were pre-treated in medium containing 0.15–0.25 M mannitol and 0.15–0.25 M sorbitol, the target distance was 4 cm, 1.6 µm gold particles were coated with large amount of DNA and the bombardment was performed twice at 2000 psi (Zhang *et al.*, 1996). In another study of GUS expression in oil palm embryogenic calli, transformation by biolistics was performed using 300 mg of gold microcarriers coated with 1.5 mg of DNA. Enhancement of GUS expression was observed when calli were placed on medium containing 0.4 M mannitol 2 h prior to bombardment (Parveez *et al.*, 1998). For matured leaf explants of *Brassica rapa*, the optimised parameters were 900 psi He pressure, 3 cm target distance and bombardment of the explants once with 1 mg of DNA (Young *et al.*, 2008). Physical parameters of 6 cm target distance and 900 psi He pressure were reported to be the best for the transient GUS expression in leaves and hypocotyls of *C. annuum*. In addition, the use of He gas resulted in higher expression than nitrogen gas (Rizwan *et al.*, 2014).

The PIG (**Figure 1.16**) was developed by Finer and co-workers (1992) to accelerate DNA-coated particles using pressurised He in partial vacuum like the PDS system, but the particles are directly accelerated in the He stream through a syringe filter instead of being held by a macrocarrier (Vain *et al.*, 1993). DNA-coated particles are loaded in the centre of the screen of a disassembled syringe filter and the syringe filter is then reassembled and then tightened onto the Luer-lock adaptor. The target sample is placed on the adjustable shelf at a specific distance from the screen of the syringe filter. Activation of the solenoid by the timer relay would release He to discharge the particles.

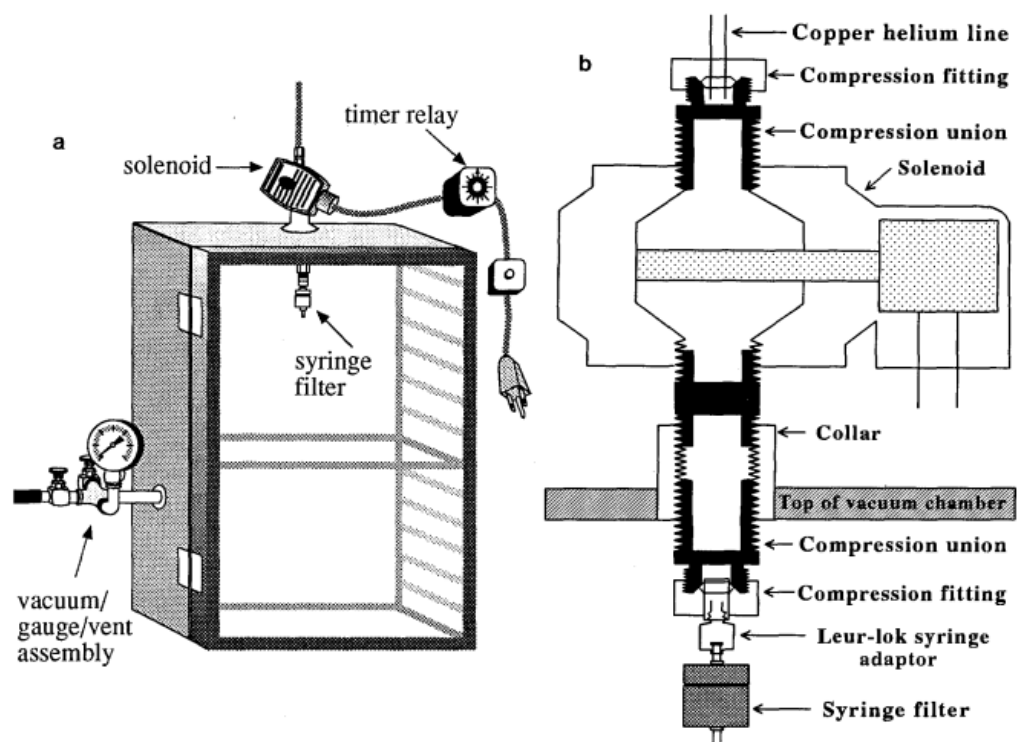


Figure 1.16 Schematic diagram of (a) the particle inflow gun and (b) connections from the copper helium line to the syringe filter in the bombardment chamber. Adapted from Finer *et al.* (1992).

PIG bombardment of the embryogenic suspension cultures of maize and soybean, and leaf tissue of cowpea achieved high transient expression

of GUS and stable expression with maize and soybean (Vain *et al.*, 1993). Using the same DNA delivery method, leaf, callus and anther cultures of tobacco, alfalfa, barley and apple were transformed with transient GUS expression. With an improved PIG protocol, higher levels of expression were achieved in scutellum-derived embryos of rice, maize, barley and wheat (Abumhadi *et al.*, 2001). Herbicide-resistant plants of bahiagrass (*Paspalum notatum*) with GUS reporter was produced with the integration of 1–5 copies of the *gus* gene in a transformant (Gondo *et al.*, 2005). Stable transgenic lines of hygromycin-resistant calli of halophyte *Kosteletzkya virginica* was also produced using the PIG method (Li and Gallagher, 1996).

1.3.6.3 Advantages

The general advantages of biolistics as a means of direct transformation are short handling time and high efficiency. Although numerous factors could affect the performance of a biolistic system (as described in **subchapter 1.3.6.2**) and should be optimized prior to the actual application, the transformation protocol is relatively simple once the important parameters have been optimized. With the use of biolistics, various transformation frequencies have been reported for soybean (9%), common bean (2.7%) and cotton (0.55%) (Rech *et al.*, 2008). Transformation frequency was calculated as a percentage of the number of transgenic explants recovered out of the total number of explants being bombarded. The transformation of two species of orchid, *Dendrobium phalaenopsis* and *Dendrobium nobile*, with a *uidA* gene and hygromycin resistance gene respectively produced 12% and 2% of transgenic plants from the bombarded calli or protocorm-like bodies (Men *et al.*, 2003).

Transformation of *C. annuum* L. cv. Mathiana with the *uidA* gene gave up to 4% of stable transformation frequency (Rizwan *et al.*, 2014). Biolistic co-bombardment of Chardonnay (*Vitis vinifera*) with a selectable marker and an antimicrobial peptide achieved up to 56% transformation frequency with confirmed expression (Vidal *et al.*, 2003). As a comparison with *Agrobacterium*-mediated transformation, the transformation of the immature embryos of maize (*Zea mays*) with *A. tumefaciens* achieved frequencies of 5–30% (Ishida *et al.*, 1996). Transformation of rice scutellum-derived calli co-cultivated with *A. tumefaciens* gave 10–30% transformation efficiency (Hiei *et al.*, 1994). A study of the phosphomannose-isomerase gene (*pmi*) as a selectable marker in maize using *Agrobacterium*-mediated transformation revealed transformation frequencies up to 30% (Negrotto *et al.*, 2000). A study of the same *pmi* selectable marker in maize and wheat (*Triticum aestivum*) using biolistics gave transformation frequencies of 45% and 20%, respectively (Wright *et al.*, 2001).

Due to its direct penetration nature, the biolistic method can be used as a delivery system for almost all plant species and organized tissues, depending on the competency of the cells for foreign DNA uptake and subsequent regeneration. In this sense, the biolistic approach is advantageous over the commonly used *Agrobacterium* method that relies on bacteria-host specificity, which limits their scope of use (Christou, 1991). Besides that, biolistics is useful not only for nuclear but also for transformation of organelles, such as mitochondria and plastids, because the delivery of microparticles into the subcellular compartments of target cells is not specific (Husaini *et al.*, 2010). The use of carrier DNA or binary vectors is not required because biolistics does not rely on extraneous genes or proteins for the localization of transgenes into the genome. In addition,

co-transformation of multiple plasmids into multiple cellular compartments is possible via biolistics. For example, Elghabi and co-workers (2011) demonstrated that particles that are coated with both nuclear and plastid transformation vectors resulted in co-transformation of the nucleus and chloroplast. However, individually coating the vectors onto the particles did not co-transform the organelles. It was also demonstrated that biolistics could be used to deliver linear DNA fragments of *npt-II* selectable marker and *MSI99* antimicrobial peptide genes into grapevine (Vidal *et al.*, 2006). In another study, linear DNA carrying the HMW-GS 1Dx5 gene was successfully introduced into a common wheat variety to improve the quality of bread-making flour (Qin *et al.*, 2014).

1.3.6.4 Limitations

A few major limitations that were identified with the use of biolistics are the shallow penetration of particles and associated cell damage if inappropriate particle size, bombardment pressure or target distance is used (Husaini *et al.*, 2010). Smaller particle size is known to minimise damage to small cells. Therefore, nano-biolistics, which uses particles as small as 40 nm, is now available as an alternative to the conventional 0.6–1.6 µm microparticles (O'Brien and Lummis, 2011). In a study of immature maize embryos, it was found that high bombardment pressure and short target distance caused excessive tissue damage, which could be prevented with the supplementation of mannitol in the culture medium pre- and post-bombardment (Kemper *et al.*, 1996). Besides that, multiple bombardments on the same tissue have been shown to increase or decrease transient expression (Janna *et al.*, 2006; Klein *et al.*, 1988).

Unlike *Agrobacterium*-mediated transformation, the biolistic method is yet to be used to deliver DNA systemically because the DNA entry into cells is difficult to control (Luo and Saltzman, 2000). In addition, the transgene is not protected and is therefore susceptible to nuclease activity, unlike the T-DNA of *A. tumefaciens* that is protected by the VirD2 protein (Gelvin, 2000; Zupan *et al.*, 2000). It is also difficult to obtain single copy transgenic events. Transformants from a biolistic method usually take in multiple copies of the transgene into their nuclear genome (Sodiende and Kindle, 1993). Different copy numbers could result in differences in the expression level. In this regard, high copy number does not always correspond to high expression level. The occurrence of multiple copies of a foreign gene could trigger post-transcriptional gene silencing in the host cell, which in turn could lead to the loss of expression (Matzke *et al.*, 1994; Tang *et al.*, 2007; Vaucheret *et al.*, 1998). Due to random integration of genes delivered by biolistics into the host genome, there is also high possibility of DNA getting inserted into a functional gene (Husaini *et al.*, 2010).

CHAPTER 2

GENERAL MATERIALS AND METHODS

Table 2.1 provides a list of materials used throughout the study (in alphabetical order) and their respective producers, unless stated otherwise. The specific brands of the consumables or kits that are not mentioned here are described, where relevant, in the subsequent chapters.

Table 2.1 The list of materials used and their respective producers.

Material	Producer
<i>Chemicals</i>	
Acetic acid, glacial	R&M Chemicals
Calcium chloride (CaCl ₂)	Sigma-Aldrich
Chloroform	Sigma-Aldrich
Diethyl pyrocarbonate (DEPC)	Sigma-Aldrich
Ethanol, 100%	R&M Chemicals
Ethylenediaminetetraacetic acid (EDTA)	Sigma-Aldrich
Glycerol	System
Hydrochloric acid (HCl), 37%	Sigma-Aldrich
Isopropanol, 99.7%	R&M Chemicals
Lithium chloride (LiCl)	Sigma-Aldrich
Methanol, 99.7%	R&M Chemicals
Phenol-chloroform-isoamyl alcohol (25:24:1)	Fluka
Polyethylene glycol (PEG) 7500 / 8000	Fluka
Potassium acetate (KOAc)	Sigma-Aldrich
Sodium dodecyl sulphate (SDS)	Sigma-Aldrich
Sodium chloride (NaCl)	Sigma-Aldrich
Sodium acetate (NaOAc)	Sigma-Aldrich
Sodium hydroxide (NaOH)	Fisher Scientific
Spermidine, 99%	Sigma-Aldrich
Tris base	R&M Chemicals
Triton X-100	Bio Basic Inc.
Tween-20	Sigma-Aldrich
TRIzol [®] Reagent	Thermo Fisher Scientific
<i>Culture media</i>	
1-naphthaleneacetic acid (NAA)	Duchefa Biochemie
2,4-dichlorophenoxyacetic acid (2,4-D)	Duchefa Biochemie
6-benzylaminopurine (BAP)	Duchefa Biochemie

Indole-3-acetic acid (IAA) Indole-3-butyric acid (IBA) Glucose Kinetin Lysogeny broth (LB) solid / liquid medium Murashige & Skoog (MS) basal salt with vitamins Phytigel™ Sucrose Super optimal broth (SOB)	Duchefa Biochemie Duchefa Biochemie Fisher Scientific Duchefa Biochemie Becton-Dickinson PhytoTechnology Laboratories Sigma-Aldrich Fisher Scientific Becton-Dickinson
<u>PCR / qPCR reagents</u> dNTPs mix PCR primers <i>Pfx50</i> ™ DNA Polymerase qPCR master mix Recombinant <i>Taq</i> DNA polymerase UltraPure™ DNase/RNase-free distilled water	Invitrogen Integrated DNA Technologies Invitrogen KAPA Biosystems Invitrogen Invitrogen
<u>Gel electrophoresis reagents, DNA / RNA ladders</u> 1 kb DNA ladder 100 bp DNA ladder 2× RNA loading dye 6× DNA loading dye 10× Tris-borate-EDTA (TBE) buffer 50× Tris-acetate-EDTA (TAE) buffer Agarose High range RNA ladder SYBR® Safe DNA gel stain, 10,000× concentrate in dimethyl sulfoxide (DMSO)	Fermentas Fermentas Fermentas Fermentas Thermo Fisher Scientific Thermo Fisher Scientific 1 st Base Fermentas Invitrogen
<u>Restriction / ligation enzymes</u> <i>Age</i> I* <i>Bam</i> HI* <i>Bsm</i> BI <i>Bbs</i> I* <i>Pst</i> I* <i>Pvu</i> I* T4 DNA ligase	New England Biolabs New England Biolabs New England Biolabs New England Biolabs New England Biolabs New England Biolabs New England Biolabs
*High fidelity enzymes	
<u>Antibiotics</u> Ampicillin Blasticidin S (BS) Chloramphenicol Kanamycin	Sigma-Aldrich Thermo Fisher Scientific Duchefa Biochemie Duchefa Biochemie
<u>Kits</u> Consumables for biolistics Gateway® cloning kit PCR and gel purification kit Plasmid purification kit Reverse transcription kit	Bio-Rad Invitrogen GeneAll GeneAll Qiagen
<u>HPLC reagents / consumables</u> 0.45 µm nylon membrane disk filter 0.45 µm nylon syringe filters 1.0 ml syringes 2.0 ml vials with polytetrafluoroethylene (PTFE)/silicone caps	Thermo Fisher Scientific Thermo Fisher Scientific Sartorius Stedim Fisher Scientific

Acetic acid, glacial	Fisher Scientific
C18 analytical column	Thermo Fisher Scientific
Capsaicin standard, 99%	Sigma-Aldrich
Column guard cartridge & cartridge holder	Thermo Fisher Scientific
Ethanol (HPLC-grade)	Fisher Scientific
Ferulic acid standard, 99%	Acros
Methanol (HPLC-grade)	Fisher Scientific
Vanillic acid standard, 97%	Sigma-Aldrich
Vanillin standard, 99%	Acros
Vanillin- β -D-glucoside standard, 99%	Santa Cruz Biotechnology
Whatman [®] 1 filter paper	GE Healthcare
<i>Other general plastic wares</i>	
0.2 μ m nylon syringe filters	Sartorius Stedim
1.5 ml microcentrifuge tubes	Labcon
2.0 ml microcentrifuge tubes	Labcon
10.0 ml luer-lock syringes	Sartorius Stedim
50.0 ml centrifuge tubes	Labcon
PCR tubes	Labcon
Petri dishes	Brandon

2.1 STANDARD REAGENTS

The standard reagents prepared for the experiments in the subsequent chapters / subchapters are listed below. The reagents, except those that were sterilised using 0.2 μ m syringe filters (Sartorius Stedim, France), were sterilised using steam autoclave for 15 min at 121°C and 15 psi.

Water (H₂O): The H₂O used for the preparation of reagents was double distilled to the purity of at least 15 M Ω , unless stated otherwise.

1 M HCl: A 1 M stock of HCl solution was prepared by mixing 8.21 ml of concentrated HCl with 91.79 ml of H₂O.

1 M NaOH: A 1 M stock of NaOH solution was prepared by dissolving 4 g of NaOH pellets in 50 ml of H₂O and then adding H₂O to a final volume of 100 ml.

1 M Tris-Cl (pH 8.0): A 1 M stock of Tris-Cl solution was prepared by dissolving 6.06 g of Tris base in 40 ml of H₂O, adjusting the pH to 8.0 using HCl and then adding H₂O to bring the final volume to 50 ml.

1 M Tris-Cl (pH 7.5): A 1 M stock of Tris-Cl solution was prepared by dissolving 6.06 g of Tris base in 40 ml of H₂O, adjusting the pH to 7.5 using HCl and then adding H₂O to bring the final volume to 50 ml.

0.5 M EDTA: A 0.5 M stock of EDTA solution was prepared by dissolving 9.31 g of EDTA disodium salt in 40 ml of H₂O and then adding H₂O to bring the final volume to 50 ml.

10% (w/v) SDS: A 10% (w/v) stock of SDS solution was prepared by dissolving 5 g of SDS powder in 40 ml of H₂O and then adding H₂O to bring the final volume to 50 ml.

0.5 M NaCl: A 0.5 M stock of NaCl solution was prepared by dissolving 4.38 g of NaCl powder in 100 ml of H₂O and then adding H₂O to bring the final volume to 150 ml.

3 M NaOAc: A 3 M stock of NaOAc was prepared by dissolving 2.46 g of NaOAc powder in 5 ml of H₂O and then adding H₂O to bring the final volume to 10 ml.

2.5 M CaCl₂: A 2.5 M stock of CaCl₂ was prepared by dissolving 2.77 g of CaCl₂ powder in 5 ml of H₂O and then adding H₂O to bring the final volume to 10 ml. The CaCl₂ solution was sterilised by filtration using a 0.2 µm syringe filter.

0.1 M spermidine: A 0.1 M stock of spermidine was prepared by dissolving 29 mg of spermidine powder in 1 ml of H₂O and then adding H₂O to bring the final volume to 2 ml. The spermidine solution was sterilised by filtration using a 0.2 µm syringe filter.

Plasmid purification solution 1 (PPS1) – Resuspension buffer: 0.45 g of glucose powder was dissolved in 40 ml of H₂O. Then, 1.25 ml of 1 M Tris-Cl (pH 8.0) and 1 ml of 0.5 M EDTA was added into the solution. H₂O

was added to make 50 ml of PPS1, followed by filtration using a 0.2 µm syringe filter. The final concentrations were 25 mM Tris-Cl, 10 mM EDTA and 50 mM dextrose.

Plasmid purification solution 2 (PPS2) – Lysis buffer: 10 ml of 1 M NaOH was mixed with 5 ml of 10% (w/v) SDS and H₂O to make 50 ml of PPS2, followed by filtration using a 0.2 µm syringe filter. The final concentrations were 0.2 M NaOH and 1% (w/v) SDS.

Plasmid purification solution 3 (PPS3) – Neutralisation buffer: 5 M of KOAc was first prepared by dissolving 29.44 g of KOAc powder in 30 ml of H₂O, and then adding H₂O to a final volume of 60 ml. The KOAc solution was supplemented with 11.5 ml of glacial acetic acid and 28.5 ml of H₂O to make 100 ml of PPS3, followed by filtration using a 0.2 µm syringe filter.

Plant callus DNA extraction buffer: 50 ml of 1.0 M Tris-Cl (pH 7.5), 125 ml of 0.5 M NaCl, 12.5 ml of 0.5 M EDTA and 12.5 ml of 10% SDS were mixed with 50 ml H₂O to make 250 ml of plant callus DNA extraction buffer, followed by filtration using a 0.2 µm syringe filter. The final concentrations were 200 mM Tris-Cl, 250 mM NaCl, 25 mM EDTA and 0.5% SDS.

Tris-EDTA (TE) buffer: 500 µl of Tris-Cl (pH 8.0) and 100 µl of 0.5 M EDTA (pH 8.0) were mixed with H₂O to make 50 ml of TE buffer, followed by filtration using a 0.2 µm syringe filter. The final concentrations were 10 mM Tris-Cl and 1 mM EDTA.

2.2 PLANT TISSUE CULTURE

2.2.1 Plant Materials

The seeds of *C. frutescens* L. cv. Skyrocket, cv. Full Sky and cv. Hot Lava (Green World Genetics Pt. Ltd., Malaysia) were germinated *in vitro* after being surface sterilized using the procedure optimised in **chapter 3**. The cultivar with the highest germination rate and the lowest infection rate was used for the subsequent plant tissue culture experiments in **chapters 3 and 5**.

2.2.2 Tissue Culture Media

Full-strength MS medium was used throughout all plant tissue culture experiments in chapters 3 and 5. For 1 L of the medium, 4.42 g of MS basal salt with vitamins (formulation is specified in **appendix A**) was dissolved in 800 ml of H₂O. Then, 30 g of sucrose was added into the solution under constant stirring. After the MS salt and the sucrose were all dissolved, the pH of the solution was adjusted to pH 5.8 (± 0.02) using 1 M NaOH. The final volume of the solution was adjusted to 1 L. To prepare agar medium, 3.5 g of gelling agent (Phytigel™ by Sigma-Aldrich, USA) was added and the media was sent for autoclaving prior to pouring into sterile culture vessels. This medium is hereinafter referred as MS medium.

2.2.3 Plant Growth Regulators / Hormones

The auxins used were 2,4-dichlorophenoxyacetic acid (2,4-D), indole-3-acetic acid (IAA), indole-3-butyric acid (IBA) and 1-naphthaleneacetic acid (NAA). The cytokinins used were 6-benzylaminopurine (BAP) and kinetin.

Stock concentration of 1 mg/ml was first prepared for each of the plant growth regulators used. For 2,4-D and IAA sodium salt, 100 mg of the growth regulator was dissolved in 100 ml of H₂O. For IBA, NAA, BA and kinetin, 100 mg of the growth regulator was first dissolved in some 1N NaOH solution before H₂O was added to make a final volume of 100 ml. The final solutions were sterilized using a 0.2 µm syringe filter.

2.2.4 Antibiotics

Blasticidin S (BS) (Thermo Fisher Scientific, USA) and kanamycin (Duchefa Biochemie, The Netherlands) were used in the MS media for the selection of transformed *C. frutescens* cultures. A 5 mg/ml stock of BS solution was prepared by dissolving 50 g of BS powder in 8 ml of H₂O and then adding H₂O to a final volume of 10 ml. A 50 mg/ml stock of kanamycin solution was prepared by dissolving 0.5 g of kanamycin powder in 8 ml of H₂O and then adding H₂O to a final volume of 10 ml. The stocks of antibiotics were separately filter sterilized using a 0.2 µm syringe filter, transferred into aliquots of 1 ml and stored at -20°C when not in use.

2.2.5 Plant Culture Incubation Conditions

In the tissue culture room, all of the plant cultures were maintained in 16 h light/8 h dark photoperiod with 40 µmol m⁻² s⁻¹, (or 2960 lux) light intensity from cool white fluorescent lamps. The temperature and humidity of the room was kept at approximately 24°C and 42%, respectively.

2.3 BACTERIAL CULTURE

2.3.1 Bacterial Strains and Plasmids

Three bacterial strains of chemically competent *E. coli* were used for the propagation of plasmids. The strains and genotypes of the *E. coli* used in **chapter 4** are listed in **Table 2.2**.

Table 2.2 The list of *E. coli* strains used and their respective genotypes.

<i>E. coli</i> strain	Genotype	Source
One Shot [®] <i>ccdB</i> Survival [™] 2 T1 ^R	F ⁻ <i>mcrA</i> Δ(<i>mrr-hsdRMS-mcrBC</i>) Φ80 <i>lacZ</i> ΔM15 Δ <i>lacX74</i> <i>recA1</i> <i>ara</i> Δ139 Δ(<i>ara-leu</i>)7697 <i>galU</i> <i>galK</i> <i>rpsL</i> (Str ^R) <i>endA1</i> <i>nupG</i> <i>fhuA::IS2</i>	Invitrogen, Thermo Fisher Scientific, USA
One Shot [®] Mach1 [™] T1 ^R	F ⁻ φ80(<i>lacZ</i>)ΔM15 Δ <i>lacX74</i> <i>hsdR</i> (r _K ⁻ m _K ⁺) Δ <i>recA</i> 1398 <i>endA1</i> <i>tonA</i>	Invitrogen, Thermo Fisher Scientific, USA
One Shot [®] TOP10	F ⁻ <i>mcrA</i> Δ(<i>mrr-hsdRMS-mcrBC</i>) Φ80 <i>lacZ</i> ΔM15 Δ <i>lacX74</i> <i>recA1</i> <i>ara</i> Δ139 Δ(<i>ara-leu</i>)7697 <i>galU</i> <i>galK</i> <i>rpsL</i> (Str ^R) <i>endA1</i> <i>nupG</i>	Invitrogen, Thermo Fisher Scientific, USA

The plasmids (individually referred as transformation vectors or holding vectors) used in **chapters 4–5** and their respective components are listed in **Table 2.3**.

Table 2.3 The list of plasmids used and their components.

Plasmid	Component	Source
pcDNA [™] 6.2/V5-pL- DEST transformation vector (abbreviated as the pcDNA6.2)	<ul style="list-style-type: none"> • T7 promoter/priming site • <i>attR1</i> and <i>attR2</i> sites • <i>ccdB</i> gene • Chloramphenicol acyltransferase gene (<i>cat</i>) for chloramphenicol resistance • V5 epitope • V5 reverse priming site • Herpes simplex virus thymidine kinase polyadenylation signal (TK pA) • f1 origin • SV40 early promoter and origin 	Invitrogen, Thermo Fisher Scientific, USA

	<ul style="list-style-type: none"> • EM7 promoter • Blasticidin S deaminase gene (<i>bsd</i>) for BS resistance • SV40 early polyadenylation signal • pUC origin • Beta-lactamase gene (<i>bla</i>) for ampicillin resistance 	
HBT-sGFP(S65T)-NOS transformation vector (abbreviated as the HBT)	<ul style="list-style-type: none"> • 35S promoter • synthetic (enhanced) green fluorescent protein gene (<i>sgfp</i>) • Beta-galactosidase gene (<i>lac</i>) • <i>lac</i> promoter • <i>bla</i> gene • M13 forward priming site • M13 reverse priming site • NOS terminator 	J. Sheen Laboratory, USA
pHBT12K transformation vector	<ul style="list-style-type: none"> • <i>attR1</i> and <i>attR2</i> sites • <i>ccdB</i> gene • Chloramphenicol resistance gene (<i>cat</i>) • synthetic (enhanced) green fluorescent protein gene (<i>sgfp</i>) • Beta-galactosidase gene (<i>lac</i>) • <i>lac</i> promoter • <i>bla</i> gene • M13 forward priming site • M13 reverse priming site • NOS terminator 	Modified from HBT vector (Leong, 2015)
pUCIDT- <i>fcs</i> holding vector	<ul style="list-style-type: none"> • <i>attB5</i> and <i>attB4</i> sites • <i>fcs</i> gene • <i>lac</i> promoter • <i>lac</i> operator • <i>bla</i> promoter • <i>bla</i> gene • pUC origin 	
pUCIDT- <i>ech</i> holding vector	<ul style="list-style-type: none"> • <i>attB4r</i> and <i>attB3r</i> sites • <i>ech</i> gene • <i>lac</i> promoter • <i>lac</i> operator • <i>bla</i> promoter • <i>bla</i> gene • pUC origin 	Integrated DNA Technologies, Singapore
pUCIDT- <i>VpVAN</i> holding vector	<ul style="list-style-type: none"> • 35S promoter • <i>VpVAN</i> gene • <i>lac</i> promoter • <i>lac</i> operator • <i>bla</i> promoter • <i>bla</i> gene 	

	<ul style="list-style-type: none"> • pUC origin 	
pUCIDT-NOSp holding vector	<ul style="list-style-type: none"> • <i>attB4r</i> and <i>attB3r</i> sites • NOS promoter • <i>lac</i> promoter • <i>lac</i> operator • <i>bla</i> promoter • <i>bla</i> gene • pUC origin 	

2.3.2 Bacterial Culture Media

Difco™ LB solid medium, Lennox (Becton Dickinson, USA) was used for the solid culture of *E. coli* colonies. For every litre of LB solid medium, 35 g of the agar powder was suspended in H₂O and was sent for autoclaving at 121°C, 15 psi for 20 min prior to pouring into Petri dishes. Each litre of LB agar contained 10 g of tryptone, 5 g of yeast extract, 5 g of NaCl and 15 g of agar.

Difco™ LB liquid medium, Lennox (Becton Dickinson, USA) was used for the liquid culture of *E. coli*. For every litre of LB liquid medium, 20 g of the broth powder was suspended in H₂O, sent for autoclaving and cooled to room temperature prior to pouring into sterile centrifuge tubes or Erlenmeyer flasks. The LB broth consisted of the same ingredients as the LB agar, but without the agar.

Super optimal broth with catabolite repression (SOC) medium was used for the recovery of *E. coli* during transformation. SOC medium was prepared from the Difco™ SOB (Becton Dickinson, USA). For every litre of SOB, 28 g of SOB powder was suspended in H₂O, sent for autoclaving and cooled to room temperature. To make SOC medium, 20 ml of filter-sterilized 20% (w/v) glucose solution was added prior to use.

2.3.3 Antibiotics

Ampicillin, kanamycin and chloramphenicol were used in the LB agar or LB broth for the selection of transformed *E. coli*. A 100 mg/ml stock of ampicillin solution was prepared by dissolving 1 g of ampicillin powder in 8 ml of H₂O and then adding H₂O to a final volume of 10 ml. A 50 mg/ml stock of kanamycin solution was prepared by dissolving 0.5 g of kanamycin powder in 8 ml of H₂O and then adding H₂O to a final volume of 10 ml. A 20 mg/ml stock of chloramphenicol solution was prepared by dissolving 0.2 g of chloramphenicol powder in ethanol and then adding H₂O to a final volume of 10 ml. The stocks of antibiotics were separately filter sterilized using a 0.2 µm syringe filter, transferred into aliquots of 1 ml and stored at -20°C when not in use. To prepare antibiotic selective media for bacteria, the antibiotic stocks were pipetted aseptically into molten LB media to a final concentration of 100 mg/l ampicillin, 50 mg/l kanamycin and 20 mg/l chloramphenicol.

2.3.4 Bacterial Culture Incubation Conditions

Agar cultures of *E. coli* were incubated at 37°C for 16 h with the Petri dishes inverted to prevent condensation (if any) from falling into cultures. Liquid cultures of *E. coli* were incubated in an incubator shaker (New Brunswick™ Innova® 42, Eppendorf, Germany) at 37°C and 220 rpm for 16 h.

2.4 POLYMERASE CHAIN REACTION (PCR)

2.4.1 PCR Reagents

PCR stock reagents, which consisted of 10× PCR buffer (200 mM Tris-HCl pH 8.4, 500 mM potassium chloride, KCl), 50 mM magnesium chloride (MgCl₂), 10 mM deoxynucleotides (dNTPs) and 1 unit of recombinant *Taq* polymerase, were obtained from Invitrogen (Thermo Fisher Scientific, USA). The PCR reagents were stored at -20°C when not in use. In the preparation for PCR, the UltraPure™ DNase/RNase-free distilled water (Invitrogen, Thermo Fisher Scientific, USA) was used as the universal diluent.

A standard PCR reaction tube for screening purposes contained the final concentrations, unless stated otherwise, 1× PCR buffer, 1.5 mM MgCl₂, 0.3 mM dNTPs, 0.3 μM forward and reverse primers (Integrated DNA Technologies, Singapore), 1 unit of recombinant *Taq* polymerase (Invitrogen, Thermo Fisher Scientific, USA) and 50 ng of template genomic DNA or 1 ng of template plasmid DNA. For vector construction, *Pfx50*™ DNA Polymerase and *Pfx50*™ PCR buffer (Invitrogen, Thermo Fisher Scientific, USA), which contained MgSO₄ at a final 1× concentration of 1.2 mM bovine serum albumin (BSA), was used (no additional MgSO₄ was added, unless stated otherwise).

2.4.2 Thermal Cycling Programme

Generally, unless stated otherwise, the PCR thermal cycling was carried out as described in **Table 2.4**:

Table 2.4 A general PCR thermal cycling programme.

Number of cycle(s)	Thermal cycling step	Temperature (°C)	Holding time
1	Initial denaturation	95	3 min
25–30	Denaturation	95	30 s
	Annealing	Varied ¹	30 s
	Elongation	72 (68 for Pfx50™ DNA Polymerase)	Varied ²
1	Final elongation	72 (68 for Pfx50™ DNA Polymerase)	5 min

¹The temperature for the annealing step would be specified in the related methods in other chapters, which varied according to the primer sets used.

²The holding time for the elongation step would be specified in the related methods in other chapters, which varied according to the expected amplicon length.

2.5 AGAROSE GEL ELECTROPHORESIS

A stock of 50× TAE gel electrophoresis buffer was diluted to 1× working concentration (40 mM Tris, 20 mM acetic acid, 1 mM EDTA) with H₂O.

All DNA products, except those from RT-qPCR, were electrophoresed through a 1% (w/v) agarose gel. The agarose powder was dissolved in 1× TAE buffer using microwave heat and the resulting gel liquid was slightly cooled before being mixed with 10,000× SYBR[®] Safe DNA gel stain to a final 1× working concentration. The gel solution was then poured into a gel cast and cooled to room temperature for 30 min to 1 h. DNA and RNA products from RT-qPCR (Chapter 6) were electrophoresed through a 1.5% (w/v) agarose gel.

The typical amount of genomic DNA, product of PCR, or product of restriction digest that was loaded into gel was approximately 100–200 ng. If more than one band were to be separated in the gel, the amount of DNA to be loaded, w_{DNA} , in ng, was calculated based on the fragment of interest to be visualized, as follows:

$$\frac{\text{Size of fragment of interest, in bp}}{\text{Total size of DNA, in bp}} \times w_{DNA} = 100 \text{ ng}$$

Hence,

$$w_{DNA} = 100 \text{ ng} \times \frac{\text{Total size of DNA, in bp}}{\text{Size of fragment of interest, in bp}}$$

The DNA products were mixed with 6× DNA gel loading dye (10 mM Tris-HCl at pH 7.6, 0.03% bromophenol blue, 0.03% xylene cyanol FF, 60% glycerol, 60 mM EDTA) to bring the loading dye to 1× working concentration prior to loading into gel for electrophoresis. For dilution purposes, H₂O was added where necessary. The RNA products were mixed with 2× RNA loading dye (95% formamide, 0.025% SDS, 0.025% bromophenol blue, 0.025% xylene cyanol FF, 0.025% ethidium bromide, 0.5 mM EDTA) to bring the loading dye to 1× working concentration prior gel electrophoresis.

The DNA ladder used was GeneRuler 1 kb Plus DNA ladder (0.5 µg/µl, ready-to-use) and/or GeneRuler 100 bp Plus DNA ladder (0.5 µg/µl, ready-to-use), which were obtained from Thermo Fisher Scientific, USA. For DNA gel electrophoresis, 0.5 µg of the DNA ladder was loaded for every 5 mm of gel lane. The RNA ladder used was RiboRuler High Range RNA Ladder, ready-to-use (Thermo Fisher Scientific, USA). For RNA gel electrophoresis, 0.6 µg of the RNA ladder was loaded for every 5 mm of gel lane. Gel electrophoresis was performed with 1× TAE buffer at 5 V/cm gel length (typically 90 V) for 45 min (1% agarose gel) or 1 h (1.5% agarose gel).

2.6 QUANTIFICATION OF NUCLEIC ACIDS

All DNA and RNA products were quantified using the NanoDrop 1000 Spectrophotometer (Thermo Scientific, USA). Prior to the start of each measurement session, the instrument was initialised with 1 µl of H₂O

according to the instructions displayed. Then, a blank measurement was taken with the respective dilution buffer (without any nucleic acid) of each sample type. After that, the concentrations of nucleic acids were measured using 1 μ l of each sample. The absorbance of the samples was measured at 280 nm, 260 nm and 230 nm ultraviolet wavelengths. Any absorbance at 280 nm indicated the presence of contaminants that absorb at or near 280 nm, such as proteins. The concentrations of nucleic acids were determined from the absorbance at 260 nm, which was absorbed strongly by nucleic acids. Any absorbance at 230 nm indicated the presence of contaminants that absorb at or near 230 nm, such as EDTA, phenol and carbohydrates. The purity of the samples was determined from the measurement of 260 nm/280 nm and 260 nm/230 nm ratios. A 260 nm/280 nm ratio of \sim 1.8 was generally accepted as pure (free from protein contaminants) for DNA samples, while a 260 nm/280 nm ratio of \sim 2.0 was generally accepted as pure for RNA samples. A 260 nm/230 nm ratio in the range of 2.0–2.2 was deemed to be pure (free from EDTA, phenol and carbohydrate contaminants) for DNA and RNA samples. Values that were substantially lower than the expected ratios might indicate the presence of contaminants.

2.7 STATISTICAL ANALYSIS

All of the numerical data and statistical analyses in **chapters 3, 5 and 6** were performed with GenStat 17th Edition (v17.1.0.14713). The presented data are shown as mean \pm standard deviation (SD) of the mean, unless stated otherwise. The data were subjected to the analysis of variance (ANOVA) to test the hypotheses statistically at a significance level or p -value of 0.05. Where multiple comparisons were performed, Tukey's post hoc test of least significant difference (LSD) was used in the ANOVA.

CHAPTER 3

PLANT TISSUE CULTURE FOR THE CALLUS REGENERATION OF *CAPSICUM FRUTESCENS* L.

3.1 INTRODUCTION

Plant tissue cultures can be established under sterile environment with appropriate aseptic techniques to multiply tissues from explants, such as leaf discs, stem cuttings, roots and nodes, for the accumulation of secondary metabolites (Karuppusamy, 2009). Unlike primary metabolites, such as nucleotides, amino acids, and organic acids, secondary metabolites do not participate directly in normal plant growth and development. Secondary metabolites are produced for functions in plant defence or competition, or to contribute to the aesthetic nature of plant organs, such as flower and fruit colours, to make them attractive to pollinators and dispersers. Examples of plant secondary metabolites include alkaloids, terpenoids, flavonoids, polyketides, glycosides, and phenols (Gunatilaka, 2012). Interests in the secondary metabolites have led to the discovery of many natural products, such as drugs, dyes, glues, polymers, flavouring agents and perfumes (Croteau *et al.*, 2015). To elevate the production of useful plant secondary metabolites, various recombinant DNA techniques

are employed to upregulate, downregulate or modify the biosynthetic pathways of the target secondary metabolites. Many of the recombinant DNA techniques require effective protocols for plant regeneration alongside a plant transformation procedure (Ravishankar *et al.*, 2003). In this chapter, the optimisation of plant tissue culture procedures for the regeneration of callus culture to be used for secondary metabolite production is described.

3.1.1 Callus Regeneration in Chilli

For tissue culture regeneration, the productivity of cultures can be regulated or stimulated by controlling the microenvironmental regime (Lila, 2005). In some cases, production requires the generation of more differentiated plant or organ cultures, but many researchers have succeeded in producing myriad of valuable chemical compounds using unorganized calli or cell suspensions (Dörnenberg and Knorr, 1997). Besides that, extraction of compounds from unorganized tissues is much easier than extraction from complex, organized tissues of a plant (Karuppusamy, 2009). For example, a protocol was developed to induce callus for large scale capsaicin production from the placental explants of *C. annuum* L. (Umamaheswari and Lalitha, 2007). Besides that, a study of the extracts from *Capsicum chinense* Jacq. found small amounts of saponins, flavonoids, terpenoids and volatile oils, and moderate amount of phenols and alkaloids in the callus (Gayathri *et al.*, 2016). These studies demonstrated the capacity of various calli that were regenerated for the purpose of secondary metabolite production in chilli. Although chilli is an economically important crop, the regeneration of *in vitro* cultures of *Capsicum* has not been reproducible with consistent efficiency. Despite

these, many of the studies indicated the existence of limitations that are yet to be overcome on the tissue culture of *Capsicum*, which was explored in the following experiments in this chapter.

3.1.2 Specific Objectives

This chapter focuses on the regeneration of sterile callus cultures of *C. frutescens* L. cv. Hot Lava. The specific objectives to be achieved include: (i) establishing sterile culture from the seeds of *C. frutescens* by examining the effects of different chilli cultivars and different concentrations of sterilising agent on the germination and infection rates, (ii) establishing an optimal hormone composition for callus regeneration from cotyledon, hypocotyl and root explants of the selected cultivar of *C. frutescens*, and (iii) determining the best explants from cotyledon, hypocotyl and root explants for high callus proliferation for the subsequent transformation studies (as reported in **chapters 5 and 6**).

3.2 MATERIALS AND METHODS

3.2.1 Surface Sterilisation of Seeds of *C. frutescens*

To establish sterile cultures of *C. frutescens*, the seeds of *C. frutescens* L. cv. Skyrocket, cv. Full Sky, and cv. Hot Lava (as described in **subchapter 2.2.1**) were surface sterilised in the laminar flow cabinet. They were soaked in 70% (v/v) denatured ethanol for 5 min and washed with sterile distilled water for 5 min. Then, the seeds were transferred into 5%, 10%, 15% and 20% (v/v) commercial bleach (Clorox, USA, containing 5.25% sodium hypochlorite, NaOCl, in undiluted stock) for 20 min. The process

was continued with washing in sterile distilled water for 10 min, followed by another wash for 5 min. The seeds were then left to dry on sterile Scott® C-fold Towels (Kimberly-Clark, USA) in the laminar flow cabinet for at least 30 min before being transferred into Petri dishes containing Murashige and Skoog (MS) media for germination. To examine the effect of the surface sterilisation procedure on seed germination, the number of seeds germinated was counted over a period of 25 days. Observation was stopped after there was no increase in number of seeds germinated for three consecutive days. To examine the effectiveness of the surface sterilisation protocol in establishing sterile samples, the number of seeds showing any emergence of microbe infection was also recorded.

For infected seeds, the colony morphology of microbes in a Petri dish could be characterised by visual observation of the form (circular, irregular, filamentous or rhizoid), size (measured by diameter or referred as punctiform for very small colonies, less than 1 mm), margin/border (entire, filiform, curled, undulate or lobate), elevation (raised, convex, flat, umbonate or crateriform), surface (smooth, glistening, rough, dull or wrinkled), opacity/density (transparent, translucent or opaque), and colour (**Figure 3.1**) (Manuselis, 2011; Vasanthakumari, 2007). The colony density could be characterised as transparent, translucent or opaque (example as shown in **figure 3.2**).

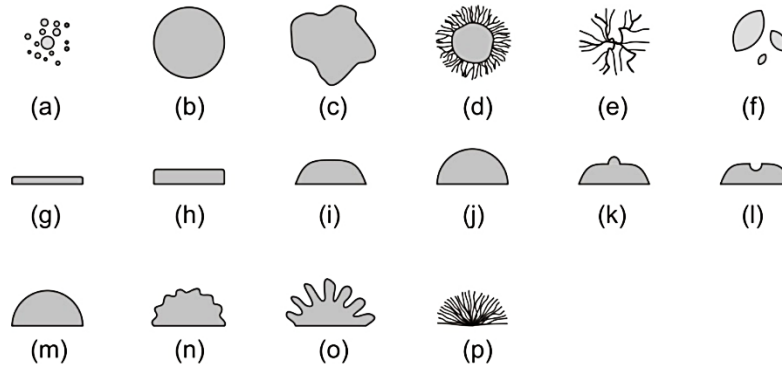


Figure 3.1 Illustration of various colony morphologies of bacteria or fungi with regards to: Form: (a) punctiform, (b) circular, (c) irregular, (d) filamentous, (e) rhizoid, (f) spindle; Elevation: (g) flat, (h) raised, (i) convex, (j) pulvinate, (k) umbonate, (l) crateriform; Margin: (m) entire, (n) undulate, (o) lobate, (p) filiform. Adapted from http://ttktamop.elte.hu/online-tananyagok/practical_microbiology/ch06s04.html.

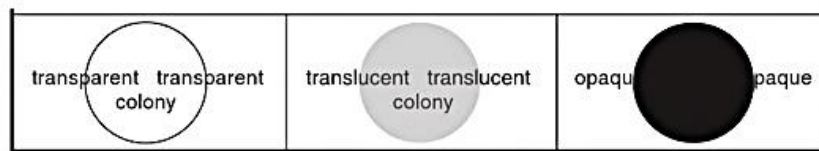


Figure 3.2 Illustration of colony density. Left: transparent or clear – agar beneath the colony can be seen clearly; Middle: translucent – almost clear but with distorted vision of the agar beneath; Right: opaque – agar beneath the colony cannot be seen through the colony. Adapted from Manuselis (2011).

The mean germination time (MGT), \bar{t} , for chilli seed germination was calculated as:

$$\bar{t} = \frac{\sum_{i=1}^k n_i t_i}{\sum_{i=1}^k n_i} \quad \dots \text{Equation 3.1}$$

where t_i is the time from the start of seed imbibition to the i^{th} observation (day or hour), n_i is the number of seeds germinated corresponding to the i^{th} observation (not the accumulated number) and k is the last time of germination (Ranal and De Santana, 2006). As a standard summation notation, the expression $i=1$ denotes that the summation equation did not consider day 0, but assumed day 1 as the start of observation time. The MGT was calculated as the weighted mean of the germination time due to

the consideration that a different number of seeds germinated at each observation time. Therefore, the number of seeds germinated in the time intervals was used as weight.

Seed vigour was evaluated using mean germination rate (MGR), \bar{v} , which was calculated by first determining the coefficient of velocity of germination (CVG), c :

$$c = \left(\sum_{i=1}^k n_i / \sum_{i=1}^k n_i t_i \right) \times 100 \quad \dots \text{Equation 3.2}$$

where n_i is the number of seeds newly germinating on i^{th} observation, t_i is the time from the start of imbibition, and k is the last day of germination. CVG is the reciprocal of the mean length of incubation time, which quotient is multiplied by 100. The MGR is then calculated as $\bar{v} = c/100$ (Ranal and De Santana, 2006). By summarising equations 3.1 and 3.2, the resulting MGR is actually the reciprocal of MGT, where $\bar{v} = 1/\bar{t}$, because the increase or decrease in \bar{v} correlates to $1/\bar{t}$, not to \bar{t} .

3.2.2 Callus Regeneration

Seedlings of *C. frutescens* L. cv. Hot Lava that germinated for 14 days in culture were each dissected into three parts – cotyledon, hypocotyl and root – which are referred to as “explants” hereinafter. The explants were then placed onto callus induction media (CIM). Every plate of CIM contained all three types of explants. Several compositions of auxins and cytokinins were used in the CIM to test for hormonal effects in callus induction. Various concentrations of 2,4-dichlorophenoxyacetic acid (2,4-D) (0.0, 0.5, 1.0, 1.5, 2.0, 2.5 and 3.0 mg/l) were tested with 0.5 mg/l kinetin to examine the effects of 2,4-D. The explants were also cultured on

MS media supplemented with (a) 5.0 mg/l 6-benzylaminopurine (BAP) and 0.1 mg/l 1-naphthaleneacetic acid (NAA), (b) 10.0 mg/l BAP and 0.1 mg/l NAA, (c) 3.0 mg/l BAP and 1.0 mg/l indole-3-acetic acid (IAA), (d) 10.0 mg/l BAP and 1.0 mg/l IAA, (e) 5.0 mg/l BAP, and (f) 10.0 mg/l BAP to examine the effects of BAP and NAA, the effects of BAP and IAA, as well as the effects of BAP alone. As negative controls, explants were cultured in standard full-strength MS agar medium without any hormone.

For each treatment, 50 seedlings were used and the experiments were replicated twice. The number of explants induced into callus and the period to callus initiation was recorded. After 30 days, the weight and the coverage area of the calli were measured.

3.2.3 Statistical Analysis

Statistical analysis was conducted by performing ANOVA to test the hypotheses statistically at a significance level or p -value of 0.05 using GenStat 17th Edition, as described in **subchapter 2.7**.

3.3 RESULTS

3.3.1 Establishment of Sterile Cultures

3.3.1.1 *Germination and Infection Frequencies from Different Concentrations of Sterilising Agent*

The effects of different concentrations of bleach on germination and infection frequencies of Skyrocket, Full Sky and Hot Lava were tested. The seeds of Skyrocket, Full Sky and Hot Lava were surface sterilized at bleach

concentrations of 5%, 10%, 15% and 20%. The germination and infection frequencies resulting from the bleach treatments are shown in **figure 3.3**. Seeds of Skyrocket and Hot Lava that were surface sterilized with higher bleach concentration generally germinated at lower frequencies. On the other hand, the infection frequencies of the three cultivars was reduced with an increase in the concentration of bleach. The results from Tukey's multiple comparisons showed that the germination frequencies of seeds treated with 20% bleach were significantly lower than those treated with 5% bleach. However, the germination frequencies of Full Sky were not significantly different across the four treatments. Skyrocket, Full Sky and Hot Lava germinated up to 95.3%, 89.6%, 96.0%, respectively, after surface sterilization using 5% bleach. However, the seeds were highly infected, up to 51.3%, 25.3% and 14%, respectively. At 20% bleach, the germination frequencies were 76.7%, 79.8% and 86.9% for Skyrocket, Full Sky and Hot Lava, with infection frequencies of 8.8%, 7.8% and 2.2%, respectively. For Full Sky and Hot Lava, 15% or 20% bleach could be used to control seed infection effectively without significant difference. For Skyrocket, surface sterilization with 20% bleach resulted in the significantly lowest amount of seed infection.

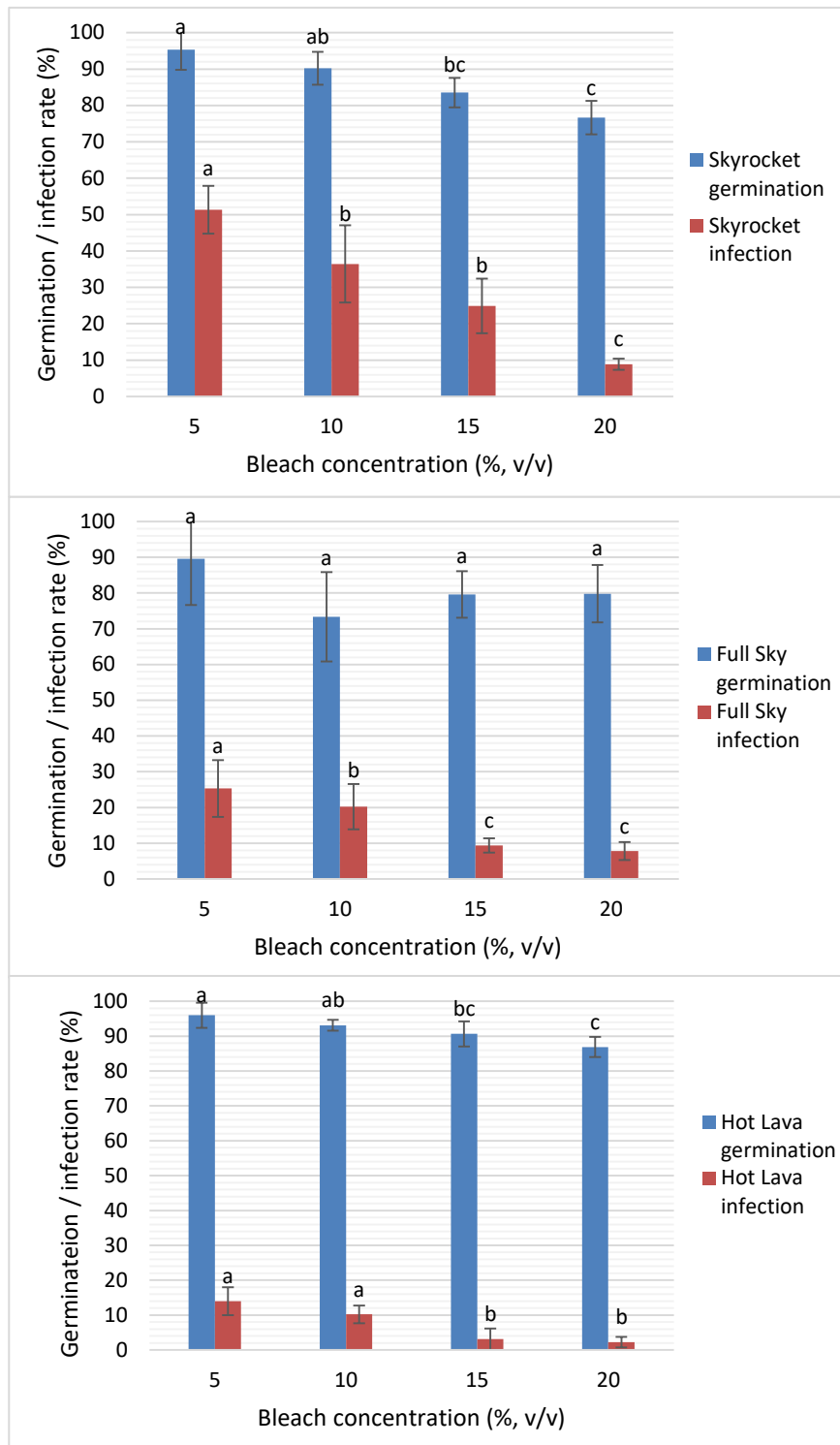


Figure 3.3 Bar charts showing the percentage of seeds of Skyrocket, Full Sky and Hot Lava that germinated and were infected after surface sterilisation with 5%, 10%, 15% and 20% bleach concentrations. Bars of mean percentage (\pm standard deviation error bars) with the same letters are not significantly different using LSD at 5% level.

Microbial infection was observed when any visible fungal or bacterial growth was spotted on any individual seed as the starting point of the microbial growth (**Figure 3.4**). The severity of seed infection indicates the degree of ineffectiveness of the surface sterilisation agent. Any microbial growth that did not appear to originate from the seeds was not regarded as “seed infection” and was excluded from the infection count. Based on the observation of colony morphology, seeds that were infected were generally manifested by the appearance of circular or irregular, and raised colonies that were smooth in early stage, but became wrinkled at approximately 2–3 cm in diameter. The colonies were translucent or opaque, and all of them (if present) were cream in colour.

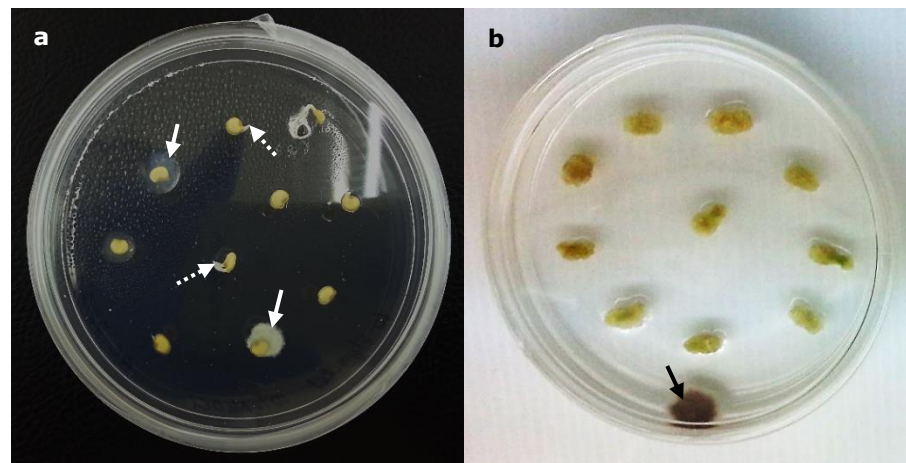


Figure 3.4 Microbial growth on culture plates. (a) Seed infection was observed when microbes grew from the seed as the origin of infection (pointed by solid arrows). Seed germination was observed when radicle emerged from the seed (pointed by dotted arrows). (b) An example of microbial growth as a result of external contamination (pointed by arrow), which did not originate from the samples.

3.3.1.2 Germination and Infection Rates of Different Cultivars

The seeds of Skyrocket, Full Sky and Hot Lava, which were surface sterilised using 20% (v/v) bleach, exhibited similar germination patterns

over the 25-day observation time course (**Figure 3.5**). Germination started from day 6 for the three cultivars. At the end of the time course, Hot Lava germinated with an average frequency of 86.9%, whereas Full Sky and Skyrocket germinated with lower frequencies of 79.8% and 76.7%, respectively. "Germination bloom" was observed from day 6 to day 13, when the number of seeds germinated increased dramatically. The number of seeds germinated generally increased until day 21 and plateaued thereafter. The calculated MGTs for Skyrocket, Full Sky and Hot Lava were 10.1, 9.7 and 9.6 days, respectively. Although the MGTs were very close among the three cultivars, the seeds of Hot Lava germinated the earliest collectively. Based on **equations 3.1 and 3.2** in **subchapter 3.2.1**, the calculated MGRs for Skyrocket, Full Sky and Hot Lava were 0.099, 0.103 and 0.104 day⁻¹, respectively, which were very close among the three cultivars.

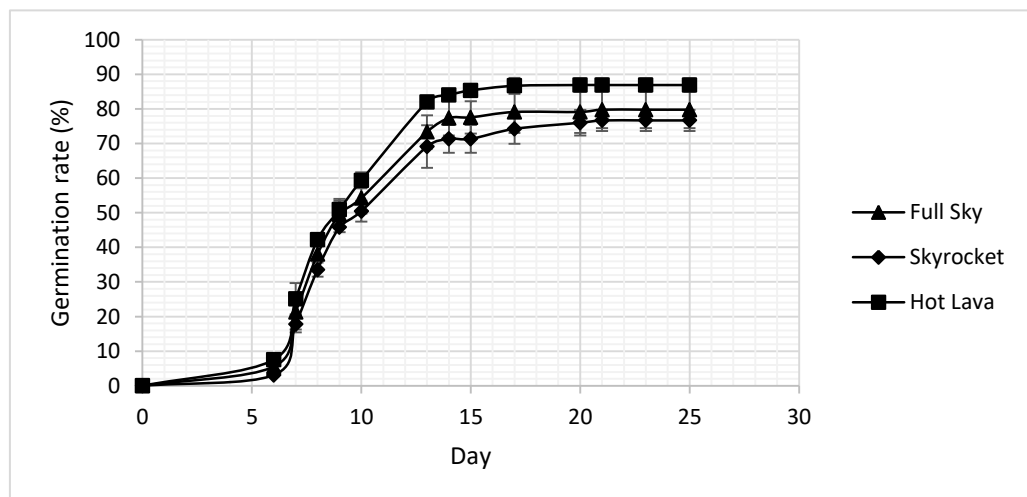


Figure 3.5 Germination rates of surface sterilised seeds of *C. frutescens* cv. Skyrocket, cv. Full Sky and cv. Hot Lava over 25 days. Error bars represent standard deviations ($n=3$).

Infection of the seeds over the observation time course appeared to occur at irregular patterns across the three cultivars (**Figure 3.6**). As a whole, Hot Lava acquired the least microbial infection (2.2%), as compared

to Full Sky (7.8%) and Skyrocket (8.9%). A drastic rise in the frequency of microbial infection was generally observed around 15–20 days for Full Sky and Skyrocket. New infections could have still occurred randomly way after 25 days, but the infection frequency was very low and inconsistent. Applying the same formula as MGT (**Equation 3.1**), the mean infection time (MIT) was calculated, where t_i is the time from the start of seed culturing to the i^{th} observation (day or hour), n_i is the number of seeds infected corresponding to the i^{th} observation (not the accumulated number) and k is the last time of detected infection. The calculated MITs for Skyrocket, Full Sky and Hot Lava were 16.3, 14.1 and 14.2 days, respectively. In general, the time taken for the emergence of infection was the shortest for Full Sky, which was also very close to Hot Lava. To give a general idea of the rate of seed infection, the mean infection rate (MIR) was calculated for Skyrocket, Full Sky and Hot Lava using the same principle as MGR. The MIRs were 0.061, 0.071 and 0.070 day⁻¹, respectively. It appeared that microbial growth emerged faster on the seeds of Full Sky and Hot Lava than those of Sky Rocket.

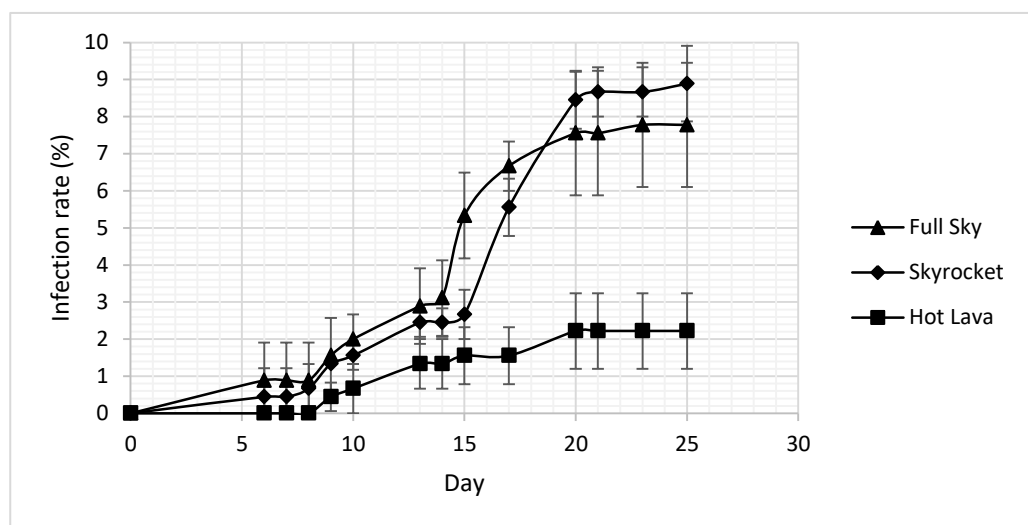


Figure 3.6 Infection rates of surface sterilised seeds of *C. frutescens* cv. Skyrocket, cv. Full Sky and cv. Hot Lava over 25 days. Error bars represent standard deviations ($n=3$).

3.3.2 Callus Regeneration

3.3.2.1 *Effects of 2,4-D and Kinetin*

In order to determine the optimal combination of 2,4-D and kinetin for callus regeneration, cotyledon, hypocotyl and root explants of Hot Lava were cultured on MS media containing different concentrations of 2,4-D (0.5, 1.0, 1.5, 2.0, 1.5 or 3.0 mg/l) and kinetin (0.5 mg/l). Explants in all treatments regenerated into visible callus starting from 7 days after culturing, except the treatment with only 0.5 mg/l kinetin and the treatment without any plant growth regulator, where callus induction was not observed (**Figure 3.7**). The percentage of explants induced into calli (out of 50 explants for each explant type per treatment per replicate) and the period taken to observe the first visible calli are shown in **table 3.1**. For cotyledon explants, the percentage of callus induction for treatment with 0.5 mg/l 2,4-D and 0.5 mg/l kinetin (78%) was significantly lower than those induced with 2.0–3.0 mg/l 2,4-D and 0.5 mg/l kinetin (100%). No significant difference was observed between the treatments for hypocotyl and root explants, although concentrations of 2,4-D at 2.0–3.0 mg/l resulted in 100% callus induction compared to treatments at 1.5 mg/l 2,4-D and lower. In short, the efficiency of callus induction appeared to be the same regardless of the type of explants used.

The mean fresh weights and the mean areas of calli regenerated from the different treatments are presented in **table 3.2**. The weights and areas of the calli induced were not significantly different ($p=0.05$) between the different types of explant. Looking at the calli weights, the treatment with 2.0–3.0 mg/l 2,4-D and 0.5 mg/l kinetin induced calli from the cotyledon explants at an average of 0.76 g and above, which was significantly higher than the treatment with 0.5–1.5 mg/l 2,4-D and 0.5

mg/l kinetin (0.54 g and below). The same outcome was observed from the calli that were generated from the hypocotyl explants. The average weight of the calli from the root explants was significantly higher (0.81 g) in the treatment with 3.0 mg/l 2,4-D and 0.5 mg/l kinetin than those in the treatments with 0.5–2.5 mg/l 2,4-D and 0.5 mg/l kinetin (0.55 g and below). With regards to the area of the calli, the average area of the calli from the cotyledon explants was significantly higher (1.92 cm²) in the treatment with 3.0 mg/l 2,4-D and 0.5 mg/l kinetin than those in the treatments with 0.5–2.5 mg/l 2,4-D and 0.5 mg/l kinetin (1.71 cm² and below). For calli from the hypocotyl explants, the treatment with 2.0 mg/l 2,4-D and 0.5 mg/l kinetin generated significantly larger calli (2.07 cm²) than the other treatments. Calli from the root explants were significantly larger (1.88 cm²) in the treatment with 3.0 mg/l 2,4-D and 0.5 mg/l kinetin than those in the treatments with 0.5–2.5 mg/l 2,4-D and 0.5 mg/l kinetin (1.53 cm² and below). In general, hypocotyl explants have generated larger calli than cotyledon and root explants. The treatment with 2.0 mg/l 2,4-D and 0.5 mg/l kinetin was the lowest auxin concentration that gave significantly high amount of calli in terms of biomass.

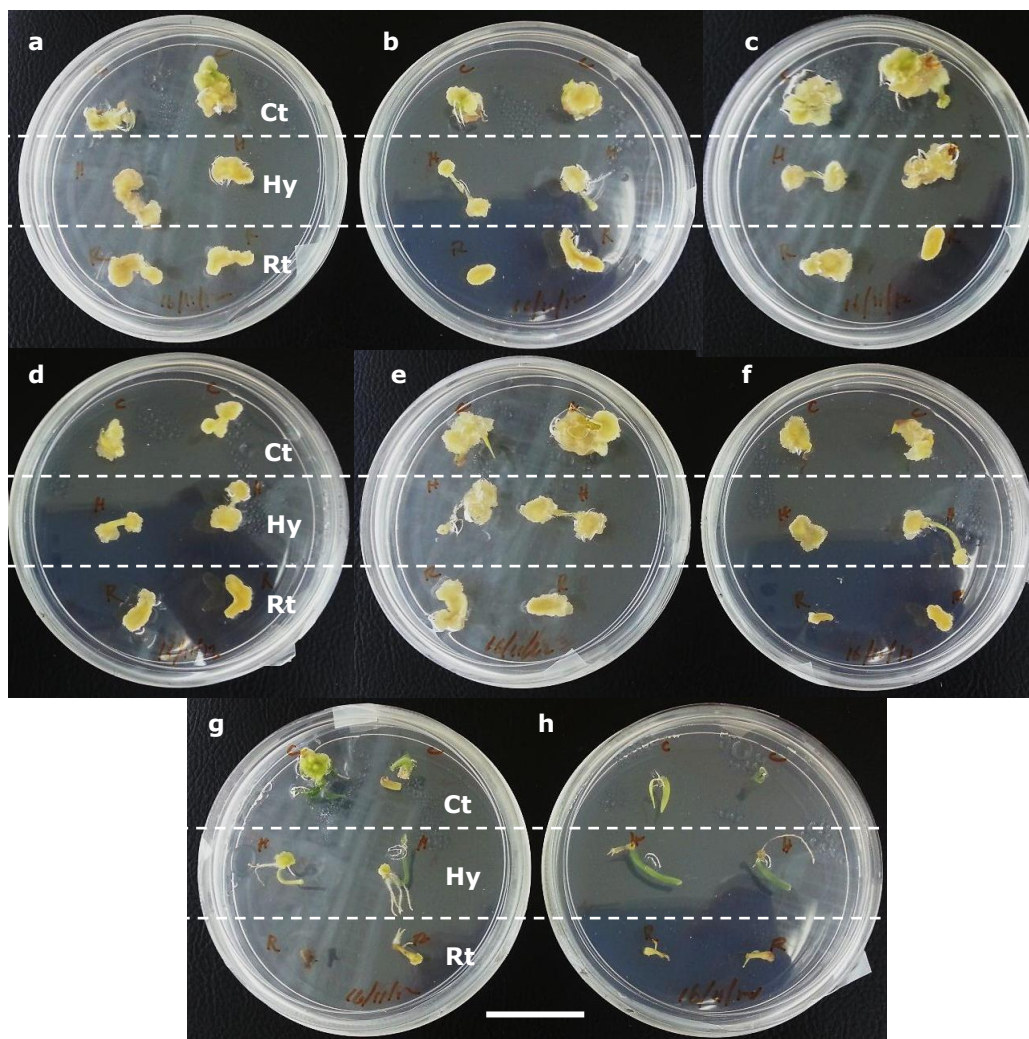


Figure 3.7. Calli induced on MS media supplemented with (a) 0.5 mg/l 2,4-D + 0.5 mg/l kinetin, (b) 1.0 mg/l 2,4-D + 0.5 mg/l kinetin, (c) 1.5 mg/l 2,4-D + 0.5 mg/l kinetin, (d) 2.0 mg/l 2,4-D + 0.5 mg/l kinetin, (e) 2.5 mg/l 2,4-D + 0.5 mg/l kinetin, (f) 3.0 mg/l 2,4-D + 0.5 mg/l kinetin, (g) 0.5 mg/l kinetin, and (h) no plant growth regulator. Explants in the same row as separated by dashed lines were of cotyledon (Ct), hypocotyl (Hy) and root (Rt) origins. Scale bar represents 3 cm.

Table 3.2 Effect of various concentrations of 2,4-D on the period and the mean number of callus induced from cotyledon, hypocotyl and root explants.

2,4-D concentration (mg/l)	Kinetin concentration (mg/l)	Mean induction period (day)	Mean number of calluses		
			Cotyledon	Hypocotyl	Root
0.5	0.5	7±0.6 ^a	39±1.2 ^c	41±1.5 ^b	41±1.2 ^c
1.0	0.5	7±0.0 ^a	43±0.6 ^b	42±1.5 ^b	45±2.6 ^{bc}
1.5	0.5	7±0.6 ^a	45±2.0 ^b	43±2.6 ^b	44±1.2 ^b
2.0	0.5	6±0.6 ^a	50±0.6 ^a	50±0.0 ^a	50±0.0 ^a
2.5	0.5	7±0.6 ^a	50±0.0 ^a	50±0.0 ^a	50±0.0 ^a
3.0	0.5	6±0.6 ^a	50±0.0 ^a	50±0.0 ^a	50±0.0 ^a
0.0	0.5	-	0 ^d	0 ^d	0 ^d
0.0	0.0	-	0 ^d	0 ^d	0 ^d

Mean values (±standard deviation) with the same superscript letters are not significantly different using LSD at 5% level.

Table 3.3. Effect of different 2,4-D concentrations on the fresh weight and area of callus induced from cotyledon, hypocotyl and root explants.

2,4-D concentration (mg/l)	Kinetin concentration (mg/l)	Mean weight (g)			Mean area (cm ²)		
		Cotyledon	Hypocotyl	Root	Cotyledon	Hypocotyl	Root
0.5	0.5	0.46±0.04 ^b	0.62±0.05 ^b	0.37±0.04 ^d	0.90±0.04 ^d	1.37±0.11 ^d	0.96±0.08 ^d
1.0	0.5	0.52±0.03 ^b	0.64±0.03 ^b	0.43±0.04 ^{cd}	1.13±0.04 ^c	1.63±0.03 ^c	1.15±0.05 ^c
1.5	0.5	0.54±0.05 ^b	0.68±0.02 ^b	0.49±0.05 ^{bc}	1.19±0.04 ^c	1.56±0.06 ^c	1.28±0.07 ^c
2.0	0.5	0.76±0.04 ^a	0.78±0.04 ^a	0.59±0.05 ^b	1.61±0.04 ^b	2.07±0.04 ^a	1.47±0.04 ^b
2.5	0.5	0.78±0.04 ^a	0.81±0.02 ^a	0.55±0.06 ^b	1.71±0.05 ^b	1.84±0.05 ^b	1.53±0.04 ^b
3.0	0.5	0.83±0.04 ^a	0.81±0.03 ^a	0.81±0.02 ^a	1.92±0.07 ^a	1.84±0.03 ^b	1.88±0.04 ^a
0.0	0.5	0.00 ^c	0.00 ^c	0.00 ^e	0.00 ^e	0.00 ^e	0.00 ^e
0.0	0.0	0.00 ^c	0.00 ^c	0.00 ^e	0.00 ^e	0.00 ^e	0.00 ^e

Mean values (±standard deviation) with the same superscript letters are not significantly different using LSD at 5% level.

3.3.2.2 Effects of BAP and NAA/IAA

Cotyledon, hypocotyl and root explants were cultured with numerous combinations of BAP and NAA/IAA to examine the effects of high concentrations of BAP on callus induction. None of the explants showed callus induction. Interestingly, organ regeneration directly from the cotyledon and hypocotyl explants was observed, although with low frequencies. The root explants failed to regenerate. The number of shoots and roots that regenerated from the cotyledon and hypocotyl explants after culturing with a number of BAP and NAA/IAA combinations is shown in **table 3.3**. The comparison between the regeneration treatments in the number of explants forming shoots and roots was performed statistically using Tukey's multiple comparisons. The number of cotyledon explants forming shoots did not differ significantly across all of the treatments tested. A similar result was observed on the number of cotyledon explants forming roots. On the other hand, the number of hypocotyls forming shoots with 5.0 mg/l BAP and 0.1 mg/l NAA was generally higher than the other treatments, although the differences were insignificant except when compared with 3.0 mg/l BAP and 1.0 mg/l IAA and with control treatment without any hormone. For the formation of root from hypocotyl explants, the most promising treatment was 5.0 mg/l BAP and 0.1 mg/l IAA, while the rest of the treatments did not result in root formation at all. On average, little root formation was observed among the cotyledon explants. Therefore, it is important to note that explants that produced a shoot did not necessarily produce a root and vice-versa. The former occurrence was more prominent in this study. In addition, the occurrence of such characteristic development was random and inconsistent.

Table 3.4 Comparison on the number of cotyledon and hypocotyl explants forming shoot and root between the different combinations of BAP and NAA or IAA in the regeneration media.

BAP concentration (mg/l)	NAA or IAA concentration (mg/l)	Cotyledon explant		Hypocotyl explant	
		Number forming shoot	Number forming root	Number forming shoot	Number forming root
5.0	NAA, 0.1	1.33±1.53 ^a	0.33±0.58 ^a	4.67±0.58 ^a	1.33±0.58 ^a
10.0	NAA, 0.1	2.67±0.58 ^a	0.00 ^a	3.33±1.53 ^{ab}	0.00 ^b
3.0	IAA, 1.0	1.67±1.52 ^a	0.00 ^a	1.33±1.15 ^b	0.00 ^b
10.0	IAA, 1.0	1.00±0.00 ^a	0.00 ^a	3.67±1.53 ^{ab}	0.00 ^b
5.0	-	2.00±1.00 ^a	0.00 ^a	3.33±0.58 ^{ab}	0.00 ^b
10.0	-	2.00±1.73 ^a	0.00 ^a	4.00±1.00 ^{ab}	0.00 ^b

Mean values (\pm standard deviation) with the same superscript letters are not significantly different using LSD at 5% level.

For explants that developed organs, the formation of the primordia structures was generally observed within ten days after culturing (**Figure 3.8a**), followed by the development of the main shoot and the first leaves, and a root within 20 days (**Figure 3.8b,c**). After two months in culture, the small plants (**Figure 3.8d,e**) were ready for acclimatization. Acclimatization was successfully achieved after the exposure of the plant to the tissue culture room environment (outside of culture jar) for one week, followed by another week of exposure to normal room conditions at $\sim 27^{\circ}\text{C}$ and 54% humidity before transplanting to soil (**Figure 3.8f**). Although a number of whole plants that were acclimatized to soil (peat compost) had been regenerated through this procedure, the success rate was low, with an average regeneration frequency of only 6.65%.

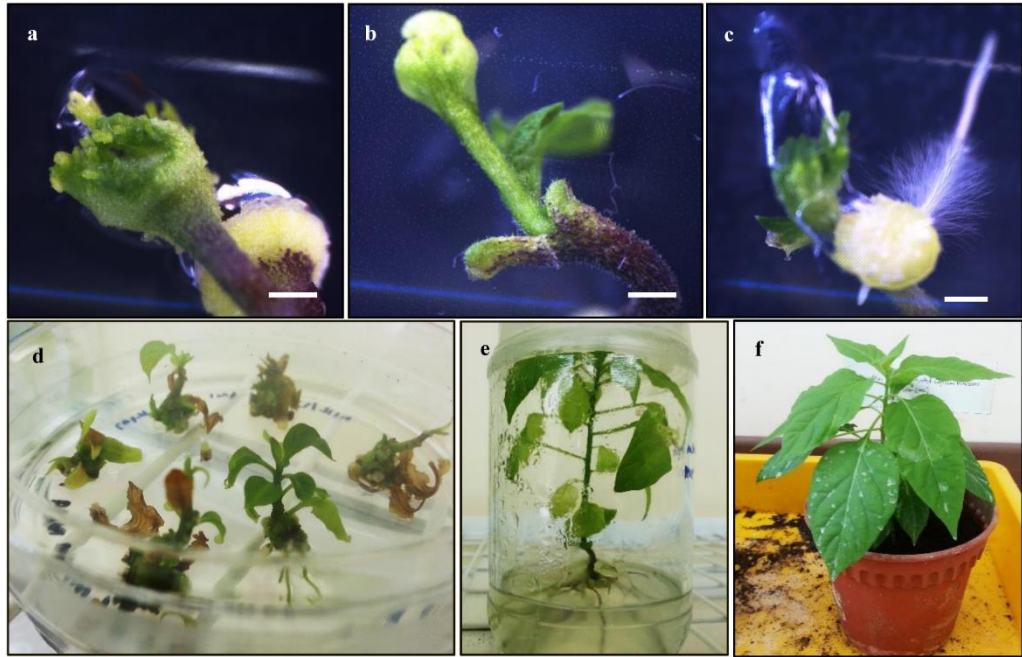


Figure 3.8 Hypocotyl explants on standard MS with 5.0 mg/l BAP and 0.1 mg/l NAA. (a, microscopic) Both ends of explant formed primordial structures after 10 days; (b, microscopic) shoot apex at one end of the explant after 20 days; (c, microscopic) root at another end of the explant after 20 days; (d) newly developed whole plant after 40 days, sub-cultured; (e) grown whole plant after 2 months, sub-cultured into tall culture jar; and (f) after 3 months, transplanted into soil. Scale bar represents 1 mm.

3.4 DISCUSSION

3.4.1 Establishment of Sterile Cultures

3.4.1.1 *Seed Viability and Seed Germination*

In the effort to establish sterile plant cultures, one notable factor that could affect the efficiency of seed germination, apart from the source of seeds, was the effect of surface sterilising agent on the viability of the embryo. Bleach with the active compound, NaOCl, is a very common agent used for disinfection. Nevertheless, at high concentrations and long exposure, NaOCl not only kills microorganisms, but can also be harmful to healthy plant cells. NaOCl causes the formation of chloramines that alter cellular metabolism and the destruction in phospholipids, the oxidative effect that inactivates enzymes irreversibly, as well as the degradation of lipids and

fatty acids (Estrela *et al.*, 2002; Miché and Balandreau, 2001). From the results in **subchapter 3.3.1.1**, it was shown that an increase in the concentration of bleach resulted in a decrease in the frequency of seed germination. This observation suggests that high concentrations of bleach could have a negative effect on the seed viability. While it was thought decades ago that the treatment of seeds with bleach could help to break dormancy and induce germination, bleaching could potentially result in the loss of seed viability (Maguire *et al.*, 1973; Okonkwo and Nwoke, 1975). As such, the use of appropriate bleach concentration to minimise seed infection should achieve a balanced compromise with the loss of seed viability. Although the loss of viability could be compensated by increasing the sample size for future preparation of explants, the surface sterilisation results suggest that bleach concentration up to 20% still gave high germination frequency (86.9% for Hot Lava). This result was comparable to those obtained by Khah and Passam (1992), who achieved 89.3% final germination with a similar sigmoid germination curve from the seeds of *C. annuum* L. c.v. E-84066 using a similar surface sterilisation procedure, i.e. treatment with 1% NaOCl (equivalent to 19% bleach) for 20 min at 25°C. The infection frequency was not reported by Khah and Passam, but it might be worth noting that freshly isolated seeds were more sensitive to inhibition by NaOCl than seeds that were stored for 10 months at ambient temperature.

In addition to seed viability, the uniformity of explant size and developmental stage is important to minimise biological variation in the downstream transformation and regeneration works. It was found that longer MGT (lower MGR) due to slower germination and larger spread in germination time in the chilli seed lot could cause the emergence of smaller and more variable seedlings (Demir *et al.*, 2008). Therefore, the selection

of chilli cultivar that gave short MGT and high MGR was critical. An alternative to the calculation of germination rate is to consider the rate, v , as the reciprocal of the median time: $v_{1/2} = 1/t_{1/2}$, where $t_{1/2}$ is time for 50% germination. However, the application of the function using median time was uncommon because the interpretation would be more complicated than using mean (Ranal and De Santana, 2006).

The efficiency of seed germination during tissue culture could also be impeded by seed dormancy. Seed dormancy is the physical or physiological characteristic of seeds, which is induced to prevent viable seeds from germinating, in order to survive extended periods of unfavourable conditions (Ekong *et al.*, 2014). It was said that newly harvested seeds of *Capsicum* could exhibit dormancy and would require approximately 6 weeks of post-ripening at room temperature to break that dormancy (Randle and Homna, 1981). Nevertheless, seed dormancy was not apparent for the seeds of *C. frutescens* L. cv. Skyrocket, cv. Full Sky and cv. Hot Lava used in this study, despite the observation of close to twenty percent of non-germinated seeds. In the event of seeds having turned dormant, the dormancy could be broken using several ways. The seeds could be soaked in water (seed-priming) prior to germination to allow the expansion of embryo and to leach off inhibitors. Besides that, subjecting the seeds briefly to high temperature or the abrasion of hard seed coats to allow the entry of water could also help to break dormancy (Ekong *et al.*, 2014). Besides that, the germination of dormant seeds of *C. annum*, *C. baccatum*, *C. chinense*, *C. frutescens* and *C. pubescens* could be promoted with the alternation of temperature regimes, such as 15/27°C or 15/30°C (Gerson and Homna, 1978).

3.4.1.2 Genotype Dependency in Seed Germination

The MGTs and MGRs were very similar for Skyrocket, Full Sky and Hot Lava, indicating the possibility of very small genotypic differences apart from the constant culture conditions during germination. Nonetheless, Hot Lava germinated the earliest with the highest vigour and the highest final germination percentage. It should be noted that different cultivars or genotypes of a given species could portray distinctive germination patterns even under optimal growth conditions, more so under suboptimal conditions. For example, different oat (*Avena sativa* L.) genotypes, such as those with different seed sizes and osmotic potential, were found to exhibit significant differences in MGT and final germination percentage (Willenborg *et al.*, 2005). Variability in seed germination was also observed in different cultivars of common bean (*Phaseolus vulgaris* L.), tomato (*Lycopersicon esculentum* Mill.) and quinoa (*Chenopodium quinoa* Willd.), which exhibited varied sensitivity to temperatures and/or salinity (Bois *et al.*, 2006; Dahal *et al.*, 1990; White and Montes-R, 1993). More specifically, seeds of different genotypes might differ in their regulation of plant hormones, abscisic acid and gibberellin, which in turn regulated dormancy and germination (Koornneel *et al.*, 2002; Ogawa *et al.*, 2003). At the molecular level, genetic studies using *Arabidopsis* have identified *DELLA* genes *GAI*, *RGA* and *RGL1* and *RGL2*, which conferred responses to gibberellin and light in seed germination, PHYTOCHROME INTERACTING FACTOR 3-LIKE5 (*PIL5*) transcription factor, which mediated the expression of abscisic acid- and gibberellin-related genes, and *DAG1* and *DAG2* genes that coded for Dof zinc finger proteins, which controlled dependence to light and cold stimuli (Cao *et al.*, 2005; Gualberti *et al.*, 2002; Oh *et al.*, 2009). In tomato, expansin genes *LeEXP4*, *LeEXP8* and *LeEXP10*, which were homologous to those of *Arabidopsis AtEXPA1* were found to be involved in

cell expansion during germination (Chen *et al.*, 2001; Zhong *et al.*, 2015). Genetic variability has been shown to determine not only seed germination characteristics, but also pollen viability and germination, such as in apricots and maize (Asma, 2008; Sari Gorla *et al.*, 1975). Nevertheless, the extent to which genotypic differences could have caused variability in seed germination among the different cultivars of *Capsicum* species has yet to be discovered extensively.

3.4.1.3 Seed Infection

Microbial infection of seeds could have been caused by microbes on the external surfaces of the seeds that survived through the surface sterilisation procedure or by microbes that resided in the internal part of the seeds, which later emerged following seed germination. The ineffectiveness of the surface sterilisation procedure could be attributed to the lack of contact between microbes and NaOCl because of air bubbles, cracks, rough surface, and/or debris on seed surfaces. In such cases, the use of wetting agents or surfactants, such as Tween-20 or Triton X-100, in the surface sterilising agent and mechanical stirring could aid in the contact of the sterilising agent with the seed surfaces. In this study, the surface sterilisation of the seeds of *C. frutescens* with 15–20% bleach (0.79–1.05% NaOCl) have effectively controlled seed infection without the use of surfactant. In addition, pre-treatment of seeds with ethanol before NaOCl could have increased the effectiveness of the sterilisation procedure. Similarly, in a study of wheat kernels that were inoculated with fungal spores of *Aspergillus glaucus*, rinsing with wetting agents did not improve the effectiveness, but rinsing in ethanol before NaOCl greatly reduced surface contamination (Sauer and Burroughs, 1986). However, despite

being a powerful sterilising agent, ethanol was also very phytotoxic (Kern *et al.*, 2009). Therefore, the seeds were normally exposed to ethanol only for a short duration prior to treatment with NaOCl. Other compounds that could be used as surface sterilising agents include calcium hypochlorite ($\text{Ca}(\text{ClO})_2$), mercury(II) chloride or mercuric chloride (HgCl_2), hydrogen peroxide (H_2O_2) or potassium permanganate (KMnO_4) (Leifert *et al.*, 1991; Yeoman, 1973).

Random infections could be detected occasionally after the 25-day observation period, but the infection frequency was very low and inconsistent. The occurrence of random infections at a later time could be due to the contaminants remaining latent for longer periods instead of expressing themselves immediately (Leifert and Cassells, 2001). Many plants, especially perennials, have been shown to be colonised intercellularly by bacteria (local endophytes). Intercellular and intracellular pathogenic microbes may be transmitted latently and be spread in nutrient-rich cultures horizontally and vertically (Cassells, 2012).

The observation of colony morphology is often the first step in the characterisation or screening of microorganisms, and hence, the control of infection. Infections by bacteria, moulds and yeast were easy to detect by visual observation, but infections by protozoa, viruses and mycoplasmas were difficult to detect (Barile, 1973; Fogh *et al.*, 1971). Although no further characterisation work was done in this study, initial observation provides an idea on the type of contamination and helps in the planning of contamination control strategies. For example, simple classification of bacteria or fungus based on colony morphology enables the determination of control agents to be used in the culture media, such as bactericidal, fungicidal or broad-spectrum antibiotics. The observed infections in the cultured seeds appeared to be circular or irregular, and were raised

colonies that were smooth in early stage, but became wrinkled at later stage. The colonies were translucent or opaque, and were cream in colour. The colonies appeared to be bacteria, or yeast (*Saccharomyces*, *Cryptococcus* or *Candida*). Antibiotics, such as cefotaxime, penicillin, carbenicillin and chloramphenicol were effective against a wide range of bacteria. Laterosporamine, basiliskamides and tupuseleiamides, are effective against *Candida* (Vos *et al.*, 2011). Isolated munumbicins from *Streptomyces* spp. NRRL 30562 exhibited broad spectrum antibiotic activity against Gram-positive and Gram-negative bacteria, as well as parasitic oomycetes, such as *Pythium ultimum* (Castillo *et al.*, 2006). However, antibiotics should be used strategically in tissue culture because incorrect or overuse of antibiotics could be detrimental. Excessive reliance on antibiotics could lead to poor aseptic techniques and increased antibiotic resistance in the culture contaminants (Barile, 1973). Combinations of antibiotics could be advantageous provided that they exhibit synergistic effect, otherwise incompatible antibiotics might offset the effect of each other. Combinations of antibiotics should also be used cautiously as combinations at bactericidal concentrations were also potentially phytotoxic (Reed and Tanprasert, 1995).

3.4.2 Callus Regeneration with 2,4-D and Kinetin

In this study, callus induction occurred at 2,4-D concentrations as low as 0.5 mg/l supplemented with 0.5 mg/l kinetin. The highest percentage of callus induction was observed for treatments with 2.0 mg/l 2,4-D and above with 0.5 mg/l kinetin (100% induction). Likewise, previous experiments of hormonal effects on callus induction and capsaicin production showed that 2.0 mg/l 2,4-D and 0.5 mg/l kinetin generated

most callus from placental explants for large scale production of capsaicin (Umamaheswari and Lalitha, 2007). Hasnat and co-workers (2007) reported the highest percentage of callus induction in the shortest time at a 2,4-D concentration of 1.5 mg/l. It was reported that the optimum concentration of auxin stimulated DNA and RNA synthesis for increased growth, whereas continuous growth of calli would not be stimulated at low auxin concentration – low concentration of 2,4-D would lead to herbicide action (Hasnat *et al.*, 2007). Rhizogenesis, which did not proceed into shoot regeneration, occurred in some of the calli on MS media containing only 0.5 mg/l kinetin (without 2,4-D) and on media without any plant growth regulator. In a previous study on the regeneration of *C. annuum* L. cv. Mathania, it was found that calli induced in media containing growth regulators apart from 2,4-D were difficult to maintain as a result of browning and rhizogenesis was prevalent (Agrawal *et al.*, 1989).

3.4.3 High BAP to NAA/IAA Ratios Stimulated Direct Organ Regeneration

High BAP to NAA or BAP to IAA ratios have been reportedly used to regenerate calli from explants of *Capsicum* spp. For example, it was reported that hypocotyls and cotyledonary leaves from red pepper cultivars formed callus, rosette leaves and ill-defined shoot buds at the cut ends when cultured on MS medium supplemented with BAP and IAA. It was further reported that shoot buds could be regenerated from hypocotyls, but not from other explants, grown in MS medium supplemented with different concentrations of BAP alone (Vinoth Kumar *et al.*, 2012). Besides that, bud forming efficiency was reported to be the most optimal with hypocotyl explants on MS supplemented with 3.0 mg/l BAP and 0.3 mg/l IAA (Mok

and Norzulaani, 2007). In this study, a similar observation was observed when high BAP to NAA or IAA ratios were used, but only single shoots were induced from an explant. Another notable drawback in the regeneration of *Capsicum* spp. was that shoot buds that were induced might not be able to elongate. Agrawal and co-workers (1989) reported an increase in shoot bud differentiation of *Capsicum annuum* L. cv. mathania on media with 5.0 mg/l BAP, but shoot elongation did not occur. Other researchers found that the maximum number of shoot buds was induced on calli of *C. annuum* L. cv. 'Morok Amuba' using 10.0 mg/l zeatin, followed by 5.0 mg/l BAP and 1.0 mg/l IAA (Sanatombi & Sharma 2007). For hypocotyl explants, addition of 5.0 mg/l humates enhanced shoot regeneration; however, the effect of supplementation with humates was genotype-specific (Grozeva *et al.*, 2012). Unlike other members of the Solanaceae family, *Capsicum* remained recalcitrant to *in vitro* morphogenesis and regeneration, especially via callus, thus posing difficulties to genetic improvement (Santana-Buzzy *et al.*, 2005; Sharma *et al.*, 2008; Ochoa-Alejo and Ramírez-Malagón, 2001; Grozeva *et al.*, 2012).

Each of the explants on media with BAP and NAA or IAA that regenerated into both shoot and root produced only one main shoot at one end of the explant and one root at the other end instead of multiple adventitious shoots and roots (**Figure 3.8**). This observation suggests that the regenerated parts exhibited strong apical dominance. Such a characteristic ensures that the resources are focused towards the main axis during the plant's growth (Müller and Leyser, 2011; Yeoman *et al.*, 1965). Auxin is known to be involved in shoot apical dominance as it represses local biosynthesis of cytokinin, which stimulates the extension of axillary buds (Tanaka *et al.*, 2006). On the other hand, while auxin is known to promote root development, cytokinin promotes root apical dominance

(Aloni *et al.*, 2006). The explants underwent dedifferentiation and differentiation processes to produce primordial structures at both ends before developing into shoot and root, respectively. These observations are the result of initial attainment of competence, followed by determination to form either a shoot or a root, and finally outgrowth to a shoot or a root (De Klerk *et al.*, 1997). Furthermore, the development of a shoot at one end and a root at the other end shows that apical-basal polarity developed during the regeneration process.

3.5 CONCLUSION

The surface sterilisation of seeds of *C. frutescens* successfully enabled the establishment of sterile *in vitro* plant cultures with high germination rates and with low microbial infection rates. Bleach concentrations at 15–20% was the most effective to surface sterilise the seeds, with the sterilisation procedure effectively reduced seed infection frequency down to 2.2%. Hot Lava has the highest germination rate, compared to Skyrocket and Full Sky. Callus regeneration was the most efficient in hypocotyl compared to cotyledon and root explants on MS media containing as low as 2.0 mg/l 2,4-D and 0.5 mg/l kinetin. The use of MS media supplemented with various combinations of BAP and NAA achieved direct organ regeneration, but with very low frequencies, so such regime is not suitable for use in subsequent works. In summary, the surface sterilisation and callus regeneration procedures have enabled the establishment of aseptic cultures from the hypocotyl explants of Hot Lava for subsequent transformation, regeneration, expression of transgenes and production of secondary metabolites.

CHAPTER 4

CONSTRUCTION OF EXPRESSION VECTORS FOR THE NUCLEAR TRANSFORMATION OF *CAPSICUM* *FRUTESCENS* L.

4.1 INTRODUCTION

The cell nucleus has long been a target organelle for genetic transformation as it is the core component that stores most of the genomic DNA of the cell. Expression of genes primarily takes place from the transcription of messenger RNAs (mRNAs) in the nucleus to the translation of polypeptides in the ribosomes. The genetic transformation work in this chapter conformed to this central dogma of molecular biology, but with the introduction of exogenous genes that code for vanillin biosynthetic enzymes into the nuclear genome. This chapter describes the cloning of genes for vanillin biosynthesis into transformation vectors (plasmid DNAs), which features are described in the following **subchapters 4.1.1 and 4.1.2**. The resulting expression vectors would then be delivered into plant cells and the target transgenes would be integrated into the nuclear genome via random recombination events.

4.1.1 The pcDNATM6.2 Transformation Vector

The pcDNA6.2 transformation vector was originally a promoterless plasmid that was designed for Gateway[®] Cloning by Invitrogen (Thermo Fisher Scientific, USA). The pcDNA6.2 harboured the *attR1* and *attR2* Gateway[®] recombination sites, which flanked the *ccdB* cytotoxicity gene and the chloramphenicol acyltransferase gene (*cat*) for chloramphenicol resistance. The *ccdB* and *cat* genes were negative and positive selectable markers, respectively, for the bacterial selection of *ccdB*-resistant *E. coli* during the replication of the original vector. A beta-lactamase gene (*bla*) for ampicillin resistance was also present as a bacterial selectable marker (Jobling and Holmes, 1990). The integrity of the original vector could be maintained by selecting the *E. coli* transformants in media containing ampicillin and chloramphenicol. The pcDNA6.2 also contained the *bsd* gene, which conferred resistance to blasticidin S (BS) antibiotic, as a eukaryotic selectable marker (Thermo Fisher Scientific, 2016). Being a versatile vector, the pcDNA6.2 contained three origins of replication (*ori*'s) for replication in different host organisms: the pUC *ori* for replication in *E. coli*, the SV40 *ori* for replication in mammalian cells, and the f1 *ori* for replication in filamentous phage (Dotto *et al.*, 1984; Piechaczek *et al.*, 1999; Wang *et al.*, 2009). The map of pcDNA6.2 is shown in **appendix B(i)**.

Gateway[®] Cloning via homologous recombination at the *attR* sites of the pcDNA6.2 vector would replace the *ccdB* and *cat* genes with the target DNA fragment(s). In addition, the presence of recognition sites of *Pst*I, *Bam*HI, *Eco*RI, *Xba*I and *Age*I restriction endonucleases (REs) allows for the cloning of a target gene by conventional double restriction and ligation method. Besides that, recognition sites for type IIS REs, such as *Bsm*BI and *Bbs*I, were also available for cloning using methods like GeneArtTM

Type IIs Assembly or Golden Gate Assembly. Type IIS REs are REs that cut at certain distances away from their recognition sites.

4.1.2 The pHBT12K Transformation Vector

The original HBT transformation vector was a plasmid with pUC18 backbone. The *bla* gene for ampicillin resistance was originally present in the pUC18 backbone to serve as a bacterial selectable marker. The pUC ori was also available for the replication of the vector in *E. coli*. In addition, the original HBT also harboured the gene of an engineered, synthetic green fluorescent protein (*sgfp*) combined with a chromophore mutation where serine was replaced with threonine at position 65 to give 100-fold higher fluorescence when excited with 490 nm blue light (Chiu *et al.*, 1996; Niwa, 2003). The region upstream of the *sgfp* reporter gene had been re-engineered by Leong (2015, personal communication), with the removal of the 35S promoter (35Sp) and the addition of an *attR1-ccdB-cat-attR2* Gateway[®] cassette. The region downstream of the *sgfp* and its NOS terminator had been re-engineered with the addition of the neomycin phosphotransferase II gene (*nptII*), which conferred resistance to kanamycin antibiotic, as a bacterial and plant selectable marker (de Vries & Wackernagel 1998; Leong 2015, personal communication). The re-engineered HBT (now renamed as pHBT12K) could be cloned using Gateway[®] recombination. Subsequently, bacteria or plants that were transformed with pHBT12K could be selected using kanamycin. Besides the availability of *attR* sites for Gateway[®] cloning, target genes could also be cloned into the pHBT12K vector via type IIS REs, such as *BbsI*, and conventionally via double restrictions using type II REs, such as *BsbI*, *NdeI*,

SfoI, *XhoI*, *SacII*, *BstBI* and *EcoRV*. The map of pHBT12K is shown in **appendix B(ii)**.

4.1.3 Specific Objectives

The *fcs*, *ech* and *VpVAN* were vanillin biosynthetic genes, which coded for feruloyl-CoA synthetase, enoyl-CoA hydratase and vanillin synthase, respectively. *Fcs* and *Ech* have been identified to sequentially catalyse the conversion of ferulic acid into vanillin in *Amycolatopsis* sp. (Achterholt *et al.*, 2000). On the other hand, *VpVAN* has been identified as a single enzyme that catalyses the conversion of ferulic acid into vanillin in the vanilla plant (Gallage *et al.*, 2014). Preceding the transformation of plants with these vanillin biosynthetic genes, expression vectors in the form of recombinant plasmids were constructed to incorporate *fcs*, *ech* and *VpVAN* into the pcDNA6.2 and the pHBT12K transformation vectors. Hence, the specific objectives in this chapter centred on the construction of six expression vectors: (i) The pcDNA6.2::35Sp-*sgfp* expression vector, which contained 35Sp and *sgfp*, was constructed for the optimisation of biolistic parameters using a GFP assay (described in **chapter 5**). (ii) The pcDNA6.2::35Sp-*fcs*-NOSp-*ech* expression vector, which comprised 35Sp and *fcs* as well as the nopaline synthase promoter (NOSp) and *ech*, was constructed to study the synergistic effect of *Fcs* and *Ech* in vanillin production. (iii) The pcDNA6.2::35Sp-*fcs* and pcDNA6.2::NOSp-*ech* expression vectors were constructed separately, to determine whether *Fcs* or *Ech* alone (expression driven by 35Sp and NOSp, respectively) could catalyse the production of vanillin. (iv) The pcDNA6.2::35Sp-*VpVAN* expression vector, which carried the 35Sp and *VpVAN*, was constructed to study the effect of *VpVAN* alone in vanillin production. (v) The pHBT12K::35Sp-*VpVAN* was constructed to

evaluate the expression of *VpVAN* that was delivered using another customised pHBT12K transformation vector and subsequently, the production of vanillin.

4.2 MATERIALS AND METHODS

The main workflow in the construction of expression vectors involved the codon optimisation and synthesis of the target genes and promoter into holding vectors, followed by the cloning of the genes and their assigned promoters into the transformation vectors. **Figure 4.1** illustrates the origin of the genes and the desired target cassettes, which were cloned into pcDNA6.2 or pHBT12K to produce the final expression vectors (specific methods to be detailed in **subchapters 4.2.1–4.2.14**).

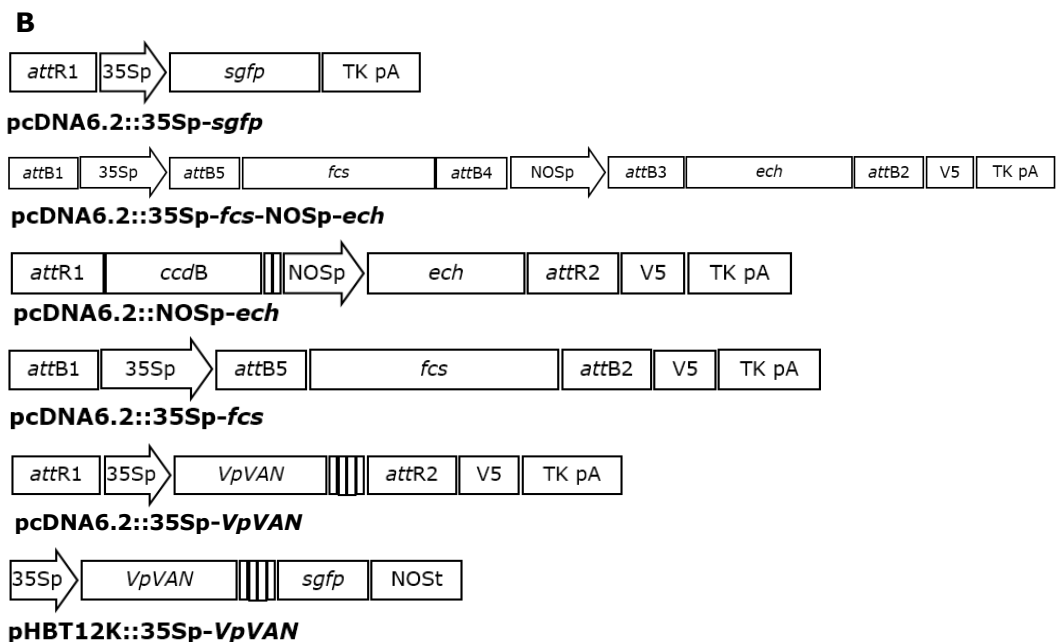
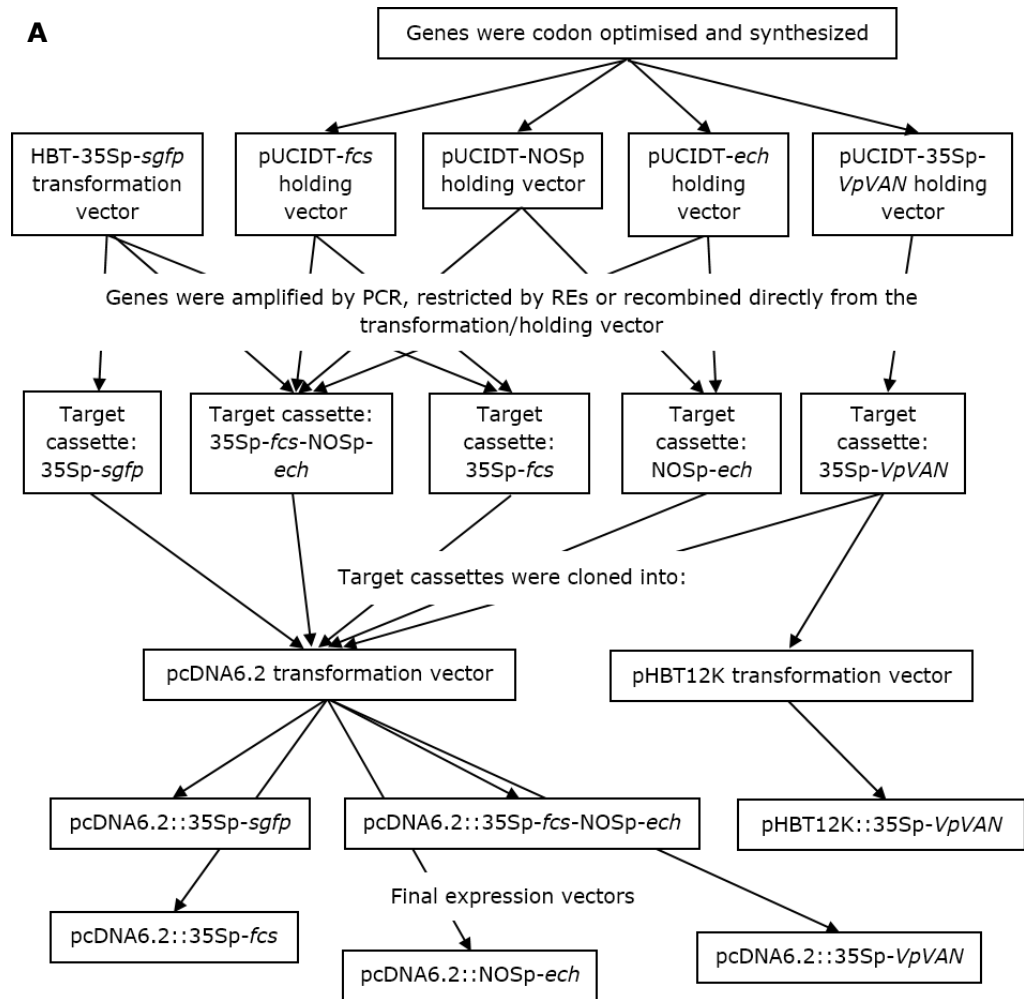


Figure 4.1 Illustration showing (A) the origins of target genes, *sgfp*, *fcs*, *ech* and *VpVAN*, and the promoters, 35Sp and NOSp, which were used for the construction of the respective target cassettes (B) that were cloned into pcDNA6.2 or pHBT12K to produce the final expression vectors, pcDNA6.2::35Sp-*sgfp*, pcDNA 6.2::35Sp-*fcs*-NOSp-*ech*, pcDNA 6.2::35Sp-*fcs*, pcDNA 6.2::NOSp-*ech*, pcDNA 6.2::35Sp-*VpVAN* and pHBT12K::35Sp-*VpVAN*.

4.2.1 Propagation and Isolation of Plasmids from *E. coli*

The plasmids (**Table 2.3, subchapter 2.3.1**) that were used in this study were transformed into chemically competent *E. coli* (Invitrogen, Thermo Fisher Scientific, USA, as listed in **Table 2.2, subchapter 2.3.1**) for propagation. After an overnight incubation of the *E. coli* cultures, during which the plasmids were replicated, the plasmids were isolated from the *E. coli* using commercial kit or alkaline lysis method. Propagation and purification of plasmids were done under sterile conditions to prevent external contamination.

4.2.1.1 Transformation of *E. coli*

Plasmid DNA was propagated using biological host, *E. coli*. Insertion of plasmid into chemically competent cells of *E. coli* was done via heat shock transformation. The competent cells, which were delivered and stored in a storage solution containing LB, 36% (v/v) glycerol, 12% (w/v) polyethylene glycol (PEG) 7500 and 12 mM magnesium sulphate (MgSO₄) were removed from -80°C and thawed on ice for 3 to 5 min. Not more than 5 µl (10 pg to 100 ng) of plasmid DNA was added into the competent cells. Then, the *E. coli* was incubated on ice for 30 min, transferred to 42°C (heat shock) for 1 min, and incubated on ice again for 2 min. Then, 900 µl of super optimal broth with catabolite repression (SOC) was added and the reaction tube was incubated horizontally at 37°C, 220 rpm for 1 h in an incubator shaker (New Brunswick™ Innova® 42, Eppendorf, Germany). After that, the tube was centrifuged for 1 min at 4,700 ×g. The supernatant was removed by decanting. Pelleted cells were re-suspended in the remaining supernatant and were spread on selective LB agar plates

containing 100 µg/ml ampicillin or 50 µg/ml kanamycin, depending on the antibiotic selection used. The plates were then incubated at 37°C for 16 h.

4.2.1.2 Propagation of Plasmid

A single colony of *E. coli* that was transformed with a target plasmid as described in subchapter 4.2.1.1 was suspended into 10 ml of liquid LB containing 100 µg/ml ampicillin or 50 µg/ml kanamycin in a 50 ml centrifuge tube. The *E. coli* culture was incubated for 16 h at 37°C and 220 rpm using an incubator shaker (New Brunswick™ Innova® 42, Eppendorf, Germany).

4.2.1.3 Isolation of Plasmids Using GeneAll® Hybrid-Q™ Plasmid Rapidprep Kit

Plasmid DNA was isolated from the pelleted cells of *E. coli* using buffers and spin columns provided in the GeneAll® Hybrid-Q™ Plasmid Rapidprep Kit (GeneAll Biotechnology, South Korea) according to a standard protocol in the protocol handbook. An overnight broth culture of transformed *E. coli* that was prepared as described in **subchapter 4.2.1.2** was centrifuged at 4°C and 4,700 ×g for 5 min using an Eppendorf 5810R Refrigerated Centrifuge (Germany). The supernatant was removed. The bacterial pellet was sequentially suspended in 250 µl of buffer S1 and transferred to a new 1.5 ml microcentrifuge tube. The lysate was sequentially mixed by inversion with 250 µl of buffer S2 and 350 µl of buffer G3, followed by centrifugation at 9,500 ×g and room temperature for 10 min. The cleared lysate was transferred into a spin column contained in a collection tube and centrifuged at 9,500 ×g and room temperature for 30 s (this speed,

temperature and duration was used for the subsequent centrifugations). The pass-through in the collection tube was discarded and 700 µl of buffer PW was added into the spin column. After another centrifugation, the pass-through was discarded and the spin column was re-inserted into the collection tube for another centrifugation for 1 min. Finally, the plasmid was eluted from the spin column using Buffer EB from the kit. The elution volume of Buffer EB could be reduced down to 40 µl for a higher concentration of plasmid DNA. Increasing the incubation time to 2 min after the addition of Buffer EB and/or repeating the elution using the spin-through eluent could help in the recovery of plasmids.

4.2.1.4 Isolation of Plasmids Using Alkaline Lysis Method

Plasmids that were propagated for use in the biolistic-mediated transformation of *C. frutescens* were isolated using an alkaline lysis method. The reagents used in this method, plasmid purification solution 1 (PPS1), plasmid purification solution 2 (PPS2), plasmid purification solution 3 (PPS3), sodium acetate (NaOAc) and Tris-EDTA (TE) buffer, was prepared as described in **subchapter 2.1**. An overnight broth culture of transformed *E. coli* that was prepared as described in **subchapter 4.2.1.2** was centrifuged at 4°C and 4,700 ×g for 5 min using an Eppendorf 5810R Refrigerated Centrifuge (Germany). The supernatant was discarded and the bacterial pellet was resuspended in 150 µl of pre-chilled PPS1. The suspension was transferred into a new 1.5 ml microcentrifuge tube. Then, 250 µl of PPS2 was added to the suspension and the tube was inverted several times to mix, followed by incubation at room temperature for 2–3 min. After that, 250 µl of PPS3 was added to the lysate and mixed by inversion and flicking of the tube several times. The tube was centrifuged

at 9,500 ×g and room temperature for 5 min (this speed, temperature and duration was used for the subsequent centrifugations). The resulting supernatant was transferred into a new 1.5 ml microcentrifuge tube and was mixed with 700 µl of 100% isopropanol (R & M Chemicals, UK), followed by incubation at room temperature for 5 min to precipitate the plasmid DNA. The tube was centrifuged and the supernatant was removed. Whitish pellet should be seen at the bottom of tube. The pellet was washed by adding 500 µl of 99% ethanol (R & M Chemicals, UK). The wash mixture was centrifuged, the supernatant was discarded and the pellet was dried in a vacuum dessicator (Concentrator plus, Eppendorf, Germany) for approximately 2 min. Subsequently, 100 µl of TE buffer was added to resuspend the pellet. RNA contaminant was eliminated with the addition of 2 µl of 10 mg/ml RNase A (Sigma-Aldrich, USA). The mixture was incubated at 70°C for 10 min, followed by incubation at room temperature for at least 30 min. Then, 10 µl of 3 M NaOAc and 100 µl of 25:24:1 phenol:chloroform:isoamyl alcohol (Sigma-Aldrich, USA) was added and the mixture was vortexed for 10–20 s for the recovery of plasmid DNA. The mixture was centrifuged and the top aqueous layer (~80 µl) of the resulting three layers was carefully transferred into a new 1.5 ml microcentrifuge tube without interrupting the middle interphase and bottom organic layers. The aqueous layer was mixed with 100 µl of isopropanol to precipitate the plasmid DNA. Centrifugation of the tube was done, followed by the removal of the supernatant. At this point, semi-transparent pellet might or might not have been seen at the bottom of tube. The pellet was washed with 500 µl of 99% ethanol. Subsequently, the wash mixture was centrifuged, the supernatant was discarded and the pellet was dried in vacuum dessicator. Finally, the pellet was resuspended in 30 µl of TE buffer.

4.2.2 Purification of DNA Fragments during the Construction of Vectors

DNA products of PCRs or RE digestions were purified prior to certain steps in the construction of vectors. Such purification was important to remove the salts and enzymes of the PCRs or RE digestions from interfering with the downstream reactions. DNA fragments of interest were purified using commercial kits or PEG method.

4.2.2.1 Purification of DNA Fragments Using GeneAll® Expin™ PCR SV and Gel SV Kits

DNA fragments from PCRs or RE digestions were purified using GeneAll® Expin™ PCR SV Kit (GeneAll Biotechnology, South Korea) according to the protocol handbook. Five volumes of buffer PB was added into one volume of DNA sample, mixed and transferred into an SV column contained in a collection tube. The mixture was centrifuged at 9,500 ×g and room temperature for 30 s (this speed, temperature and duration was used for the subsequent centrifugations). The pass-through was discarded and the SV column was re-inserted into the collection tube. Buffer NW (700 µl) was added into the SV column, followed by another centrifugation. The pass-through was discarded, the SV column was re-inserted into the collection tube and the tube was centrifuged for 1 min to remove the residual wash buffer. Finally, the plasmid was eluted from the spin column using Buffer EB from the kit.

DNA fragments of interest were purified from agarose gels following agarose gel electrophoresis using GeneAll® Expin™ Gel SV Kit (GeneAll Biotechnology, South Korea) according to the protocol handbook. Three

volumes of buffer GB mixed with one volume of excised agarose gel containing DNA (1 mg is equivalent to 1 μ l). The mixture was incubated at 50°C with occasional vortexing until the agarose gel is completely melted. One gel volume of isopropanol was added into the tube. The mixture transferred into an SV column contained in a collection tube. The mixture was centrifuged at 9,500 \times g and room temperature for 30 s (this speed, temperature and duration was used for the subsequent centrifugations). The pass-through was discarded and the SV column was re-inserted into the collection tube. Buffer NW (700 μ l) was added into the SV column, followed by another centrifugation. The pass-through was discarded, the SV column was re-inserted into the collection tube and the tube was centrifuged for 1 min to remove the residual wash buffer. Finally, the plasmid was eluted from the spin column using Buffer EB from the kit.

At the final elution step, the volume of the eluent (Buffer EB) could be increased to obtain more diluted DNA samples or be decreased to obtain more concentrated DNA samples. After purification, the concentration and purity of the eluted DNA was measured using a NanoDrop 1000 Spectrophotometer (Thermo Scientific, USA).

4.2.2.2 Purification of DNA Fragments Using PEG Method

PCR products in Gateway[®] Cloning were purified using a PEG protocol provided by the Invitrogen Multisite Gateway[®] Pro User Manual. After PCR, TE buffer, pH 8.0, was added to the PCR product, followed by 30% PEG 8000 / 30 mM MgCl₂. The mixture was mixed thoroughly by vortexing and was centrifuged at 10,000 \times g for 15 min at room temperature. The supernatant was then carefully removed, leaving clear pellet. The pellet

was re-dissolved in 30 µl of TE buffer. Quantification of DNA was done using a NanoDrop 1000 Spectrophotometer (Thermo Scientific, USA).

4.2.3 Polymerase Chain Reactions (PCRs)

PCRs were performed for the amplification of target genes or DNA fragments for the cloning process. The annealing temperature of each primer pair that was synthesised for PCR was optimised by running a PCR with gradient annealing temperatures ranging from 15°C below to 15°C above the melting temperature of a primer pair. The information and sequences of the primers used are given in **appendix C**. PCR was performed according to the concentrations of reagents and thermal cycling programme as described in **subchapter 2.4**. The elongation time was set according to the length of target DNA to be amplified (1 min per kb of DNA). PCR thermal cycling was performed for 25–30 cycles. Where amplification resulted in a low yield or unspecific priming, a PCR with gradient concentrations of 1.5–3.0 mM MgCl₂ was run. The specific PCR conditions for the cloning processes are described in **subchapters 4.2.9–4.2.14**. All PCRs were done in 20 µl reaction volumes in 200 µl PCR tubes. Where a higher amount of a PCR product was required, multiple tubes of 20 µl reaction volume were prepared for PCR and then pooled together after the PCR.

4.2.4 Restriction Endonuclease (RE) Digestions

RE digestions were performed during double restriction-ligation cloning and Golden Gate Cloning. The REs and their respective buffers used in this study were acquired from New England Biolabs (USA). RE digestions were

conducted in 20 µl reaction volumes according to the incubation temperatures and durations as instructed by the manufacturer. For each RE digestion, 5 units of each RE was mixed with the RE buffer to a final 1× concentration in 200 µl PCR tube and incubated using a water bath (Mettler WWB 29, Germany) or a thermomixer (Thermomixer comfort, Eppendorf, Germany).

4.2.5 Ligation of DNA

The digested DNA was ligated during the cloning process using T4 DNA ligase from New England Biolabs (USA). In each ligation reaction, 400 units of T4 DNA ligase, T4 DNA ligase buffer (1× final concentration) and DNA samples were mixed to a final volume of 20 µl in a 200 µl PCR tube. The typical 3:1 molar ratio of insert DNA to vector DNA was used for the ligation reactions. All of the ligation reactions were performed at 16°C overnight or at room temperature for 2 h.

4.2.6 Codon Optimisation and Gene Synthesis

The genes of *fcs*, *ech* and *VpVAN* were codon optimised using Integrated DNA Technologies Codon Optimization Tool (<http://sg.idtdna.com/CodonOpt>) based on the codon usage of *Nicotiana benthamiana*. This was because *Nicotiana benthamiana* was a close relative of *Capsicum* spp. from the Solanaceae family with a complete database of codon usage available in the codon optimization tool. Sequences of the codon optimised genes are given in **appendix D**. The *fcs*, *ech* and *VpVAN* sequences were then synthesized into pUCIDT holding vectors by IDT (Singapore) as pUCIDT-*fcs*, pUCIDT-*ech* and pUCIDT-35Sp-*VpVAN*,

respectively. *VpVAN* was synthesized with a 35Sp upstream. NOSp was also synthesized and the resulting holding vector was known as pUCIDT-NOSp.

4.2.7 Gateway® Cloning

Gateway® Cloning was a recombinational cloning system that enabled simultaneous cloning of up to four DNA fragments into a transformation vector. This cloning system was carried out in two phases. Phase 1 involved the recombination between PCR products (flanked by Gateway® *attB* sites) and Gateway® pDONR™ donor vectors (containing Gateway® *attP* sites that were homologous to the corresponding *attB* sites) to produce entry clones. The target DNA fragments in the entry clones were now flanked by *attL* and/or *attR* sites, a result of the recombination between *attB* and *attP*. This phase 1 reaction was termed the BP reaction, taking the names of *attB* and *attP*. Phase 2 involved recombination between the entry clones and a transformation vector (also known as destination vector, which carried Gateway® *attR* sites like pcDNA6.2) to produce the final expression vector. This phase 2 reaction was termed the LR reaction, taking the names of *attL* and *attR*. The general workflow of Gateway® Cloning is illustrated in **Figure 4.2**. In this study, Gateway® Cloning was performed using Multisite Gateway® Pro Kit (Invitrogen, Thermo Fisher Scientific, USA).

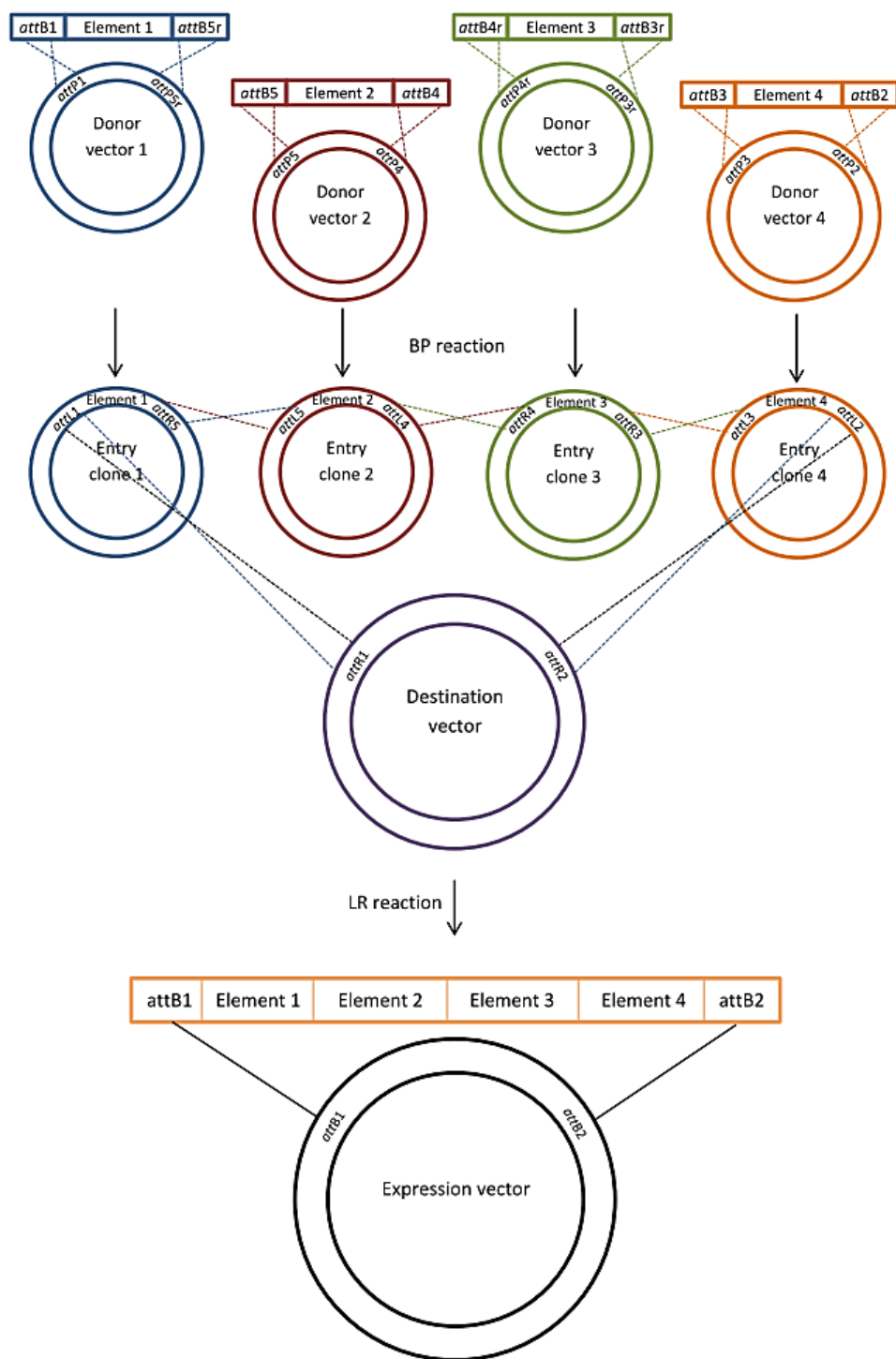


Figure 4.2 The general workflow of Gateway® Cloning of four DNA elements into a destination vector through BP and LR reactions to produce a final expression vector. Published in Chee and Chin (2015).

4.2.7.1 BP Reaction

For each BP reaction, 50 femtomole (fmole) of *attB*-flanked PCR product was required. The *attB* sites have been incorporated into the primer pair for PCR according to the sequences given in the user's manual. Conversion of DNA amount from fmole to ng was done according to the following formula:

$$\text{Amount of DNA in ng} = (x \text{ fmole})(N)\left(\frac{660 \text{ fg}}{\text{fmole}}\right)\left(\frac{1 \text{ ng}}{10^6 \text{ fg}}\right) \dots \text{Equation 4.1}$$

where x is the amount of DNA required in fmole and N is the size of the target DNA or PCR product in bp.

Each BP reaction (for each target DNA fragment) was carried out by mixing the *attB*-flanked PCR product or plasmid containing the *attB*-flanked target DNA fragment (50 fmole or 15–150 ng, up to 7 μ l) with 1 μ l (150 ng) of the corresponding Gateway[®] donor vector, pDONR[™], which was provided by the kit, in a 1.5 ml microcentrifuge tube. Then, TE buffer, pH 8.0, was added to the mixture to make up the reaction volume to 8 μ l. Then, BP Clonase[™] II enzyme mix (Invitrogen, Thermo Fisher Scientific, USA) was removed from -20°C storage, thawed on ice for 2 min and mixed twice by vortex (2 s each time). To each reaction tube, 2 μ l of the BP Clonase[™] II enzyme mix was added and mixed by vortex twice (2 s each time). The reactions were incubated at 25°C for 1 h. Overnight incubation up to 18 h could yield more *E. coli* colonies after downstream transformation than 1 h incubation. After incubation, 1 μ l of Proteinase K (Invitrogen, Thermo Fisher Scientific, USA) was added to each reaction, followed by incubation at 37°C for 10 min. Finally, 2 μ l of the reaction product (entry clones) was transformed into One Shot[®] Mach1[™] T1[®] Chemically Competent *E. coli* (Thermo Fisher Scientific, USA) according to

the protocol described in **subchapter 4.2.1.1** and the transformed *E. coli* was plated on LB agar supplemented with 50 µg/ml kanamycin to select for kanamycin-resistant *E. coli*.

After an overnight broth culture of the selected *E. coli* colonies, the entry clones were isolated from the bacteria for subsequent LR reaction according to the protocol described in **subchapter 4.2.1.3**. The entry clones were sequenced to verify the integrity of the target DNA fragments.

4.2.7.2 LR Reaction

The resultant entry clones (10 fmoles each) from BP reactions (as described in **subchapter 4.2.7.1**) were mixed with pcDNA6.2 transformation vector (20 fmoles) for each LR reaction. TE buffer, pH 8.0, was added to the mixture to make up the reaction volume to 8 µl. Conversion of DNA amount from fmole to ng was done according to **equation 4.1** in **subchapter 4.2.7.1**. LR Clonase™ II enzyme mix (Invitrogen, Thermo Fisher Scientific, USA) was removed from -20°C storage, thawed on ice for 2 min and mixed twice by vortex (2 s each time). Then, 2 µl of LR Clonase™ II enzyme mix was added to the DNA mixture and mixed by vortex twice (2 s each time). The reactions were incubated at 25°C for 16 h. Then, 1 µl of Proteinase K was added, followed by incubation at 37°C for 10 min. The reaction was then transformed into One Shot® TOP10 Chemically Competent *E. coli* (Thermo Fisher Scientific, USA) according to the protocol described in **subchapter 4.2.1.1**. The transformed *E. coli* was plated on LB agar supplemented with 100 µg/ml ampicillin to select for ampicillin-resistant *E. coli*.

After an overnight broth culture of the selected *E. coli* colonies, the expression vectors were isolated from the bacteria according to the

protocol described in **subchapter 4.2.1.4**. The expression vectors were sequenced to verify the integrity of the assembled DNA fragments.

4.2.8 Golden Gate Cloning

Golden Gate Cloning was a one-pot reaction that combined the restriction and ligation of multiple DNA modules and a target transformation vector in a single tube. In Golden Gate Cloning, a single type IIS RE site was incorporated into the primer pairs to flank both 5' and 3' ends of the target DNA fragments. After PCR, target DNA fragments were then assembled into the transformation vector through repeated cycles of restriction-ligation (**Figure 4.3**).

In a 200 µl PCR tube, 100–200 ng of transformation vector was mixed with the PCR products in a 2:1 molar ratio of insert DNA to vector DNA. Then, 2.0 µl of T4 DNA ligase buffer (New England Biolabs, USA), which contained adenosine triphosphate (ATP), and 2.0 µl of 10× BSA (Thermo Fisher Scientific, USA) was added into the reaction tube. After that, 200–400 units of T4 DNA ligase (New England Biolabs, USA) and 10 units of the type IIS RE were added. Sterile H₂O was added to top up the reaction volume to 20 µl. Restriction-ligation was carried out according to the following thermal cycling programme: one cycle at 37°C for 20 s, 15 cycles at 37°C for 3 min and 16°C for 4 min, one cycle at 50°C for 5 min, and one cycle at 80°C for 5 min. The reaction product was cooled to 16°C and 5 µl of the product was transformed into One Shot[®] *ccdB* Survival[™] 2 T1^R Chemically Competent *E. coli* (Thermo Fisher Scientific, USA) according to the protocol described in **subchapter 4.2.1.1**. The transformed *E. coli* was plated on LB agar supplemented with 100 µg/ml ampicillin to select for ampicillin-resistant *E. coli*.

After an overnight broth culture of the selected *E. coli* colonies, the expression vectors were isolated from the bacteria according to the protocol described in **subchapter 4.2.1.4**. The expression vectors were sequenced to verify the integrity of the assembled DNA fragments.

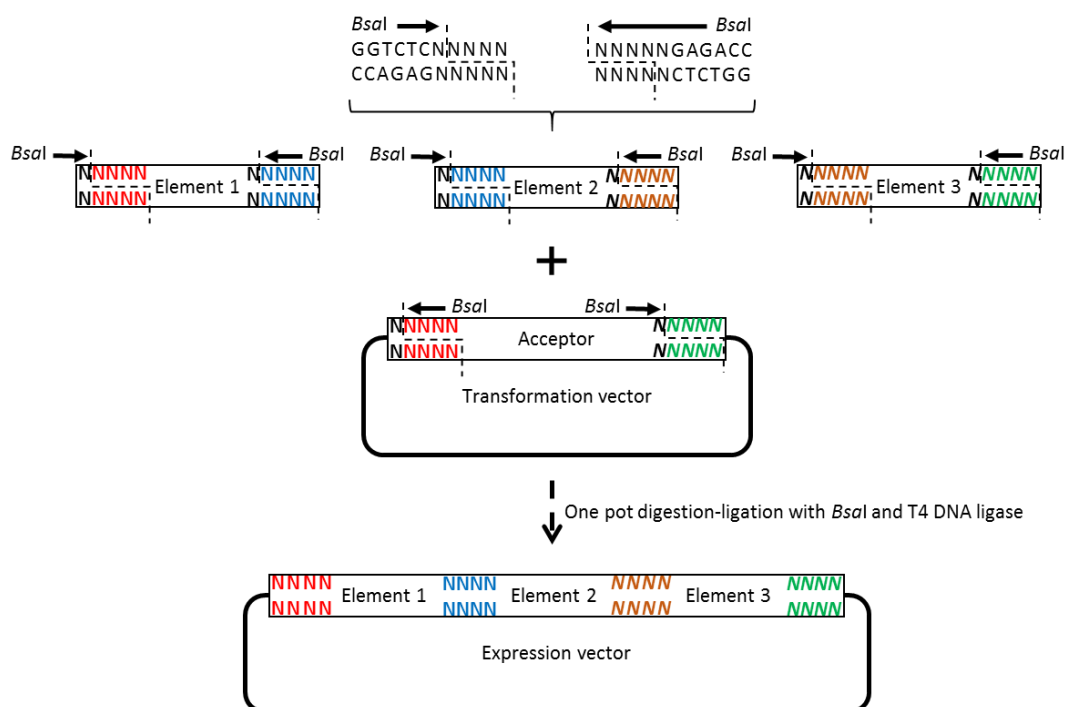


Figure 4.3 The general workflow of Golden Gate Cloning. The PCR products of target DNA fragments (elements 1, 2 and 3) were flanked by, for example, *Bsa*I recognition sites (5'-GGTCTC-3' or 5'-GAGACC-3') with their corresponding "NNNN" cutting sites downstream of the recognition sites. The **NNNN** overhang of element 1 was complementary to the **NNNN** overhang of element 2 so that they could be ligated together. The **NNNN** overhang of element 2 was complementary to the **NNNN** overhang of element 3. The **NNNN** overhang of element 1 and the **NNNN** overhang of element 3 were complementary to the **NNNN** and **NNNN** overhangs of the transformation vector, respectively. In a single tube, repeated restriction-ligation cycles with *Bsa*I and T4 DNA ligase would assemble elements 1, 2 and 3 into the transformation vector, thereby producing the final expression vector.

4.2.9 Double Restriction and Ligation for the Construction of pcDNA6.2::35Sp-sgfp

The pcDNA6.2::35Sp-sgfp expression vector was constructed using conventional double restrictions and ligation method. Primers PF/*Pst*I-35Sp-sgfp and PR/35Sp-sgfp-*Age*I (**appendix C**) were used for the

amplification of 35Sp-*sgfp* cassette from HBT vector in a 30-cycle PCR. The annealing temperature was set at 64°C and the elongation time was set at 1 min and 30 s. The PCR product was purified and then double restricted using *Pst*I and *Age*I, followed by another purification of the restriction product. The pcDNA6.2 was also double digested using *Pst*I and *Age*I. The restriction product of pcDNA6.2 was subjected to electrophoresis in an agarose gel to separate the vector backbone from the unwanted DNA fragment (*ccdB-cat*). The vector backbone was then purified from the gel. The purified 35Sp-*sgfp* cassette and the pcDNA6.2 backbone were ligated using T4 DNA ligase.

The ligation product was transformed into One Shot® TOP10 Chemically Competent *E. coli* (Thermo Fisher Scientific, USA) according to the protocol described in **subchapter 4.2.1.1**. The transformed *E. coli* was plated on LB agar supplemented with 100 µg/ml ampicillin to select for ampicillin-resistant *E. coli*. After an overnight broth culture of the selected *E. coli* colonies, the pcDNA6.2::35Sp-*sgfp* expression vector was isolated from the bacteria according to the protocol described in **subchapter 4.2.1.4**. The cloning process to produce pcDNA6.2::35Sp-*sgfp* is illustrated in **Figure 4.4**. The expression vector was sequenced to verify the integrity of the assembled cassette.

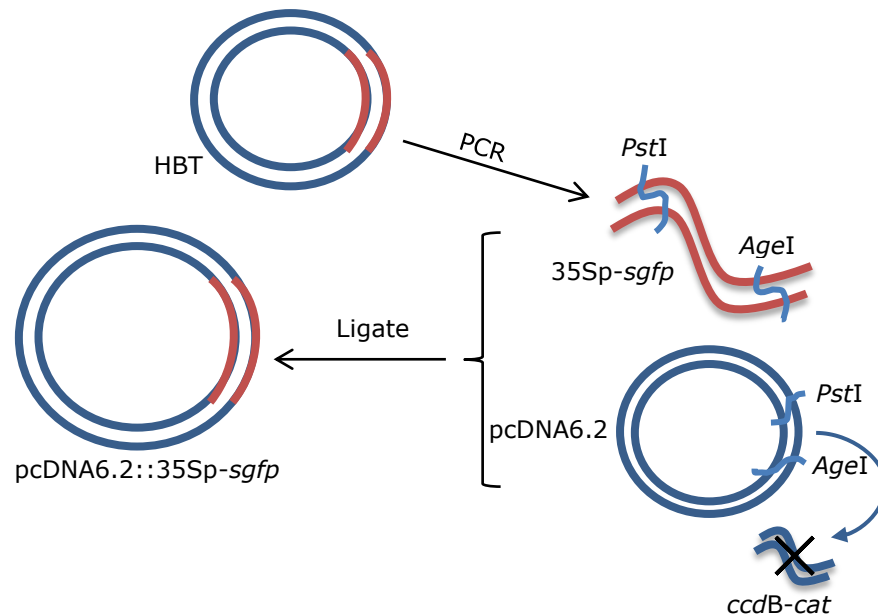


Figure 4.4 Illustration of the cloning process for pcDNA6.2::35Sp-sgfp expression vector. The 35Sp-sgfp cassette was first amplified from the HBT vector by PCR. The PCR product and pcDNA6.2 transformation vector were cut separately using *Pst*I and *Age*I to produce sticky ends. After the RE digestion of pcDNA6.2, a *ccdB-cat* fragment was removed. The sticky ends in the 35Sp-sgfp cassette was then ligated with the complementary sticky ends in the pcDNA6.2 backbone to produce pcDNA6.2::35Sp-sgfp, which was transformed and propagated in *E. coli*.

4.2.10 Gateway® Cloning for the Construction of pcDNA6.2::35Sp-fcs-NOSp-ech Expression Vector

The pcDNA6.2::35Sp-fcs-NOSp-ech expression vector was constructed using a MultiSite Gateway® Pro Kit as described in **subchapter 4.2.7**. The cloning process involved the recombination of four fragments, 35Sp, fcs, NOSp and ech, and hence the 4-fragment recombination method was used, according to the instructions in the user's manual.

4.2.10.1 BP Reactions to Create pENTR L1-35Sp-R5, pENTR L5-fcs-L4, pENTR R4-NOSp-R3 and pENTR L3-ech-L2

BP reactions were first performed to create four entry clones, pENTRs, from the recombination between the *attB*-flanked target DNA fragments (35Sp, *fcs*, NOSp and *ech*) and their corresponding pDONRTM vectors as illustrated in **Figure 4.5**. The first fragment, *attB1-35Sp-attB5r*, was amplified by PCR using PF/*attB1-35Sp* and PR/35Sp-*attB5r* primers. In the 25-cycle amplification of *attB1-35Sp-attB5r*, the annealing temperature was set at 52°C and the elongation time was set at 30 s. Then, a BP reaction was carried out between the *attB1-35Sp-attB5r* PCR product and pDONRTM P1-P5r to produce pENTR L1-35Sp-R5. The second fragment, *fcs*, was cloned directly from pUCIDT-*fcs*, which contained *fcs* flanked by *attB5* and *attB4*. A BP reaction was carried out between pUCIDT-*fcs* and pDONRTM P5-P4 to produce pENTR L5-*fcs*-L4. The third fragment, NOSp, was cloned directly from pUCIDT-NOSp, which contained the NOSp flanked by *attB4r* and *attB3r*. A BP reaction was carried out between pUCIDT-NOSp and pDONRTM P4r-P3r to produce pENTR R4-NOSp-R3. The fourth fragment, *ech*, was cloned directly from pUCIDT-*ech*, which contained the *ech* flanked by *attB3* and *attB2*. BP reaction was carried out between pUCIDT-*ech* and pDONRTM P3-P2 to produce pENTR L3-*ech*-L2.

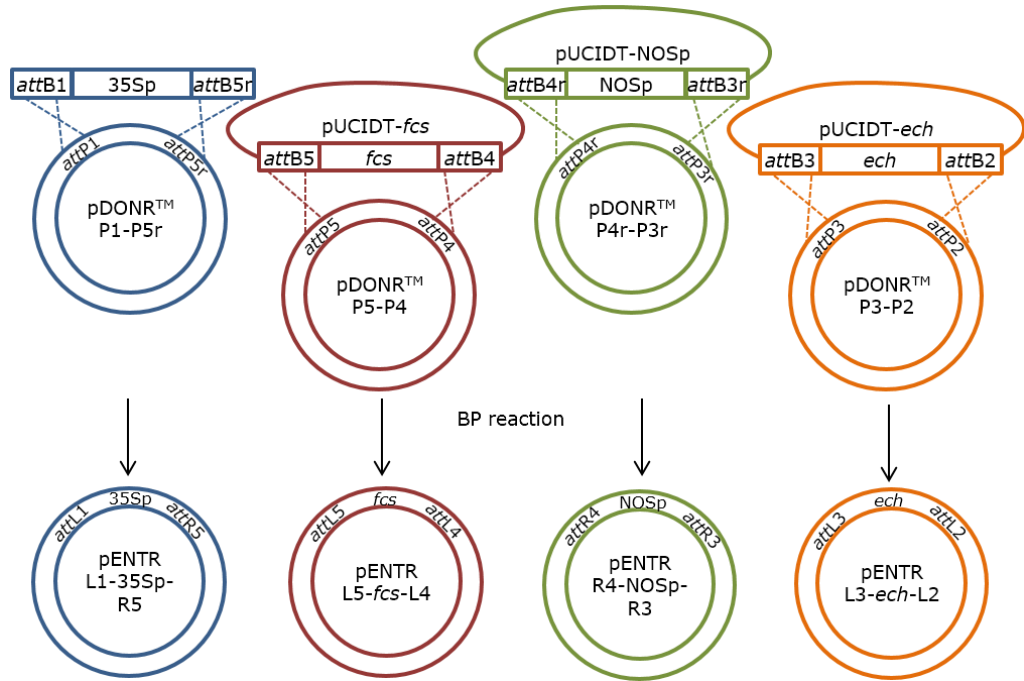


Figure 4.5 Illustration of the cloning process for BP recombination reactions between PCR amplified *attB1-35Sp-attB5r* PCR product, pUCIDT-*fcs*, pUCIDT-NOSp and pUCIDT-*ech*, and their respective donor vectors, pDONR™ P1-P5r, pDONR™ P5-P4, pDONR™ P4r-P3r and pDONR™ P3-P2, to produce entry clones, pENTR L1-35Sp-R5, pENTR L5-*fcs*-L4, pENTR R4-NOSp-R3 and pENTR L3-*ech*-L2, respectively.

4.2.10.2 LR Reaction to Create *pcDNA6.2::35Sp-fcs-NOSp-ech*

An LR reaction was performed between the entry clones, pENTR L1-35Sp-R5, pENTR L5-*fcs*-L4, pENTR R4-NOSp-R3 and pENTR L3-*ech*-L2, which was produced from the previous BP reactions (as described in **subchapter 4.2.10.1**), and the destination vector, pcDNA6.2. The cloning process in the LR reaction is illustrated in **Figure 4.6**. The recombination reaction was carried out in a 1.5 ml microcentrifuge tube by mixing 10 fmoles of each of the four pENTRs (19.5 ng of pENTR-L1-35Sp-R5, 26.7 ng of pENTR L5-*fcs*-L4, 19.2 ng of pENTR R4-NOSp-R3 and 22.6 ng of pENTR L3-*ech*-L2), and 20 fmoles (88.4 ng) of pcDNA 6.2. Subsequent steps were conducted as described in **subchapter 4.2.7.2**.

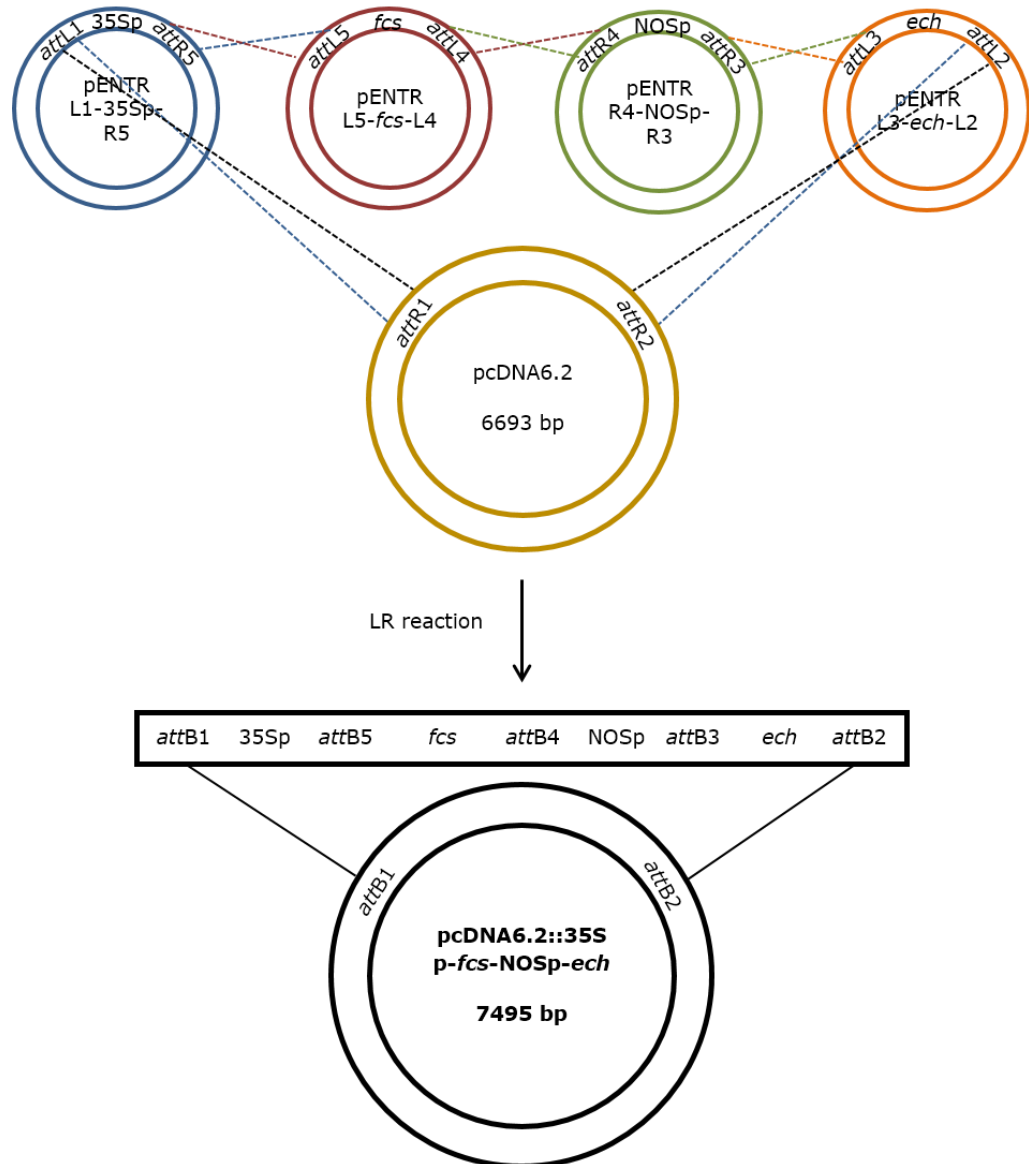


Figure 4.6 Illustration of the cloning process for LR recombination reaction between entry clones, pENTR L1-35Sp-R5, pENTR L5-*fcs*-L4, pENTR R4-NOSp-R3 and pENTR L3-*ech*-L2, and, pcDNA6.2 to produce the final expression vector, pcDNA6.2::35Sp-*fcs*-NOSp-*ech*.

4.2.11 Gateway® Cloning for the Construction of pcDNA6.2::35Sp-*fcs* Expression Vector

The pcDNA6.2::35Sp-*fcs* expression vector was constructed using MultiSite Gateway® Pro Kit as described in **subchapter 4.2.7**. The cloning process involved the recombination of two fragments, 35Sp and *fcs*, hence the 2-

fragment recombination method was used, according to the instructions in the user's manual.

4.2.11.1 BP Reaction to Create pENTR L5-fcs-L2

For the 35Sp fragment, pENTR L1-35Sp-R5 that was previously produced (as described in **subchapter 4.2.10.1**) was used. A BP reaction was performed to produce another entry clone carrying *fcs* from the recombination between *attB*-flanked *fcs* and the corresponding pDONR™ vectors, as illustrated in **Figure 4.7**. The *attB5-fcs-attB2* fragment was amplified by PCR using PF/*attB5-fcs(2)* and PR/*fcs-attB2(2)* primers. In the 25-cycle amplification of *attB1-35Sp-attB5r*, the annealing temperature was set at 54.5°C and the elongation time was set at 1.5 min. Then, BP reaction was carried out between the *attB5-fcs-attB2* PCR product and pDONR™ P5-P2 to produce pENTR L5-*fcs*-L2.

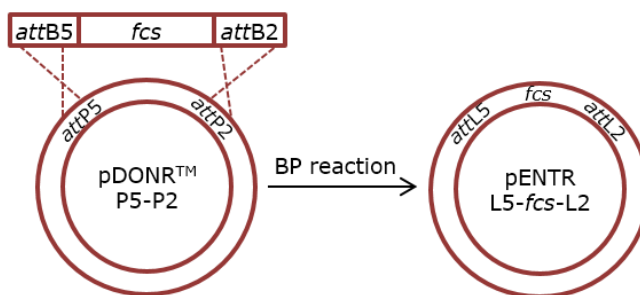


Figure 4.7 Illustration of the cloning process for BP recombination reaction between PCR amplified *attB5-fcs-attB2* cassette from pUCIDT-*fcs* and donor vector, pDONR™ P5-P2, to produce entry clone, pENTR L5-*fcs*-L2.

4.2.11.2 LR Reaction to Create pcDNA6.2::35Sp-fcs

LR reaction was performed between the entry clones, pENTR L1-35Sp-R5 and pENTR L5-*fcs*-L2, and the destination vector, pcDNA6.2. The cloning

process in the LR reaction is illustrated in **Figure 4.8**. The recombination reaction was carried out in a 1.5 ml microcentrifuge tube by mixing 10 fmoles of each of the two pENTRs (19.5 ng of pENTR-L1-35Sp-R5 and 26.7 ng of pENTR L5-*fcs*-L2), and 20 fmoles (88.4 ng) of pcDNA 6.2. Subsequent steps were conducted as described in **subchapter 4.2.7.2**.

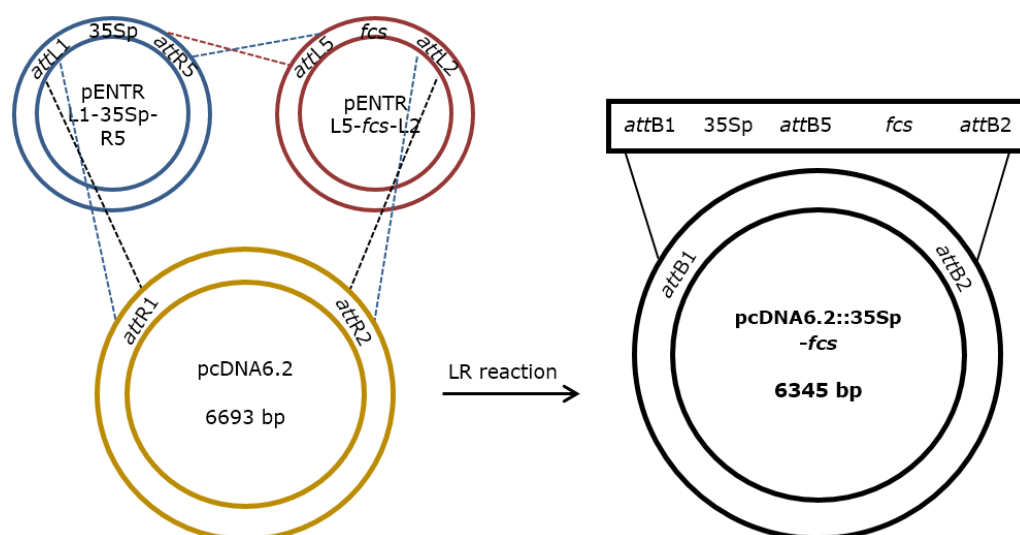


Figure 4.8 Illustration of the cloning process for LR recombination reaction between entry clones, pENTR L1-35Sp-R5 and pENTR L5-*fcs*-L2, and, pcDNA6.2 to produce the final expression vector, pcDNA6.2::35Sp-*fcs*.

4.2.12 Golden Gate Cloning for the Construction of pcDNA6.2::NOSp-*ech* Expression Vector

The pcDNA6.2::NOSp-*ech* expression vector was constructed using Golden Gate Cloning. The cloning process involved the assembly of two fragments, NOSp and *ech*, which were both incorporated with *Bsm*BI flanking sites at the 5' and 3' ends. The NOSp fragment was PCR amplified using PF/*Bsm*BI-NOSp and PR/NOSp-*Bsm*BI primers at 71°C annealing temperature and 30 s elongation time for 30 cycles. The *ech* fragment was PCR amplified using PF/*Bsm*BI-*ech* and PR/*ech*-*Bsm*BI primers at 81°C annealing temperature and 1 min elongation time for 30 cycles. PCR

products of NOSp (8.9 ng) and *ech* (30 ng) were mixed with pcDNA6.2 (100 ng), 400 units of T4 DNA ligase and 10 units of *Bsm*BI in 1× T4 DNA ligase buffer for the Golden Gate one-pot reaction (10 µl total volume). Subsequent steps were carried out according to the protocol as described in **subchapter 4.2.8**. The cloning process to produce pcDNA6.2::NOSp-*ech* is illustrated in **Figure 4.9**.

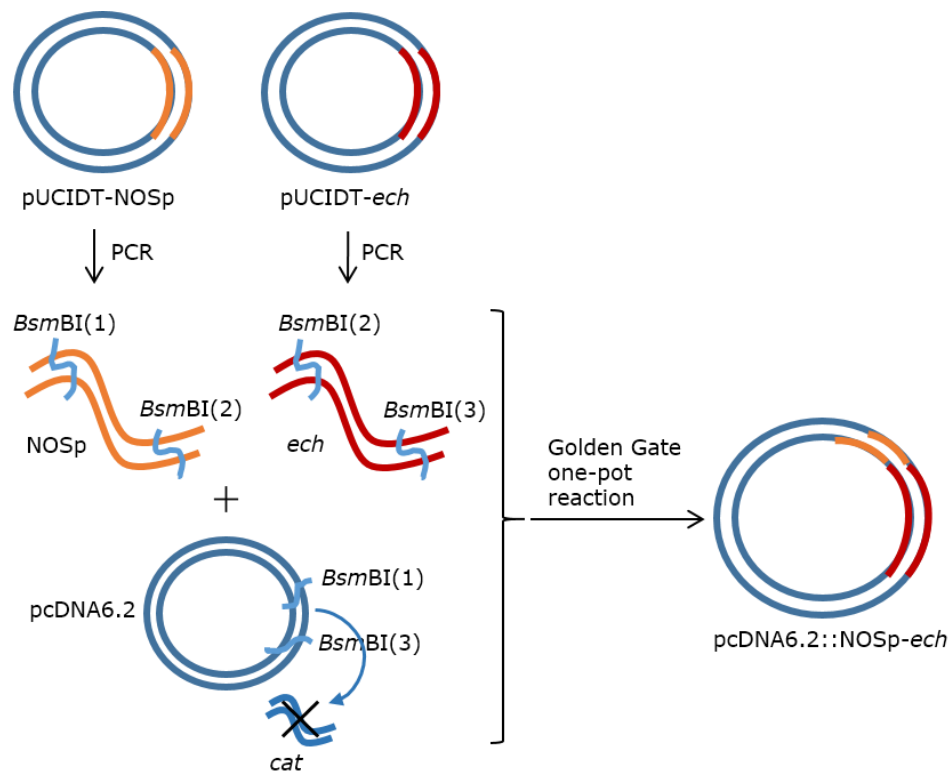


Figure 4.9 Illustration of Golden Gate Cloning to produce pcDNA6.2::NOSp-*ech* expression vector. The NOSp and *ech* fragments were first amplified by PCR from holding vectors, pUCIDT-NOSp and pUCIDT-*ech*, respectively. The PCR products and pcDNA6.2 transformation vector were mixed with *Bsm*BI and T4 DNA ligase for the one-pot reaction. During the one-pot reaction, RE digestion by *Bsm*BI left sticky ends (1) in the NOSp fragment and pcDNA6.2, which were complementary to each other. Sticky ends (2) in the NOSp fragment and the *ech* fragment were complementary to each other. Sticky ends (3) in the *ech* fragment and pcDNA6.2 were complementary to each other. RE digestion by *Bsm*BI would result in the removal of a *cat* region from pcDNA6.2. Ligation of the complementary sticky ends would result in the assembly of the NOSp-*ech* cassette into pcDNA6.2 to produce pcDNA6.2::NOSp-*ech*.

4.2.13 Double Restriction and Ligation for the Construction of pcDNA6.2::35Sp-VpVAN Expression Vector

The pcDNA6.2::35Sp-VpVAN expression vector was constructed using conventional double restrictions and ligation method. Holding vector, pUCIDT-35Sp-VpVAN, and transformation vector, pcDNA6.2, were double digested separately using *Pst*I and *Bam*HI. The restriction product of pUCIDT-35Sp-VpVAN was electrophoresed in an agarose gel to separate the unwanted vector backbone from the target cassette (35Sp-VpVAN). The target cassette was purified from the gel. The restriction product of pcDNA6.2 was electrophoresed in an agarose gel to separate the vector backbone from the unwanted DNA fragment (*Pst*I-*Bam*HI). The vector backbone was then purified from the gel. The purified 35Sp-VpVAN cassette and the pcDNA6.2 backbone were ligated using T4 DNA ligase.

The ligation product was transformed into One Shot[®] TOP10 Chemically Competent *E. coli* (Thermo Fisher Scientific, USA) according to the protocol described in **subchapter 4.2.1.1**. The transformed *E. coli* was plated on LB agar supplemented with 100 µg/ml ampicillin to select for ampicillin-resistant *E. coli*. After an overnight broth culture of the selected *E. coli* colonies, the pcDNA6.2::35Sp-VpVAN expression vector was isolated from the bacteria according to the protocol described in **subchapter 4.2.1.4**. The cloning process to produce pcDNA6.2::35Sp-VpVAN is illustrated in **Figure 4.10**. The expression vector was sequenced to verify the integrity of the assembled cassette.

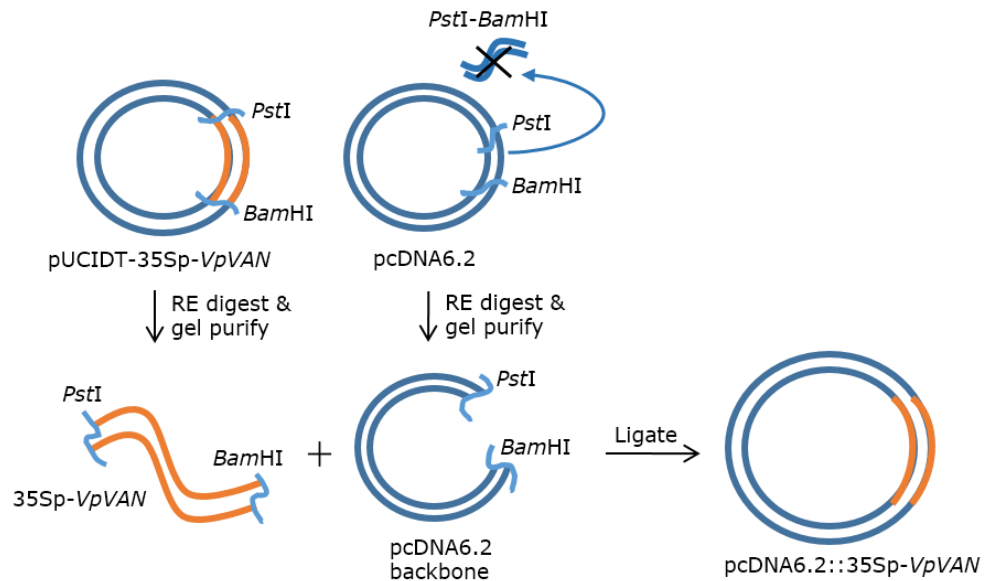


Figure 4.10 Illustration of the cloning process for *pcDNA6.2::35Sp-VpVAN* expression vector. The *35Sp-VpVAN* cassette was obtained from holding vector, *pUCIDT-35Sp-VpVAN*, by RE digestion using *PstI* and *AgeI*, followed by purification of the cassette from an agarose gel after gel electrophoresis. The *pcDNA6.2* transformation vector was also cut using *PstI* and *AgeI*. After the RE digestion of *pcDNA6.2*, a *PstI-BamHI* fragment was removed. The sticky ends in the *35Sp-sgfp* cassette was then ligated with the complementary sticky ends in the *pcDNA6.2* backbone to produce *pcDNA6.2::35Sp-VpVAN*, which was transformed and propagated in *E. coli*.

4.2.14 Golden Gate Cloning for the Construction of *pHBT12K::35Sp-VpVAN* Expression Vector

The *pHBT12K::35Sp-VpVAN* expression vector was constructed using Golden Gate Cloning. The cloning process involved the assembly of an expression cassette, *35Sp-VpVAN*, which was incorporated with *BbsI* flanking sites at the 5' and 3' ends. The *35Sp-VpVAN* cassette was PCR amplified using *PF/BbsI-35Sp-VpVAN* and *PR/35Sp-VpVAN-BbsI* primers at 60°C annealing temperature and 1.5 min elongation time for 30 cycles. PCR product of *35Sp-VpVAN* (84.9 ng) was mixed with *pHBT12K* (200 ng), 200 units of T4 DNA ligase and 10 units of *BbsI* in 1× T4 DNA ligase buffer for the Golden Gate one-pot reaction (15 µl total volume). Subsequent steps were carried out according to the protocol as described in

subchapter 4.2.8. The cloning process to produce pHBT12K::35Sp-VpVAN is illustrated in **Figure 4.11**.

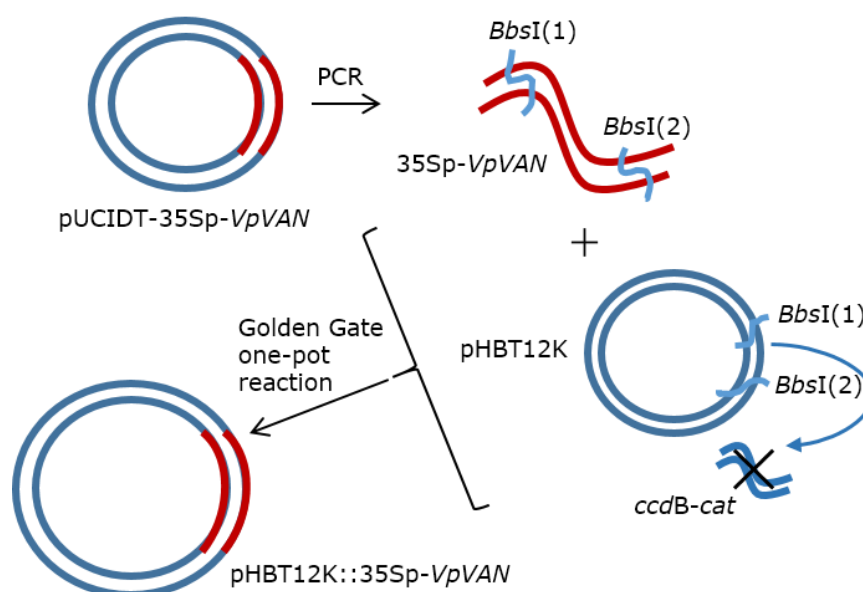


Figure 4.11 Illustration of Golden Gate Cloning to produce pHBT12K::35Sp-VpVAN expression vector. The 35Sp-VpVAN cassette was amplified by PCR from holding vectors, pUCIDT-35Sp-VpVAN. The PCR product and pHBT12K transformation vector were mixed with *BbsI* and T4 DNA ligase for the one-pot reaction. During the one-pot reaction, RE digestion by *BbsI* left sticky ends (1) in the 35Sp-VpVAN cassette, which were complementary to each other. Sticky ends (2) in the 35Sp-VpVAN cassette were complementary to each other. RE digestion by *BbsI* would result in the removal of a *ccdB-cat* region from pHBT12K. Ligation of the complementary sticky ends would result in the assembly of the 35Sp-VpVAN cassette into pHBT12K to produce pHBT12K::35Sp-VpVAN.

4.3 RESULTS

4.3.1 Construction of pcDNA6.2::35Sp-sgfp

A PCR of 35Sp-sgfp cassette from HBT using PF/*PstI*-35Sp-sgfp and PR/35Sp-sgfp-*AgeI* primers (**Appendix C**) was performed during the construction of pcDNA6.2::35Sp-sgfp via double restrictions and ligation. A band of ~1.3 kb was obtained, which corresponded to the size of the 35Sp-sgfp cassette (~1303 bp) (**Figure 4.12**). After that, RE digestion of pcDNA6.2 with *PstI* and *AgeI* yielded two DNA bands of ~4.9 kb and ~1.8

kb, which corresponded to the expected sizes of the resulting vector backbone (4879 bp) and the disposed *PstI*-*AgeI* fragment (1814 bp), respectively (**Figure 4.13**). Following subsequent ligation, propagation and isolation from *E. coli*, the recombinant vector was evaluated by PCR and sequencing. PCR using PF/*PstI*-35Sp-*sgfp* and PR/35Sp-*sgfp*-*AgeI* primers (**Appendix C**) gave a band of ~1.3 kb, confirming the presence of the 35Sp-*sgfp* in the recombinant expression vector (**Figure 4.14**). The sequencing results further confirmed the presence of 35Sp-*sgfp* in the correct orientation in the expression vector, pcDNA6.2::35Sp-*sgfp* (**Appendix E(i)**). A schematic diagram of the resulting 35Sp-*sgfp* cassette in the construction of pcDNA6.2::35Sp-*sgfp* is shown in **figure 4.15**.

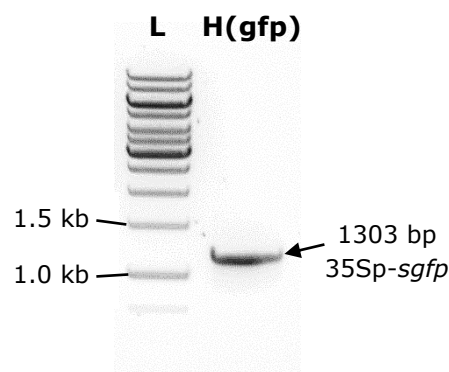


Figure 4.12 PCR profile of the 35Sp-*sgfp* cassette (1303 bp) amplified from plasmid, HBT, using PF/*PstI*-35Sp-*sgfp* and PR/35Sp-*sgfp*-*AgeI* primers. L: GeneRuler 1kb DNA ladder, H(gfp): 35Sp-*sgfp* from HBT.



Figure 4.13 RE digestion profile of pcDNA6.2 using REs, *PstI* and *AgeI*, resulting in two fragments, the pcDNA6.2 backbone (4879 bp) and the *PstI*-*AgeI* region (1814 bp). L: GeneRuler 1kb DNA ladder, pc: pcDNA6.2.

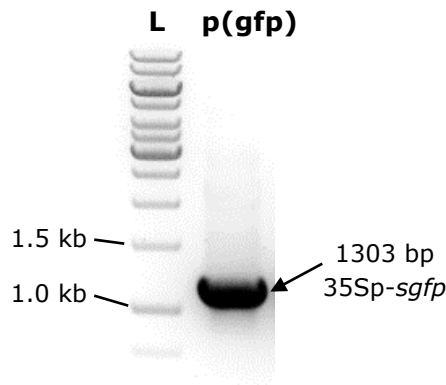


Figure 4.14 PCR profile of the 35Sp-*sgfp* cassette (1303 bp) amplified from the expression vector, pcDNA6.2::35Sp-*sgfp*, using PF/*Pst*I-35Sp-*sgfp* and PR/35Sp-*sgfp*-*Age*I primers. L: GeneRuler 1kb DNA ladder, p(gfp): 35Sp-*sgfp* from pcDNA6.2::35Sp-*sgfp*.

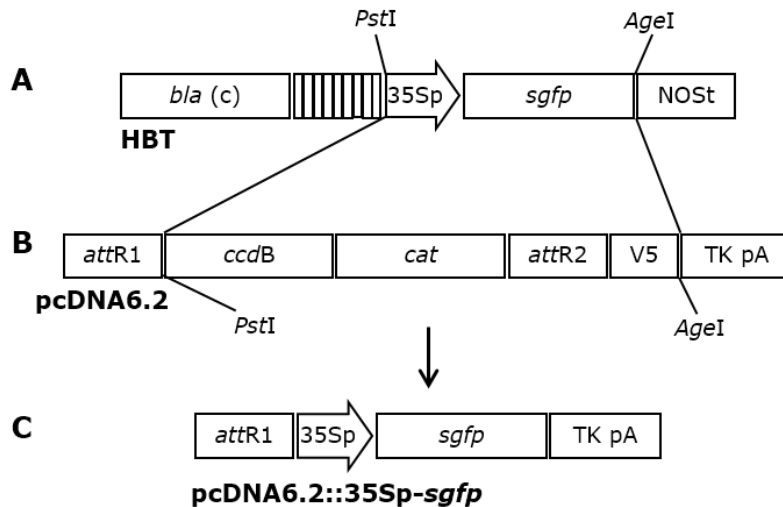


Figure 4.15 Schematic diagram for the resulting 35Sp-*sgfp* cassette in the construction of pcDNA6.2::35Sp-*sgfp*. A: The 35Sp-*sgfp* cassette was amplified from HBT. B: The *Pst*I-*Age*I fragment containing *ccdB* and *cat* genes, *attR2* site and V5 epitope was removed from pcDNA6.2 after double RE digestion with *Pst*I and *Age*I. The amplified 35Sp-*sgfp* cassette was cloned into the backbone of pcDNA6.2 via ligation. C: The final expression vector, pcDNA6.2::35Sp-*sgfp*, contained the 35Sp-*sgfp* cassette.

4.3.2 Construction of pcDNA6.2::35Sp-*fcs*-NOSp-*ech*

In the construction of pcDNA6.2::35Sp-*fcs*-NOSp-*ech* via Gateway® Cloning, four target DNA fragments, *attB1*-35Sp-*attB5r*, *attB5-fcs-attB4*, *attB4r*-NOSp-*attB3r* and *attB3-ech-attB2*, were cloned separately into the corresponding donor vectors through BP reactions. For the *attB1*-35Sp-*attB5r* fragment, PCR of *attB1*-35Sp-*attB5r* from HBT using PF/*attB1*-35Sp and PR/35Sp-*attB5r* primers (**Appendix C**) produced a band of ~400 bp, which corresponded to the size of the 35Sp fragment (~407 bp) (**Figure 4.16**). After the BP reaction to clone *attB1*-35Sp-*attB5r* into pDONR™ P1-P5r, the resulting entry clone (pENTR L1-35Sp-R5) was produced. For the *attB5-fcs-attB4* fragment, a direct BP reaction between pUCIDT-*fcs* and pDONR™ P5-P4 produced pENTR L5-*fcs*-L4 entry clone. For the *attB4r*-NOSp-*attB3r* fragment, a direct BP reaction between pUCIDT-NOSp and pDONR™ P4r-P3r produced the entry clone, pENTR R4-NOSp-R3. For the *attB3-ech-attB2* fragment, a direct BP reaction between pUCIDT-*ech* and pDONR™ P3-P2 produced the entry clone, pENTR L3-*ech*-L2. The individual entry clones were linearised with *PvuI* and resulted in DNA bands of ~3.0 kb, ~4.0 kb, ~3.0 kb and ~3.5 kb, which corresponded to the expected sizes of pENTR L1-35Sp-R5 (~2958 bp), pENTR L5-*fcs*-L4 (~4050 bp), pENTR R4-NOSp-R3 (~2906 bp) and pENTR L3-*ech*-L2 (~3418 bp), respectively (**Figure 4.17**).

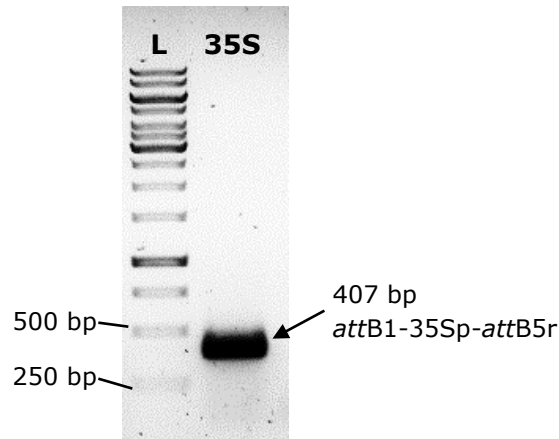


Figure 4.16 PCR profile of the *attB1-35Sp-attB5r* fragment (407 bp) amplified from HBT plasmid, using PF/*attB1-35Sp* and PR/*35Sp-attB5r* primers. L: GeneRuler 1kb DNA ladder, 35S: *attB1-35Sp-attB5r*.

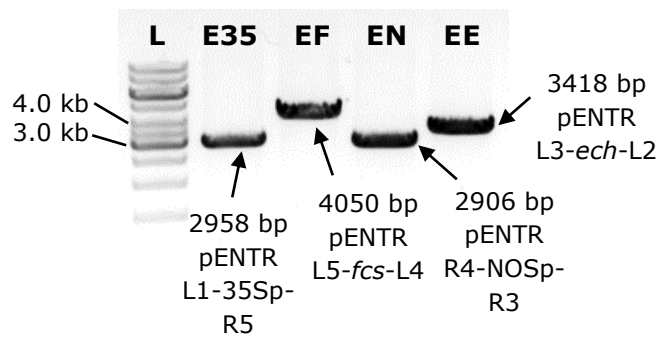


Figure 4.17 RE digestion profiles of pENTR L1-35Sp-R5 (2958 bp), pENTR L5-*fcs*-L4 (4050 bp), pENTR R4-NOSp-R3 (2906 bp) and pENTR L3-*ech*-L2 (3418 bp) using RE, *PvuI*. L: GeneRuler 1kb DNA ladder, E35: pENTR L1-35Sp-R5, EF: pENTR L5-*fcs*-L4, EN: pENTR R4-NOSp-R3, EE: pENTR L3-*ech*-L2.

An LR reaction between the four entry clones, pENTR L1-35Sp-R5, pENTR L5-*fcs*-L4, pENTR R4-NOSp-R3, pENTR L3-*ech*-L2, and the destination vector, pcDNA6.2, produced the final expression vector (pcDNA6.2::*35Sp-fcs-NOSp-ech*). Individual PCRs using the corresponding primer pairs and their respective annealing temperatures (**Appendix C**) confirmed the presence of individual target fragments in pcDNA6.2::*35Sp-*

fcs-NOSp-*ech* (**Figure 4.18**), as follows (the final MgCl₂ concentration in each PCR reaction tube was 1.5 mM, unless stated otherwise): PCR using PF/*attB1*-35Sp and PR/35Sp-*attB5r* primers produced a band of ~400 bp, which corresponded to the correct size of 35Sp (~407 bp). PCR at a final MgCl₂ concentration of 3.0 mM using PF/*fcs* and PR/*fcs* primers produced a band of ~1.5 kb, which corresponded to the correct size of *fcs* (~1473 bp). PCR using PF/NOSp and PR/NOSp primers produced a band of ~250 bp, which corresponded to the correct size of NOSp (~233 bp). PCR using PF/*ech* and PR/*ech* primers produced a band of ~900 bp, which corresponded to the correct size of *ech* (~861 bp). DNA sequencing of the expression cassette confirmed the integrity of the cloned DNA fragments in the correct orientation (**Appendix E(ii)**). A schematic diagram of the resulting 35Sp-*fcs*-NOSp-*ech* cassette in the construction of pcDNA6.2::35Sp-*fcs*-NOSp-*ech* is shown in **figure 4.19**.

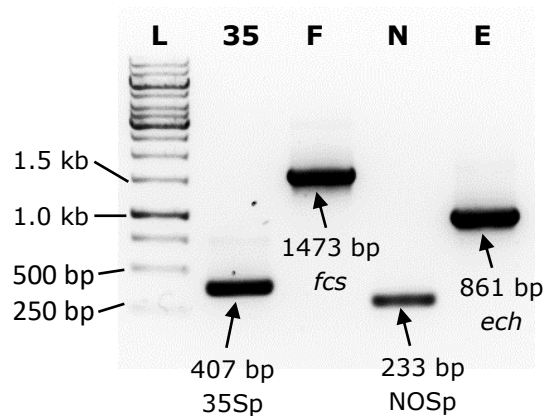


Figure 4.18 PCR profiles of 35Sp (407 bp), *fcs* (1534 bp), NOSp (233 bp) and *ech* (922 bp) from the expression vector, pcDNA6.2::35Sp-*fcs*-NOSp-*ech*. L: GeneRuler 1kb DNA ladder, 35: 35Sp, F: *fcs*, N: NOSp, E: *ech*.

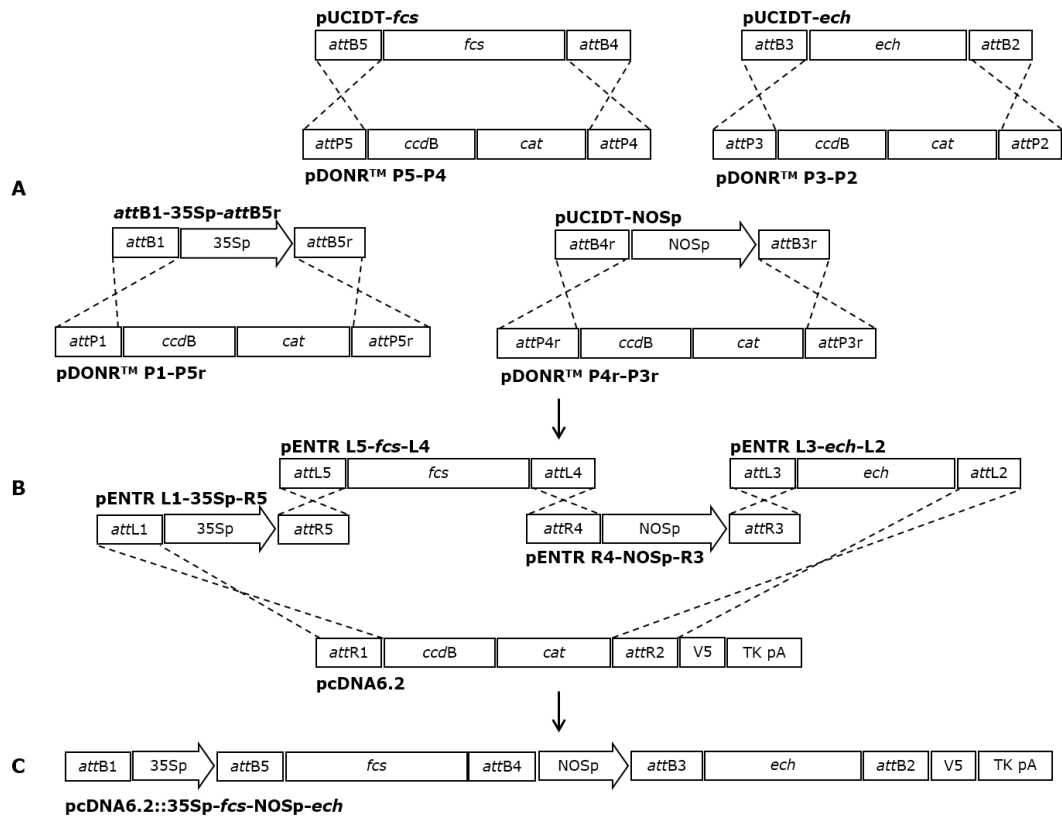


Figure 4.19 Schematic diagram for the resulting 35Sp-*fcs*-NOSp-*ech* cassette in the construction of pcDNA6.2::35Sp-*fcs*-NOSp-*ech*. A: The *attB1*-35Sp-*attB5r* fragment, pUCIDT-*fcs*, pUCIDT-NOSp and pUCIDT-*ech* underwent recombination through BP reactions with pDONR™ P1-P5r, pDONR™ P5-P4, pDONR™ P4r-P3r and pDONR™ P3-P2, respectively. B: The resulting pENTR L1-35Sp-R5, pENTR L5-*fcs*-L4, pENTR R4-NOSp-R3 and pENTR L3-*ech*-L2 from BP reactions then underwent another recombination with each other and with pcDNA6.2 through LR reaction. C: The product of the LR reaction was the final expression vector, pcDNA6.2::35Sp-*fcs*-NOSp-*ech*, which contained the 35Sp-*fcs*-NOSp-*ech* cassette.

4.3.3 Construction of pcDNA6.2::35Sp-*fcs*

In the construction of pcDNA6.2::35Sp-*fcs* via Gateway® Cloning, *attB5-fcs-attB2* was cloned into pDONR™ P5-P2 through a BP reaction. A PCR of *attB5-fcs-attB2* from pUCIDT-*fcs* using PF/*attB5-fcs*(2) and PR/*fcs-attB2*(2) primers (**Appendix C**) produced a band of ~1.5 kb, which corresponded to the correct size of *attB5-fcs-attB2* (~1576 bp) (**Figure 4.20**). After the BP reaction, entry clone, pENTR L5-*fcs*-L2, was produced. The entry clone was linearised with *PvuI* and resulted in a DNA band of ~4.0 kb, which

corresponded to the expected size of pENTR L5-*fcs*-L2 (~4075 bp) (**Figure 4.21**).

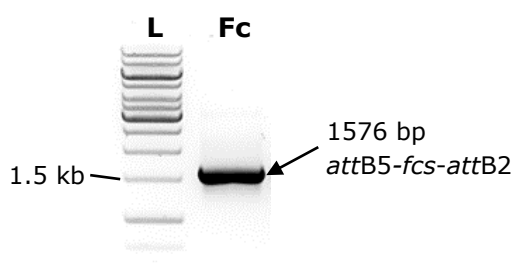


Figure 4.20 PCR profile of the *attB5-fcs-attB2* fragment (1576 bp) amplified from holding vector, pUCIDT-*fcs*, using PF/*attB5-fcs*(2) and PR/*fcs-attB2*(2) primers. L: GeneRuler 1kb DNA ladder, Fc: *attB5-fcs-attB2*.

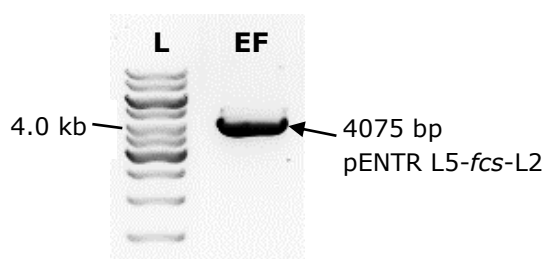


Figure 4.21 RE digestion profile of pENTR L5-*fcs*-L2 (4075 bp) using RE, PvuI. L: GeneRuler 1kb DNA ladder, EF: pENTR L5-*fcs*-L2.

An LR reaction between the two entry clones, pENTR L1-35Sp-R5 (from **subchapter 4.2.10.1**) and pENTR L5-*fcs*-L2, and the destination vector, pcDNA6.2, produced the final expression vector (pcDNA6.2::35Sp-*fcs*). Individual PCRs using the corresponding primer pairs (**appendix C**) confirmed the presence of the individual target fragments in the expression vector, pcDNA6.2::35Sp-*fcs* (**Figure 4.22**), as follows: PCR using PF/*attB1*-35Sp and PR/35Sp-*attB5r* primers produced a band of ~400 bp, which corresponded to the correct size of 35Sp (~407 bp). PCR using PF/*attB5-fcs*(2) and PR/*fcs-attB2*(2) primers produced a band of ~1.5 kb, which corresponded to the correct size of *fcs* (~1576 bp). DNA sequencing

of the expression cassette confirmed the integrity of the cloned DNA fragments in the correct orientation (**appendix E(iii)**). A schematic diagram of the resulting 35Sp-*fcs* cassette in the construction of pcDNA6.2::35Sp-*fcs* is shown in **figure 4.23**.

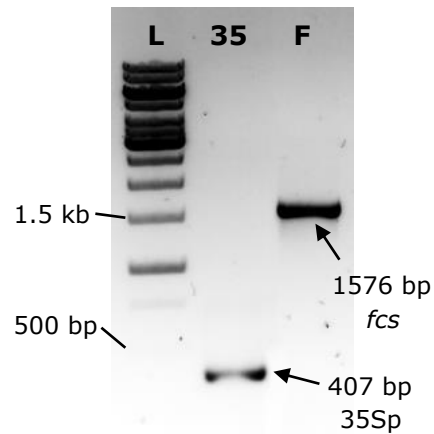


Figure 4.22 PCR profile of the 35Sp fragment (407 bp) and the *fcs* fragment (1576 bp), which were amplified from pcDNA6.2::35Sp-*fcs* expression vector using primer pairs "PF/*attB1*-35Sp and PR/35Sp-*attB5r*" and "PF/*attB5-fcs*(2) and PR/*fcs-attB2*(2)," respectively. L: GeneRuler 1kb DNA ladder, 35: 35Sp, F: *fcs*.

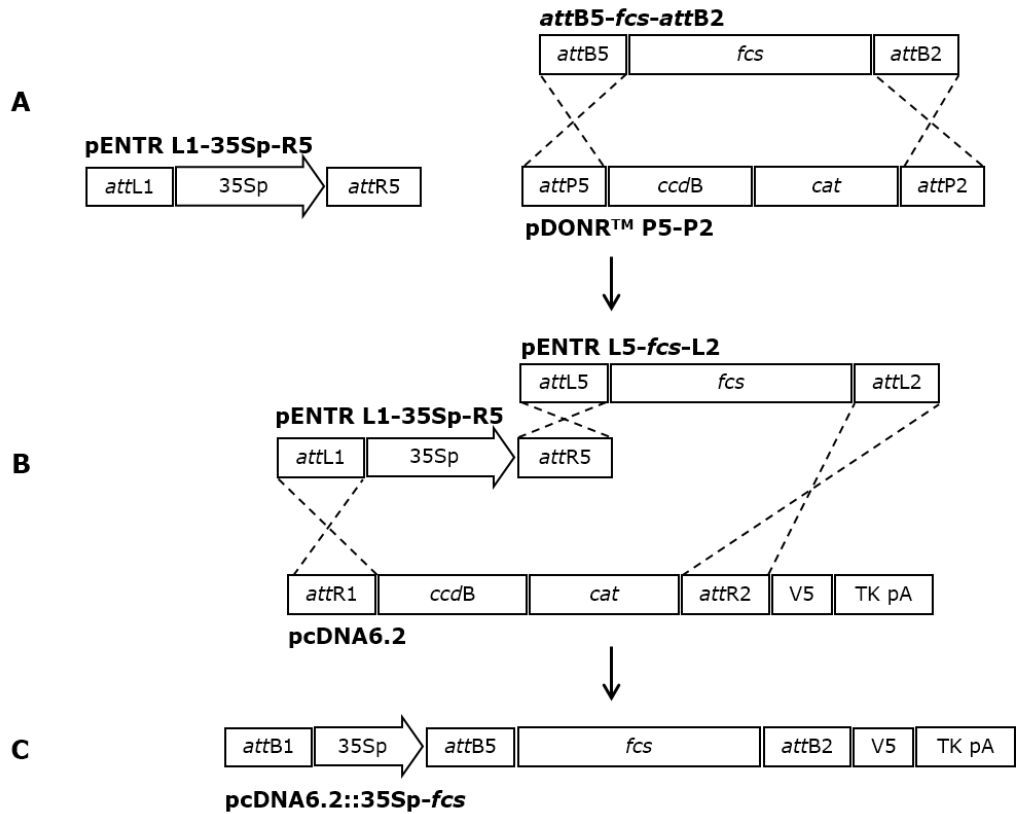


Figure 4.23 Schematic diagram for the resulting 35Sp-*fcs* cassette in the construction of pcDNA6.2::35Sp-*fcs* A: The PCR amplified *attB5-fcs-attB2* fragment from pUCIDT-*fcs* underwent recombination through BP reaction with pDONR™ P5-P2. Entry clone carrying the *attL1-35Sp-attR5* fragment, pENTR L1-35Sp-R5, was previously created as described in subchapter 4.2.10.1. B: The resulting pENTR L5-*fcs-L2* from the BP reaction and the pENTR L1-35Sp-R5 then underwent another recombination with each other and with pcDNA6.2 through LR reaction. C: The product of the LR reaction was the final expression vector, pcDNA6.2::35Sp-*fcs*, which contained the 35Sp-*fcs* cassette.

4.3.4 Construction of pcDNA6.2::NOSp-*ech*

In the construction of pcDNA6.2::NOSp-*ech* expression vector using Golden Gate Cloning, PCR of NOSp from pUCIDT-NOSp using PF/*BsmBI*-NOSp and PR/NOSp-*BsmBI* primers (**Appendix C**) produced a band of ~300 bp, which corresponded to the correct size of NOSp (~273 bp) (**Figure 4.24**). PCR of *ech* from pUCIDT-*ech* using PF/*BsmBI*-*ech* and PR/*ech*-*BsmBI* primers (**Appendix C**) produced a band of ~900 bp, which corresponded to the correct size of *ech* (~922 bp) (**Figure 4.25**).

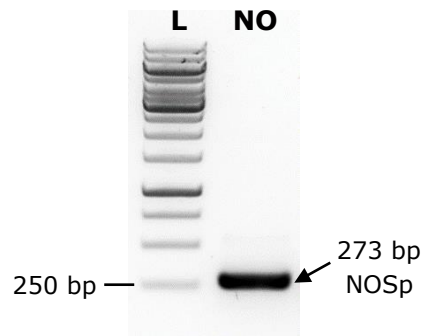


Figure 4.24 PCR profile of the NOSp fragment (273 bp) amplified from holding vector, pUCIDT-NOSp, using PF/*Bsm*BI-NOSp and PR/NOSp-*Bsm*BI primers. L: GeneRuler 1kb DNA ladder, NO: NOSp.

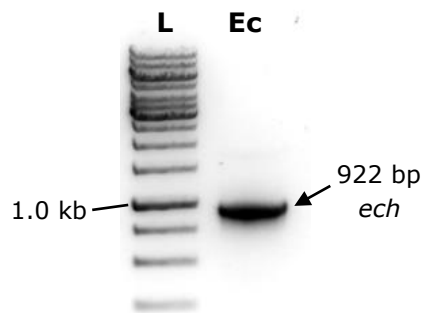


Figure 4.25 PCR profile of the *ech* fragment (922 bp) amplified from holding vector, pUCIDT-*ech*, using PF/*Bsm*BI-*ech* and PR/*ech*-*Bsm*BI primers. L: GeneRuler 1kb DNA ladder, Ec: *ech*.

Following the one-pot reaction, propagation and isolation from *E. coli*, the recombinant vector was evaluated by PCR and sequencing. Individual PCRs using the corresponding primer pairs (**Appendix C**) confirmed the presence of the individual target fragments in the expression vector, pcDNA6.2::NOSp-*ech* (**Figure 4.26**), as follows: PCR using PF/*Bsm*BI-NOSp and PR/NOSp-*Bsm*BI primers produced a band of ~300 bp, which corresponded to the correct size of NOSp (~273 bp). PCR using

PF/*Bsm*BI-*ech* and PR/*ech*-*Bsm*BI primers produced a band of ~900 bp, which corresponded to the correct size of *fcs* (~922 bp). DNA sequencing of the expression cassette confirmed the integrity of the cloned DNA fragments in the correct orientation (**Appendix E(iv)**). Schematic diagram of the resulting NOSp-*ech* cassette in the construction of pcDNA6.2::NOSp-*ech* is shown in **figure 4.27**.

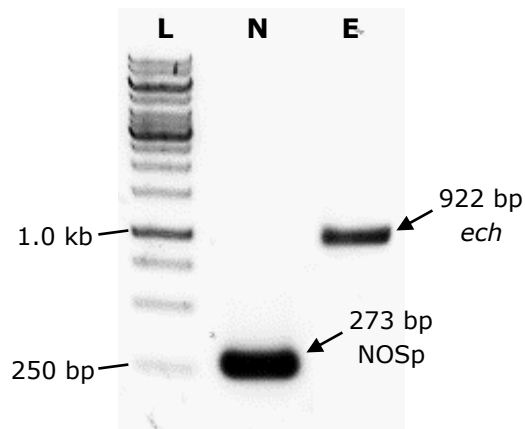


Figure 4.26 PCR profile of the NOSp fragment (273 bp) and the *ech* fragment (922 bp), which were amplified from pcDNA6.2::NOSp-*ech* expression vector using primer pairs "PF/*Bsm*BI-NOSp and PR/NOSp-*Bsm*BI" and "PF/*Bsm*BI-*ech* and PR/*ech*-*Bsm*BI," respectively. L: GeneRuler 1kb DNA ladder, N: NOSp, E: *ech*.

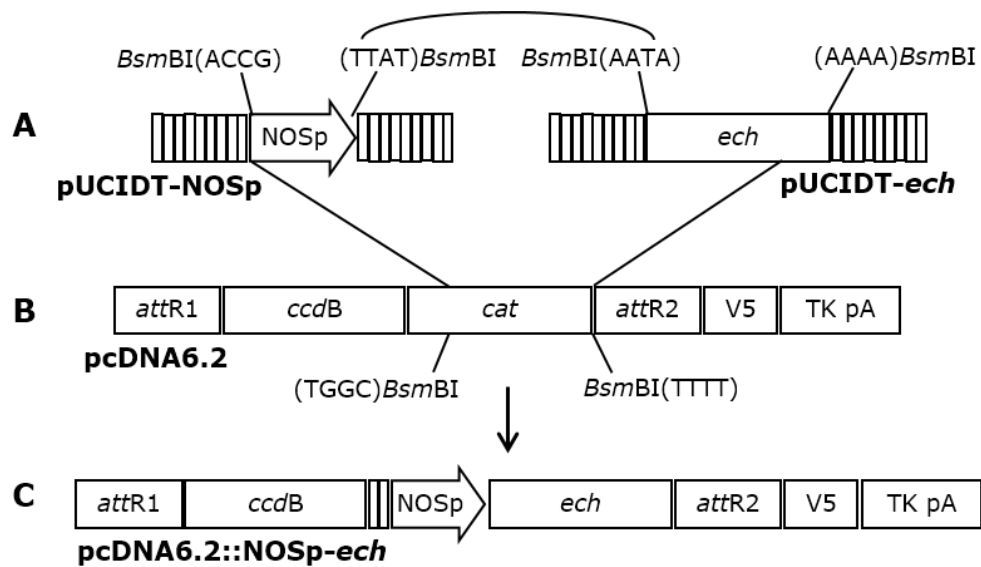


Figure 4.27 Schematic diagram for the resulting NOSp-*ech* cassette in the construction of pcDNA6.2::NOSp-*ech*. A: The NOSp fragment was amplified from pUCIDT-NOSp, and the *ech* fragment was amplified from pUCIDT-*ech*. B: During the one-pot reaction, repeated RE digestion with *Bsm*BI resulted in the removal of *cat* region and ligation of the complementary sticky ends resulted in the assembly of NOSp and *ech* into pcDNA6.2. *Bsm*BI(NNNN) and (NNNN)*Bsm*BI denote the overhang sequences of the sticky ends that were produced downstream and upstream of the *Bsm*BI recognition sites, respectively, following RE digestion. C: The final expression vector, pcDNA6.2::NOSp-*ech*, contained the NOSp-*ech* cassette.

4.3.5 Construction of pcDNA6.2::35Sp-VpVAN

RE digestions with *Pst*I and *Bam*HI, followed by purification of 35Sp-VpVAN cassette from pUCIDT-35Sp-VpVAN, were performed during the construction of pcDNA6.2::35Sp-VpVAN via double restrictions and ligation. Two bands of ~2.8 kb and ~1.5 kb were obtained, which corresponded to the sizes of the separated pUCIDT backbone (~2786 bp) and 35Sp-VpVAN cassette (~1460 bp), respectively (**Figure 4.28**). After that, the RE digestion of pcDNA6.2 with *Pst*I and *Bam*HI yielded two DNA bands of ~6.0 kb and ~700 bp, which corresponded to the expected sizes of the resulting vector backbone (6028 bp) and the disposed *Pst*I-*Bam*HI fragment (665 bp), respectively (**Figure 4.29**). Following subsequent ligation, propagation and isolation from *E. coli*, the recombinant expression vector was evaluated by RE digestion using *Pst*I and *Bam*HI. Two bands of ~6.0

kb and ~1.5 kb were obtained, confirming the correct sizes of the pcDNA6.2 backbone (~6028 bp) and the 35Sp-VpVAN cassette (~1460 bp), respectively (**Figure 4.30**). Sequencing results further confirmed the presence of 35Sp-VpVAN in the correct orientation in the expression vector, pcDNA6.2::35Sp-VpVAN (**Appendix E(v)**). Schematic diagram of the resulting 35Sp-VpVAN cassette in the construction of pcDNA6.2::35Sp-VpVAN is shown in **figure 4.31**.

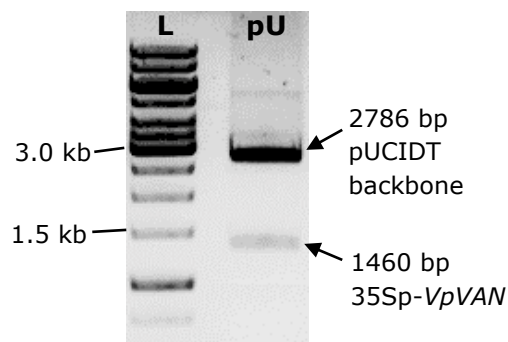


Figure 4.28 RE digestion profile of pUCIDT-35Sp-VpVAN using REs, *Pst*I and *Bam*HI, resulting in two fragments, the pUCIDT backbone (2786 bp) and the 35Sp-VpVAN cassette (1460 bp). L: GeneRuler 1kb DNA ladder, pU: pUCIDT-35Sp-VpVAN.

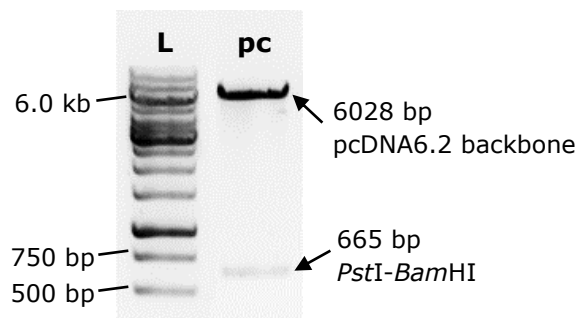


Figure 4.29 RE digestion profile of pcDNA6.2 using REs, *Pst*I and *Bam*HI, resulting in two fragments, the pcDNA6.2 backbone (6028 bp) and the *Pst*I-*Bam*HI region (665 bp). L: GeneRuler 1kb DNA ladder, pU: pcDNA6.2.

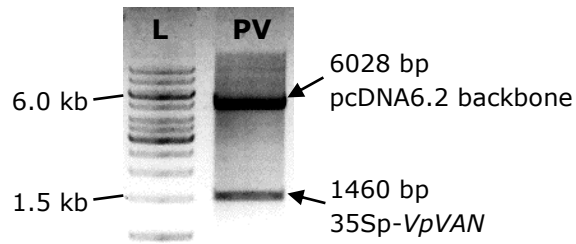


Figure 4.30 RE digestion profile of pcDNA6.2::35Sp-VpVAN using REs, *Pst*I and *Bam*HI, resulting in two fragments, the pcDNA6.2 backbone (6028 bp) and the 35Sp-VpVAN cassette (1460 bp). L: GeneRuler 1kb DNA ladder, PV: pcDNA6.2::35Sp-VpVAN.

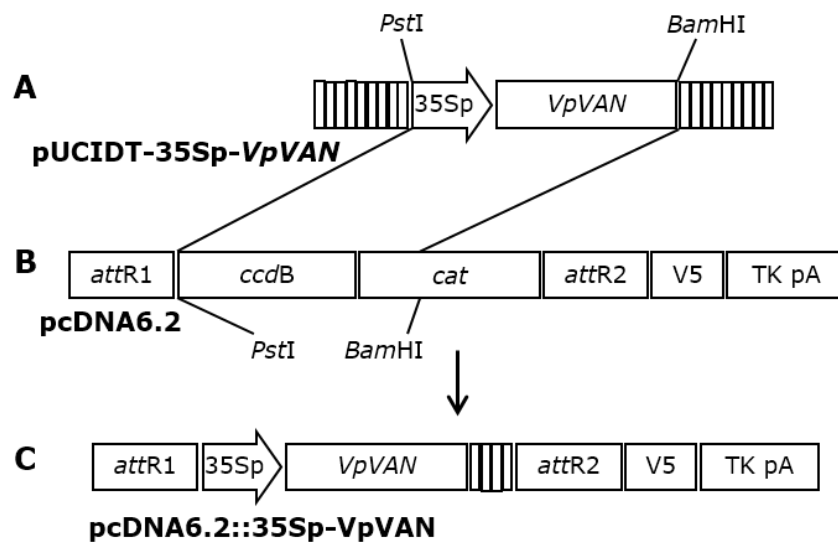


Figure 4.31 Schematic diagram for the resulting 35Sp-VpVAN cassette in the construction of pcDNA6.2::35Sp-VpVAN. A: The 35Sp-VpVAN cassette was purified after RE digestion with *Pst*I and *Bam*HI. B: The *Pst*I-*Bam*HI fragment containing *ccd*B and *cat* genes was removed from pcDNA6.2 after double RE digestion with *Pst*I and *Bam*HI. The 35Sp-VpVAN cassette was cloned into the backbone of pcDNA6.2 via ligation. C: The final expression vector, pcDNA6.2::35Sp-VpVAN, contained the 35Sp-VpVAN cassette.

4.3.6 Construction of pHBT12K::35Sp-VpVAN

In the construction of pHBT12K::35Sp-VpVAN expression vector using Golden Gate Cloning, a PCR of 35Sp-VpVAN from pUCIDT-35Sp-VpVAN using PF/BbsI-35Sp-VpVAN and PR/35Sp-VpVAN-BbsI primers (**Appendix C**) produced a band of ~1.5 kb, which corresponded to the correct size of 35Sp-VpVAN (~1505 bp) (**Figure 4.32**).

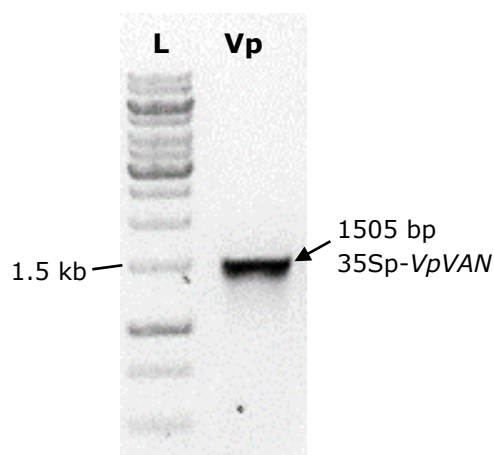


Figure 4.32 PCR profile of the 35Sp-VpVAN cassette (1505 bp) amplified from holding vector, pUCIDT-35Sp-VpVAN, using PF/BbsI-35Sp-VpVAN and PR/35Sp-VpVAN-BbsI primers. L: GeneRuler 1kb DNA ladder, Vp: 35Sp-VpVAN.

Following the one-pot reaction, propagation and isolation from *E. coli*, the recombinant expression vector was evaluated by RE digestion using *BbsI* and sequencing. Two bands of ~4.5 kb and ~1.5 kb were obtained, confirming the correct sizes of the pHBT12K backbone (~4595 bp) and the 35Sp-35Sp-VpVAN cassette (~1477 bp), respectively (**Figure 4.33**). Sequencing results further confirmed the presence of 35Sp-VpVAN in the correct orientation in the expression vector, pHBT12K::35Sp-VpVAN (**Appendix E(vi)**). A schematic diagram of the resulting 35Sp-VpVAN

cassette in the construction of pHBT12K::35Sp-VpVAN is shown in **figure 4.34**.

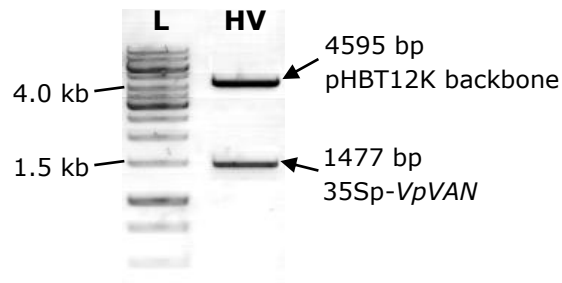


Figure 4.33 RE digestion profile of pHBT12K::35Sp-VpVAN using RE, *BbsI*, resulting in two fragments, the pHBT12K backbone (4595 bp) and the 35Sp-VpVAN cassette (1477 bp). L: GeneRuler 1kb DNA ladder, HV: pHBT12K::35Sp-VpVAN.

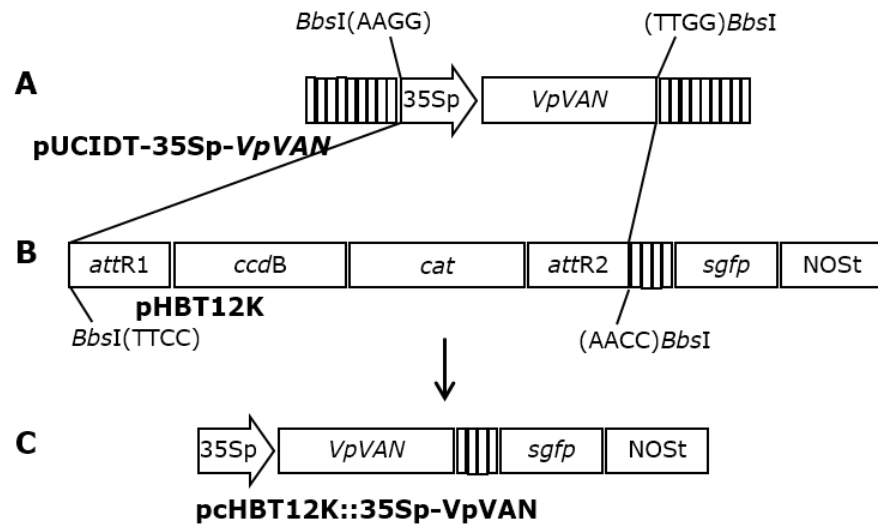


Figure 4.34 Schematic diagram for the resulting 35Sp-VpVAN cassette in the construction of pHBT12K::35Sp-VpVAN. A: The 35Sp-VpVAN cassette was amplified from pUCIDT-35Sp-VpVAN. B: During the one-pot reaction, repeated RE digestion with *BbsI* resulted in the removal of the *attR1-ccdB-cat-attR2* region and ligation of the complementary sticky ends resulted in the assembly of 35Sp-VpVAN into pHBT12K. *BbsI*(NNNN) and (NNNN)*BbsI* denote the overhang sequences of the sticky ends that were produced downstream and upstream of the *BbsI* recognition sites, respectively, following RE digestion. C: The final expression vector, pHBT12K::35Sp-VpVAN, contained the 35Sp-VpVAN cassette.

4.4 DISCUSSION

4.4.1 Restriction-Ligation, Gateway[®], and Golden Gate Cloning Systems

This study involved the utilisation of three cloning methods (restriction-ligation, Gateway[®] Cloning and Golden Gate Cloning) for the construction of the expression vectors. The conventional restriction-ligation method was a very commonly used method to create recombinant vectors. Restriction-ligation was easy to perform and could be carried out as far as the availability of REs and RE sites was not a concern. As such, the restriction-ligation method was employed in the cloning of single cassettes, 35Sp-*sgfp* and 35Sp-*VpVAN*, into pcDNA6.2. However, the versatility of the restriction-ligation method was often hampered by the lack of desirable restriction sites for cloning into the desired open reading frames (ORFs), such as in pcDNA6.2 and pHBT12K (van den Ent and Lowe, 2006). Due to such limitation, the assembly of multiple DNA fragments into the vectors was also difficult.

Using Gateway[®] Technology, the simultaneous transfer of multiple DNA fragments into one destination vector was done using a site-specific recombinase known as the Integrase (Hartley *et al.*, 2000). Although the current Gateway[®] Technology only enabled the cloning of two, three or four DNA fragments, this intriguing cloning technology was sufficient for the cloning works in this study. A notable drawback of the Gateway[®] system, besides its relatively higher cost than the conventional restriction-ligation cloning and Golden Gate Cloning, was the requirement of two bacterial transformation steps before obtaining the final expression vector. Compared to just one step in many other cloning methods, the Gateway[®] system required a bacterial transformation step after the BP reaction and

another bacterial transformation step after the LR reaction. Nonetheless, it has been reported that both BP and LR reactions could be performed in a single reaction. In the reaction product, more entry clones could be produced at a high BP/LR ratio or more expression vector could be produced at low BP/LR ratio (Liang *et al.*, 2013). Performing a single reaction would mean that only one bacterial transformation step was needed. However, the single-reaction approach would then require additional downstream work for the separation of entry clones from the expression vector. Besides that, the BP and LR reactions required the availability of *att* sites for targeted recombination to take place. Subsequently, the cloning products were left with *att*-scar regions in the expression cassette. Such a characteristic was not favourable because extra amino acids might be incorporated into the expressed protein and might contribute to the addition of functional or non-functional peptides affecting the protein characteristics (Buj *et al.*, 2013). Despite these limitations, the Gateway[®] system was very versatile for the application in this study considering that there were no perfect recombination-based strategies. With just a modification to the primer designs, the number of modules to be assembled could be changed using the same kit, for example, from 4-fragment recombination to 2-fragment recombination.

The problem with extraneous sequences that might arise during the cloning process could be alleviated with the use of non-recombination cloning system like Golden Gate Cloning. The Golden Gate technique utilised type IIS restriction enzymes that cut outside their recognition regions. As such, the design of primers with unique overhang sequences at the cutting sites enabled precise and targeted cloning of multiple DNA fragments. With appropriate incorporation of the restriction sites into the transgene, two or more digested fragments could be ligated to produce an

assembly lacking the original restriction sites (Engler *et al.*, 2008). The use of Golden Gate Cloning avoided time-consuming steps of gel purification, but requires PCR amplification of target DNA fragments with primers that provided the appropriate restriction sites. As such, the application of Golden Gate Cloning posed a limitation, which was the need for the infrequent recognition sites of type IIS REs to be available in the ORFs of transformation vectors, but not in the target DNA fragments (Buj *et al.*, 2013). The Golden Gate Cloning was nevertheless versatile, as this cloning system has been recently adapted into CRISPR technology for the insertion of guide RNAs into Cas9-containing plasmids (Sakuma *et al.*, 2014; Vad-Nielsen *et al.*, 2016). As there were no perfect cloning strategies, a few methods were used in this study. In the construction of the expression vectors, the cloning method that was considered the most feasible for the cloning of the target DNA fragments/cassette into pcDNA6.2 or pHBT12K was used. The justifications of the cloning system used to construct each of expression vectors in this study are summarised in **Table 4.1**.

Table 4.1 The selection and justification of the cloning methods used for the construction of target DNA into pcDNA6.2 and pHBT12K to produce the final expression vectors.

Expression vector (Target DNA fragments/cassette)	Cloning method and justification
pcDNA6.2::35Sp- <i>sgfp</i> (Target DNA cassette: 35Sp- <i>sgfp</i>)	Single-cassette cloning using restriction-ligation cloning <ul style="list-style-type: none"> • <i>Pst</i>I and <i>Age</i>I sites were present at the ORF of pcDNA6.2, but not in the 35Sp-<i>sgfp</i> cassette.
pcDNA6.2::35Sp- <i>fcs</i> - NOSp- <i>ech</i> (Target DNA fragments: 35Sp; <i>fcs</i> ; NOSp; <i>ech</i>)	4-fragment recombination using Gateway® Cloning <ul style="list-style-type: none"> • The lack of multiple cloning sites in the transformation vector posed difficulty for cloning via restriction-ligation. • Type IIS RE site, <i>Bsm</i>BI, was present at the ORF of pcDNA6.2, but <i>Bsm</i>BI also cut in <i>fcs</i>. Hence cloning via Golden Gate was not possible.
pcDNA6.2::35Sp- <i>fcs</i> (Target DNA fragments: 35Sp; <i>fcs</i>)	2-fragment recombination using Gateway® Cloning <ul style="list-style-type: none"> • Feasibility was lower for cloning via

	<p>restriction-ligation than via Gateway[®] and Golden Gate due to the lack of multiple cloning sites and the requirement of multiple steps to clone in one fragment after another.</p> <ul style="list-style-type: none"> • Although <i>BsmBI</i> cut in pcDNA6.2, the type IIS RE also cut in <i>fcs</i>, making Golden Gate Cloning not possible.
pcDNA6.2::NOSp- <i>ech</i> (Target DNA fragments: NOSp; <i>ech</i>)	<p>2-fragment assembly (one-pot reaction) using Golden Gate Cloning</p> <ul style="list-style-type: none"> • The lack of multiple cloning sites and the requirement of multiple steps to clone in one fragment after another made cloning via restriction-ligation difficult. • <i>BsmBI</i> cut in pcDNA6.2, but did not cut in NOSp and <i>ech</i> – Golden Gate Cloning was possible. <i>BsmBI</i> sites were removed after cloning, leaving no extraneous sequences in the cloning product. • The cost of cloning using Golden Gate was lower than Gateway[®]
pcDNA6.2::35Sp- <i>VpVAN</i> (Target DNA cassette: 35Sp- <i>VpVAN</i>)	<p>Single-cassette cloning using restriction-ligation cloning</p> <ul style="list-style-type: none"> • <i>PstI</i> and <i>BamHI</i> sites were present in both pUCIDT-35Sp-<i>VpVAN</i> holding vector and pcDNA6.2 transformation vector. Transfer of 35Sp-<i>VpVAN</i> cassette could be done directly from pUCIDT-35Sp-<i>VpVAN</i> to pcDNA6.2 via restriction-ligation without the need for PCR.
pHBT12K::35Sp- <i>VpVAN</i> (Target DNA cassette: 35Sp- <i>VpVAN</i>)	<p>Single-cassette cloning (one-pot reaction) using Golden Gate Cloning</p> <ul style="list-style-type: none"> • Cloning of the 35Sp-<i>VpVAN</i> cassette into pHBT12K could be done via restriction-ligation or Golden Gate, which cost was lower than Gateway, although <i>attR</i> sites have been customized into pHBT12K. • The efficacy of a type IIS RE site, <i>BbsI</i>, in the ORF of the pHBT12K was tested for Golden Gate.

4.4.2 Construction of Expression Vectors

The pcDNA6.2 transformation vector was readily available with the *attR* sites for seamless cloning of multiple DNA fragments using Multisite Gateway[®] Technology. The *attR* sites previously incorporated into pHBT12K by Leong (2015, personal communication) so that it was compatible with Gateway[®] Cloning for the ease of cloning of multiple DNA elements. The

promoterless feature of pcDNA6.2 and pHBT12K was desirable because this feature enabled flexibility in the assembly of modules in the expression cassettes. In addition, *fcs*, *ech* and NOSp were synthesised into separate pUCIDT holding vectors to facilitate modular cloning of the target fragments. The use of promoterless vectors coupled with the modular cloning approach could enable the modification of regulatory elements, such as changing the constitutive promoters to tissue/organ-specific or inducible promoters in future studies. In this study, constitutive promoters, 35Sp and NOSp, were used to prove the concept of constitutive expression of *fcs*, *ech* and *VpVAN* in *C. frutescens*. The 35Sp was a strong, constitutive promoter derived from cauliflower mosaic virus that was very commonly used in the genetic engineering of eukaryotes (Seternes *et al.*, 2016; Wilkinson *et al.*, 1997). It has been discovered that the promoter activity of 35Sp was so strong that the tissue- or organ-specific promoters of adjacent genes could be converted into universally active promoters by the 35Sp (Zheng *et al.*, 2007). However, despite the constitutive nature of 35Sp, it was reported that the activity of 35S was weak in tissues that were grown in the dark (Saidi *et al.*, 2009). Similar to 35Sp, the NOSp was another constitutively active promoter, which originated from *Agrobacterium tumefaciens* (Ebert *et al.*, 1987). It was also found that the activity of NOSp was not organ-specific, but was wound- and auxin-inducible, as the activity of NOSp was higher in wounded tissues and in roots, which contained high levels of auxin (An *et al.*, 1990; Bouchez *et al.*, 1989). In the construction of pcDNA6.2::35Sp-*fcs*-NOSp-*ech* where two genes of interest (*fcs* and *ech*) were present consecutively in the same expression vector, two different promoters (35Sp for *fcs*, NOSp for *ech*) were used. This was because the presence of homologous promoters could induce silencing of the gene(s) of interest at the transcriptional or post-transcriptional level through the methylation of the promoter(s) (Park *et al.*,

1996). Gene silencing could also be prevented with the introduction of a silencing suppressor, such as p19 protein from tombusviruses or helper component-proteinase (HC-Pro) from a potyvirus (Anandalakshmi *et al.*, 1998; Danielson and Paul, 2013; Lakatos *et al.*, 2004; Soitamo *et al.*, 2011). Out of the two promoters used in this study, the 35Sp was used more widely than the NOSp because the transcription levels of genes in transgenic plants were found to be higher with 35Sp than with NOSp (Harpster *et al.*, 1988; Sanders *et al.*, 1987).

In pcDNA6.2, the target DNA fragments were assembled upstream of the herpes simplex virus thymidine kinase polyadenylation signal (TK pA), which served to terminate transcription efficiently and to protect the mRNA by polyadenylation (Cole and Stacy, 1985; Kim and Martinson, 2003; Proudfoot, 2011). In pHBT12K, the expression cassette, 35Sp-*VpVAN*, was cloned in upstream of *sgfp* reporter gene. As such, the translated protein was fused with the sGFP reporter gene without a translation stop codon at the 3'-end of the 35Sp-*VpVAN* cassette. The presence of NOS terminator (NOST) downstream of the *sgfp* gene served to terminate transcription.

In the construction of pHBT12K::35Sp-*VpVAN*, the presence of a *BbsI* site has enabled cloning via Golden Gate, albeit with limited options of type IIS RE at the target ORF. One disadvantage of the *BbsI* used was the occurrence of star activity during prolonged RE digestion in this study. Such star activity was also reported by Patron (2013) from The Sainsbury Laboratory, UK. With that in mind, the number of cycles in Golden Gate Cloning was reduced from 25 to 15 cycles, which proved to have avoided star activity (**Appendix F**).

The vector construction in this study was often faced with a loss of vector, which was possible due to vector instability. The constructed

vectors were propagated in bacterial host, *E. coli*, but it was important to note that the vectors were not always stable in the bacterial cells. Vector instability could be attributed to the metabolic burden imposed for vector maintenance, the presence of large vectors or large copy numbers of vectors, the presence of toxic genes, and the use of strong positive selection pressure (for example, antibiotic resistance) (Al-allaf *et al.*, 2013; Friehs, 2004; Kumar *et al.*, 1991). In the construction of pcDNA6.2::35Sp-*fcs*-NOSp-*ech*, the target DNA fragments were assembled into a large module of ~3 kb, making the expression vector ~7.5 kb in total size. The problem with vector instability was resolved when the One Shot[®] Mach1[™] T1^R Chemically Competent *E. coli*, which was initially used for vector propagation after the LR reaction, was replaced with One Shot[®] TOP10 Chemically Competent *E. coli*, a strain for general plasmid cloning and storage. Similar to Mach1[™] T1^R *E. coli* that had *recA1398* mutation, TOP10 *E. coli* also had a *recA1* mutation that could increase vector stability and reduce recombination (Ferenc, 2015). Several other *E. coli* strains have been reported to maintain the stability of vectors that have the potential to recombine, such as the Stbl2[™] and Stbl4[™] strains from Invitrogen (Thermo Fisher Scientific, USA), the SURE[®] strain from Stratagene (Agilent Technologies, USA) and the Stbl3 strain (Al-allaf *et al.*, 2013; Trinh *et al.*, 1994). Vectors to be selected for, which expressed the intact *ccdB* gene, were propagated using One Shot[®] *ccdB* Survival T1^R Chemically Competent *E. coli*, which was resistant to the cytotoxic activity of *ccdB* (Bernard and Couturier, 1992). With respect to positive selection pressure that could also result in vector instability, the antibiotics concentrations were kept to the minimal working concentration of 100 µg/ml for ampicillin and 50 µg/ml for kanamycin (Patrick, 2015). The culture temperature and period of *E. coli* during the positive selection was always 37°C and 16 h, which was typical for the bacteria to reach mid to late log phase of exponential growth

(optical density at 600 nm = 0.6–1.0) in LB liquid medium (Kelley *et al.*, 2010; Sezonov *et al.*, 2007). Culture growth conditions, such as pH and temperature, could be optimised to raise *E. coli* for the maintenance of vectors (Kumar *et al.*, 1991). Given many possible reasons that could cause the loss of vector, this problem could be minimised, if not totally prevented, with careful assessment of the DNA fragments to be cloned, using the appropriate transformation vector, selecting the suitable bacterial host for vector propagation, and minimising the selection pressure while maintaining effective selection.

4.5 CONCLUSION

In summary, six expression vectors have been assembled and were ready for transformation into *C. frutescens*: (i) pcDNA6.2::35Sp-*sgfp* for the optimisation and evaluation of biolistic-mediated transformation of *C. frutescens* using sGFP reporter assay (subsequent **Chapter 5**); (ii) pcDNA6.2::35Sp-*fcs*-NOSp-*ech* for the evaluation of vanillin production by the expression of *fcs* and *ech* (subsequent **Chapters 5 and 6**); (iii) pcDNA6.2::35Sp-*fcs* for the evaluation of vanillin production possibly by the expression of *fcs* alone (subsequent **Chapters 5 and 6**); (iv) pcDNA6.2::NOSp-*ech* for the evaluation of vanillin production possibly by the expression of *ech* alone (subsequent **Chapters 5 and 6**); (v) pcDNA6.2::35Sp-*VpVAN* for the evaluation of vanillin production by the expression of *VpVAN* delivered in pcDNA6.2 (subsequent **Chapters 5 and 6**); and (vi) pHBT12K::35Sp-*VpVAN* for the evaluation of vanillin production by the expression of *VpVAN* delivered in pHBT12K (subsequent **Chapters 5 and 6**).

CHAPTER 5

MICROPROJECTILE BOMBARDMENT AND ANTIBIOTIC SELECTION OF *CAPSICUM FRUTESCENS* L.

5.1 INTRODUCTION

Many research studies have been carried out on *Capsicum* to explore its growth and developmental physiology in different environments, as well as its potential for genetic improvements, metabolite utilisation, and pre-harvest and post-harvest enhancements (Chitravathi *et al.*, 2014; Kothari *et al.*, 2010; Kumar *et al.*, 2011; Lee and Kader, 2000; Li *et al.*, 2003a; Toivonen and Bowen, 1999). Among these, genetic engineering techniques and plant tissue culture are useful tools that can advance improvements of *Capsicum*. The success of a genetic improvement approach requires an optimized plant transformation procedure and an effective selective agent for the isolation of transformed plant tissues. A brief overview of the transformation of chilli by biolistics and the use of blasticidin S (BS) to select for putative transformants is discussed in **subchapters 5.1.1 and 5.1.2**, respectively.

5.1.1 Transformation of *C. frutescens* by Biolistics

In many recombinant DNA techniques that are commonly used, an effective plant transformation procedure is required alongside a protocol for plant regeneration (Ravishankar *et al.*, 2003). The genetic engineering of *Capsicum* is hampered by its low morphogenetic capability (Ochoa-Alejo and Ramírez-Malagón, 2001). So far, most of the transformation studies on *Capsicum* have centred on *Agrobacterium*-mediated gene transfer (Li *et al.*, 2003a; Manoharan *et al.*, 1998; Steinitz *et al.*, 1999; Wang *et al.*, 1991; Zhu *et al.*, 1996) while reports on the transformation of *Capsicum* by particle bombardment are still very lacking, more so for *C. frutescens*. Gilardi and co-workers (1998) described the introduction of pepper mild mottle virus coat protein into *Capsicum chinense* by biolistics. More recently, the same group reported the introduction of tobamovirus coat protein into *C. frutescens* L. cv. Tabasco, also by biolistics (Gilardi *et al.*, 2004). In another study, a biolistic hand gun was used to deliver the beta-glucuronidase (GUS) reporter gene into *Capsicum annuum* L. (Nianiou *et al.*, 2002).

In this study, the direct transformation of *C. frutescens* L. cv. Hot Lava via particle bombardment was optimized using GFP as the reporter protein. Despite several reported drawbacks, such as the susceptibility to photobleaching and sensitivity to pH changes (Campbell and Choy, 2001; Dickson *et al.*, 1997; Greenbaum *et al.*, 2000), GFP is advantageous because it does not rely on any exogenous cofactor to fluoresce and it is useful as a non-destructive reporter assay for *in vivo* visualization (Hanson and Köhler, 2001; Tee and Maziah, 2005).

In biolistics, parameters that contribute to major effects on transformation are microparticle size, target distance (travel distance of

microparticles to target explants), and vacuum (pressure) (Klein *et al.*, 1991). An increase in the size of microparticles, vacuum or He pressure causes an increase in the velocity of microcarriers, while an increase in the target distance causes a decrease in the velocity of microcarriers. The effects of He pressure on transformation are variable. Studies on yeast (*Saccharomyces cerevisiae*) and cauliflower have shown that the optimum transformation occurred at a broad range of He pressures (900–1550 psi), while other studies on bacteria and plants obtained a narrower range of optimum He pressures (Heiser, n.d.; Russell *et al.*, 1992; Smith *et al.*, 1992). As microprojectile bombardment could cause damage to cells, gentle conditions that contribute to the optimum transformation should be applied. A summary of parameters that affect the velocity of microcarriers and consequently on transformation, is described in **Table 5.1**.

Table 5.1 The parameters that affect transformation using PDS. An increase (+) or decrease (-) in the velocity of microcarriers are theoretically affected an increase or decrease in a respective parameter.

Parameter	Theoretical effect on velocity	Effect on transformation
Microcarrier size [†]	Size (+), velocity (+)	Major
Target distance [†]	Distance (+), velocity (-)	Major
He pressure [†]	Pressure (+), velocity (+)	Variable
Vacuum [‡]	Vacuum (+), velocity (+)	Major
Rupture disk-macrocarrier gap distance	Distance (+), velocity (-)	Minor
Macrocarrier flight distance	Distance (+), velocity (+)	Minor

^aThe effect on transformation could be more dependent on the size of the target cells than on the velocity of the microcarriers.

^bThe effect of vacuum is more pronounced with smaller particle size.

[†]Parameters that have major effects on transformation were tested.

[‡]The vacuum, which has major effect on transformation, was fixed according to the protocol by Klein *et al.* (1987).

5.1.2 Blasticidin S Antibiotic as a Selective Agent

The use of a selectable marker is very common in genetic engineering work in order to select for transformants that are expressing the transgene, which is challenging due to the low-frequency transgene integration event

(Jones and Sparks, 2009). The selectable markers used are often antibiotic or herbicide resistance genes. The resistance genes confer upon host tissues the resistance to the corresponding antibiotic, which is added into the culture media to serve as the selective media (Goodwin *et al.*, 2005). Therefore, only tissues carrying the transgene can survive in the selective media. An efficient selective antibiotic that works on eukaryotic and prokaryotic cells is blasticidin S (BS). BS is a nucleoside antibiotic found to be produced by *Streptomyces griseochromogenes* (Cone *et al.*, 2003). First developed in Japan as an agricultural antibiotic to control rice blasts, BS inhibits peptide synthesis in cells by binding to the ribosomal P-site, hence weakening tRNA binding (Misato *et al.*, 1977; Petropoulos *et al.*, 2004). BS causes fast cell death at low antibiotic concentrations (Thermo Fisher Scientific, 2016). A number of resistance genes for BS had been identified. The blasticidin S acyltransferase gene (*bls*), which itself produces BS, was originally isolated from *Streptoverticillum* sp. (Pérez-González *et al.*, 1990). The other most commonly used resistance genes against BS in many transgenic studies of eukaryotic cells are the blasticidin S deaminase gene (*bsr*) from *Bacillus cereus* (Izumi *et al.*, 1991) and the blasticidin S deaminase gene (*bsd*) from *Aspergillus terreus* (Kimura *et al.*, 1994; Tamura *et al.*, 1995). The *bsd* gene was the selectable marker used in pcDNA6.2 in subsequent transformation works.

5.1.3 Specific Objectives

Prior to the transformation of *C. frutescens*, the effect of different concentrations of BS antibiotic in the culture media on the explants of *C. frutescens* was tested. The purpose of this study was to determine (i) the minimal inhibitory concentration of BS for the selection of plant

transformants; (ii) the optimised parameters (microcarrier size, explant target distance and bombardment He pressure) for the direct transformation of *C. frutescens* via particle bombardment for stable expression using GFP as the reporter protein; and (iii) achieve putative chilli transformants that were delivered with vanillin biosynthetic genes by particle bombardment.

5.2 MATERIALS AND METHODS

5.2.1 Minimal Inhibitory Concentration of Blastidicin S

Cotyledon, hypocotyl and root explants were excised from germinated seedlings of *C. frutescens* L. cv. Hot Lava. Each of the explant types was cultured on callus induction media (CIM), which contained 2.0 mg/l 2,4-D and 0.5 mg/l kinetin, supplemented with various concentrations of BS at 0.0, 1.0, 3.0, 5.0, 7.5, 10.0, 12.5, 15.0 and 20.0 mg/l. Mortality rates of the explants were observed for two weeks (observation 1). Based on the results from observation 1, the experiment was repeated with a narrower range of BS concentrations, at 0.00, 0.25, 0.50, 0.75 and 1.00 mg/l. Mortality rates of the explants were observed for two weeks (observation 2). Based on the results from observation 2, the experiment was repeated with an even narrower range of BS concentrations, at 0.00, 0.10, 0.20 and 0.25 mg/l. Mortality rates of the explants were observed for two weeks. All experiments were conducted in triplicates. Twenty explants were used for each explant type in each replicate.

5.2.2 Optimisation of Biolistic Parameters

5.2.2.1 Preparation of Explants

One day prior to the bombardment procedure, hypocotyls from 14-day-old seedlings were excised to the length of 5 mm and were laid on MS media in Petri plates. Fifteen explants were arranged at the centre of each Petri plate. Each experiment for every set of the studied biolistic parameters was conducted in triplicates, with a total of 45 hypocotyl explants per replicate.

5.2.2.2 Preparation of Microcarriers

The amount of materials given in the procedure below, according to the methods of Sanford *et al.* (1993), was enough for 120 bombardments using 0.5 mg of gold particles per bombardment. For each batch of 0.6, 1.0 and 1.6 μm gold particles, 60 mg of gold particles were weighed into sterile 1.5 ml microcentrifuge tubes. Then, 1 ml of 70% (v/v) ethanol was added and mixed by vigorous vortex for 5 min. The gold particles were pelleted by spinning down for 5 s and the supernatant was discarded. The pellet was washed three times as follows: adding 1 ml of sterile H_2O , followed by mixing by vortex for 1 min, allowing the particles to settle for 1 min, spinning down the particles for 2 s and discarding the supernatant. Finally, 50% (v/v) glycerol was added to the pellet to bring the concentration of the gold particles to 60 mg/ml (assuming no loss of particles during the preparation). The 50% glycerol was sterilised by autoclaving and cooled to room temperature prior to use. The suspended gold particles that were not used were stored at 4°C.

5.2.2.3 Coating DNA on Microcarriers

The amount of materials given in the procedure below was enough for six bombardments. Where more or fewer bombardments were needed, the amount was adjusted accordingly. For example, all volumes were doubled to prepare for 12 bombardments.

For each of the gold particle sizes (0.6, 1.0 and 1.6 μm), 3 mg or 50 μl of 60 mg/ml gold particles (suspended in 50% (v/v) glycerol) was mixed with 5 μg of pcDNA6.2::35Sp-*sgfp* expression vector, 50 μl of 2.5 M calcium chloride (CaCl_2), and 20 μl of 0.1 M spermidine under constant vortex to mix well in a sterile 1.5 ml microcentrifuge tube. The gold-DNA suspension was then pelleted and the supernatant was removed. The gold-DNA pellet was washed once with 140 μl of 70% (v/v) ethanol, followed by another washing with 140 μl of 100% ethanol before being finally re-suspended in 48 μl of 100% ethanol.

5.2.2.4 Microprojectile Bombardment

Delivery of DNA-coated microcarriers was performed using the Bio-Rad PDS-1000/HeTM Particle Delivery System (USA) (instrument illustrated in **Figure 5.1**). Before each bombardment session, pipette tips, stopping screens, forceps, the microcarrier holder, the microcarrier launch assembly and the rupture disk retaining cap were autoclaved and dried. Non-autoclavable items, such as the macrocarrier insertion tool, were wiped with 70% (v/v) ethanol. During a bombardment session, rupture disks and macrocarriers were sterilised by brief soaking in 70% ethanol and then allowing the ethanol to evaporate completely prior to use. The pressure of the He tank was set at 1600 psi.

For each bombardment, a rupture disk was placed in the rupture disk retaining cap and the retaining cap was tightened against the chamber end of the He acceleration tube using a torque wrench in the bombardment chamber. The centre (~1 cm diameter) of each macrocarrier was spread with the 6 μ l of gold-DNA suspension. Aliquots of the gold-DNA suspension were pipetted under continuous vortex. Ethanol traces on the macrocarrier were left to evaporate completely. The microcarrier launch assembly was set up by putting a stopping screen in the centre of the brass nest in the microcarrier launch assembly. The macrocarrier was fitted into the macrocarrier holder, which was then inserted into the microcarrier launch assembly with the dried microcarriers facing down, towards the stopping screen. The macrocarrier cover lid was replaced on the assembly. The microcarrier launch assembly was placed on the top shelf of the bombardment chamber. After that, the Petri dish containing target explants (without the lid) was placed on the target plate on the shelf of the bombardment chamber according to the desired target distance. The door of the bombardment chamber was closed, the vacuum switch was turned on until the vacuum gauge showed 28 inches Hg (94.82 kPa), and the vacuum switch was set to "hold." The instrument was fired until the rupture disk burst and the He pressure shown on the instrument gauge dropped to zero. The vacuum switch was set to "vent" to release the vacuum. Finally, the Petri dish was removed from the bombardment chamber and covered with the lid.

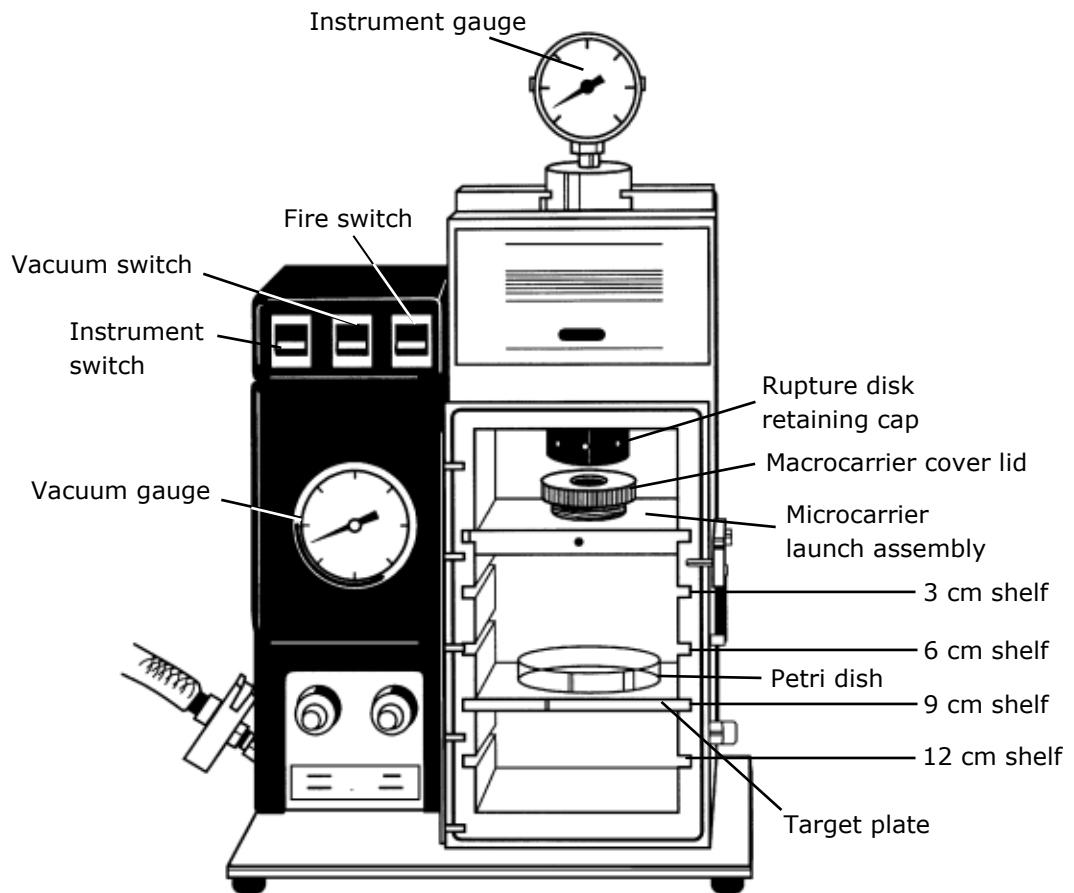


Figure 5.1 Illustration of the He-driven PDS system and its components. Adapted from Biolistic® PDS-1000/He Particle Delivery System Catalog Numbers 165-2257 and 165-2250LEASE to 165-2255LEASE Manual.

For each of the 0.6, 1.0 and 1.6 μm gold particle sizes tested, the He pressure was tested at 900, 1100 and 1350 psi. For each of the gold particle sizes and each of the He pressures used, the target distance (distance between stopping screen and explants) was tested at 3, 6 and 9 cm. The rupture disk-macrocarrier gap distance was fixed at 0.64 cm while the macrocarrier travel distance was set at 8 mm all the time (**Figure 5.2**).

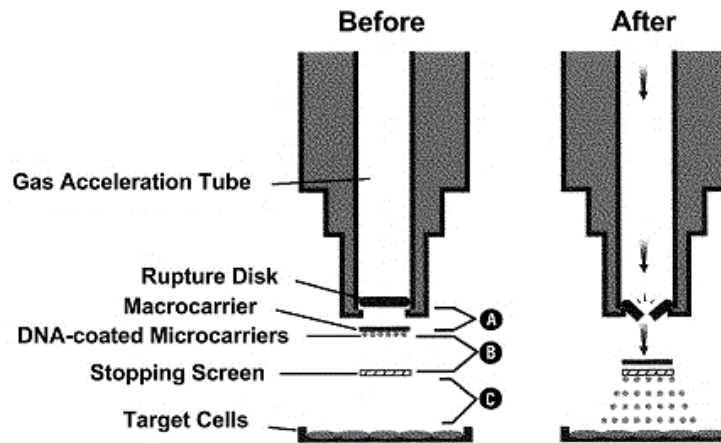


Figure 5.2 The process of microprojectile bombardment before and after the rupture disk burst. The direction of He gas flow is shown by arrows. A: Rupture disk-macrocarrier gap distance, B: Macrocarrier travel distance, C: Target distance (distance between the stopping screen and target explants).

5.2.2.5 Selection and Regeneration of Plant Transformants

Bombarded explants were incubated in the dark for 48 h before being transferred to MS media containing 0.25 mg/l BS, 2.0 mg/l 2,4-D and 0.5 mg/l kinetin for antibiotic selection and regeneration. The explants were incubated for one month, and then transferred to the same, fresh medium for another month of selection and regeneration. Callus tissues that grew away from the culture medium were submerged back into the medium to ensure a thorough selection with continuous exposure to the antibiotic.

5.2.2.6 Screening of Plant Transformants

Bombarded explants were observed for GFP expression using a Nikon SMZ1500 stereomicroscope (Japan) under blue light illumination. Observations were done every day up to five days post-bombardment, then every five days subsequently up to 60 days. Microscopic photographs were captured and the intensity of GFP fluorescence was measured using

NIS Elements D v3.22.00 (Build 710) software. Mean green intensity, which was used as the measurement of GFP fluorescence, was determined quantitatively from the signal of the green channel (excluding red and blue channels) from the microscopic images (example of green fluorescence measurement is shown in **Figure 5.3**). Mean green intensity was calculated by the software as the sum of green intensity (measured by arbitrary unit, AU) over a given area. To eliminate the signal intensity caused by autofluorescence or background noise, the pixel-by-pixel brightness of microscopic photographs was analysed using Corel® PHOTO-PAINT® X8 (Canada) to determine the signal threshold (example of signal threshold correction is shown **Figure 5.4**) (Billinton and Knight, 2001). The background-subtracted intensity of sGFP fluorescence, $I_{BG\ sub}$, was calculated as $I_{BG\ sub} = \bar{I} - \frac{I_{BG}}{A_{BG}}$, where \bar{I} is the mean green intensity of a fluorescent spot, I_{BG} is the green intensity of a background region, and A_{BG} is the area of a background region (Verdaasdonk *et al.*, 2014).

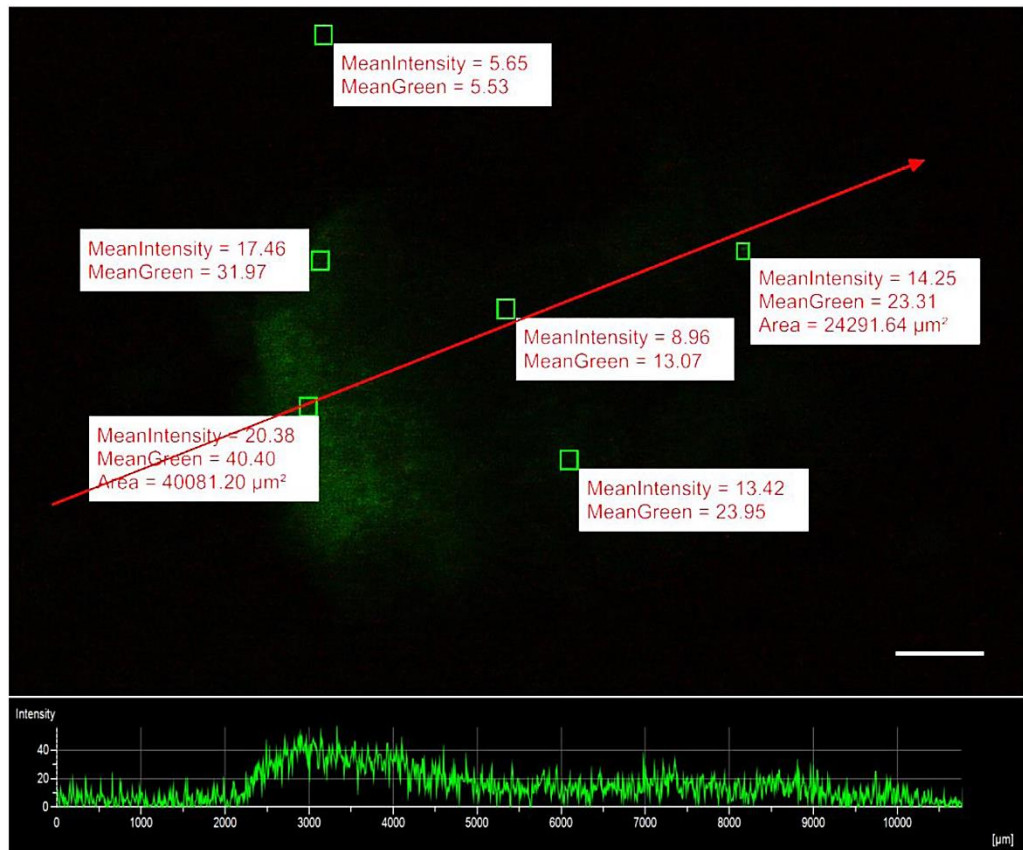


Figure 5.3 Microscopic diagram showing the measurement of GFP intensity across an explant. The graph below the diagram shows the intensity plot of green signal across the distance as indicated by the red arrow in the diagram. Mean intensity indicates the sum of intensity, combining red, green and blue channels, over a given area. Mean green indicates the sum of intensity from the green channel only over a given area. Scale bar represents 1 mm (Original).

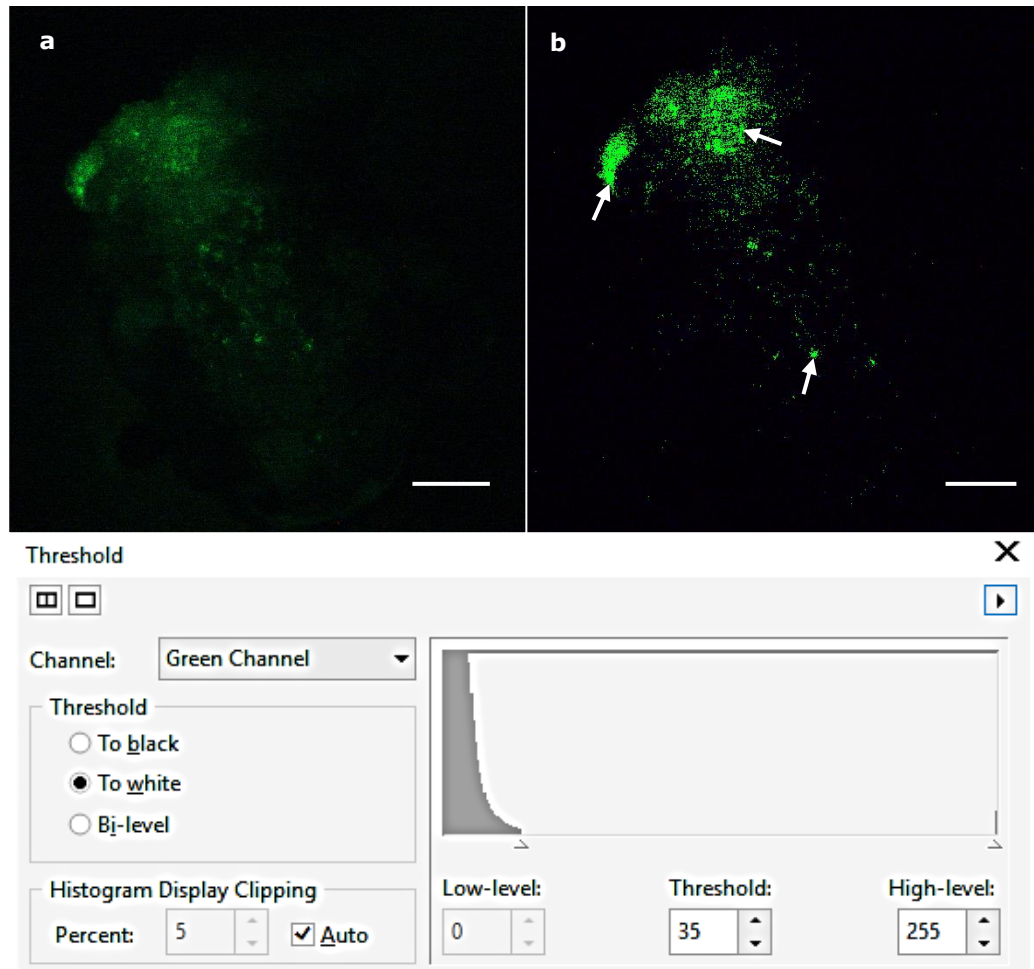


Figure 5.4 An example of microscopic photograph of a callus expressing sGFP (a) before and (b) after analysis using Corel® PHOTO-PAINT®. Pixels of the photograph analysed and spots with signal intensities greater than 35 AU (threshold beyond which autofluorescence was eliminated) were highlighted, as pointed by arrows (Original).

5.2.2.7 Purification of Plant Genomic DNA

After two months post-bombardment, genomic DNA of the selected calli was purified. For each sample, about 200 mg of callus tissues was ground in a 1.5 ml microcentrifuge tube with a Kimble™ pestle (Fisher Scientific, USA) until the tissues became mushy. Then, 600 µl of plant callus DNA extraction buffer (preparation as described in **subchapter 2.1**) was added and the sample was homogenized. Tris-saturated phenol (500 µl) was added and mixed. Then, the aqueous phase was transferred into a new 1.5 ml microcentrifuge tube following a centrifugation at maximum speed for

10 min at 4°C using a refrigerated centrifuge (Eppendorf 5810R, Germany). The aqueous phase was mixed with 450 µl of chloroform/isoamyl alcohol (24:1, v/v). After another centrifugation, 400 µl of isopropanol was added to the aqueous phase and the DNA was allowed to precipitate at room temperature for 30 min. The DNA was then pelleted, the isopropanol was removed and the pellet was washed with 70% (v/v) ethanol. Following centrifugation and removal of ethanol, the DNA pellet was dried in a vacuum desiccator (Concentrator plus, Eppendorf, Germany) for 2 min and then dissolved in H₂O. The purified DNA was quantified using a NanoDrop 1000 Spectrophotometer (Thermo Scientific, USA).

5.2.2.8 Confirmation by PCR to Detect *sgfp* Gene

The detection of the *sgfp* gene in the extracted genomic DNA was done by PCR using SCREEN*gfp*-F and SCREEN*gfp*-R primers (**Appendix C**). The 25-cycle PCR amplification was performed according to the procedure described in **subchapter 2.4**. The annealing temperature was set at 53°C and elongation was held for 45 s. Gel electrophoresis of the PCR products was performed according to the procedure described in **subchapter 2.5**.

5.2.3 Statistical Analysis

Binomial data collected on the number of transformants were subjected to logistic regression in the generalized linear model in GenStat 17th Edition (v17.1.0.14713). Mean values were predicted and compared using a LSD test at 5% level.

5.2.4 Transformation of *C. frutescens* with Vanillin Biosynthetic Genes

Hypocotyl explants of *C. frutescens* (20 explants per replicate of three replicates) were transformed with the expression vectors, pcDNA6.2::35Sp-*fcs*-NOSp-*ech*, pcDNA6.2::35Sp-*fcs*, pcDNA6.2::NOSp-*ech*, pcDNA6.2::35Sp-pcDNA6.2::35Sp-*VpVAN*, and pHBT12K::35Sp-*VpVAN* using the PDS based on the optimised parameters, which were 1.6 µm of gold particle size, 1350 psi of He pressure and 6 cm of target distance. The bombarded explants were selected and regenerated, as described in **subchapter 5.2.2.5**.

The genomic DNA of two-month cultures of the selected calli were purified according to the protocol in **subchapter 5.2.2.7**, followed by screening for genes of interest using PCR. Calli that were transformed with pcDNA6.2::35Sp-*fcs*-NOSp-*ech* were screened for *fcs* and *ech* using primer pairs, PF/*fcs* and PR/*fcs*, and PF/*ech* and PR/*ech*, respectively. Calli that were transformed with pcDNA6.2::35Sp-*fcs* were screened for *fcs* using PF/*fcs* and PR/*fcs* primers. Calli that were transformed with pcDNA6.2::NOSp-*ech* were screened for *ech* using PF/*ech* and PR/*ech* primers. Calli that were transformed with pcDNA6.2::35Sp-*VpVAN* and pHBT12K::35Sp-*VpVAN* were screened for *VpVAN* using primer pairs, PF/*VpVAN* and PR/*VpVAN*, and PF/*BbsI*-35Sp-*VpVAN* and PR/35Sp-*VpVAN*-*BbsI*, respectively. Sequences and annealing temperatures of the primers are given in **appendix C**.

5.3 RESULTS

5.3.1 Minimal Inhibitory Concentration of Blastocidin S

To determine the lowest concentration of BS that killed the explants, cotyledon, hypocotyl and root explants of *C. frutescens* were cultured on CIM containing 2.0 mg/l 2,4-D and 0.5 mg/l kinetin and various concentrations of BS (0.00, 0.10, 0.20, 0.25, 0.50, 0.75, 1.00, 3.0, 5.0, 7.5, 10.0, 12.5, 15.0 and 20.0 mg/l). Out of a total number of twenty explants per replicate for each explant type and each BS concentration, the average number of explants induced into calli was recorded (**Table 5.2**). Statistically, the lowest significant concentration of BS that gave complete mortality, E_{100} , was 0.25 mg/l for cotyledon and root explants and 0.20 mg/l for hypocotyl explants. However, an average of two escapes was observed for hypocotyl explants at 0.20 mg/l. Therefore, the concentration of BS that achieved the E_{100} for all explant types without escapes was 0.25 mg/l. Explants that were inhibited turned brown after one week in culture, did not proliferate into healthy calli and deteriorated, whereas explants that were not inhibited proliferated into white, healthy calli (**Figure 5.5**).

Table 5.2 The average number of explants callusing from cotyledon, hypocotyl and root explants of *C. frutescens* L. cv. Hot Lava across different concentrations of BS.

BS concentration (mg/l)	Average number of explants callusing		
	Cotyledon	Hypocotyl	Root
0.00	20±0.0 ^a	20±0.0 ^a	20±0.0 ^a
0.10	18±1.5 ^b	15±1.2 ^b	16±1.0 ^b
0.20	2±1.0 ^c	2±2.6 ^c	3±1.2 ^c
0.25	0 ^d	0 ^c	0 ^d
0.50	0 ^d	0 ^c	0 ^d
0.75	0 ^d	0 ^c	0 ^d
1.00	0 ^d	0 ^c	0 ^d
3.00	0 ^d	0 ^c	0 ^d
5.00	0 ^d	0 ^c	0 ^d
7.50	0 ^d	0 ^c	0 ^d
10.00	0 ^d	0 ^c	0 ^d
12.50	0 ^d	0 ^c	0 ^d
15.00	0 ^d	0 ^c	0 ^d
20.00	0 ^d	0 ^c	0 ^d

Mean values (±standard deviation) with the same superscript letters are not significantly different using LSD at 5% level.

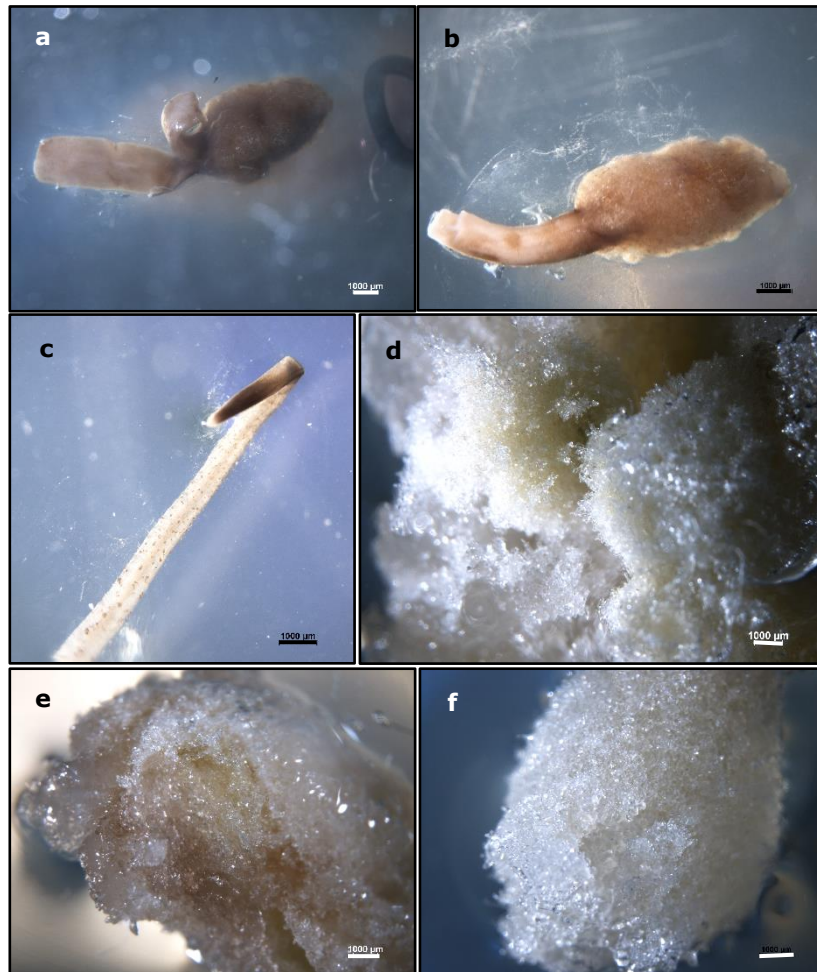


Figure 5.5 One-month culture of cotyledon, hypocotyl and root explants on MS media with 0.25 mg/l BS (a, b and c, respectively) turned brown and deteriorated. The cotyledon, hypocotyl and root explants on media without BS (d, e and f, respectively) proliferated into white, healthy callus. Scale bar represents 1 mm.

5.3.2 Effects of Microparticle Size, Target Distance and Bombardment He Pressure on Transformation

During the optimisation of biolistic parameters, each of the microparticle sizes, 0.6, 1.0 and 1.6 μm , was tested in combination with 3, 6 and 9 cm target distances and with 900, 1100 and 1350 psi He pressures. The percentage of transformants that proliferated into calli and displayed the expression of *sgfp* was recorded for each parameter (**Figure 5.6**).

Appendix G(i) shows the number of transformants obtained and the highest achievable sGFP intensities across the parameters tested. The

summary of statistical analysis using logistic regression in a generalized linear model is also shown in **appendix G(ii)**. The combination of 1.6 μm gold particles with 6 cm target distance and 1350 psi He pressure gave the highest number of transformants and the highest GFP intensity. This combination gave up to 18% transformation efficiencies (14.8% in average), which was calculated as the percentage of effective number of transformed calli (integration of *sgfp* into genomic DNA confirmed by PCR, **(Figure 5.7)** divided by the total number of bombarded explants. A total of 67.4% of the bombarded explants were BS-resistant and 14.8% of the total were expressing sGFP (**Table 5.3**).

Table 5.3 The transformation frequency of hypocotyl explants bombarded using the optimum parameters.

Number of explants bombarded	Number of calli	
	BS-resistant	sGFP-expressed ¹
135	91 (67.4%)	20 (14.8%)

¹The result was calculated from the sum of data across three replicates obtained in **appendix G(i)**.

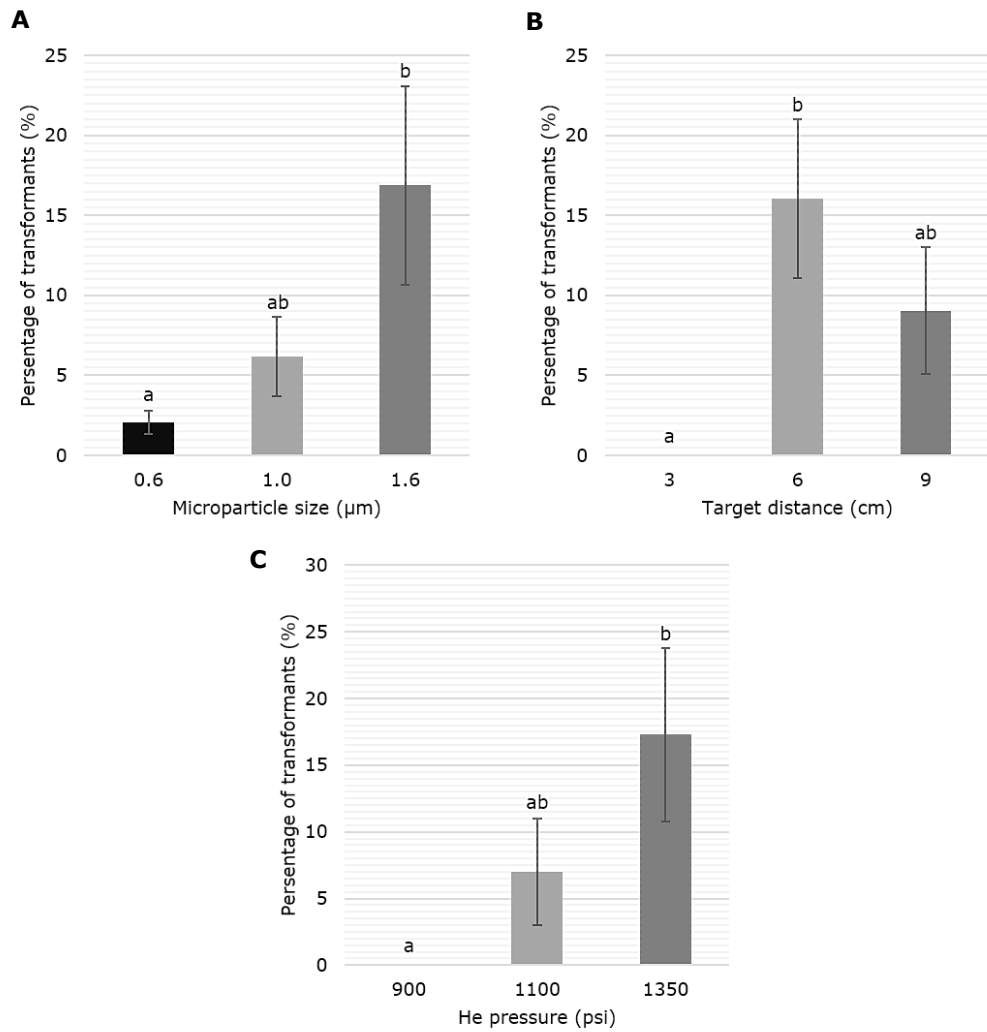


Figure 5.6 Bar chart representing the mean percentage of transformants expressing *sgfp* achieved under different (A) microparticle sizes, (B) target distances and (C) He pressures. Error bars represent standard deviation ($n=3$). Bars denoted with different letters are significantly different at $p=0.05$.

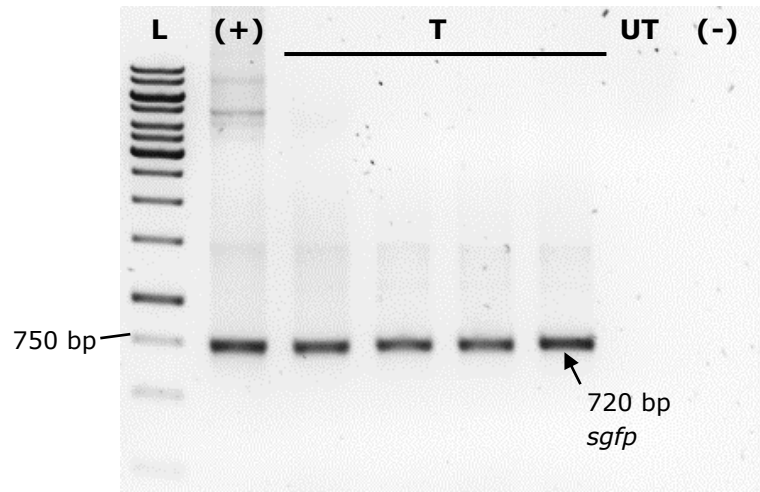


Figure 5.7 PCR of *sgfp* gene (720 bp) from the genomic DNA of transformed calli (T). L: GeneRuler 1kb DNA ladder, (+): PCR positive control using pcDNA6.2::35Sp-*sgfp* as the DNA template, UT: PCR using the genomic DNA of untransformed calli as the DNA template, (-): PCR negative control without any DNA template.

5.3.3 Intensity of sGFP Over Time and Distribution in Transformants

Explants that were bombarded using the best tested parameters, i.e. 1.6 μm gold particle size, 6 cm target distance and 1350 psi He pressure, were observed over a period of 60 days to examine the pattern of stable GFP expression over time. Transient expression of GFP was observed starting one day post-bombardment, but was inconsistent (i.e. gain and loss of spots occurred at different rates) among the bombarded explants and declined five days after bombardment. Besides that, a wounded part of an explant was more susceptible to transformation (**Figure 5.8**). A few new foci of GFP expression could be observed around 15 days post-bombardment and purportedly stable expression was observed in the same explants over the time course. The GFP intensity increased slowly over the days until the highest level of intensity was seen 50 days post-bombardment, after which the GFP intensity declined sharply (**Figure 5.9**).

Besides that, it was also observed that the GFP intensity was not consistent among the transformed explants. Some of the bombarded explants displayed a lower expression of GFP, whereas some displayed a higher expression of GFP (**Figure 5.10**).

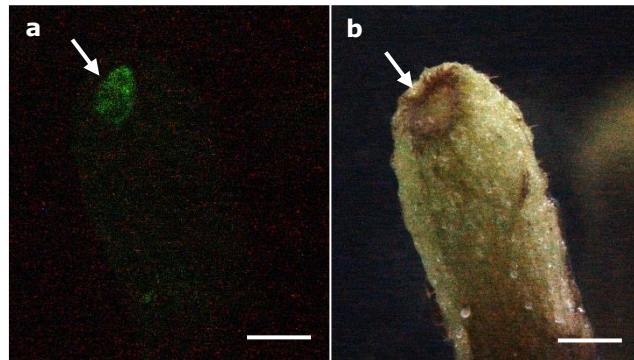


Figure 5.8 The transient expression of sGFP at the wounded part of a hypocotyl explant. a: Blue light microscopy in the dark, b: Bright field microscopy. Scale bar represents 1 mm.

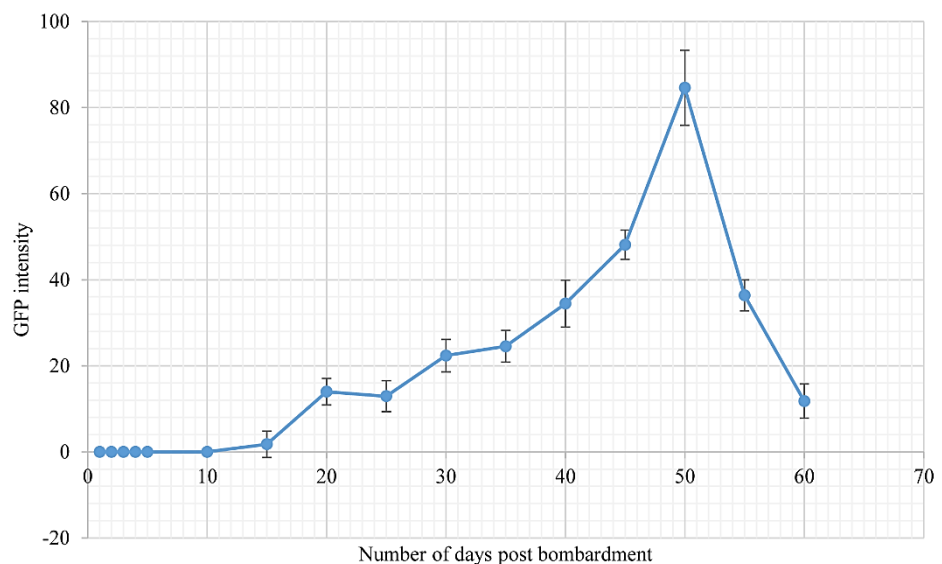


Figure 5.9 Plot of the highest mean intensities (background-subtracted) of purportedly stable sGFP fluorescence over 60 days after bombardment. Error bars represent the standard deviation of the mean values (n=3).

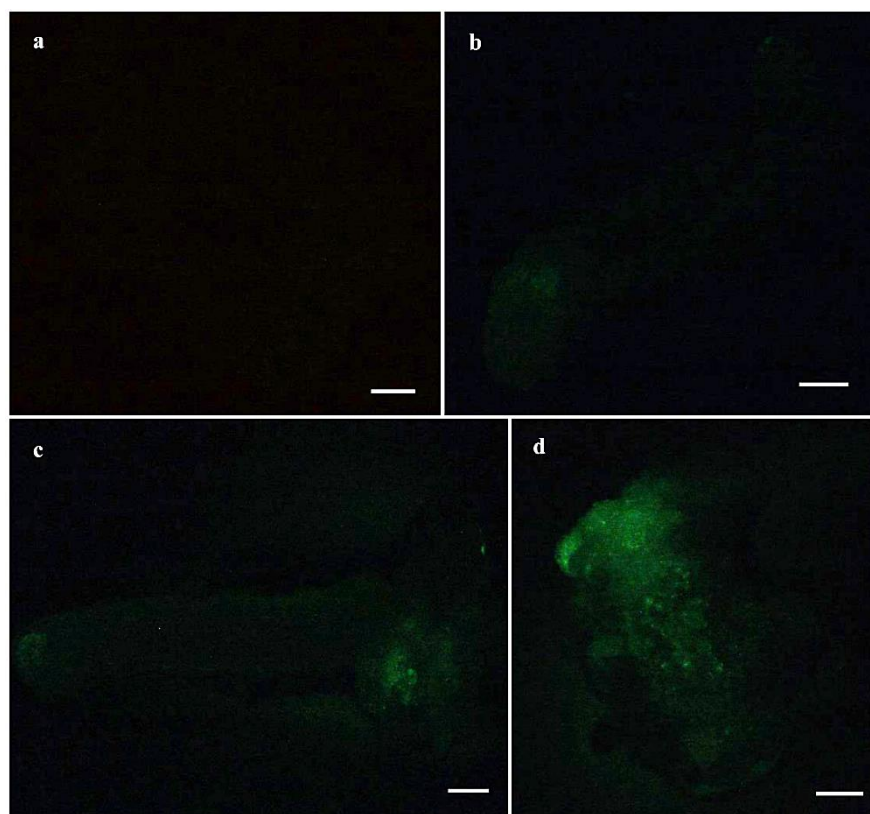


Figure 5.10 Regenerated tissues of calli expressing sGFP at different intensities after bombardment. Callus not expressing GFP is shown in a (negative control) and calli expressing GFP at different intensities are shown from b (lower intensity) to d (higher intensity). Scale bar represents 1 mm.

5.3.4 Verification of Gene Integration in Calli Transformed with Vanillin Biosynthetic Genes

Purification of genomic DNA from 50-day transformed calli was successful, as shown by the intact genomic DNA profiles in **Figure 5.11**. Following the purification of genomic DNA, PCR amplification of *fcs* and *ech* genes from selected calli that were transformed with pcDNA6.2::35Sp-*fcs*-NOSp-*ech* gave the desired bands of ~1.5 kb and ~900 bp, respectively (**Figure 5.12**). PCR amplification of the *fcs* gene from selected calli that were transformed with pcDNA6.2::35Sp-*fcs* gave the desired bands of ~1.5 kb (**Figure 5.13**). PCR amplification of the *ech* gene from selected calli that were transformed with pcDNA6.2::NOSp-*ech* gave the desired bands of

~900 bp (**Figure 5.14**). PCR amplification of the *VpVAN* gene and the 35Sp-*VpVAN* cassette from selected calli that were transformed with pcDNA6.2::35Sp-*VpVAN* and pHBT12K::35Sp-*VpVAN* gave the desired bands of ~1.1 kb (**Figure 5.15**) and ~1.5 kb (**Figure 5.16**), respectively.

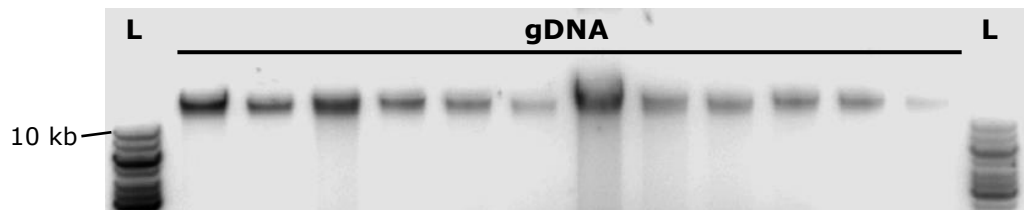


Figure 5.11 Genomic DNA profiles of transformed calli. L: GeneRuler 1kb DNA ladder, gDNA: Purified genomic DNA.

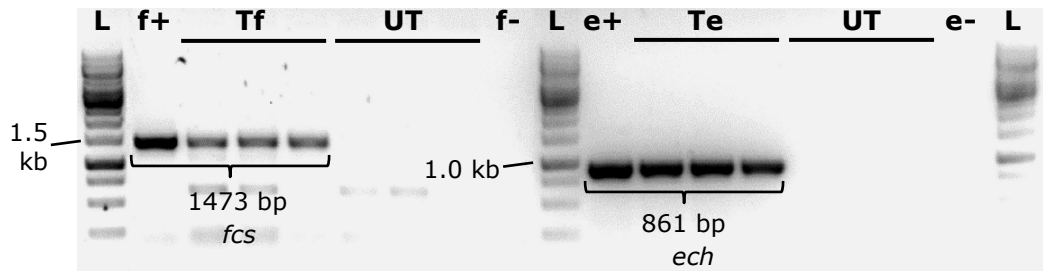


Figure 5.12 PCR of *fcs* and *ech* genes (1473 and 861 bp, respectively) from the genomic DNA of calli transformed with pcDNA6.2::35Sp-*fcs*-NOSp-*ech*. L: GeneRuler 1kb DNA ladder, f+: PCR positive control using the pUCIDT-*fcs* as the DNA template, e+: PCR positive control using the pUCIDT-*ech* as the DNA template, Tf: *fcs* gene from transformed calli, Te: *ech* gene from transformed calli, UT: Untransformed calli, f- and e-: PCR negative controls without any DNA template.

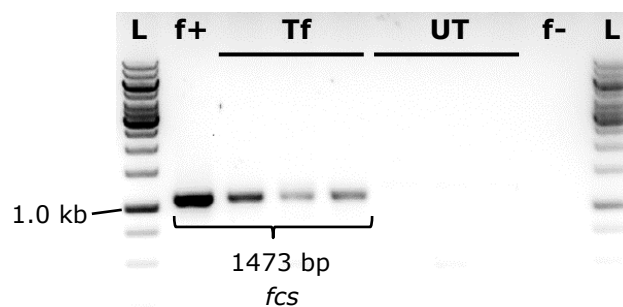


Figure 5.13 PCR of *fcs* gene (1473 bp) from the genomic DNA of calli transformed with pcDNA6.2::35Sp-*fcs*. L: GeneRuler 1kb DNA ladder, f+: PCR positive control using the pUCIDT-*fcs* as the DNA template, Tf: *fcs* gene from transformed calli, UT: Untransformed calli, f-: PCR negative controls without any DNA template.

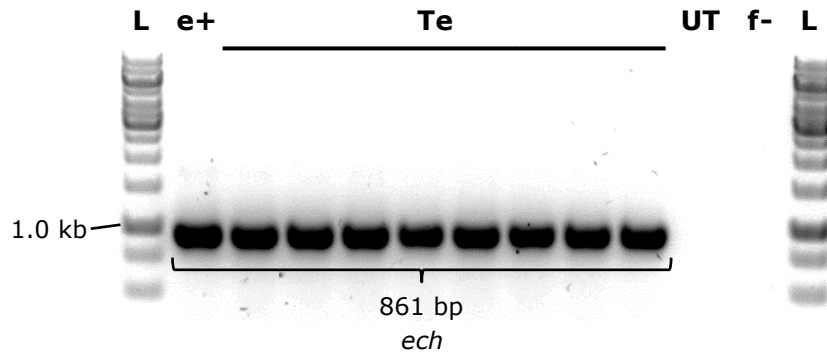


Figure 5.14 PCR of *ech* gene (861 bp) from the genomic DNA of calli transformed with pcDNA6.2::NOSp-*ech*. L: GeneRuler 1kb DNA ladder, e+: PCR positive control using the pUCIDT-*ech* as the DNA template, Te: *ech* gene from transformed calli, UT: Untransformed calli, e-: PCR negative controls without any DNA template.

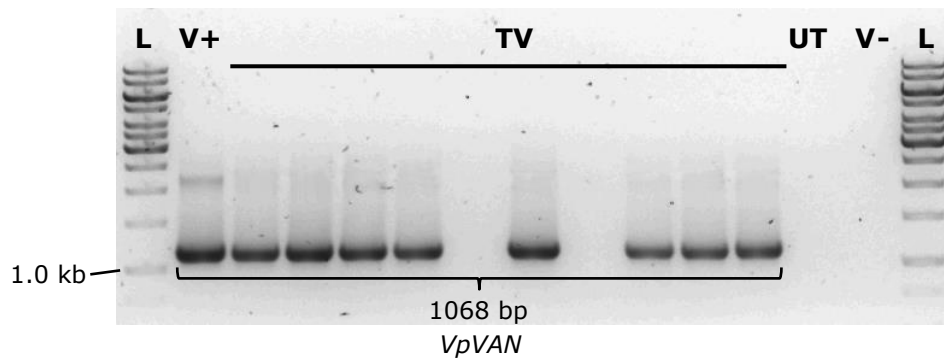


Figure 5.15 PCR of *VpVAN* gene (1068 bp) from the genomic DNA of calli transformed with pcDNA6.2::35Sp-*VpVAN*. L: GeneRuler 1kb DNA ladder, V+: PCR positive control using the pUCIDT-35Sp-*VpVAN* as the DNA template, TV: *VpVAN* gene from transformed calli, UT: Untransformed calli, V-: PCR negative control without any DNA template.

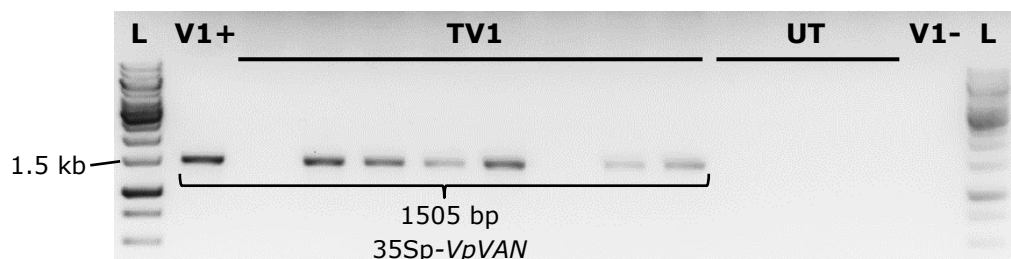


Figure 5.16 PCR of 35Sp-*VpVAN* cassette (1505 bp) from the genomic DNA of calli transformed with pHBT12K::35Sp-*VpVAN*. L: GeneRuler 1kb DNA ladder, V1+: PCR positive control using the pUCIDT-35Sp-*VpVAN* as the DNA template, TV1: 35Sp-*VpVAN* gene from transformed calli, UT: Untransformed calli, V1-: PCR negative controls without any DNA template.

5.4 DISCUSSION

5.4.1 Inhibitory Effects of Blastidicin S

BS is a potent antibiotic, which could cause rapid cell death at low concentrations (Thermo Fisher Scientific, 2016). In a previous study by Tamura and co-workers (1995), BS was found to prevent callus formation completely from the roots of *Arabidopsis thaliana* at 20 mg/l concentration and reduced callus formation tremendously at 5 mg/l. In another study, transgenic tobacco shoots were selected at 2.5–5.0 mg/l BS (Kamakura *et al.*, 1990). In this study, the E_{100} for BS was found to be relatively low, at 0.25 mg/l for the hypocotyl explants of *C. frutescens* L. cv. Hot Lava that were used in this study. It was possible that the explants were more susceptible to BS and required a more gentle selection pressure as they were harvested from chilli seedlings in an early stage (juvenile) of growth. Nevertheless, it was thought that transformed calli expressing the *bsd* gene could be potentially resistant to higher concentrations of BS, although the hypocotyl explants were initially selected at 0.25 mg/l BS. As an example, shoots of *Arabidopsis thaliana* and *Nicotiana tabacum*, which were transformed with the *bsd* gene, were initially selected at 10 mg/l BS. Later, the resulting transgenic plants showed resistance to 100 mg/l BS sprayed on their leaves (Tamura *et al.*, 1995).

It was interesting to observe a uniformity in the response to various BS concentrations across all of the tested explant types (cotyledons, hypocotyls and roots). The E_{100} for cotyledon, hypocotyl and root explants was in a very narrow range of 0.20–0.25 mg/l. This result suggests that different organs of the same seedling age had similar susceptibility to the selective agent. Nevertheless, only hypocotyls were used in subsequent studies as hypocotyls were found to be the most suitable explant type that

regenerated into calli with higher biomass than the other two explant types, as described in chapter 3.

5.4.2 Optimisation of Biolistic Parameters

In biolistics, there are many factors affecting transformation efficiencies that interact in complex ways. Due to the difficulty of addressing all possible variables in a single, large experiment, many researchers would prioritise the parameters based on their magnitude of effects and then optimise and test their interactions on a smaller scale. Generally, this optimisation study was conducted around the variables recommended by the Biolistic[®] PDS-1000/He Particle Delivery System Catalog Numbers 165-2257 and 165-2250LEASE to 165-2255LEASE Manual. For plant callus or cell cultures, the use of osmoticum was not recommended, and the other recommended variables were 28 inches Hg vacuum, 9 cm target distance, 1100 psi He pressure and 1.0 µm gold particle size. In this study, the combination of 1.6 µm gold particle size, 6 cm target distance and 1350 psi He pressure gave the highest number of transformants (14.8%), which was confirmed by PCR, as well as the highest GFP intensity. The vacuum was set constant at 28 inches Hg, which was in the recommended range that minimised the damage to tissues due to the He force and deceleration of microparticles on target tissues (Rech *et al.*, 2008). The bombardment chamber was made partial vacuum to reduce frictional drag on microcarriers as they decelerate towards the target tissues. As the rupture disk bursts, a shock wave of He gas passes through the vacuum and hits the target tissues at a force that can damage the target tissues. In a study reported by Heiser (n.d.), the magnitude of vacuum pressure used for the transformation of yeast and cauliflower was the same (28 inches Hg),

suggesting that the variability caused by vacuum could be minimal across a wide range of target tissues (plant and microbial tissues). In this study, a mock bombardment termed "the vacuum control" was performed without gold particles to assess the damage that could potentially result from the vacuum and the He shock wave. Results from the vacuum control showed no damage in any of the tested explants, all of which later proliferated into healthy calli in the CIM. Nevertheless, it was reported that the bombardment impact of smaller particles was more pronounced at the same vacuum (Heiser, n.d.). In this study, the most optimum gold particle size was 1.6 μm , which was relatively larger than the other two available sizes (0.6 and 1.0 μm). As such, the vacuum effect would be less pronounced. Besides that, although smaller particle sizes were claimed to cause less damages to tissues, particles as large as 1.6 μm did not seem to result in lower transformation efficiencies. The same gold particle size was used by Furutani and Hidaka (2004) to produce 11% of hygromycin-resistant soybean clones which expressed GFP.

Transformation efficiencies across different combinations of the tested parameters were generally less than 10% and more rarely, less than 20%. This could be due to the nature of transgene integration in biolistic transformation, which is complex and could be affected by random occurrences, such as DNA breakage and premature ligation of DNA before integration (Hansen and Wright 1999). Separate analysis within each of the respective groups (microcarrier size, target distance and He pressure) showed significant interactions (F probability <0.05) (**Appendix G(ii)**, within groups). The 1.6 μm microcarrier performed better than the 0.6 μm and 1.0 μm microcarriers, and the 6 cm target distance was significantly more effective than the 3 cm and 9 cm target distances. For He pressure, 1350 psi was significantly more efficient than 900 psi and 1100 psi.

Subsequent combination of these outcomes showed that 1.6 μm gold particles, 6 cm target distance and 1350 psi He pressure were the most suitable parameters for the biotistic-mediated transformation of hypocotyl explants of *C. frutescens* based on this study.

In a standard fluorescence microscopy, noise from autofluorescence can contribute to errors in the measurement of GFP intensity when the GFP intensity to noise ratio is less than 1.5, which is considered low (Coffman and Wu, 2014; Waters, 2009). The reported data of the highest GFP intensities had signal/noise ratios of more than 1.5, a threshold below which error is said to arise (Heinrich *et al.*, 2013). This shows that the GFP signals detected in this study were significantly higher than those detected from the autofluorescence or background. Furthermore, signal intensities arising from autofluorescence have been analysed using Corel[®] PHOTO-PAINT[®] X8 (Billinton and Knight, 2001) and was subtracted from the GFP intensities henceforth (Verdaasdonk *et al.*, 2014).

5.4.3 Expression Pattern of GFP

The decline in the transient expression of *sgfp* five days after bombardment was followed by a more stable expression starting 15 days post-bombardment using the optimum parameters i.e., 1.6 μm gold particles, 6 cm target distance and 1350 psi He pressure. A similar expression pattern was reported by Lonsdale and co-workers (1998) in a study of bombarded wheat scutellar tissues, where transient expression of luciferase (similar to GFP) was visible shortly after bombardment, peaked after 2 days and declined to an undetectable level after 10 to 20 days. New areas of gene expression, presumably from the clones of single cells that had integrated the luciferase gene stably, was observed approximately

after 30 days. This suggests that gene integration could happen days or weeks after the introduction of the exogenous DNA (Blechl and Jones, 2009). In this case, care should be taken as the parameters for transient expression might not be effectively extrapolated to achieve stable expression because cells could have displayed false positives in transient expression, but could not divide and regenerate into transformants with stable expressions later on (Heiser, n.d.). GFP intensities increased slowly over the days until the highest level of intensity was seen 50 days post-bombardment, after which the GFP intensity declined sharply (Figure 5.9). This could be due to the slow proliferation of transformed tissues as the presence of selective antibiotic in the regeneration medium caused metabolic stress to the explants (Wang *et al.*, 2015; Zampieri *et al.*, 2017). Although slow, the increase in GFP intensity up to 50 days suggests that the rate of GFP production had increased with the proliferation of transformed tissues. From the time-point observations, it was hypothesized that the onset of transgene expression to a detectable level (as in the case of GFP) had started 15 days post-bombardment. Assuming a similar expression pattern for the BS resistance selectable marker, it was thought that the bombarded explants should be transferred to the selective media 15 days post-bombardment to minimise selection against actually transformed explants that had yet to express the resistance gene to a level sufficient to confer resistance on the explants.

The GFP fluorescence was observed more often at the wounded parts of the explants, which resulted from the excision of hypocotyls from the seedlings of *C. frutescens* during the pre-bombardment tissue culture procedure. Although wound-assisted transformations were frequently associated with *A. tumefaciens*-mediated transformations but not in the light of biolistic-mediated transformations (Christou, 1991; Ibrahim *et al.*,

2014; Spokevicius *et al.*, 2006; Zuker *et al.*, 1999), this observation suggests that the expression of *sgfp* was more apparent at the wounded parts possibly due to active multiplication of cells, which were transformed with the *sgfp* gene. It has been well-known that wounding promotes callus and organ regeneration (Hofmann, 2014; Ikeuchi *et al.*, 2013). Therefore, any cells in the wounded parts that were transformed with the *sgfp* gene could have multiplied and produced more GFP in those regions.

The detection of the *sgfp* gene by PCR two months post-bombardment confirmed the presence of the gene in the genome of transformants (Figure 5.7). Although the gene was present, a drastic decline of GFP fluorescence after 50 days post-bombardment suggests that the protein might have ceased expression or the protein was still expressed, but had lost its fluorescence. The GFP (S65T) reporter gene used in the plasmid construct was a modified *sgfp* gene, encoding a protein in which serine was replaced with threonine in a chromophore mutation at position 65 of the amino acid sequence, to give 100-fold higher fluorescence signal compared to the original jellyfish GFP (Chiu *et al.*, 1996). Transcription of this reporter gene was driven by a reliable, constitutive CaMV 35S promoter to give constant expression of GFP in cells where it was expressed. Nevertheless, there could have been a loss of expression over time due to systemic gene silencing by the host's defence mechanism. Transcribed messenger RNA (mRNA) of GFP was possibly removed with the production of small interfering RNA (siRNA) to target the mRNA of GFP for degradation (Kim *et al.*, 2006; Voinnet and Baulcombe, 1997). A small amount of siRNA could also trigger spontaneous local silencing of GFP where there was no systemic silencing (Kalantidis *et al.*, 2006). In addition, the number of copies of the *sgfp* gene that was integrated was uncertain, although transformants from a biolistic method usually take multiple copies

of the transgene into their nuclear genome (Sodiende and Kindle, 1993). Different copy number could result in difference in the expression level. In this regard, a high copy number does not always correspond to a high expression level. The occurrence of multiple copies of a foreign gene could trigger post-transcriptional gene silencing in the host cell, which in turn could lead to the loss of expression (Matzke *et al.*, 1994; Tang *et al.*, 2007; Vaucheret *et al.*, 1998).

Apart from that, the chromophore of GFP could have lost its fluorescence following constant light irradiation, a phenomenon known as photobleaching that is seemingly irreversible (Dickson *et al.*, 1997). Light irradiation of GFP generates endogenous singlet oxygen (1O_2), which induces damage to the GFP chromophore (Greenbaum *et al.*, 2000). However, the rate of photobleaching of GFP could be lower than other fluorescent proteins because the key GFP chromophore is located in the core of a β -barrel structure, thus somewhat protecting it from reaction with 1O_2 (Ormo *et al.*, 1996). Besides irradiation that causes photobleaching, the spectral properties of GFP *in vitro* are also sensitive to pH. As an example, the fluorescence of wild-type GFP is stable at pH 6–10, but a decrease below pH 6 causes a reduction in the fluorescence (Campbell and Choy, 2001). Therefore, any changes in the ionic strength of the tissue culture that lead to pH change could result in the loss of fluorescence. In the case that the GFP did not cease expression, it was possible that the rate of GFP production could not overcome the rate of fluorescence decline due to photobleaching or pH change after 50 days.

It was observed that GFP intensities were not consistent throughout a transformed explant and among the transformed explants (Figure 5.10), indicating that GFP was randomly distributed and was not expressed at the same level across the explants. This could be due to random uptake of the

exogenous plasmid into the cells, as well as random integration of the *sgfp* DNA into the genome of the host cells. Integration of target DNA into the genome in a nuclear transformation takes place *via* random recombination (Kindle, 1998; Sodiende and Kindle, 1993). Other than depending on the nature of the DNA, the gene expression also depends on the position in the genome where it is integrated. Integration into a transcriptionally active region may result in high expression, while positioning in a non-active region may cause reduced or no expression (Ingelbrencht *et al.*, 1991).

Despite being “transformed,” certain regions of the proliferating tissues did not necessarily express the GFP. The results from the bombardment using the optimum parameters gave 67.4% of BS-resistant calli, but only 22% of them expressed the GFP. The rest of the BS-resistant calli were considered untransformed. Transformed tissues expressing the GFP were presumed to have also acquired the *bsd* gene, which was included as a selectable marker. Hence, BS was used in the regeneration medium to kill untransformed tissues in order to select for transformed tissues. However, untransformed tissues that proliferated on this selective medium could have incorporated the *bsd* gene but not the *sgfp* gene due to the random integration nature of DNA into the host genome, as discussed earlier. Besides that, untransformed tissues could have developed resistance to the antibiotic through the induction of somaclonal variation. Somaclonal variation may occur in the form of cytological abnormalities, phenotypic and genetic mutations, gene activation and silencing, as well as epigenetic changes in the DNA (Kaepler *et al.*, 2000). The underlying epigenetic mechanisms may not be targeted, so methylation or demethylation events could occur randomly genome-wide. For example, the exposure of *Arabidopsis thaliana* callus to kanamycin has been reported to cause extensive genome-wide methylation, predominantly

hypomethylation, which had a greater effect with higher antibiotic dosage (Bardini *et al.*, 2003). The introduction of plants into tissue culture, the transformation procedure and the use of selective agents impose stresses that may lead to such genomic changes (Jain, 2001; Pluhar *et al.*, 2001). Genome-wide mutations can occur from hundreds to thousands of events every diploid genome and the frequency of transformation-induced mutations is not exactly understood. Furthermore, biolistics is notably correlated with deletion and disorganization of transgenic and chromosomal DNA (Latham *et al.*, 2006). Certain locations like the transgene itself may be activated or deactivated based on the requirements of the cell (Bardini *et al.*, 2003). Likewise, cells that are initially not resistant to the selective agent may be rendered resistant as a result of the genetic changes.

5.4.4 Genomic Integration of Vanillin Biosynthetic Genes

The vanillin biosynthetic genes, *fcs*, *ech* and *VpVAN*, have been successfully integrated into the genome of *C. frutescens* as shown by the results from the PCR analysis, a universal tool to identify the presence of the transgene in the genomic DNA (Glaeser and Heermann, 2015; Ivics *et al.*, 2014; Zhang *et al.*, 2016). However, not all of the BS-resistant calli have been integrated with the *VpVAN* gene (Figure 5. and 5.16). Two out of ten and two out of eight of the screened BS-resistant calli that were transformed with *pcDNA6.2::35Sp-VpVAN* and *pHBT12K::35Sp-VpVAN*, respectively, did not show the presence of the *VpVAN* gene. This observation was similar to the finding where not all BS-resistant calli expressed the *sgfp* gene, as discussed in subchapter 5.4.3. Again, such a phenomenon could be attributed to the random uptake of DNA into the host genome, which resulted in the incorporation of the *bsd* gene but not

the *sgfp gene*, or the acquisition of BS resistance by untransformed tissues possibly due to somaclonal variation (Bardini *et al.*, 2003; Kindle, 1998; Sodiende and Kindle, 1993).

5.5 CONCLUSION

The findings from this study have demonstrated that the minimal inhibitory concentration of BS at 0.25 mg/l was effective for the selection of bombarded hypocotyls. The optimum biolistic parameters were 6 cm of target distance and 1350 psi of He pressure, in combination with 28 inches Hg of vacuum, using 1.6 µm gold particles coated with DNA in the presence of CaCl₂ and spermidine. The delivery of pcDNA6.2::35Sp-*fcs*-NOSp-*ech*, pcDNA6.2::35Sp-*fcs*, pcDNA6.2::NOSp-*ech*, pcDNA6.2::35Sp-*VpVAN* and pHBT12K::35Sp-*VpVAN* separately into hypocotyls of *C. frutescens* was successful as the explants regenerated into calli and the genomic integration of the target genes, *fcs*, *ech* and *VpVAN*, was verified using PCR.

CHAPTER 6

EVALUATION OF GENE EXPRESSION LEVELS AND PHENOLIC CONTENTS IN CALLUS CULTURES OF *CAPSICUM FRUTESCENS* L.

6.1 INTRODUCTION

A wide range of tools are available for the study of gene expression at the molecular level, be it for clinical diagnostics or for analytical research. Among these tools is reverse transcription-quantitative PCR (RT-qPCR). For the analysis of plant secondary metabolites, such as phenolic compounds, high performance liquid chromatography (HPLC) is one of the most robust and reliable technologies available. The reliability of RT-qPCR and HPLC technologies (as described in **subchapters 6.1.1 and 6.1.2**, respectively) is attributed to the specificity, sensitivity and precision of both systems, which allows the detection of a target molecule down to very low quantities with reproducible results (Begas *et al.*, 2014; Gotfred-Rasmussen *et al.*, 2016).

6.1.1 RT-qPCR for the Quantification of Gene Expression

Levels

qPCR has come a long way since its discovery in the 1990's to becoming the "gold standard" in the quantification of nucleic acids because of high sensitivity and reproducibility, broad range of quantification, and ease of use of the method (Pfaffl, 2010). The highly sensitive nature of qPCR has enabled the quantification of small amounts of target molecules or the detection of small changes in the expression levels based on RNA molecules (Lockey *et al.*, 1998). qPCR is now used widely, with the development of myriad techniques for the application of qPCR in different types of DNA-, RNA- or protein-based assays. The advantages of qPCR have also extended towards its ability to quantify nucleic acids in unprocessed biological or pharmaceutical samples, making qPCR a leading resource over an extensive range of applications (Hussain, 2015; Liu, 2014). Besides being used in research, many applications in the diagnostic sector have been explored, which include quantification of microbes, determination of gene quantity, identification of exogenous genes in genetically modified foods, risk assessment of cancer relapse, and forensic applications (Bustin *et al.*, 2009).

The use of RNA as the starting material with the addition of an RT step has made the RT-qPCR a more powerful method in the analysis of changes in RNA levels. In this method, RNA is first transcribed into cDNA through an RT reaction, followed by using the cDNA as the template for the qPCR reaction. The RT-qPCR can be performed in a one-step or two-step reaction. The one-step reaction combines RT and qPCR in a single tube, using a reverse transcriptase and a DNA polymerase along with a single buffer. In the two-step reaction, the RT and qPCR are carried out separately using different buffers, reaction conditions and primers. Despite

being a robust technique for the comparison of gene transcripts within samples of interest, RT-qPCR relies on the use of appropriate calibration and reference materials. The effectiveness of PCR is often restricted by inefficient RNA purification protocols, which result in low quality templates or the presence of impurities that inhibit the PCR. As the preparation of samples for qPCR starts with the isolation of nucleic acids, many of the methods for gene expression studies are designed to prepare nucleic acids that are pure and free from bound proteins (Deepak *et al.*, 2007). Isolation of RNA is challenging due to the sensitivity of RNA to increased temperatures and degradation by RNases, which should be quickly inactivated during cell lysis.

For qPCR, the design of species-specific or gene-specific primers is needed for an accurate analysis of a target nucleic acid region. The qPCR assay can be performed using probe-based detection, such as hydrolysis probes, hybridisation probes, molecular beacons or Scorpions™, or dye-based detection, such as SYBR®, YoYo™, BOXTO, Ampifluor™, quencher-labelled primers or LUX™ primers (Sigma-Aldrich, n.d.). Focusing on the dye-based detection that was used in this study, DNA-binding dyes can bind non-specifically to double-stranded DNA. Hence, the specificity of the primers is often indicated through the analysis of a melt (dissociation) curve, whereby the final PCR product is denatured at a temperature gradient from 50–95°C to detect the decrease in fluorescence as the dye dissociates. PCR amplicons of different lengths and sequences would melt at different temperatures, resulting in the observation of distinct melt peaks (Pryor and Wittwer, 2006).

A variety of kits and instruments are available for qPCR. The real-time capability of the qPCR enables immediate data output from the kinetics of the PCR and produces a visual representation of the PCR

amplification simultaneous to the PCR cycles. Despite the extensive use of qPCR, it is important to understand the basic principles, potential sources of errors and potential problems that might arise with the RT-qPCR. Therefore, there is a need for proper validation to develop a qPCR assay that is reproducible, sensitive, truly quantitative and reliable with biologically valid experimental designs. Nevertheless, RT-qPCR is a common tool for the quantification of expression levels of desired genes, as employed in this study—a dramatic increase in use and application has been observed over the past couple of years (Deepak *et al.*, 2007).

6.1.2 HPLC for the Quantification of Plant Metabolites

HPLC is a robust technique for separating, identifying and quantifying individual chemical components in liquid samples. HPLC is used for various applications, such as in the medical, forensic, environmental and manufacturing arena. Generally, this technique is fast, automated, highly accurate and precise, but it can also be complicated and expensive.

There are two common types of HPLC applications, normal-phase and reverse-phase, depending on the relative solvent polarity and the stationary phase (Cazes, 1997). The normal-phase HPLC is technically similar to the conventional column chromatography (Bird, 1989). The HPLC separation column is filled with small particles of silica. The solvent used is non-polar, such as hexane. A typical column has an internal diameter of 4.6 mm (or less), with 150 to 250 mm length (Hemstrom and Irgum, 2006). Polar compounds in the sample that pass through the column will adsorb longer to the polar silica compared to the non-polar compounds. With that, the non-polar compounds will elute faster through the column

(Waters, 2014). Despite being termed as "normal", normal phase HPLC is not the most commonly used form of HPLC.

Reverse-phase HPLC is the most common type of HPLC being used. The column size used in reversed phase HPLC is the same as the normal-phase HPLC. However, the silica is modified to a non-polar state with the attachment of long hydrocarbon chains (eight or eighteen carbon atoms) at its surface (Waters, 2014). A polar solvent is used, such as the combination of water and an alcohol like methanol (Amersham Biosciences, 1999). There is a strong attraction between the polar solvent and the polar molecules in the sample passing through the column. Less attraction between the hydrocarbon chains on the silica in the stationary phase and the polar molecules in the sample-solvent mixture (mobile phase) will therefore cause the polar molecules in the mixture to elute of their time more with the solvent. Non-polar compounds have higher affinity to form attractions with the hydrocarbon groups as a result of Van der Waals bondings (Hemstrom and Irgum, 2006). These compounds are less soluble in the solvent due to the need to release from hydrogen bonds as the compounds move in the polar mobile phase. Therefore, non-polar compounds elute more slowly through the column as compared to polar compounds (Waters, 2014).

The HPLC separation can be performed *via* isocratic elution or gradient elution. In an isocratic elution, the composition of the mobile phase remains constant throughout the HPLC programme. In a gradient elution, the ratio of polar to non-polar compounds in the mobile phase is changed gradually during the HPLC programme. This technique is applied when a sample contains components of different polarities. The gradient elution enables the separation of compounds of various polarities in a

shorter time without causing the loss of resolution of earlier peaks or the much broadening of later peaks (Barkovich, 2017).

This study utilised the reverse-phase HPLC, where hydrophobic molecules are adsorbed to the hydrophobic stationary phase in the chromatography column comprising of alkyl chains bound to solid support. The detection of phenolic compounds that were potentially present in target samples was done by separating sample matrices into individual components after extracting them from the target samples. Effective separation by HPLC could only be achieved with optimal conditions, such as appropriate mobile phase composition, run programme and detection wavelength.

6.1.3 Specific Objectives

The analysis of transgene expressions of *fcs*, *ech* and *VpVAN* using RT-qPCR and subsequently, the analysis of metabolic compounds (vanillin, vanillic acid, vanillin- β -D-glucoside (hereinafter referred to as vanillin glucoside), ferulic acid and capsaicin (collectively referred to as the phenolic compounds) involved with the expressed enzymes using HPLC would provide further verifications in this bioengineering study of vanillin biosynthesis. Therefore, the specific objectives of this study were to: (i) obtain high quality total RNA from transformed and untransformed calli of *C. frutescens* for cDNA conversion; (ii) achieve specific and efficient qPCR with the inclusion of stable housekeeping (reference) genes; (iii) obtain significant differences in the relative expression levels of transgenes between transformed and untransformed calli; (iv) achieve optimised mobile phase composition and validated HPLC method for the analyses of phenolic compounds; (v) obtain significant differences in the phenolic

contents between transformed and untransformed callus cultures of *C. frutescens*, which might correlate to the transgene expression levels.

6.2 MATERIALS AND METHODS

Calli samples (and their respective RNA and phenolic extracts) that were transformed with the following expression vectors are hereinafter denoted as:

- (i) "FcsEch" for pcDNA6.2::35Sp-*fcs*-NOSp-*ech* expression vector
- (ii) "Fcs" for pcDNA6.2::35Sp-*fcs* expression vector
- (iii) "Ech" for pcDNA6.2::NOSp-*ech* expression vector
- (iv) "pcVAN" for pcDNA6.2::35Sp-*VpVAN* expression vector
- (v) "pHVAN" for pHBT12K::35Sp-*VpVAN* expression vector
- (vi) "Neg" for negative controls (untransformed samples)

6.2.1 Analysis of RNA Levels by RT-qPCR

Prior to any RNA-related work, the following procedures were conducted to eliminate any possible RNase that might be present and cause degradation to RNA samples: All working surfaces, micropipettes, tube holders, pipette tip boxes and gel electrophoresis tanks were wiped with RNaseZap[®] RNase Decontamination Solution (Thermo Fisher Scientific, USA). Other tubes and plastic wares were soaked in 0.5 M NaOH for at least 10 min, then rinsed three times with 0.1% (v/v) diethyl pyrocarbonate (DEPC)-treated ultrapure (18 M Ω) H₂O and dried completely before use. UltraPure[™] DNase/RNase-free distilled water (Invitrogen, Thermo Fisher Scientific, USA) was used as the universal diluent in all RT-qPCR preparations.

6.2.1.1 Purification of RNA Using TRIzol® Reagent

Approximately 100 mg of callus for each sample was ground with 1 ml of TRIzol® Reagent in a 1.5 ml microcentrifuge tube using a Kimble™ pestle (Fisher Scientific, USA). Then, 200 µl of chloroform was added into the lysate and the mixture was incubated for 3 min at room temperature. The mixture was centrifuged for 15 min at 12,000 ×g and 4°C in a refrigerated centrifuge (Eppendorf 5810R, Germany). The colourless upper aqueous phase containing the RNA was separated from the middle interphase and the red lower phenol-chloroform phase and was transferred into a new 1.5 ml microcentrifuge tube. Isopropanol (500 µl) was added to the aqueous phase and the mixture was incubated for 10 min at room temperature to precipitate the RNA. The mixture was centrifuged for 10 min at 12,000 ×g and 4°C. The supernatant was then discarded using a micropipette. The translucent gel-like RNA pellet was re-suspended in 75% (v/v) ethanol and mixed by vortexing to wash the RNA. The sample was centrifuged for 5 min at 7,500 ×g and 4°C and the supernatant was discarded using a micropipette. The RNA pellet was air-dried for 15 min and subsequently re-suspended in UltraPure™ DNase/RNase-free distilled water (Invitrogen, Thermo Fisher Scientific, USA) and incubated at 55°C for 10 min for complete dissolution. The purified RNA was divided into three aliquots: The first aliquot was used for quantification using the NanoDrop 1000 Spectrophotometer (Thermo Scientific, USA) and then stored at -80°C, the second aliquot was sent for RNA integrity number (RIN) check, and the third aliquot was used for copy DNA (cDNA) conversion *via* reverse transcription.

6.2.1.2 Quantification of RNA

The analysis of RNA quantity and quality was first performed using the NanoDrop 1000 Spectrophotometer (Thermo Scientific, USA), as described in **subchapter 2.6**, to estimate the purity of the RNA based on the 260 nm/280 nm ratio. After that, an aliquot of the purified RNA was sent to 1st Base Laboratories (Malaysia) for the analysis of the RIN using an Agilent 2100 Bioanalyzer and RNA LabChip[®] (Agilent Technologies, USA). A 260 nm/280 nm ratio of ≥ 1.8 was accepted as pure, while a RIN of ≥ 7.0 (from the scale of 1, degraded, to 10, intact) was considered as good quality (Bustin *et al.*, 2009; Bustin *et al.*, 2010; Marx, 2013; Taylor *et al.*, 2010).

6.2.1.3 Design and Synthesis of Primers

Primers for four reference genes—actin (*ACT*), β -tubulin (*β -TUB*), glyceraldehyde-3-phosphate dehydrogenase (*GAPDH*) and ubiquitin-conjugating enzyme (*UBI-1*)—were designed based on the reference gene sequences for RT-qPCR in pepper, as recommended by Wan *et al.* (2011). Primers for the target genes (*fcs*, *ech* and *VpVAN*) were designed using Integrated DNA Technologies PrimerQuest Tool (<http://sg.idtdna.com/PrimerQuest/Home/Index?Display=AdvancedParams>) with the amplicon size settings set to min=100, opt=150, max=200. All primers were synthesised by Integrated DNA Technologies (Singapore). The primer sequences are listed in **appendix H**.

6.2.1.4 Synthesis of cDNA by Reverse Transcription

The synthesis of cDNA was carried out using QuantiTect® Reverse Transcription Kit (Qiagen, Germany) according to the protocol handbook. For each sample, 1 µg of RNA was converted into cDNA. A genomic DNA elimination reaction was first performed using the gDNA Wipeout Buffer provided in the kit. The volumes and concentrations of the components for the genomic DNA elimination reaction are given in **Table 6.1**. The sample was incubated for 2 min at 42°C, and then placed on ice immediately.

Table 6.1 The components in a genomic DNA elimination reaction.

Component	Volume/reaction	Final concentration
7× gDNA Wipeout Buffer	2 µl	1×
Template RNA	Variable (to 1 µg)	1 µg/reaction
RNase-free water	Variable	-
Total volume	14 µl	

Subsequently, the RT reaction was carried out on the product of the genomic DNA elimination reaction using the components as specified in **Table 6.2**. The RT reaction was performed for 15 min at 42°C, followed by 3 min at 95°C to inactivate the reverse transcriptase. The resulting cDNA was stored at -20°C until further use in qPCR.

Table 6.2 The components in a reverse transcription reaction.

Component	Volume/reaction	Final concentration
QuantiScript Reverse Transcriptase	1 µl	-
5× QuantiScript RT Buffer	4 µl	1×
RT primer mix	1 µl	-
Entire gDNA elimination reaction from above (Table 6.1)	14 µl	1000 ng/20 µl = 50 ng/µl
Total volume	20 µl	

6.2.1.5 qPCR Analysis

Samples which were analysed included calli that were transformed with pcDNA6.2::35Sp-fcs-NOSp-ech, pcDNA6.2::35Sp-fcs, pcDNA6.2::NOSp-

ech, pcDNA6.2::NOSp-*ech*, pcDNA6.2::35Sp-*VpVAN* and pHBT12K::35Sp-*VpVAN*, and those that were untransformed. For each sample type, selected samples that were pooled into three biological sets were analysed on the target gene(s) and two reference genes (*ACT* and *UBI-1*). The two reference genes were selected from four reference genes (*ACT*, β -*TUB*, *GAPDH* and *UBI-1*), which were initially analysed for suitability using untransformed controls (results in **subchapter 6.3.1.3**). Three technical replications were carried out for each qPCR sample.

All qPCR samples were prepared using the master mix provided in the KAPA SYBR[®] FAST qPCR Kit (KAPA Biosystems, USA) according to the protocol handbook. The kit contained KAPA SYBR FAST qPCR Master Mix consisting of KAPA SYBR FAST DNA Polymerase, reaction buffer, dNTPs, SYBR Green I dye, and MgCl₂ at a final concentration of 2.5 mM (**Table 6.3**).

Table 6.3 The components in a qPCR reaction.

Component	Volume/reaction	Final concentration
DNase/RNase-free water	8.8 μ l	-
2 \times KAPA SYBR FAST qPCR Master Mix Universal	10 μ l	1 \times
10 μ M forward primer	0.4 μ l	200 nM
10 μ M reverse primer	0.4 μ l	200 nM
Template from RT reaction	0.4 μ l	20 ng/reaction
Total volume	20 μ l	

The thermal cycling and fluorescence acquisition was done using the CFX Connect[™] Real-Time PCR Detection System (Bio-Rad, USA) with the following conditions: (i) One cycle of initial denaturation at 95°C for 3 min (no acquisition, i.e. no fluorescence detection); (ii) 40 cycles of denaturation (95°C for 3 s, no acquisition), annealing (60°C for 20 s, no acquisition) and elongation (72°C for 12 s, single acquisition); (iii) one cycle of dissociation (melting) curve measurement—95°C for 1 min (no

acquisition), 60°C for 20 s (no acquisition) and 95°C at 3°C/s (continuous acquisition).

6.2.1.6 Validation of qPCR Amplification Efficiency

The qPCR amplification efficiency was validated using plasmid DNA (pUCIDT-*fcs*, pUCIDT-*ech* and pUCIDT-35Sp-*VpVAN*) and the respective primers for target genes, *fcs*, *ech* and *VpVAN* (**Appendix H**). Eight dilution steps of ten-fold (1:10) serial dilutions were done for each plasmid DNA using DNase/RNase-free water. Each of the nine dilutions (the 0th to the 8th dilution) were amplified by qPCR in triplicates. A calibration curve was plotted for each target gene by the CFX Manager software (Bio-Rad, USA) and the qPCR amplification efficiency, *E*, was calculated from the slope of each concentration curve, as follows (Bustin *et al.*, 2009; Svec *et al.*, 2015):

$$E = (10^{-(1/\text{slope})} - 1) \times 100\%$$

6.2.1.7 Analysis of Relative RNA Levels

The amount of mRNA transcripts, which reflected the expression level, was determined relative to those of reference genes to normalise variations in individual reactions that were caused by initial quantities of DNA templates. Therefore, the Cq values of the three target genes (*fcs*, *ech* and *VpVAN*) in transformed and untransformed samples were normalised with the geometric Cq mean of *ACT* and *UBI-1* reference genes (Vandesompele *et al.*, 2002). The geometric mean was calculated as follows:

$$\left(\prod_{i=1}^n x \right)^{\frac{1}{n}} = \sqrt[n]{x_1 x_2 \dots x_n}$$

where a capital pi notation is used to show a series of multiplications, and x_n is the Cq value of the n th reference gene. In this study, two reference genes were used (therefore, $n=2$). As such, the geometric mean of Cq values would be the square root of the product of two Cq values ($\sqrt{(Cq_{ACT})(Cq_{UBI-1})}$).

The relative expression of each target gene in each sample type was calculated using the $2^{-\Delta\Delta Cq}$ method (Livak and Schmittgen, 2001; Pfaffl, 2001; Yuan *et al.*, 2006). For each target gene, the delta Cq of each sample of interest and control sample ($\Delta Cq_{\text{sample or control}}$) was first calculated by deducting the geometric Cq mean of the reference genes from the Cq mean of biological sets for the target gene ($\Delta Cq_{\text{sample or control}} = Cq_{\text{target}} - Cq_{\text{reference}}$). Then, the delta delta Cq of each target gene in the sample of interest ($\Delta\Delta Cq$) was calculated by deducting the $\Delta Cq_{\text{control}}$ from the $\Delta Cq_{\text{sample}}$ ($\Delta\Delta Cq = \Delta Cq_{\text{sample}} - \Delta Cq_{\text{control}}$). For the comparison of relative expression, the *VpVAN* level from calli transformed with pcDNA6.2::35Sp-*VpVAN*, (denoted as *VpVAN*: pcVAN), was used as a control (calibrator). Finally, the relative expression, R, of a target gene in a sample of interest was calculated as $R = 2^{-\Delta\Delta Cq}$. With that, the relative expression level of *VpVAN*[pcVAN] was 1.00, and the expression levels of other target genes in other samples (denoted as *target gene*[sample]) were compared against *VpVAN*[pcVAN].

6.2.2 Analysis of Plant Phenolic Contents by Reverse-Phase HPLC

The preparation of solvents and eluents were done using ultrapure (18 M Ω) H₂O, where required. All glass wares were washed thoroughly and rinsed three times with ultrapure H₂O before being dried and used.

The preparation of analytical standards and the optimisation of HPLC mobile phase compositions were performed based on the methods recommended by Robert Linforth (method in **subchapter 6.2.2.1**) and Stuart Wilkinson (method in **subchapters 6.2.2.3–6.2.2.4**) (personal communications) from the University of Nottingham, UK.

6.2.2.1 Preparation of Standards

HPLC-grade analytical standards, vanillin (Acros, Thermo Fisher Scientific, USA), vanillic acid (Sigma-Aldrich, USA), vanillin glucoside (Santa Cruz Biotechnology, USA), ferulic acid (Acros, Thermo Fisher Scientific, USA) and capsaicin (Sigma-Aldrich, USA), were prepared in stock solutions of 4000 ppm (0.4%, w/v, or 4 mg/ml). For each standard, 8 mg of powder was dissolved in 1.6 ml of methanol, and then topped up to 2 ml with H₂O. With that, each standard was finally dissolved in 80% (v/v) methanol as the solvent. The stock solutions were diluted into desired working concentrations or stored at -80°C when not in use.

6.2.2.2 Preparation of Mobile Phase Eluents

In this study, three types of eluents were used in the mobile phase for the reverse-phase HPLC: Methanol (Fisher Scientific, USA), 1% (v/v) acetic acid, and H₂O. For every litre of 1% acetic acid, 10 ml of glacial acetic acid (Fisher Scientific, USA) mixed with 990 ml of H₂O. Each eluent was filtered through a 0.45 µm nylon membrane disc filter using a glass vacuum filtration unit (**Figure 6.1**). After that, the eluents were degassed for 30 min using a bath sonicator (Thermo-3D Ultrasonic Cleaner, Thermo-Line, Australia) prior to use.

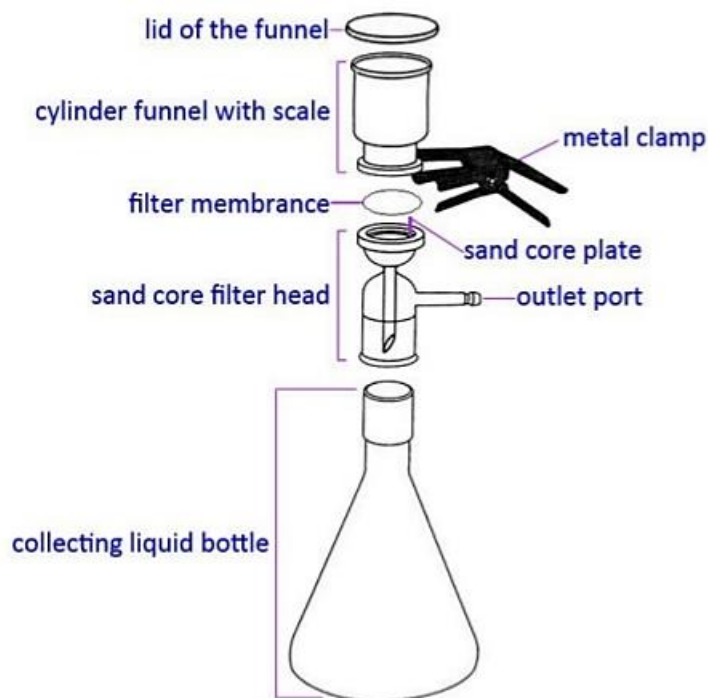


Figure 6.1 Illustration of a vacuum filtration unit. The nylon membrane disc filter was placed between the cylinder funnel and the sand core filter head, both of which were then clamped with the metal clamp. The filtration unit was connected to a vacuum pump through the outlet port. Eluents were poured into the cylinder funnel (without the lid) and were filtered through the nylon membrane to the collecting bottle. Adapted from <https://image.slidesharecdn.com/2014environmentalengineeringlabmanual-141017163332-conversion-gate02/95/2014-environmental-engineeringlabmanual-31-638.jpg?cb=1413563725>

6.2.2.3 HPLC Specifications and Settings

All HPLC analyses were performed using Agilent Infinity 1260 HPLC System (USA). The analytical column used was Hypersil GOLD™ C18 Analytical Column (250 mm length × 4.6 mm internal diameter, 5 μm pore size) (Thermo Scientific, USA). One column volume was 1.32 ml.

Before the start of each HPLC session, the three mobile phase diluents (methanol, 1% acetic acid and H₂O) were connected to three channels of tubing, respectively. Each channel was purged with its respective diluent for at least 10 min at a flow rate of 5 ml/min. Purging

was done without the diluents passing through the analytical column. After that, the column was flushed with approximately 20 column volumes (26.5 ml) of the storage eluent (80% methanol, v/v). Then, the column was equilibrated by flushing with the eluents of the optimised mobile phase composition. The total flush time was approximately 1.5 h.

For each HPLC run, 10 µl of sample was injected. The flow rate was fixed at 1 ml/min. Detection was performed by a photodiode array (PDA) detector in the UV region, which was set in the range of 230–325 nm wavelengths. The optimum wavelengths for the detection of each phenolic compound were determined based on peaks maxima in an isoabsorbance plot. To protect the column, the maximum back pressure was set to 400 bar (40,000 kPa), beyond which the HPLC run would be terminated automatically.

At the end of a HPLC session, the column was flushed with 10 column volumes of 100% methanol for the removal of late-eluted compounds, followed by H₂O for the removal of acid and hydrophilic compounds. The column was finally reconditioned by flushing with 20 column volumes of 100% methanol and gradually with 80% (v/v) methanol for storage. The total flush time was approximately 2 h.

6.2.2.4 Optimisation of Mobile Phase Composition

The idea of optimising the HPLC programme in terms of mobile phase composition was to achieve the optimum resolution (separation between compounds of interest) in the minimum time. The starting composition of the mobile phase (x:y methanol–1% acetic acid) was optimised with a gradient HPLC to a final composition of 50:50 methanol–1% acetic acid in 20 min using vanillin and ferulic acid standards. The starting composition of

the mobile phase (x:y methanol–1% acetic acid) was optimised with a gradient HPLC to a final composition of 50:50 methanol–1% acetic acid in 20 min. The optimisation was initially performed based on the gradient HPLC programme (**Table 6.4**) provided by Stuart Wilkinson (personal communication) using the PerkinElmer Series 200 HPLC System (USA). Starting compositions of 50:50, 45:55, 40:60, 35:65, 30:70, 25:75 and 20:80 methanol–1% acetic acid were tested. The optimised method was later transferred to the Agilent Infinity 1260 HPLC System (USA) with minor modifications to the programme (as described in **subchapter 6.3.2.1**) for subsequent analyses of vanillin, vanillic acid, vanillin glucoside and ferulic acid. The run time for each HPLC cycle was 37.5 min.

Table 6.4 The HPLC programme for the optimisation of mobile phase composition and for the analysis of phenolic compounds extracted from plant tissues.

Step	Time (min)	Flow rate (ml/min)	Composition (%)		Remark
			Methanol	1% acetic acid	
0	0.5	1.00	x	y	Initial
1	20.0	1.00	50	50	Gradient
2	1.0	1.00	100	0	Short flush
3	5.0	1.00	100	0	Short flush
4	1.0	1.00	x	y	Reconditioning
5	10.0	1.00	x	y	Reconditioning

The HPLC of capsaicin was performed separately from those of vanillin, vanillic acid, vanillin glucoside and ferulic acid due to the inability of the optimised gradient HPLC parameters to elute capsaicin. The mobile phase composition for the HPLC of capsaicin was fixed at 80:20 methanol–1% acetic acid for 10 min (isocratic HPLC) using the Agilent Infinity 1260 HPLC System (USA).

To determine the optimum resolution, a resolution (R_s) value was calculated, as follows (Skoog *et al.*, 2007):

$$R_s = \frac{t_{R2} - t_{R1}}{(w_{b2} + w_{b1})/2} = \frac{2(t_{R2} - t_{R1})}{w_{R1} + w_{R2}}$$

where t_{R1} and t_{R2} are the retention times of two adjacent peaks ($t_{R2} > t_{R1}$), and w_{b1} and w_{b2} are the corresponding peak widths at the base. An R_s value of 1.5 or greater between two peaks indicated that the compounds were separated well.

6.2.2.5 Concentration Curve of Standards

The stock solutions of analytical standards, except capsaicin, were mixed and diluted to concentrations of 1000, 500, 250, 125, 62.5, 31.25 and 15.625 ppm in two-fold (1:2) serial dilutions using 80% (v/v) methanol. HPLC was performed using the optimised gradient HPLC method for each concentration of standards. For capsaicin, a similar two-fold serial dilutions to concentrations of 1000, 500, 250, 125, 62.5, 31.25 and 15.625 ppm were done, followed by the isocratic HPLC for each concentration of the standard. After the HPLC, a concentration curve was plotted for each compound and the correlation value, R^2 , was calculated.

6.2.2.6 Extraction of Phenolic Compounds

About 2 g of plant tissues or culture media was harvested for the extraction of phenolic compounds. The extraction of phenolic compounds was done according to the procedure modified from (Jadhav *et al.*, 2009; Singh *et al.*, 2007; Johnson *et al.*, 1996). Each sample was ground with 80% (v/v) ethanol using a pestle and mortar. Then, the mixture was transferred into a 50 ml centrifuge tube and sonicated at 45°C for 25 min. Culture media were dried for 72 h at 60 °C prior to grinding and sonication with the 80%

ethanol. The mixture was then centrifuged at 6500 ×g for 15 min at 4°C. The supernatant was filtered through a filter paper (Whatman® 1, GE Healthcare, USA) placed in a funnel into a clean 250 ml round-bottom flask (Favorit, Ukraine). Steps from the addition of 80% ethanol to the pelleted sample, followed by vortex, sonication, centrifugation and filtration of the supernatant into the round-bottom flask were repeated twice. The filter paper was rinsed with 80% ethanol and the absorbed solution was wrung out of the filter paper into the round-bottom flask. The pooled filtrate in the round-bottom flask was then evaporated at 40°C using a rotary evaporator (Rotavapor® R-200, BUCHI, Switzerland) until the ethanol was removed, leaving a paste. The paste was finally resolubilised in 80% (v/v) methanol. The extract containing phenolic compounds was filtered through a 0.45 µm syringe filter (Sartorius Stedim, France) and degassed using a bath sonicator (Thermo-3D Ultrasonic Cleaner, Thermo-Line, Australia) prior to HPLC.

6.2.2.7 HPLC Analysis of Phenolic Compounds

Before the analyses of plant samples, the accuracy, precision, limit of detection (LOD) and limit of quantitation (LOQ) of the HPLC method were validated. The accuracy was determined using a spike recovery method (Betz *et al.*, 2011). Usually, a sample matrix that was originally devoid of the target compound was spiked with a known amount of the compound and the analysis was carried out from sample preparation to HPLC measurement of the compound. A comparison was then performed between the amount found and the added amount to determine the accuracy of the method. However, in this study, the target analyte might potentially occur in the sample matrix. Hence, a comparison was performed

between spiked and unspiked samples. The amount of the target compound recovered from the spiked sample would be the sum of the amount of added compound and the amount of naturally occurring analyte (as determined in unspiked samples). The difference between the amount of naturally occurring analyte and the total amount in the spiked matrix measured by HPLC gave an estimate of accuracy, which was quantified as a percentage of the target compound measured by HPLC (normalised with the naturally occurring analyte) over the known amount (300 ppm) added into the sample matrix.

The precision of the retention time and peak area was estimated from the relative standard deviation (RSD), also known as coefficient of variance (CV), as follows:

$$CV = \frac{SD}{\bar{x}}$$

where SD is the standard deviation and \bar{x} is the mean value. The retention time and peak area of each compound was measured three times.

The LOD and LOQ were determined based on signal-to-noise ratios, according to the International Conference on Harmonisation of Technical Requirements for Registration of Pharmaceuticals for Human Use (ICH) Harmonised Tripartite Guideline. Signal-to-noise ratios were determined by the Agilent ChemStation software based on the pre-determined range of noise occurrence. A signal-to-noise ratio of 3 or more for a target compound was acceptable as beyond the detection limit. A signal-to-noise ratio of 10 or more for a target compound was acceptable for reliable quantification.

The analysis of each extract was carried out by optimised gradient HPLC (for the detection of vanillin, vanillic acid, vanillin glucoside and ferulic acid), followed by isocratic HPLC (for the detection of capsaicin).

The chromatography peaks of individual phenolic compounds were identified by the Agilent HPLC ChemStation software based on calibration with the retention times of the analytical standards. Subsequently, data of HPLC peak areas (in mAU·s), which were acquired from the UV absorbance of the compounds, were collected. Using the concentration curves of standards (presented in **subchapter 6.3.2.3**), corresponding concentrations of the phenolic compounds were computed based on Beer-Lambert's Law (**Equation 6.1**).

$$A = \varepsilon \cdot c \cdot L \dots\dots \text{Equation 6.1}$$

where A is the measured absorbance, ε is the molar absorptivity or extinction coefficient (constant), c is the concentration of the absorbing species, and L is the pathlength through the extract.

After determining the concentrations of the extracts using **equation 6.1**, concentrations (contents) of phenolic compounds in the culture samples, as expressed in μg per g of sample weight ($\mu\text{g/g}$ or ppm), were calculated using **equations 6.2 and 6.3**:

$$m_{\text{extract}} = c \times V_{\text{extract}} \dots\dots \text{Equation 6.2}$$

where m_{extract} is the amount of phenolic compound in the extract (in mg), c is the concentration of phenolic compound in the extract (in ppm), and V_{extract} is the volume of the extract (in litre);

$$C_{\text{sample}} = \frac{m_{\text{extract}} \times 1000}{w_{\text{sample}}} \dots\dots \text{Equation 6.3}$$

where c_{sample} is the concentration (content) of phenolic compound in the culture sample (in $\mu\text{g/g}$ or ppm), $m_{extract} \times 1000$ is the amount of phenolic compound in the extract (in μg), and w_{sample} is the weight of the sample (in g).

6.3 RESULTS

6.3.1 Reverse Transcription-Quantitative PCR

6.3.1.1 RNA Quality

Prior to any RT-qPCR work, the quality of the purified RNA was checked using a NanoDrop 1000 Spectrophotometer (Thermo Scientific, USA). In addition, the RIN of the RNA was analysed. Generally, all purified RNA samples were of good quality and concentrations. **Table 6.5** shows the concentrations, 260 nm/280 nm ratios and RINs of the RNA samples analysed in this study. Results from the agarose gel electrophoresis and the Agilent 2100 Bioanalyzer analyses of the purified RNA are shown in **figure 6.2**.

Table 6.5 The measured concentrations, 260 nm/280 nm ratios and RINs of the RNA samples analysed.

RNA sample*	Concentration (ng/μl)	260/280 ratio	RIN
FcsEch-1	593	2.02	9.1
FcsEch-2	643	2.00	9.4
FcsEch-3	573	2.02	9.2
Fcs-1	256	1.99	9.0
Fcs-2	219	1.99	9.7
Fcs-3	688	2.04	9.8
Ech-1	1920	1.96	9.8
Ech-2	870	1.92	9.5
Ech-3	1100	1.92	9.8
pcVAN-1	860	1.90	9.8
pcVAN-2	1840	1.83	9.5
pcVAN-3	1130	1.75	9.5
pHVAN-1	172	1.92	9.0
pHVAN-2	452	2.02	9.8
pHVAN-3	337	2.00	9.3
Neg-1	140	1.95	9.3
Neg-2	296	1.95	9.2
Neg-3	366	1.98	9.2

*RNA samples were named according to calli that were transformed with the following expression vectors:

FcsEch: pcDNA6.2::35Sp-*fcs*-NOSp-*ech*

Fcs: pcDNA6.2::35Sp-*fcs*

Ech: pcDNA6.2::NOSp-*ech*

pcVAN: pcDNA6.2::35Sp-*VpVAN*

pHVAN: pHBT12K::35Sp-*VpVAN*

Neg: Negative controls (untransformed)

Numbers 1, 2 and 3 denote biological sets 1, 2 and 3, respectively.

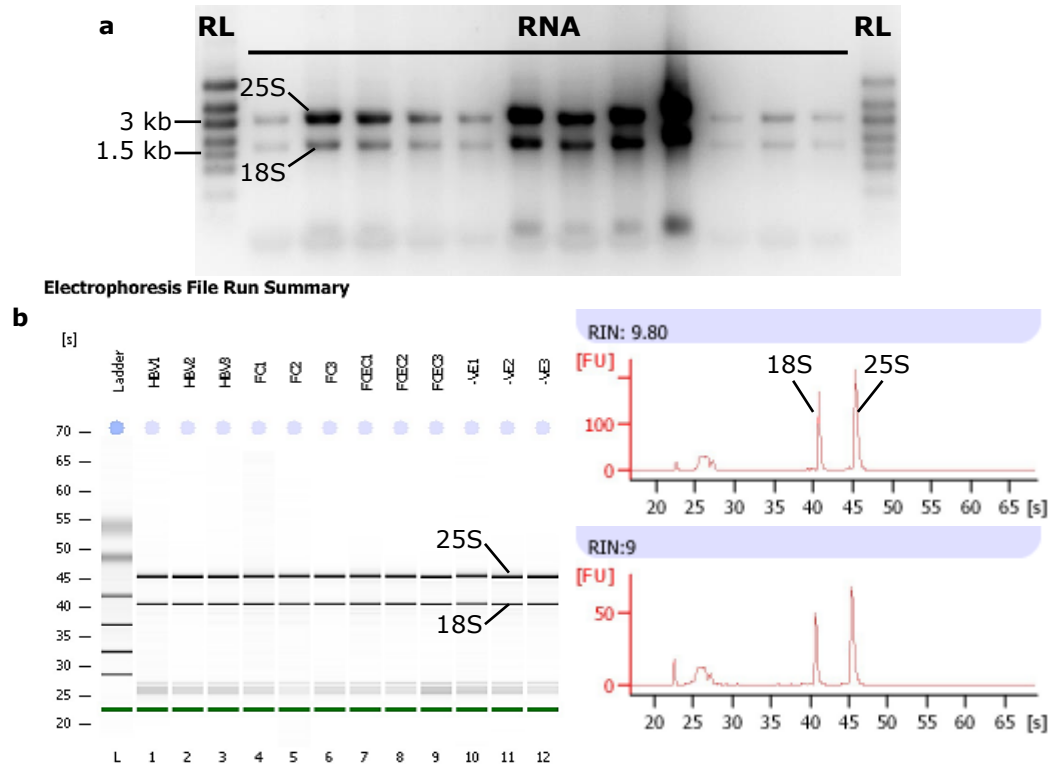


Figure 6.2 The RNA profiles after (a) agarose gel electrophoresis and (b) Agilent 2100 Bioanalyzer analysis. Intact bands of 18S and 25S ribosomal RNAs (rRNAs) were shown in the agarose gel and the virtual gel, with their distinct peaks for the highest RIN (9.8) and the lowest RIN (9.0) obtained. RL: RiboRuler high range RNA ladder

6.3.1.2 Validation of Primers

The primers were designed using Integrated DNA Technologies PrimerQuest Tool. The specificity of the primers was verified by conducting a BLAST query of the primer sequences against the European Molecular Biology Laboratory-European Biotechnology Institute (EMBL-EBI) and the National Center for Biotechnology Information (NCBI) databases.

For each of the seven genes, a PCR with gradient annealing temperatures (45.0, 45.4, 46.3, 47.7, 49.7, 51.6, 53.4, 55.3, 57.3, 58.7, 59.6, 60.0°C) was performed to verify the optimum annealing temperature and the amplicon size. Reference genes (*UBI-1*, *GAPDH*, *β -TUB* and *ACT*) were amplified from the cDNA of an untransformed callus (**Figure 6.3**).

Target genes (*fcs*, *ech* and *VpVAN*) were amplified from the respective holding vectors, pUCIDT-*fcs*, pUCIDT-*ech* and pUCIDT-35Sp-*VpVAN*, which served as positive controls (**Figure 6.4**). All tested genes were amplified at temperatures as high as 60.0°C and gave the expected amplicon sizes— 278 bp for *UBI-1*, 276 bp for *GAPDH*, 167 bp for β -*TUB*, 228 bp for *ACT*, 155 bp for *fcs*, 150 bp for *ech* and 160 bp for *VpVAN* (**Appendix H**). The no reverse transcriptase (NRT) control showed no amplification for all reference genes (**Figure 6.5**).

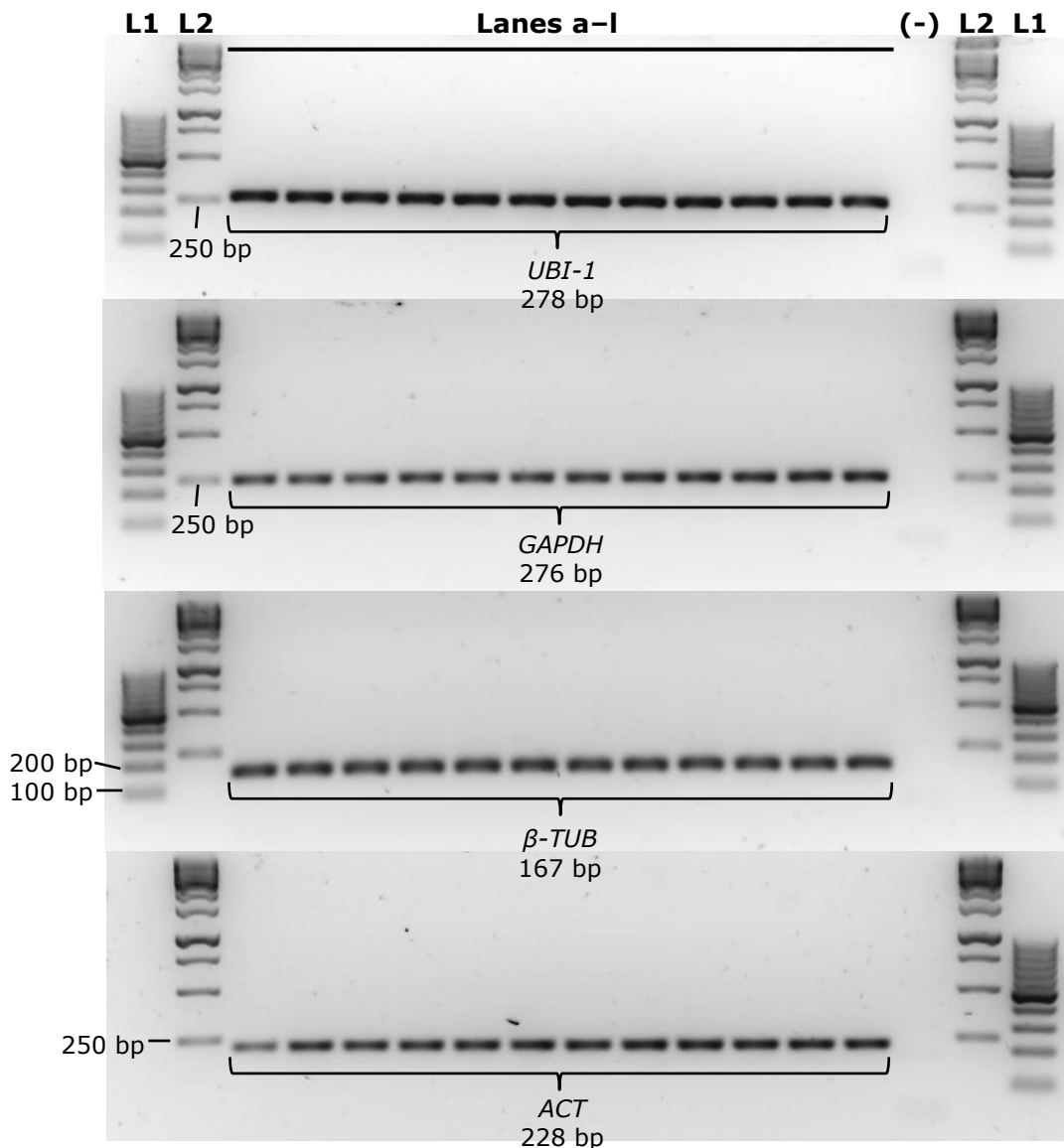


Figure 6.3 PCR profiles of reference genes, *UBI-1*, *GAPDH*, β -*TUB* and *ACT*, at gradient annealing temperatures, (from lanes a to l) 45.0, 45.4, 46.3, 47.7, 49.7, 51.6, 53.4, 55.3, 57.3, 58.7, 59.6, 60.0°C. L1: GeneRuler 100 bp DNA ladder, L2: GeneRuler 1 kb DNA ladder, (-): PCR negative control without the cDNA template.

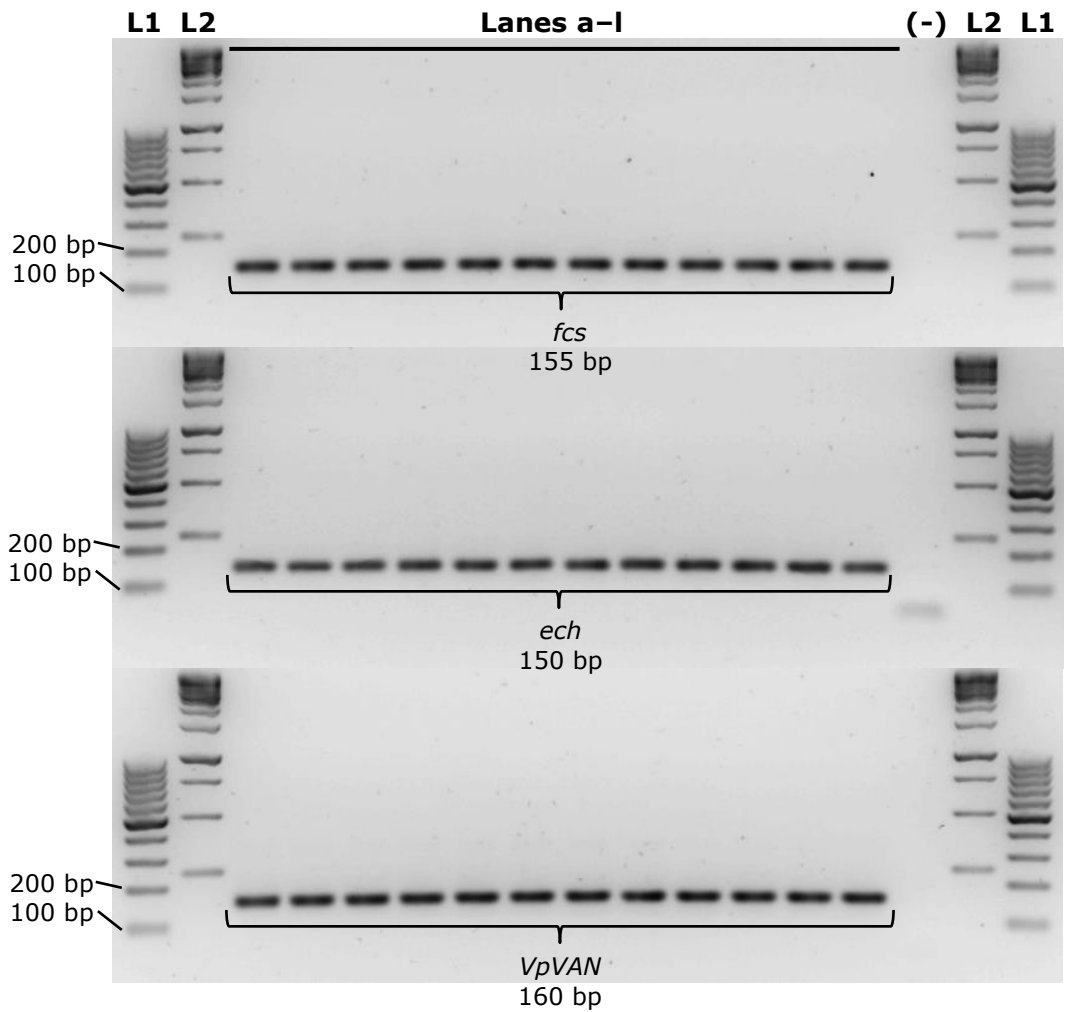


Figure 6.4 PCR profiles of target genes, *fcs*, *ech* and *VpVAN*, at gradient annealing temperatures, (from lanes a to I) 45.0, 45.4, 46.3, 47.7, 49.7, 51.6, 53.4, 55.3, 57.3, 58.7, 59.6, 60.0°C. L1: GeneRuler 100 bp DNA ladder, L2: GeneRuler 1 kb DNA ladder, (-): PCR negative control without the DNA template.

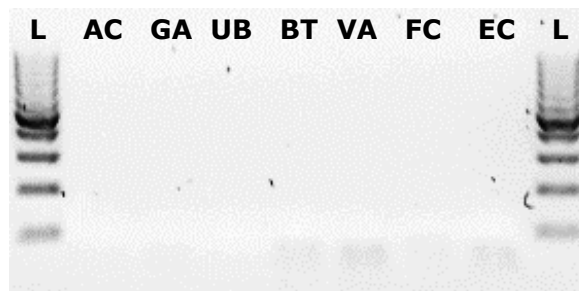


Figure 6.5 Amplification of reference genes and target genes with NRT. L: GeneRuler 100 bp ladder, AC: *ACT* gene, GA: *GAPDH* gene, UB: *UBI-1* gene, BT: β -*TUB* gene, VA: *VpVAN* gene, FC: *fcs* gene, EC: *ech* gene.

6.3.1.3 Analysis of Reference Genes

Each of the four reference genes (*UBI-1*, *GAPDH*, β -*TUB* and *ACT*) was subjected to qPCR using the cDNA of calli (two biological sets each) to determine the number of cycles (C_q) required for the amplification fluorescence of the qPCR to reach a specific threshold level of detection (baseline-corrected, Figure 6.6). The stability of each reference gene was analysed using Excel-based geNorm v3 and the stability value, M, of less than 1.5 indicated stable expression (**Figure 6.7**) (Bustin *et al.*, 2010; De Spiegelaere *et al.*, 2015; Vandesompele *et al.*, 2002). The lower the M value (lower standard deviation), the more stable the expression. The reference genes were ranked according to their M values, from the lowest to the highest: *ACT* (M = 0.091), *UBI-1* (M = 0.091), β -*TUB* (M = 0.107), *GAPDH* (M = 0.108). With that, *ACT* and *UBI-1* were selected for subsequent normalisation in qPCR analyses of cDNA samples from transformed and untransformed calli.

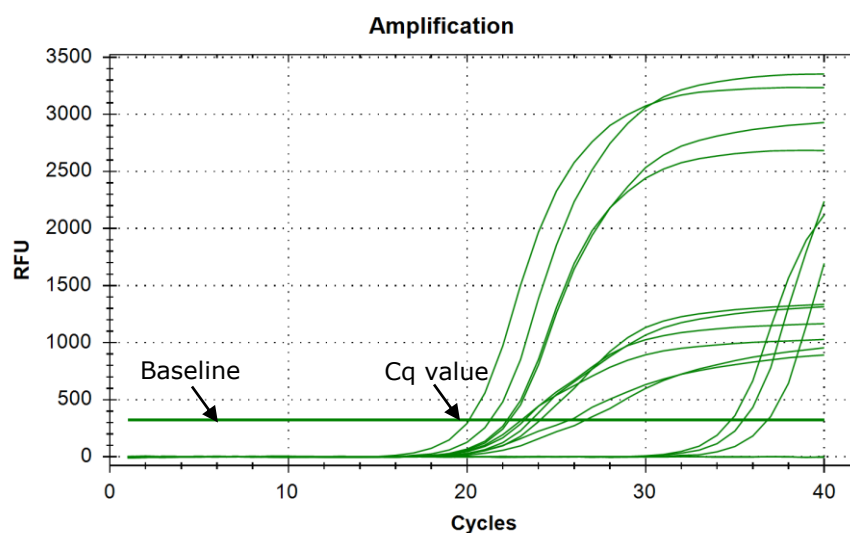


Figure 6.6 An example of the amplification curve showing baseline correction in the determination of C_q values.

 					
Change Data	ACT	UBI-1	GADPH	B-TUB	Normalisation Factor
1	2.36E+01	2.01E+01	2.30E+01	2.22E+01	0.9995
2	2.24E+01	2.13E+01	2.13E+01	2.41E+01	1.0005
M < 1.5	0.091	0.091	0.108	0.107	

Figure 6.7 The summary of preliminary geNorm analysis indicating the M values for the expression stability of *ACT* (0.091), *UBI-1* (0.091), *GADPH* (0.108), and β -*TUB* (0.107).

After the qPCR of cDNA samples from transformed and transformed calli, the *ACT* and *UBI-1* reference genes were re-evaluated. A box plot graph of Cq values of the reference genes was plotted using GenStat 18th Edition (**Figure 6.8**). Cq values of *ACT* were within the median range of 21.23–24.10, while those of *UBI-1* were within the median range of 20.82–23.04. The expression stability of both genes (M values) was calculated again using geNorm v3, and the results indicated that the expressions of *ACT* (M = 0.030) and *UBI-1* (0.030) were stable (**Figure 6.9**). It was found that the expression stability of *ACT* was the same as *UBI-1* in the preliminary and post-experimental analyses.

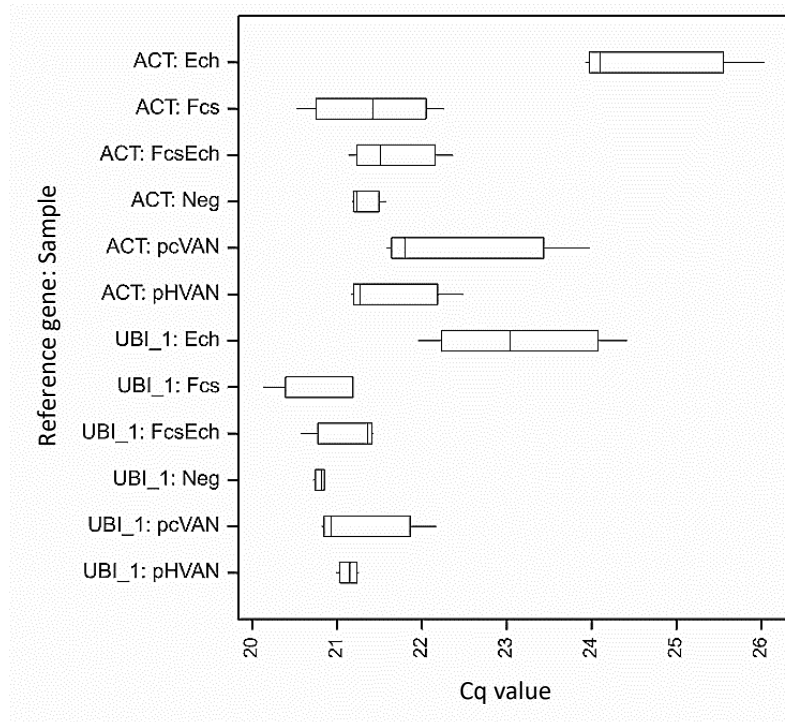


Figure 6.8 Box plot graph of Cq values of *ACT* and *UBI-1* in transformed calli (Ech, Fcs, FcsEch, pcVAN and pHVAN) and untransformed control (Neg). Boxes indicate values in the first and third quartiles separated by vertical lines, which indicate median values. Horizontal lines indicate the range of values.

		geNorm		PrimerDesign
Change Data	ACT	UBI-1	Normalisation Factor	
pHVAN	2.13E+01	2.12E+01	0.9758	
pHVAN	2.25E+01	2.13E+01	1.0060	
pHVAN	2.12E+01	2.10E+01	0.9698	
Neg	2.16E+01	2.08E+01	0.9752	
Neg	2.12E+01	2.07E+01	0.9638	
Neg	2.12E+01	2.09E+01	0.9682	
M < 1.5	0.030	0.030		

Figure 6.9 The summary of post-experimental geNorm analysis indicating the M values for *ACT* (0.030) and *UBI-1* (0.030).

6.3.1.4 qPCR Amplification Efficiency of Target Genes

The efficiency of qPCR amplifications was determined by constructing concentration curves using plasmid DNA through ten-fold serial dilutions. Concentration curves for target genes, *fcs*, *ech* and *VpVAN*, were generated by the CFX Manager software (Bio-Rad, USA) (**Figure 6.10**). For the concentration curves of *fcs* and *ech*, two points from the lowest concentrations (log starting quantities 1.5 and 2.5) and two points from the highest concentrations (log starting quantities 8.5 and 9.5) were omitted from the calculation of amplification efficiencies (**discussed in subchapter 6.4.4**). Similarly, two points of the log starting quantities 1.5 and 2.5 were also omitted for the concentration curve of *VpVAN*, whereas the other two highest concentrations (log starting quantities 8.5 and 9.5) have already been excluded from the qPCR amplification. As such, five points were included in the calculation of the amplification efficiency from the slope of each concentration curve. With that, the amplification efficiencies were 98.8% for *fcs* (slope -3.352), 106.9% for *ech* (slope -3.168), and 90.0% for *VpVAN* (slope -3.586).

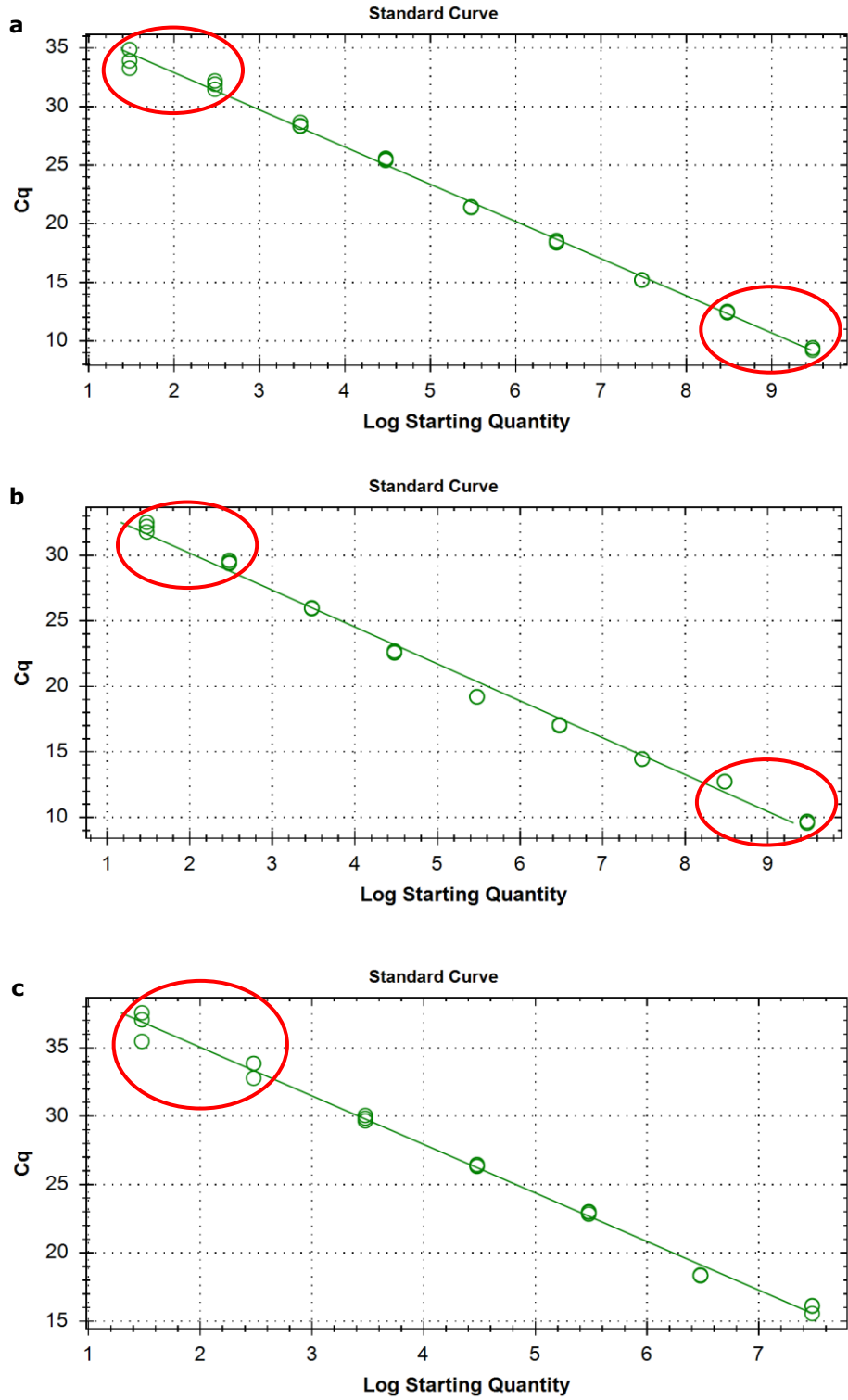


Figure 6.10 Concentration curves of (a) *fcs*, (b) *ech*, and (c) *VpVAN* plotted with Cq values against log starting quantities, and R^2 values of 0.997, 0.992 and 0.994, respectively. Red circles mark the points that were omitted from the calculation of amplification efficiencies.

6.3.1.5 Melt Curve Analysis

A melt curve analysis was conducted at the end of the qPCR to check whether a single, specific product was produced based on the dissociation characteristics of the amplicons. All of the individual reactions showed single melt peaks indicating the amplification of reference genes or target genes (**Figure 6.11**).

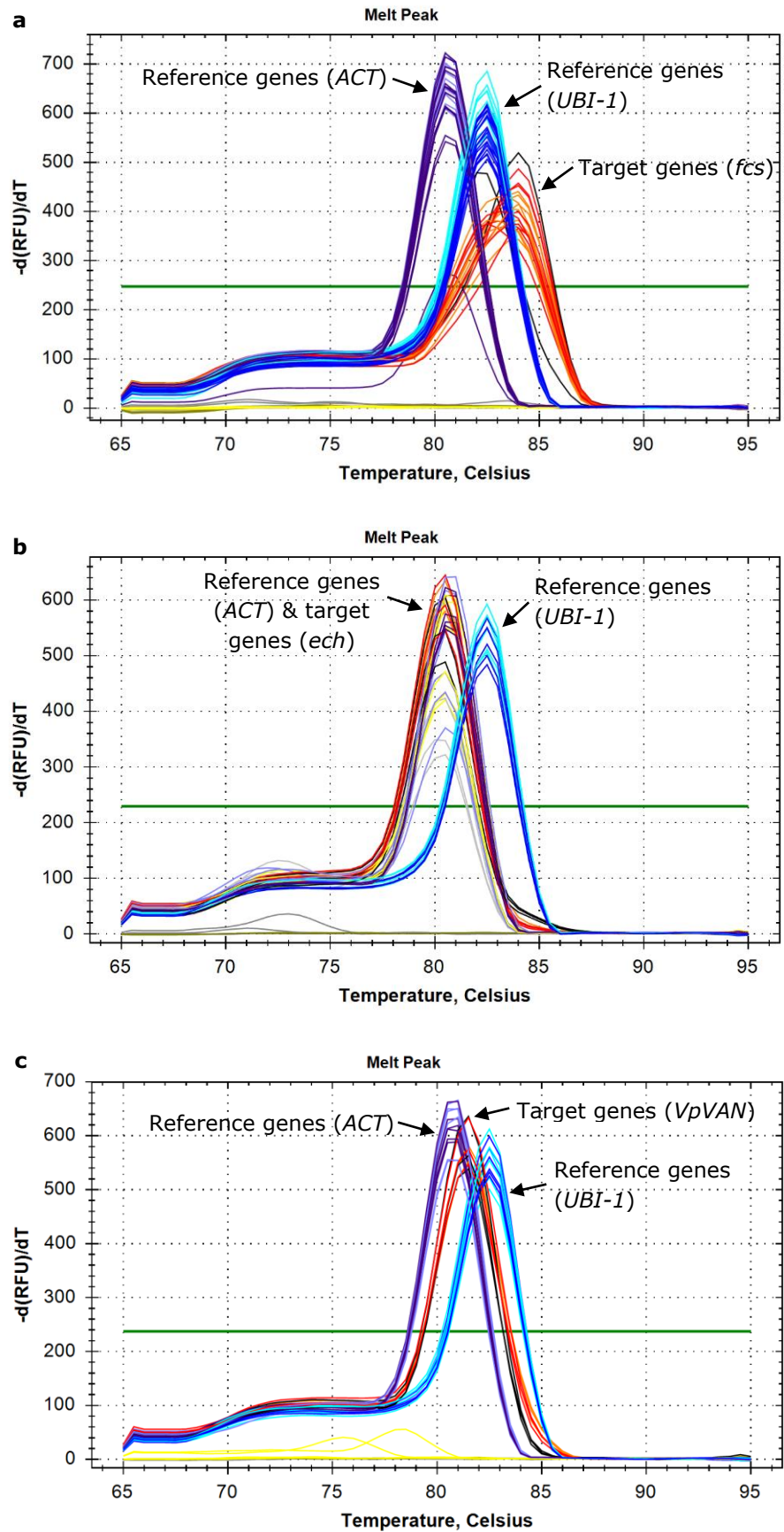


Figure 6.11 Melt peaks for individual reactions indicating single amplification products of target genes, (a) *fcs*, (b) *ech*, and (c) *VpVAN*, and the accompanying reference genes (*ACT* and *UBI-1*) included for normalisation.

6.3.1.6 Expression Levels in Transformed and Untransformed Calli

The relative expression, R , of a target gene in a sample of interest was calculated using the " $R = 2^{-\Delta\Delta Cq}$ " method. The relative expression level of $VpVAN$ [$pcVAN$] was 1.00, and the expression levels of other target genes in other samples (denoted as *target gene*[sample]) were compared against it (**Figure 6.12**). The mean Cq values of the target and reference genes, and the corresponding ΔCq , $\Delta\Delta Cq$ and $2^{-\Delta\Delta Cq}$ calculations are shown in **appendix I**. A Tukey's multiple comparisons of LSD on the $\Delta\Delta Cq$ values showed that the expression levels of the target genes in transformed samples were significantly different from untransformed samples, which showed no expression of the target genes at all. In transformed samples, expression levels of the *fcs* gene in *FcsEch* and *Fcs* samples were approximately the same. Expression levels of the *ech* gene in *FcsEch* and *Ech* samples were not significantly different. In *FcsEch* samples, expression levels of the *ech* gene was significantly much higher than the *fcs* gene. In general, expression levels of the *ech* gene was significantly higher than the *fcs* and *VpVAN* genes, except those of the *VpVAN* gene in *pHVAN* samples, where the difference was not significant. *pcVAN* and *pHVAN* samples were transformed with the 35Sp-*VpVAN* cassette that was cloned into *pcDNA6.2* and *pHBT12K* vectors, respectively. Expression levels of the *VpVAN* gene in *pcVAN* and *pHVAN* samples were not significantly different, although the *VpVAN* gene was expressed in *pHVAN* samples at a level of 8.42-fold higher than in *pcVAN* sample.

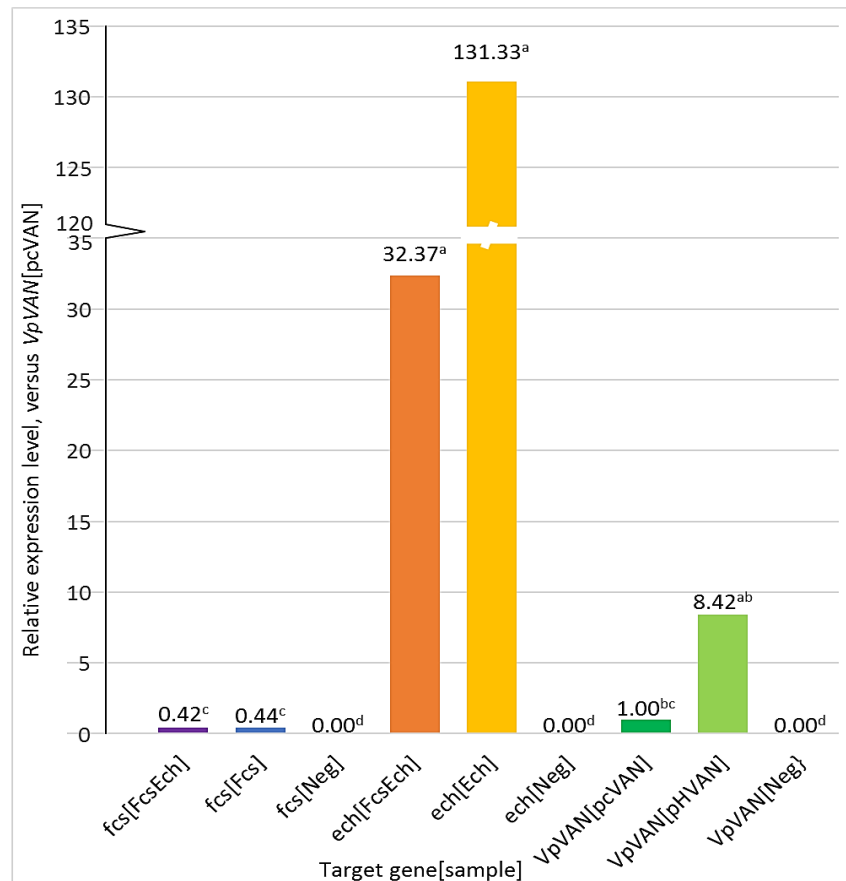


Figure 6.12 Bar chart showing the relative expression levels (fold-change) of *fcs* gene in FcsEch and Fcs samples, *ech* gene in FcsEch and Ech samples, and *VpVAN* gene in pcVAN and pHVAN samples. The expression levels were compared with *VpVAN*[pcVAN] (fold-change 1.00). Neg: Untransformed samples. Bars with the same pattern indicate that the sample was transformed with the same expression vector (for example, FcsEch sample was transformed with pcDNA6.2::35Sp-*fcs*-NOSp-*ech*). Bars with the same letters are not significantly different at $p=0.05$ ($n=3$).

6.3.2 Reverse-Phase HPLC

6.3.2.1 Mobile Phase Compositions

The starting composition of the mobile phase (x:y methanol–1% acetic acid) was optimised with a gradient HPLC to a final composition of 50:50 methanol–1% acetic acid in 20 min using vanillin and ferulic acid standards, which was later transferred to the Agilent Infinity 1260 HPLC System (USA) with minor modifications to the programme for the analyses of vanillin, vanillic acid, vanillin glucoside and ferulic acid. An initial run with isocratic

HPLC at 50:50 methanol–1% acetic acid resulted in the elution of ferulic acid in less than one minute after vanillin, but with an R_s value of 2.04. Subsequently, the gradient HPLC of all tested $x:y$ compositions gave R_s values of 1.86–8.37, all of which indicated good separation (**Table 6.6**). Considering potential interference and drag caused by other compounds in plant samples during subsequent analyses, a minimum of 2 min separation time between two adjacent compounds ($t_{R2} - t_{R1} = 2$) was preferred. Hence, the optimum starting mobile phase composition was set at 30:70 methanol–1% acetic acid. However, after transferring to the Agilent Infinity 1260 HPLC System (USA), the starting composition of 25:75 with a gradient HPLC to 50:50 methanol–1% acetic acid in 15 min was found to resolve the peaks in a shorter run time compared to 20 min of gradient used previously (total run time 32.5 min). Optimum peak resolutions were also achieved using the same parameter when vanillic acid and vanillin glucoside were added for analyses (**Figure 6.13**). The optimised gradient HPLC programme for the analysis of vanillin, vanillic acid, vanillin glucoside and ferulic acid is shown in **table 6.7**.

Table 6.6 The starting mobile phase compositions of $x:y$ methanol–1% acetic acid and their corresponding retention times, peak widths at the base and R_s values for the separation of vanillin and ferulic acid.

Starting mobile phase composition (%)		Retention time [peak width] (min)		Resolution, R_s
x	y	Vanillin	Ferulic acid	
50	50	6.94 [0.30]	7.45 [0.20]	2.04
45	55	7.43 [0.40]	8.08 [0.30]	1.86
35	65	8.91 [0.50]	10.21 [0.50]	2.60
30	70	10.09 [0.60]	13.51 [0.60]	5.70
25	75	12.25 [1.00]	18.64 [1.00]	6.39
20	80	15.60 [1.20]	27.32 [1.60]	8.37

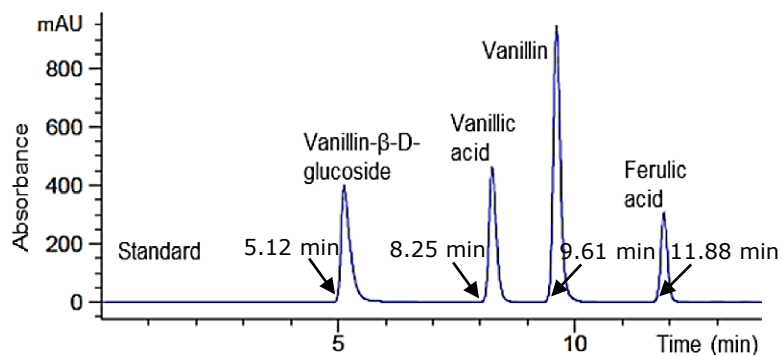


Figure 6.13 A HPLC chromatogram showing the peaks and retention times of vanillin glucoside (5.12 min), vanillic acid (8.25 min), vanillin (9.61 min) and ferulic acid (11.88 min) at 280 nm wavelength.

Table 6.7 The optimised gradient HPLC programme for the analysis of vanillin, vanillic acid, vanillin glucoside and ferulic acid.

Step	Time (min)	Flow rate (ml/min)	Composition (%)	
			Methanol	1% acetic acid
0	0.5	1.00	25	75
1	15.0	1.00	50	50
2	1.0	1.00	100	0
3	5.0	1.00	100	0
4	1.0	1.00	25	75
5	10.0	1.00	25	75

Capsaicin could not be eluted using the optimised gradient HPLC, hence analyses of capsaicin were performed separately using isocratic HPLC at 80:20 methanol–1% acetic acid, which consisted of higher organic phase (**Figure 6.14**).

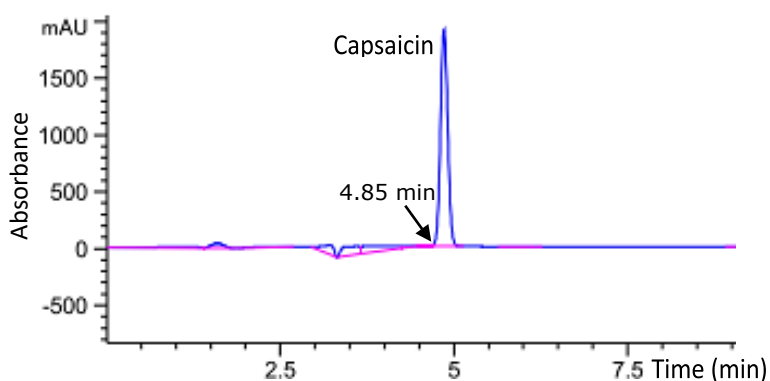


Figure 6.14 A HPLC chromatogram showing the peak and retention time of capsaicin (4.85 min) at 222 nm wavelength.

6.3.2.2 UV Wavelengths for Compound Detection

Phenolic compounds were detected during the HPLC using a PDA detector, which enabled the detection at multiple UV wavelengths. After the HPLC of the analytical standards, an isoabsorbance plot was constructed using Agilent HPLC ChemStation software. From the isoabsorbance plot, the peak maximum for each compound was analysed with comparison to the corresponding peak areas at the individual wavelengths to determine the optimum UV wavelength for the detection of the compound. The optimum UV wavelengths for the detection were 280 nm for vanillin, 270 nm for vanillin glucoside, 260 nm for vanillic acid, 325 nm for ferulic acid, and 222 nm for capsaicin (**Figure 6.15**).

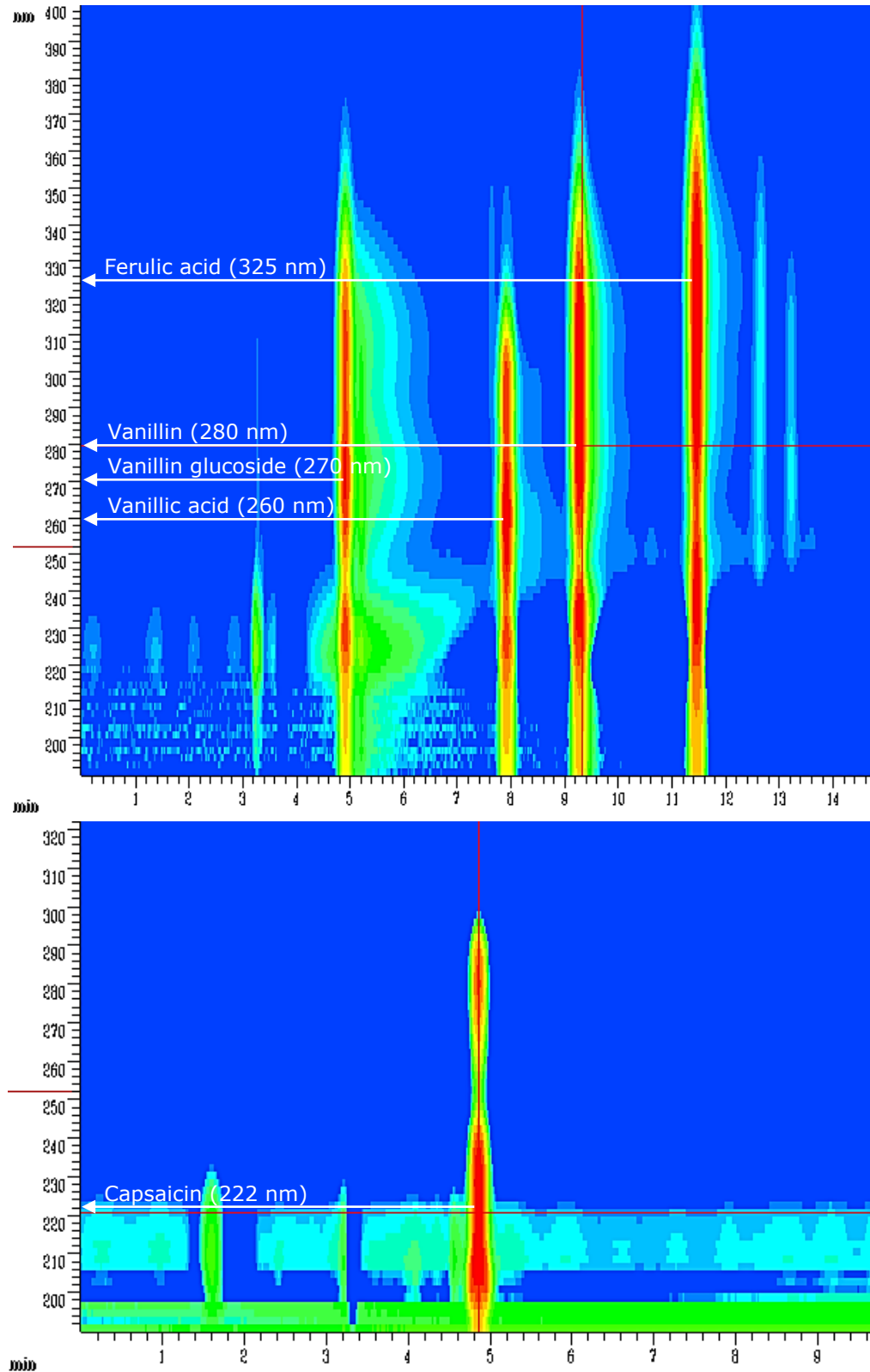


Figure 6.15 Isoabsorbance plots showing the intensities of absorbance signals (from blue, very low or nothing, to red, very high) over a range of wavelengths. The x-axis represents the retention time (min). The y-axis represents the wavelength (nm). Arrows point from the individual absorbance signals of compounds showing the maximum intensities to the corresponding optimum wavelengths.

6.3.2.3 Concentration Curve of Standards

For each standard, HPLC runs of seven dilutions (15.625, 31.25, 62.5, 125, 250, 500 and 1000 ppm) were performed and a concentration curve was plotted (**Figure 6.16**). R^2 values of 0.9995 for vanillin, 0.9999 for vanillin glucoside, 0.9999 for vanillic acid, 0.9996 for ferulic acid and 0.9998 for capsaicin indicated high linearity. The concentration curve was later used for the determination of the respective compounds in analysed samples.

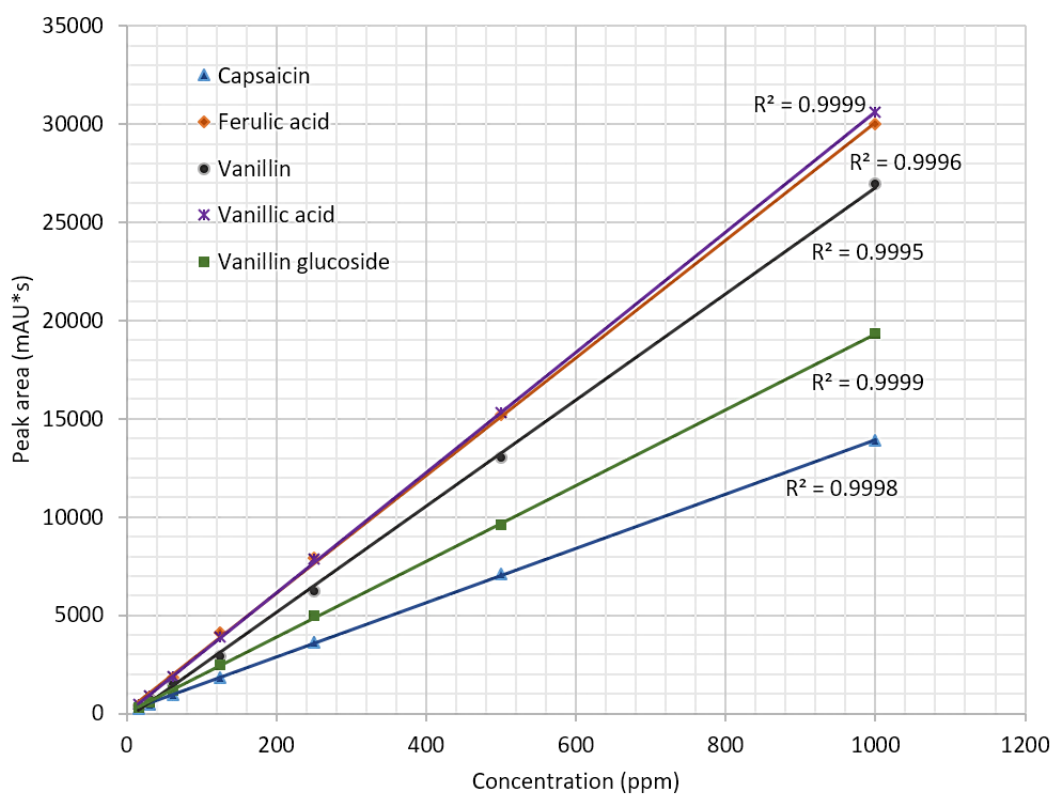


Figure 6.16 Concentration curves of analytical standards—capsaicin ($R^2 = 0.9998$, $y = 13.999x$), ferulic acid ($R^2 = 0.9996$, $y = 30.171x$), vanillin ($R^2 = 0.9995$, $y = 26.614x$), vanillic acid ($R^2 = 0.9999$, $y = 30.632x$) and vanillin glucoside ($R^2 = 0.9999$, $y = 19.34x$).

6.3.2.4 Accuracy, Precision, Limit of Detection and Limit of Quantitation

Prior to the analyses of plant samples, the accuracy, precision, LOD and LOQ of the HPLC method were validated. The accuracy was determined using a spike recovery method. The estimated accuracy for each target compound was ~95% or more (**Table 6.8**).

Table 6.8 The accuracy for each target compound that was estimated using spike recovery method ($n=3$).

Target compound	Amount spiked, c_s (ppm)	Total amount measured, c_T (ppm)	Amount naturally occurring, c_n (ppm)	Accuracy, $A = \frac{c_T - c_n}{c_s} \times 100\%$
Vanillin	300	289.08±7.63	1.34±0.45	95.91±2.62
Vanillin glucoside	300	289.46±5.93	4.70±1.69	94.92±1.69
Vanillic acid	300	296.68±8.42	8.68±1.95	95.58±2.74
Ferulic acid	300	285.95±1.85	0.42±0.08	95.18±0.64
Capsaicin	300	288.31±5.16	0	96.10±1.72

Average values from triplicate measurements of the retention time and peak area of each compound are shown in **Table 6.9 and 6.10**, respectively. All calculated CV values were well below 2.0%, indicating very high precision in the measurement of retention time and peak area.

Table 6.9 The precision of retention time for each target compound as estimated from the coefficient of variance ($n=3$).

Target compound	Average retention time, \bar{x} (min)	Standard deviation, SD (min)	Coefficient of variance, CV (%)
Vanillin	9.42	0.05	0.55
Vanillin glucoside	5.00	0.02	0.48
Vanillic acid	8.07	0.05	0.58
Ferulic acid	11.67	0.09	0.76
Capsaicin	4.83	0.03	0.60

Table 6.10 The precision of peak area for each target compound as estimated from the coefficient of variance ($n=3$).

Target compound	Average peak area, \bar{x} (mAU*s)	Standard deviation, SD (mAU*s)	Coefficient of variance, CV (%)
Vanillin	16967.73	60.43	0.36
Vanillin glucoside	10165.83	55.55	0.55
Vanillic acid	17918.03	67.37	0.38
Ferulic acid	17337.57	104.21	0.60
Capsaicin	8108.03	83.40	1.03

The LOD and LOQ were determined based on signal-to-noise ratios for each target compound. The signal-to-noise ratios for each compound were shown by the Agilent ChemStation software based on the pre-determined range of noise occurrence (**Figure 6.17**). Target compounds that were considered to be detected showed a signal-to-noise ratio of 3 or more, while target compounds that were considered for quantification analyses showed a signal-to-noise ratio of 10 or more.

Noise determination:

Time range		Noise	Noise	Noise	Wander	Drift
from	to	(6*SD)	(PtoP)	(ASTM)	[mAU]	[mAU/h]
[min]	[min]	[mAU]	[mAU]	[mAU]	[mAU]	[mAU/h]
14.500	14.700	2.415e-2	1.369e-2	-	-	-5.053e-1
13.000	14.000	0.5207	0.3046	-	-	4.079
16.000	17.000	0.1156	6.097e-2	-	-	5.880

Range for noise determination

RetTime	k'	Area	Height	Symm.	Width	Plates	Resol	Signal
[min]		[mAU*s]	[mAU]		[min]		ution	/Noise
3.112	0.25	69.62524	6.42415	3.13	0.1704	1853	-	12.3
3.351	0.34	206.83478	12.42224	0.99	0.2680	865	0.64	23.9
3.750	0.50	13.99605	2.57960	1.79	0.0945	8716	1.29	5.0
3.934	0.58	53.88414	4.43443	1.23	0.2266	1672	0.67	8.5
4.658	0.87	113.31886	9.01423	1.90	0.2119	2675	1.94	17.3
4.969	0.99	529.48840	44.48011	1.27	0.1829	4092	0.92	85.4
5.406	1.17	309.43991	23.43763	1.75	0.2078	3755	1.32	45.0
5.962	1.39	27.16015	2.75281	1.20	0.1533	8378	1.81	5.3
6.920	1.78	1.47656	9.41148e-2	1.32	0.2880	3201	2.55	1.8e-1
7.642	2.07	10.19371	1.03861	1.14	0.1517	14068	1.93	2.0
8.064	2.23	672.61902	74.07303	1.06	0.1427	17681	1.68	142.3
9.422	2.78	3274.77637	348.02142	0.91	0.1422	24317	5.60	668.4
10.431	3.18	4.18075	3.38859e-1	0.93	0.1878	17090	3.59	6.5e-1

Signal-to-noise ratio

Figure 6.17 An example of performance and noise report from the chromatography of a plant extract containing vanillin (retention time 9.42 min). The blue box indicates the range for noise determination. The red box indicates the signal-to-noise ratio of the vanillin signal (668.4), which was very much above the LOD and LOQ limits of 3 and 10, respectively. As such, the compound was not only detected effectively, it could also be quantified reliably. Any signal below the LOD was not considered as detected, while those below the LOQ was not considered for subsequent quantification.

6.3.2.5 Native Phenolic Contents in Various Tissues of *C.*

frutescens

In a preliminary study of the native phenolic compounds, extracts from cotyledon-, hypocotyl- and root-generated calli, as well as leaves, stems and roots from *in vitro* whole plants of *C. frutescens* were analysed together with the extract from vanilla pod as a reference (**Figure 6.18**). All tissue types showed much lower amounts of vanillin and ferulic acid than

vanilla pods or none at all. Separate statistical analyses of vanillin and ferulic acid contents showed that vanillin contents were not significantly different across different tissue types ($\leq 2.62 \mu\text{g/g}$), except vanilla pods ($1548.29 \mu\text{g/g}$). Ferulic acid contents were not significantly different between the analysed tissue types, including vanilla pods ($\leq 6.18 \mu\text{g/g}$).

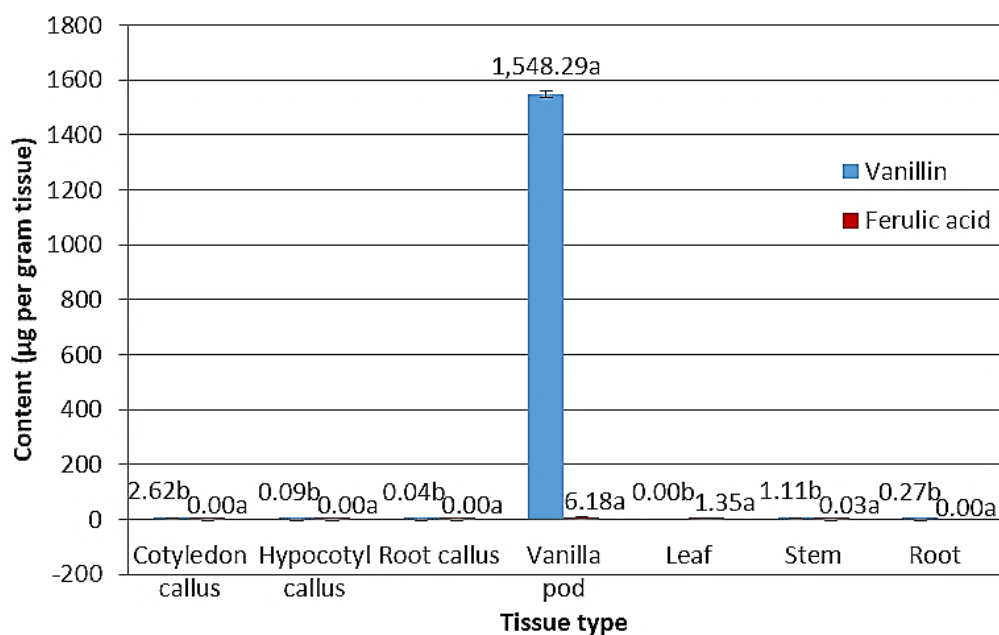


Figure 6.18 Native contents of vanillin and ferulic acid, which were the product and the precursor in the vanillin biosynthetic pathway, respectively, in different tissue types of *C. frutescens* with the extract from vanilla pod as a reference. Error bars indicate standard deviations ($n=3$). Bars with the same letters for the same compound are not significantly different at $p=0.05$.

6.3.2.6 Phenolic Contents in Callus Cultures Fed with Ferulic Acid

Wild-type calli from the hypocotyl explants of *C. frutescens* were subjected to ferulic acid feeding, whereby one-month old calli were cultured on callus induction media (CIM) supplemented with 0.0, 0.2, 0.4, 0.6 and 1.0 mM ferulic acid over a period of 28 days, to examine the possibility of vanillin elicitation upon ferulic acid feeding. The calli showed similar responses for all phenolic compounds when the concentration of ferulic acid fed was

increased (**Figure 6.19**). When the concentration of ferulic acid feeding increased from 0.0 mM to 0.2 mM, concentrations of all phenolic compounds produced in the calli increased. A decrease in the tissue compounds was seen when the feeding concentration further increased to 0.4 mM. However, the phenolic contents increased again when the feeding concentration increased to 0.6 mM, followed by another decrease and increase when the feeding concentration of ferulic acid was increased to 0.8 and 1.0 mM, respectively. Nevertheless, it was important to note that changes in phenolic contents that resulted from different feeding concentrations were very small and were not significantly different. Besides that, the contents of vanillin, vanillic acid and ferulic acid were relatively much lower than vanillin glucoside in general. A similar pattern was observed in the time-point analysis of calli with 0.6 mM ferulic acid over 0, 7, 14, 21 and 28 days. A decrease in phenolic contents was seen after 7 days, which was particularly significant for vanillin glucoside but not for other phenolic compounds. A slight increase in the contents of all phenolic compounds, except vanillin glucoside, was seen after 14 days, followed by a decrease after 21 days and another increase after 28 days. However, the changes in phenolic contents at the tested time points were not significantly different, except for vanillin glucoside, as described earlier. Capsaicin was not detected at all ferulic acid feeding concentrations at all tested time points.

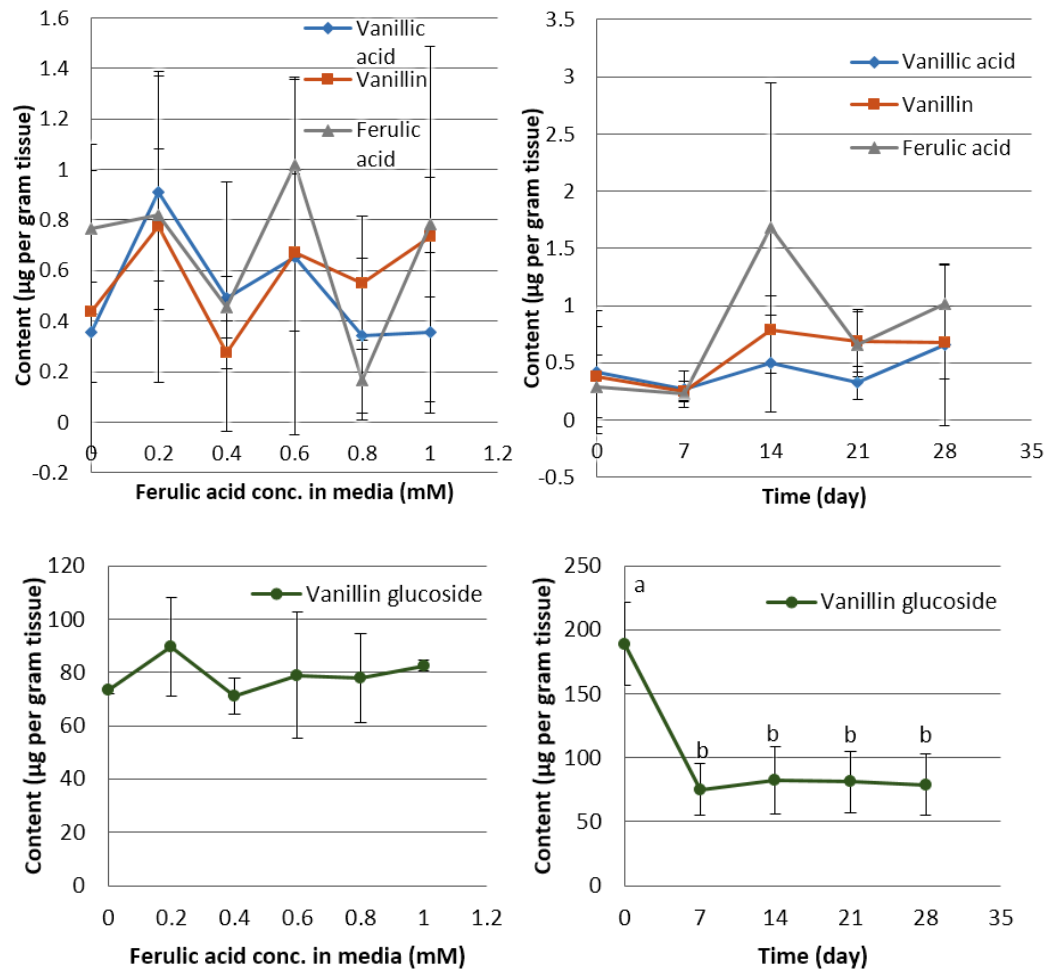


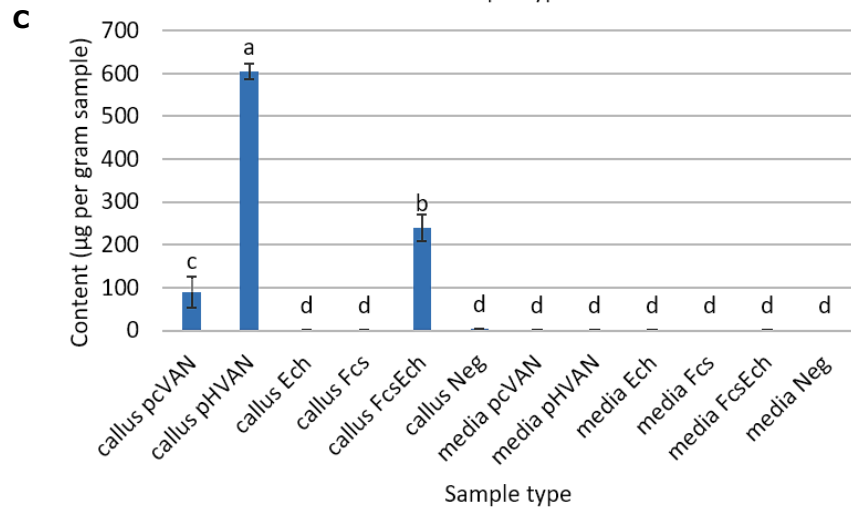
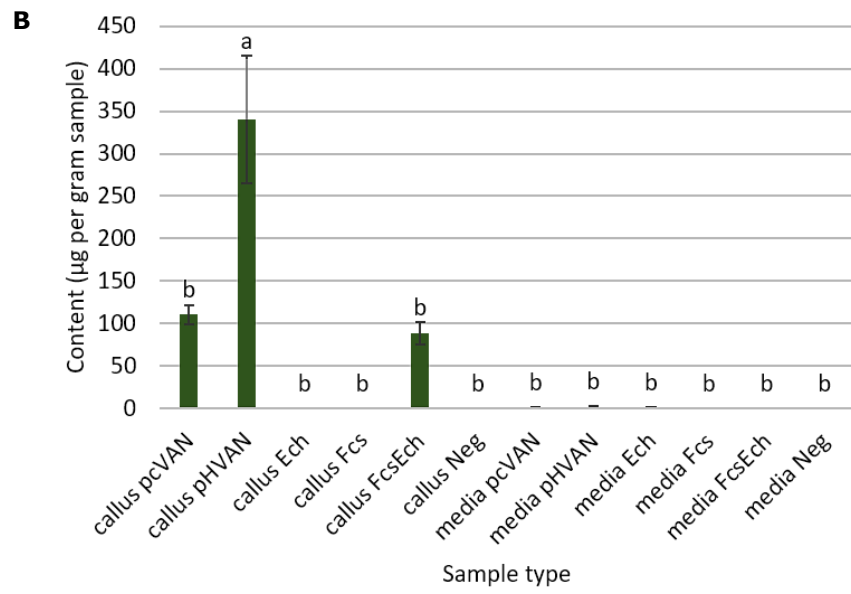
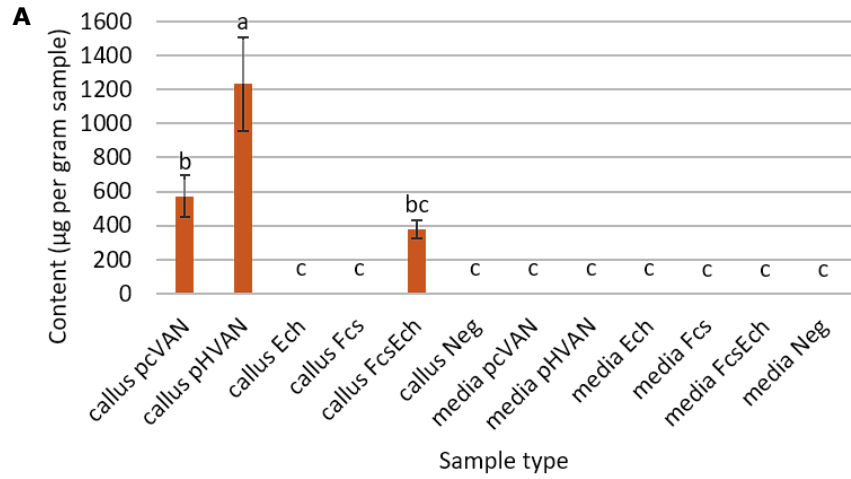
Figure 6.19 Analysed contents of vanillin, vanillic acid, vanillin glucoside and ferulic acid in callus cultures of *C. frutescens* after feeding with 0.0, 0.2, 0.4, 0.6, 0.8 and 1.0 mM ferulic acid. Calli fed with 0.6 mM ferulic acid were analysed at 5 time points (0, 7, 14, 21 and 28 days). Error bars indicate standard deviations ($n=3$). Data points with the same letters are not significantly different at $p=0.05$.

6.3.2.7 Phenolic Contents in Transformed and Untransformed Callus Cultures

Calli that were transformed with pcDNA6.2::35Sp-VpVAN (pcVAN), pHBT12K::35Sp-VpVAN (pHVAN), pcDNA6.2::35Sp-fcs-NOSp-ech (FcsEch), pcDNA6.2::35Sp-fcs (Fcs) and pcDNA6.2::NOSp-ech (Ech), untransformed calli (Neg), and their corresponding growth media were analysed for phenolic contents (**Figure 6.20**). The retention times in HPLC chromatograms acquired for the target samples were compared with those

of the analytical standards (**Figure 6.21**). Vanillin contents were significantly higher in pHVAN (1231.73 $\mu\text{g/g}$) than pcVAN (573.39 $\mu\text{g/g}$) and FcsEch (377.87 $\mu\text{g/g}$). Other samples showed negligible contents of vanillin (≤ 1.10 $\mu\text{g/g}$). Similarly, vanillin glucoside contents were significantly higher in pHVAN (340.46 $\mu\text{g/g}$) than pcVAN (110.32 $\mu\text{g/g}$) and FcsEch (88.83 $\mu\text{g/g}$). Other samples showed minute (≤ 1.68 $\mu\text{g/g}$) or no vanillin glucoside content at all.

Vanillic acid contents were also significantly higher in pHVAN (604.60 $\mu\text{g/g}$) than FcsEch (239.67 $\mu\text{g/g}$), which in turn, were significantly higher than pcVAN (89.29 $\mu\text{g/g}$). Other samples showed trace amounts of vanillic acid (≤ 3.14 $\mu\text{g/g}$). Ferulic acid contents in all samples, which were very low (≤ 3.56 $\mu\text{g/g}$), were not significantly different from each other. Capsaicin was not detected in all analysed samples. To double check, an extract of chilli fruit purportedly containing capsaicin was included in the analysis (HPLC chromatograms in **figure 6.22**). Capsaicin was detected at 4.85 min in the chilli fruit extract, but not in the callus extract.



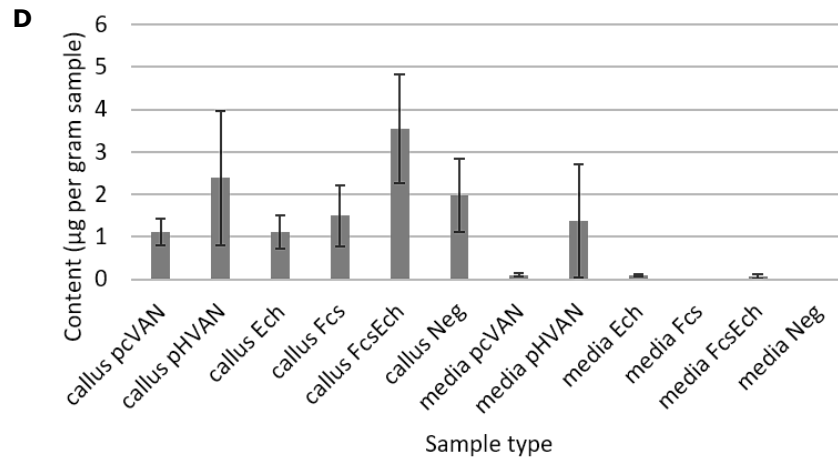


Figure 6.20 Analysed (A) vanillin, (B) vanillin glucoside, (C) vanillic acid and (D) ferulic acid contents of transformed calli (pcVAN, pHVAN, Ech, Fcs and FcsEch) and untransformed calli (Neg) and their corresponding growth media. Error bars indicate standard deviation ($n=3$). Bars with the same letters are not significantly different at $p=0.05$.

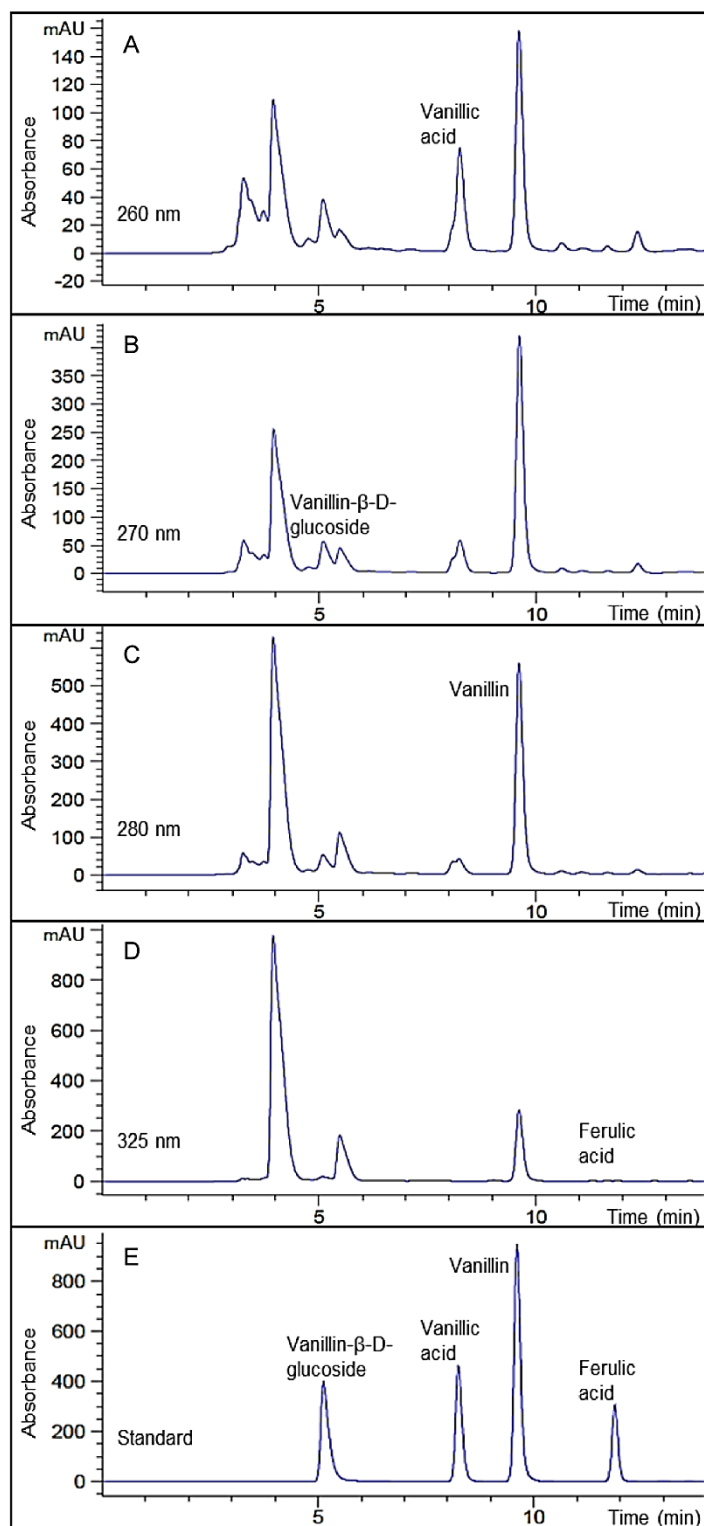


Figure 6.21 Example HPLC chromatograms of phenolic compounds extracted from a transformed pcVAN callus of *C. frutescens*. UV absorbance at (A) 260 nm, (B) 270 nm, (C) 280 nm, and (D) 325 nm wavelengths were measured for vanillic acid, vanillin glucoside, vanillin, and ferulic acid, respectively. Retention times for compounds in chromatograms A–D were compared with that of the analytical standards (E) measured at 280 nm wavelength. Published in Chee *et al.* (2016).

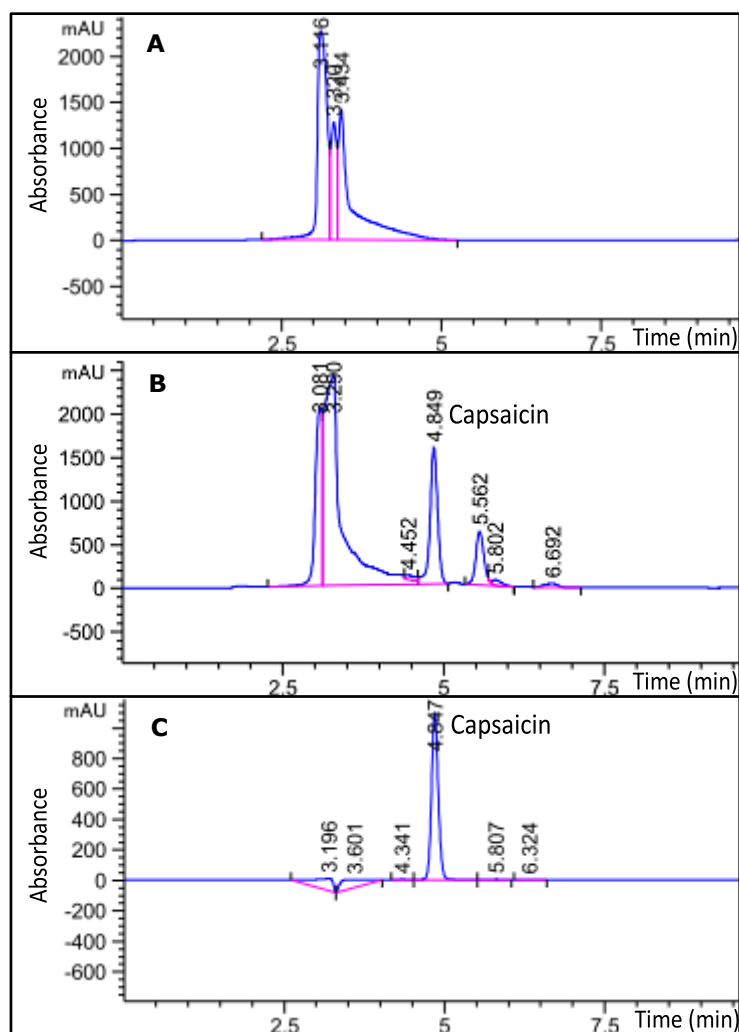


Figure 6.22 Example HPLC chromatograms of phenolic compounds extracted from (A) a transformed pcVAN callus of *C. frutescens* and (B) a chilli fruit. UV absorbance at 222 nm wavelength was measured for capsaicin. Retention times for compounds in chromatograms A–B were compared with that of the capsaicin standard (C), which was eluted at 4.85 min.

6.4 DISCUSSION

6.4.1 Native Phenolic Contents and Ferulic Acid Feeding of *C. frutescens*

In a preliminary study, native contents of vanillin and ferulic acid in various parts of a *C. frutescens* plant and regenerated calli were in trace amounts. This finding was parallel with the results reported by Singh and co-workers

(2007), where total phenolic contents in the leaves, stems and roots of *C. annuum* were below 1.00 µg/g, except for the presence of 64.82 µg/g of caffeic acid in roots. Ferulic acid, the precursor of vanillin biosynthesis, was found at 0.49, 0.15 and 0.39 µg/g in leaves, stems and roots, respectively.

Subsequently, an elicitation experiment with ferulic acid feeding found that all of the ferulic acid feeding concentrations tested did not elicit the production of vanillin at significant levels. The findings by Kang and co-workers (2005) formed the basis of this elicitation experiment, whereby elicitation of vanillin production was expected. It was reported that 0.6 mM was the optimum ferulic acid feeding concentration that elicited the maximal production of vanillin in cell cultures of *C. annuum* L. cv. P1482. Therefore, the feeding concentration at 0.6 mM ferulic acid was used as a reference concentration in the time-point study. It remained puzzling that vanillin glucoside was detected at relatively higher levels than other phenolic compounds at the time of experiment, and the exposure to ferulic acid seemed to lower the vanillin glucoside content over time. Nevertheless, this occurrence was not consistent as subsequent experiments did not find any vanillin glucoside in untreated calli. A possible reason could be the inability of undifferentiated cultures, such as calli, to compartmentalise metabolites or enzymes as cellular differentiation could be the prerequisite for enzymatic activities. Having said that, the lack of accumulation compartments does not necessarily negate the potential for the biosynthesis of secondary metabolites in general (Cresswell *et al.*, 2012).

Apparently, ferulic acid feeding did not increase the contents of endogenous ferulic acid contents in the callus tissues. This finding suggests that an uptake of the fed ferulic acid by the callus tissues did not take place. However, the possibility of no uptake due to toxicity could be ruled out as ferulic acid has very low toxicity properties and is present naturally

in plant cells for the maintenance of cell wall structures and the synthesis of other organic compounds, such as coniferyl alcohol, vanillin, sinapic, diferulic acid and curcumin (Kumar and Pruthi, 2014; Ou and Kwok, 2004). Furthermore, ferulic acid has been shown to exhibit antioxidant properties and inhibit cytotoxic enzymes (Mancuso and Santangelo, 2014).

6.4.2 The Expression Levels of Vanillin Biosynthetic Genes and the Phenolic Contents

Transformed pHVAN calli produced the highest amount of vanillin (up to 1231.73 µg per gram tissue or 0.123%), followed by transformed pcVAN calli (up to 573.39 µg per gram tissue or 0.057%) and transformed FcsEch calli (up to 377.87 µg per gram tissue or 0.038%). Such vanillin contents correlate to the expression levels of *VpVAN*[pcVAN], *VpVAN*[pHVAN], and *fcs* and *ech*[FcsEch]. The *VpVAN*[pcVAN] was expressed at 2.3- to 2.4-fold higher levels than the *fcs*[FcsEch], but the *ech*[FcsEch] was expressed at 77.1-fold higher levels than the *fcs*. It appeared that the catalytic activity of Fcs enzyme was the limiting factor due to its much lower expression than the Ech enzyme. The *VpVAN*[pHVAN] was expressed at 8.4-fold higher levels than the *VpVAN*[pcVAN].

Fcs and Ech enzymes catalyse the synthesis of vanillin from ferulic acid synergistically in a two-step pathway (Walton *et al.*, 2000; Yoon *et al.*, 2005). The consequential activities of Fcs and Ech enzymes were proven through the findings whereby calli expressing both *fcs* and *ech* genes produced vanillin at lower levels than those expressing the *VpVAN* gene, despite much higher expression levels of the *ech* gene because of the limiting expression levels of the *fcs* gene. The expression of *fcs* alone did not result in a rise in phenolic contents. Similarly, although being

expressed at very high levels, the expression of *ech* alone also did not result in a rise in phenolic contents.

The bioconversion of vanillin could have been catalysed from endogenous ferulic acid as free and bound ferulic acid is one of the most abundant phenylpropanoids in plant tissues. Being an important molecule in the plant cell wall, ferulic acid is present either as free homodimers or as dehydrodimers and dehydrotrimers esterified with proteins or sugars (Dobberstein and Bunzel, 2010; Gallage and Møller, 2015; Matthew and Abraham, 2004). A study by Yahiaoui and co-workers (1998) showed that the downregulation of cinnamyl alcohol dehydrogenase (CAD, an enzyme in lignin biosynthesis) in transgenic tobacco (*Nicotiana tabacum*) caused up to ten-fold increase in vanillin content (>4 µmol per gram of extracted xylem residue) compared to the untransformed control. This finding suggested that instead of being converted into lignin, more ferulic acid was available for vanillin biosynthesis. Looking at the capsaicinoid biosynthetic pathway, the suppression of a *pAMT* in *C. frutescens* resulted in no vanillylamine production and very low levels of capsaicinoid, which is downstream of vanillin in the capsaicinoid biosynthetic pathway. This in turn stimulated an increase in metabolites, such as vanillin and vanillic acid (Gururaj *et al.*, 2012).

The HPLC results of transformed and untransformed calli (**subchapter 6.3.2.7**) show that ferulic acid was found at low levels in transformed (1.12 µg per gram tissue) and untransformed (1.53 µg per gram tissue) calli. It is possible that most of the ferulic acid in plant tissues was esterified in cell walls rather than being free dimers (Dobberstein and Bunzel, 2010; Matthew and Abraham, 2004). As such, it would not have been released during the extraction process. Other than that, free ferulic acid that appeared as intermediate in the phenylpropanoid pathway could have been instantly degraded or converted into other phenolic derivatives,

such as feruloyl-CoA, vanillyl-CoA, 4-hydroxy-3-methoxyphenyl- β -hydroxypropionyl CoA, vanillic acid and vanillin, based on the possible routes for bioconversion of ferulic acid to vanillin (Gallage and Møller, 2015). Despite the low levels of ferulic acid detected, it is shown that the level of ferulic acid in transformed and untransformed tissues appeared to be similar, suggesting that there could be compensation of intracellular ferulic acid that was converted into vanillin. It is known that ferulic acid is a source of feruloyl-CoA in lignin biosynthesis. In a study of transgenic poplar (family Salicaceae), the downregulation of cinnamoyl CoA reductase (CCR, one of the key enzymes involved in the conversion of feruloyl-CoA from the general phenylpropanoid pathway to monolignols in lignin biosynthesis) resulted in a decreased flux of feruloyl-CoA to lignin, which in turn stimulated an increased flux of ferulic acid deposition (Harris and Trethewey, 2010; Pilate *et al.*, 2010). In the case of vanillin biosynthesis, the ability of *VpVAN* to release ferulic acid from plant cell wall material is still unknown. Hence, the biosynthesis of vanillin by *VpVAN* could have taken place *via* ferulic acid and feruloyl-CoA in the phenylpropanoid pathway. The diversion of ferulic acid for the synthesis of vanillin could have caused a reduced flux to lignin, thereby inducing a compensation of ferulic acid in return.

VpVAN catalyses the synthesis of vanillin and its glucoside from ferulic acid and its glucoside, respectively (Gallage *et al.*, 2014). Therefore, the detection of significant levels of vanillin glucoside (110.32 and 340.46 μg per gram tissue in *pcVAN* and *pHVAN* calli, respectively) suggests the presence of ferulic acid glucosides in the callus tissues that were used in the conversion by *VpVAN*. Although *Fcs* and *Ech* are yet to be known to produce vanillin glucoside, the presence of vanillin glucoside in calli expressing the *fcs* and *ech* genes (88.83 μg per gram tissue) sheds light on the possibility of the glucosylation of vanillin to its conjugated β -D-

glucoside form to overcome the toxicity caused by high levels of vanillin (Brochado *et al.*, 2010). Although the glucosylation activity in *Capsicum* has not been studied extensively, certain plant cells, such as those of *Eucalyptus perriniana* (Spinning Gum) and *Apium graveolens* L. (celery), are able to glucosylate exogenous compounds into their glucosides (Lin *et al.*, 2007; Sato *et al.*, 2012). The ability to glucosylate vanillin has also been demonstrated in cultured cells of *Coffea arabica* (coffee), *Gardenia jasminoides* (Cape jasmine), *Medicago sativa* (alfalfa), *Nicotiana tabacum* (tobacco), *Theobroma cacao* (cocoa) and *Prunus amygdalus* (almond) (Kometani *et al.*, 2014). Detectable amounts of vanillic acid (89.29, 604.60 and 239.67 μg per gram tissue in pcVAN, pHVAN and FcsEch calli, respectively) also suggest the presence of intermediary forms of vanillic acid glucosides and vanillic acid in the vanillin biosynthetic pathway or a downstream conversion of vanillin into vanillic acid in the plant tissues (Gallage and Møller, 2015).

Negligible traces of phenolic compounds found in the growth media, including those of calli with elevated phenolic contents, showed that there was no excretion of phenolic compounds into the growth media. Most metabolic products are accumulated intracellularly by the cultured plant cells, despite reports of metabolite excretion into the media (Cresswell *et al.*, 2012; Rao and Ravishankar, 2002; Zenk *et al.*, 1977). In addition, the aggregation of metabolites also depends on the species or strain of the cultured cells (Misawa, 1985).

6.4.3 Comparison of pcDNA6.2 and pHBT12K Vectors for Vanillin Production

The expression of the *VpVAN* gene after transformation with pHBT12K::35Sp-*VpVAN* was 8.4-fold higher than those transformed with pcDNA6.2::35Sp-*VpVAN*. Despite being the same expression cassette, it seemed that the expression of transgenes after delivery with the pHBT12K vector was more efficient than the pcDNA6.2 vector. One notable difference is the size of the expression vectors, which was 6.0 kb for pHBT12K::35Sp-*VpVAN* and 7.5 kb for pcDNA6.2::35Sp-*VpVAN*. Larger plasmids have been reported to result in lower transformation efficiencies and hence, lower expression of transgenes (Chan *et al.*, 2002; Curtis, 2010; Grosser and Omer, 2011; Kung *et al.*, 2013; Lakshmanan *et al.*, 2015; Ohse *et al.*, 1995). However, such a phenomenon should be regarded on a case-by-case basis as large plasmids of tens to hundreds of kilobases have been shown to be effectively transformed into plant cells (Frary and Hamilton, 2001). Another difference between the two expression vectors is the use of different selectable markers. pcDNA6.2::35Sp-*VpVAN* utilises the *bsd* gene, while pHBT12K::35Sp-*VpVAN* utilises the *nptII* gene. The selection of transformants using BS could have asserted a different magnitude of selection pressure compared to using kanamycin. As such, the resulting metabolic stress, gene expression levels and metabolite production could have differed among the two types of transformed calli.

6.4.4 Limitations in qPCR Analysis

One of the main challenges in establishing a reliable qPCR analysis is the identification of suitable reference genes for the normalization of target gene expression levels (Pfaffl, 2010; Radonic *et al.*, 2004; Reddy *et al.*,

2013). Such reference genes are rare single biological genes that are expressed stably in different cells under different conditions (De Spiegelaere *et al.*, 2015). Besides that, it has been reported that “classical” reference genes, such as those of β -actin and GAPDH, were unsuitable due to significant regulation of their expression under different experimental conditions and in different tissues (Radonic *et al.*, 2004). However, results suggest that the reference genes used in this study were stably transcribed across different samples, indicating homogeneity in the tissue culture conditions and similar growth stages of the same sample type (callus). In addition, the reference genes used were suggested by Wan and co-workers (2011) in their study to discover suitable reference genes for *C. annuum* with two biological replications, in which the expression stability of the reference genes were analysed using three software packages.

Another challenge in the qPCR analysis lies in the estimation of amplification efficiencies. The analysis of qPCR amplification efficiency by sample dilutions could be affected by the stochastic effect at very low concentrations of samples, when very few target molecules were present in replicates from the same dilution. On the other hand, the presence of PCR inhibitory compounds, such as ethanol, phenol and salts, at high concentrations could lead to an overestimation of efficiency (Best *et al.*, 2015; Cankar *et al.*, 2006; Wong and Medrano, 2005). Assuming a perfect doubling of the DNA template in each cycle of the qPCR, $E = 100\%$ and the slope of the concentration curve would be -3.33 (Svec *et al.*, 2015). PCR inhibition at high concentrations and subsequent removal of inhibition at low concentrations could lead to a slope of standard curve that is higher than -3.33 and affect the subsequent calculation. Bearing this in mind, the calculated amplification efficiencies in this study were within the acceptable range of 90–110% after removing the affected points from the

concentration curves and using at least five points for the estimation of amplification efficiency (Heid *et al.*, 1996; Nybo, 2011; Ruijter *et al.*, 2009; Taylor *et al.*, 2010).

A limitation was encountered in the computation of relative gene expression levels using the widely used $2^{-\Delta\Delta Cq}$ method because the absence of Cq values for negative controls (untransformed calli) rendered the negative controls unsuitable as a calibrator in the calculation of $\Delta\Delta Cq$. Many reports have seen the assignment of a calibrator among the transgenic lines or the transgenes of interest for comparison purposes (Beltrán *et al.*, 2009; Deepak *et al.*, 2007; Fletcher, 2014; Kovalchuk *et al.*, 2013; Toplak *et al.*, 2004). Employing this technique, pcVAN samples, which showed intermediate expression levels, were used as the calibrator (relative expression 1.00) in this study. A useful comparison is seen in this case as the untransformed samples were computed as 0.00 in expression levels, while those of other samples were compared against pcVAN.

6.4.5 Limitations in HPLC Analysis

A general limitation of HPLC is the compromise between good separation and column length. Longer columns are needed for a better separation power, which means that a HPLC run would take a longer time to complete. Although satisfactory separation has been achieved using short columns of narrow internal diameters and small particles with ultra-high performance liquid chromatography (UHPLC), transferring the HPLC system to a UHPLC setup requires operations at very high pressures of above 6000 psi, which is usually the upper limit of a HPLC system (Dong and Zhang, 2014; Kivilompolo and Hyötyläinen, 2008; Wu *et al.*, 2013). In this study, the

standard 250 mm HPLC column was sufficient for good separations in a moderate total run time of 32.5 min per HPLC sample.

Large volumes of expensive organic chemicals are usually used in the extraction of target compounds and the mobile phase of HPLC runs. Therefore, it is desirable to determine the range of chemicals that is suitable for the extraction and elution of target compounds while considering their use in large amounts and the chemical hazards posed. Various extraction solvents have been tested for the extraction of phenolic compounds, as reported by Jadhav and co-workers (2009). Ethanol was the best solvent for the ultrasonic-assisted extraction of vanillin, followed by methanol, acetone and acetonitrile, while chloroform was the least effective solvent. Ethanol concentration of up to 50% (v/v) was found to be optimal for the extraction of vanillin (up to 120 ppm) at 100 ml per 1 g of sample (Jadhav *et al.*, 2009), but 80% ethanol at 5 ml per 1 g of sample has been used effectively for the extraction of phenolic compounds in other studies, including this study (1548 ppm vanillin) (Castro-Concha *et al.*, 2014; Khoddami *et al.*, 2013; Sujalmi and Supriyanto, 2005). Ethanol was also used as the solvent for the extraction of capsaicin from plant samples, although acetone and acetonitrile were also reported to be ideal (Chinn *et al.*, 2011; Gayathri *et al.*, 2016; Juangsamoot *et al.*, 2012; Sudhakar Johnson *et al.*, 1992). Methanol, in some methods mixed with acetic acid, has been used widely as the eluent in the HPLC mobile phase (Jadhav *et al.*, 2009; Juangsamoot *et al.*, 2012; Khoddami *et al.*, 2013; Mradu *et al.*, 2012; Waliszewski *et al.*, 2006). This mobile phase composition is in conjunction with the composition recommended by Stuart Wilkinson (personal communications). Acetonitrile has also been used in the UHPLC mobile phase for methanolic extracts of phenolic compounds (Becerra-Herrera *et al.*, 2014; Peng *et al.*, 2009). It seems that a number organic

chemicals are suitable for the extraction and elution of phenolic compounds from various plant samples. Hence, it could be overconclusive to mention just one solvent and/or eluent that is the most effective for all methods and sample types in the analysis of phenolic compounds.

The LOD provides an estimate to differentiate between the absence and the presence of a compound, while the LOQ is the minimum benchmark for the reliable measurement of low levels of a compound (Armbruster and Pry, 2008; Shrivastava and Gupta, 2011). As described in the ICH Harmonised Tripartite Guideline, the determination of LOD and LOQ can be done based on visual evaluation, signal-to-noise ratios (as used in this study), or standard deviation of responses and the slope, as follows:

$$LOD = \frac{3.3\sigma}{S}$$

or

$$LOQ = \frac{10\sigma}{S}$$

where σ is the standard deviation (of responses of blank samples, residuals of the calibration curve, or y-intercepts of the calibration curve) and S is the slope of the calibration curve. Alternatively, the LOD can be calculated based on the limit of blank (LOB) (Armbruster and Pry, 2008):

$$LOD = LOB + 1.645(SD_{\text{low concentration analyte}})$$

where $SD_{\text{low concentration analyte}}$ is the standard deviation of responses of the minimum concentration analyte at which $\geq 95\%$ of the values should exceed the LOB. The LOQ should be equivalent or higher than the LOD ($LOQ \geq LOD$) at which the pre-determined conditions of imprecision ($CV=20\%$) is met. LOB is calculated as:

$$\text{LOB} = \text{Mean}_{\text{blank}} + 1.645(\text{SD}_{\text{blank samples}})$$

where $\text{mean}_{\text{blank}}$ is the mean value of background responses of the blank sample and $\text{SD}_{\text{blank sample}}$ is the standard deviation of the corresponding background responses of the blank sample. However, these methods were recommended for estimation using large numbers of sample replicates (for example, ≥ 60 replicates), more than one analyser, and many reagents (Armbruster and Pry, 2008). Estimations of LOD and LOQ based on signal-to-noise ratios would require a pre-determined magnitude of noise, which could also differ among different samples, different analysers, different reagents and different researchers who evaluate the noise range. Notwithstanding the limitations mentioned above, the presentation of data or chromatograms is acceptable for the justification of LOD and LOQ based on visual evaluation or signal-to-noise ratio (ICH Harmonised Tripartite Guideline).

6.5 CONCLUSION

In summary, a reliable RT-qPCR method has been established for the analysis of gene expressions in *C. frutescens* using *ACT* and *UBI-1* as the reference genes, which were found to be stably expressed across all tested samples. An optimised HPLC method for the analyses of phenolic compounds in *C. frutescens* has also been developed. Native vanillin and ferulic acid contents in various parts of a whole plant and in calli of *C. frutescens* were present only in trace amounts. Ferulic acid feeding at the tested concentrations did not elicitate the production of target phenolic compounds, especially vanillin. Calli that were transformed with pcDNA6.2::35Sp-*fcs*-NOSp-*ech*, pcDNA6.2::35Sp-*VpVAN* and pHBT12K::35Sp-*VpVAN* produced significantly higher levels of vanillin,

vanillin glucoside and vanillic acid than the untransformed calli. Vanillin was produced the most in calli that were transformed with pHBT12K::35Sp-*VpVAN*, followed by those transformed with pcDNA6.2::35Sp-*VpVAN* and subsequently those transformed with pcDNA6.2::35Sp-*fcs-NOSp-ech*. The production of phenolic compounds corresponded to the expression levels of the transgenes. The expression of *fcs* or *ech* alone was not capable of catalysing the biosynthesis of vanillin.

CHAPTER 7

GENERAL DISCUSSION AND FUTURE PERSPECTIVES

Various studies in this research have achieved numerous objectives, which include: (i) the optimised callus regeneration media consisting of MS media supplemented with 2.0 mg/l 2,4-D and 0.5 mg/l kinetin; (ii) the determination of 0.25 mg/l as the minimum inhibitory concentration of blasticidin S; (iii) the successful construction of pcDNA6.2::35Sp-*sgfp*, pcDNA6.2::35Sp-*fcs*-NOSp-*ech*, pcDNA6.2::35Sp-*fcs*, pcDNA6.2::NOSp-*ech*, pcDNA6.2::35Sp-*VpVAN* and pHBT12K::35Sp-*VpVAN* expression vectors; (iv) the optimised biolistic parameters with the use of 0.6 µm microparticles, 6 cm target distance, 1350 psi He pressure for the transformation of *C. frutescens*; (v) positive detection of target transgenes in genomic DNA of callus transformants; (vi) significantly higher RNA levels of target transgenes were quantified in transformed calli than untransformed calli; and (vii) significantly higher levels of vanillin, vanillic acid and vanillin glucoside levels were quantified in calli that were transformed with both *fcs* and *ech* genes or *VpVAN* compared to untransformed calli. These findings have led to an agreement with the concept of a possible vanillin production alternative through genetic manipulation of chilli plant with vanillin biosynthetic genes. Nevertheless,

the use of plant systems as the host for metabolite productions poses numerous advantages and disadvantages (discussed in **subchapter 7.1**). Besides that, the nuclear transformation approach used in this research has several possible limitations due to the underlying mechanisms surrounding the cellular and nuclear biology (discussed in **subchapter 7.2**). Furthermore, many more aspects in the phenylpropanoid pathway leading to vanillin biosynthesis, which could be amenable for elevated production of vanillin, remained to be understood (discussed in **subchapter 7.3**). As such, several recommendations are discussed so as to provide insights into possible improvements for consideration in future works (**subchapter 7.4**).

7.1 PROS AND CONS OF PLANT SYSTEMS AS BIOFACTORIES FOR METABOLITE PRODUCTION THROUGH TRANSGENESIS

Synthetic biology has emerged as the forefront technology of genetic engineering, which enables the “customisation” of biological functions and systems. Biological organisms can now be engineered to perform specific functions for the manufacturing of beneficial proteins or chemical products (Jenkins *et al.*, 2011). Therefore, the existing biochemical diversity within the vast pool of crop species could be exploited through synthetic biology to produce various desired compounds for research and industrial uses. Stereo- and regio-specific biotransformations can be conducted on plant cells to produce novel compounds from cheap precursors (Rao and Ravishankar, 2002). Hence, specific metabolic pathways could be introduced into crops or existing pathways could be modified to create a potential for the biomanufacturing of precursors or chemical products,

which could be purified or used readily *in vivo*. The application of synthetic biology in plants is often faced with drawbacks. Under extraneous manipulation, the overproduction of natively present chemicals or induced non-native chemicals could result in autotoxicity or a reduction in crop yield due to metabolic burden (Baldwin and Callahan, 1993; Suriyamongkol *et al.*, 2007). Moving on to this study, prospective overproduction of vanillin from ferulic acid could result in the reduction of ferulic acid available for lignin biosynthesis and jeopardise the structural integrity of the plant if indigenous compensation of the used ferulic acid did not take place. This is because ferulic acid is one of the components in lignocellulosic fibres, which provide structural integrity through the formation secondary cell walls (Chen, 2014). Although this aspect was not explored in this study, such possibility could be worth considering as the compromise between ferulic acid availability and plant structural integrity could be a major limiting factor in the sustainable production of vanillin using genetically modified plants. Having said that, wild-type calli of *C. frutescens* seemed to be lacking a network of cross-linked fibres, which consists of hemicelluloses that bind with pectin and cellulose to form secondary cell walls together with lignin, as shown in the scanning electron microscopy (SEM) of cellular surfaces (Betekhtin *et al.*, 2016; Harris, 2006; Kumar *et al.*, 2016; Leppard and Colvin, 1971) (**Appendix J**). The absence of secondary cell wall structures suggests that lignin biosynthesis could be absent in the calli and the jeopardy caused by excessive ferulic acid usage for vanillin production could be questionable.

The success of genetic manipulations relies largely on the transformation method used. One of most commonly used methods, biolistic-mediated transformation, has its own set of advantages and disadvantages. Biolistic-mediated transformation requires cells' ability to

regenerate into organs or callus mass *via* tissue culture, except in the case of direct *in vivo* transformation using the gene gun (Kikkert *et al.*, 2004). Recalcitrant species, such as those of *Capsicum* spp., are relatively harder to regenerate into whole plantlets compared to their other relatives within the Solanaceae family, such as *Nicotiana* spp., despite reports of successes in the whole-plant regeneration of *Capsicum* spp. (Kothari *et al.*, 2010; Li *et al.*, 2003a; Rizwan *et al.*, 2014; Valadez-Bustos *et al.*, 2009). However, the induction of healthy calli with satisfactory transformation efficiencies through biolistic-mediated transformation is achievable, as demonstrated in this study.

Many approaches in synthetic biology that are applied in microbial biotechnology for chemical production are now directed towards plant biotechnology for similar biorefining applications. However, it is apparent that the bioengineering of plants is more complex than microbes, although plant systems are scalable for large-scale production at cheaper costs than large fermentation bioreactors used for microbes (Urreta and Castañón, 2012). This is due to more extensive biochemical pathways and complicated regulation of gene expression in plants than in microbes (Jenkins *et al.*, 2011). However, multiple methods for the efficient transformation of many crops have been established, including this study. These methods involved not only microprojectile bombardment, but also *Agrobacterium*-mediated gene transfer, electroporation and floral dip (Pena, 2004). The establishment of various transformation methods has enabled deeper understanding of plant primary and secondary metabolic pathways and allowed the manipulation of these metabolic pathways.

The idea of using terrestrial crops for an integrated production of target metabolites is that the plants should be flexible to be amenable for the manufacture of different types of products. However, the dilemma

comes in the sense that plants that are non-food crops could be preferred, depending on the target products. For example, plants that are grown for their biomass for energy or fuel production should not enter the food supply chain (Jenkins *et al.*, 2011). On the contrary, plants that are useful for their edible crop status are preferred for the production of edible or food-related products, such as edible vaccines or flavouring compounds like vanillin. A more practical approach in the light of plant genetic engineering could be to supply to the agricultural chain using the edible portions, such as grains, fruits or tubers, whereas parts, such as stems or roots, could be harvested for the purification of target chemical products.

The utilisation of plant tissue cultures as spin-offs from intact plant systems for the production of secondary metabolites is beneficial as plant tissue culture is not dependent on environmental factors, such as geographical and seasonal variations. Besides that, the defined production system ensures that products are more rapidly and constantly supplied with uniform quality and yield compared to the conventional intact plant system. Furthermore, plant tissue culture is often facilitated by efficient downstream recovery of the products. Another important point is the tissue culture system is usually free from political interference that may impose restrictions on the genetic manipulation activity (Rao and Ravishankar, 2002).

7.2 CHALLENGES IN NUCLEAR TRANSFORMATION

Stable nuclear transformation of plants often stems from random integrations of the transgene into the plant genome. As such, expression levels may be affected by the transcriptional activity of neighbouring regions in the chromosomes. In addition, the insertion of transgenes within

the functional endogenous genes can prevent the transcription of genes regulating essential morpho-physiological pathways, resulting in atypical or lethal phenotypes (Lico *et al.*, 2005). Therefore, molecular characterisation of plant transformants, for example, the determination of the transgene position in the nuclear genome, would be helpful. Besides that, high levels of expression are not always beneficial due to the potential activation of gene silencing mechanisms, causing the suppression of the transgene (Tang *et al.*, 2007; Voinnet and Baulcombe, 1997). An alternative that could possibly resolve these problems is plastid transformation, as plastid transformation overcomes positional effects with targeted gene integration regions, hence eliminating any possible disruption of genes taking part in important cell functions (Daniell and Dhingra, 2002; Wani *et al.*, 2010). Moreover, the activation of gene silencing is not apparent in transplastomic plants, although high expressions of exogenous genes due to the high number of transformed chloroplasts in every cell have been reported (Sidorov *et al.*, 1999; Singh *et al.*, 2010). Unfortunately, this technique may not be applied for all plant species and there has been difficulty in achieving homoplastomy after successful transformations (Lico *et al.*, 2005). Furthermore, leaf chloroplasts are usually targeted using this technique as the organelle is abundant in leaf tissues and the plastid genome copy number is high in chloroplasts (Langbecker *et al.*, 2004). Hypocotyl tissues that were used in this study lacked developed plastids, especially chloroplasts (Waters and Langdale, 2009). Plastid transformation could be disadvantageous for *VpVAN*, which might require post-translational modifications, as such modifications do not occur in plastids. It was demonstrated that the pro-peptide sequence at the N-terminus of *VpVAN* may serve to regulate intracellular targeting, correct folding and post-translational modification of the mature enzyme, which are yet to be clearly understood (Gallage *et al.*, 2014).

The quality of expressed proteins can be maintained by targeting the proteins to the cellular secretory pathway (endoplasmic reticulum and Golgi apparatus), where proper folding and post-translational modifications can be done. Post-translational modifications might be essential for *VpVAN*, which originated from the plant system, but not for *Fcs* and *Ech*, which originated from the prokaryote system. The polypeptides of *Fcs* and *Ech* might be interfered with by post-translational modifications, but these characteristics were not explored in this study. Nevertheless, it seemed that the increase in vanillin production correlated well to the expressions of both *fcs* and *ech*, thereby suggesting that the activities of *Fcs* and *Ech* were likely to have been retained in the callus cells of *C. frutescens*. Retention of proteins to organelles (e.g. endoplasmic reticulum) can be achieved by fusing, for example, a H/KDEL peptide, to the recombinant protein if it is detrimental for the protein to proceed further in the secretory pathway or to avoid undesirable plant-specific glycosylation (Conrad and Fiedler, 1998). However, the retention of recombinant proteins might not be beneficial, such as in the case of vanillin biosynthetic enzymes, because vanillin biosynthesis purportedly takes place in the cytoplasm of cells based on the locations of capsaicin biosynthetic pathway, where ferulic acid and vanillin are the intermediates (**Figure 7.1**).

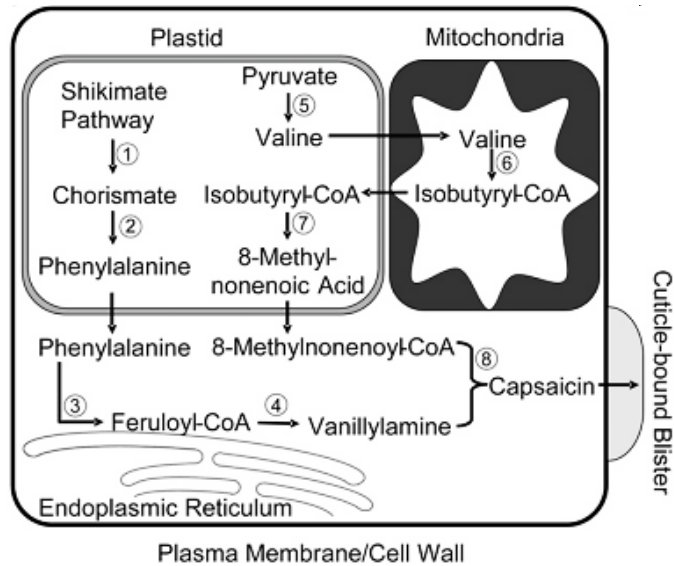


Figure 7.1 The model of capsaicin biosynthetic pathway in a cell. Chorismate from the shikimate pathway (1) is used to synthesise phenylalanine in the plastid (2). Phenylalanine is converted into feruloyl-CoA by phenylpropanoid metabolism (3) in the cytoplasm. Feruloyl-CoA is converted into vanillylamine by an unknown enzyme in an unknown compartment (4). Ferulic acid and vanillin are found within (3) and (4), respectively. In another pathway, pyruvate is converted into valine (5) and exported to the mitochondria to be catabolised to isobutyryl-CoA (6). Isobutyryl-CoA is transported to the plastid, where it is converted into 8-methylnonenoic acid (7). The location and mechanism of the final conversion and secretion of capsaicin out of the cell (8) are not confirmed. Adapted from Mazourek *et al.* (2009).

7.3 MODIFICATIONS TO THE PHENYLPROPANOID PATHWAY FOR VANILLIN BIOSYNTHESIS

In this study, the phenylpropanoid pathway in capsaicin biosynthesis is purportedly focused towards vanillin biosynthesis with the overexpression of *fcs* and *ech* or *VpVAN* (Figure 7.2). However, subsequent conversions of vanillin into other compounds, such as vanillin glucoside, vanillylamine and/or vanillic acid are still debatable. The detection of vanillin glucoside and vanillic acid in transformed calli suggests the possibility of downstream conversion of vanillin to produce vanillin glucoside and vanillic acid, which could be reversible (Achterholt *et al.*, 2000; Gallage *et al.*, 2014; Gallage

and Møller, 2015). With that, the downstream conversion of vanillin might have to be downregulated to further improve the accumulation of vanillin. For example, the knockdown of pAMT, an aminotransferase responsible for the conversion of vanillin into vanillylamine, has been shown to decrease the levels of capsaicin in *C. annuum* and *C. frutescens* (Chapa-Oliver and Mejía-Teniente, 2016; Gururaj *et al.*, 2012; Ogawa *et al.*, 2015). However, the detrimental effect of vanillin accumulation should be considered as mechanisms of such conversions could be an adaptation by plant cells to reduce possible toxicity caused by high concentrations of vanillin (Brochado *et al.*, 2010). The absence of capsaicin and the presence of only minute amounts of other phenolic compounds tested in callus tissues of *C. frutescens* suggest that the capsaicin biosynthesis has yet to be activated at an unknown step in the pathway. However, this explanation does not dismiss the availability of ferulic acid and/or feruloyl-CoA precursors in one form or another.

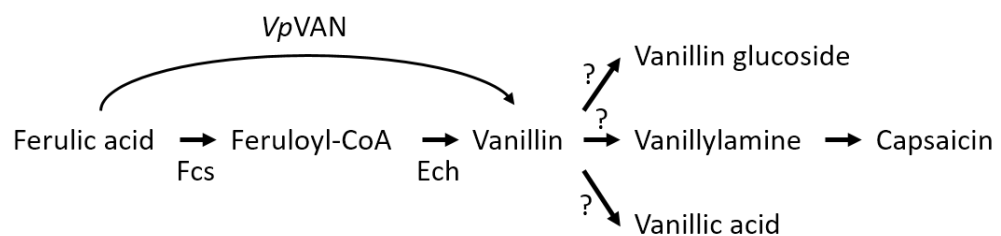


Figure 7.2 The metabolic pathway showing the purported focusing of vanillin biosynthesis from ferulic acid with the overexpression of *fcs* and *ech* or *VpVAN* in the transformed callus cells of *C. frutescens*. *Fcs* catalyses the conversion of ferulic acid into feruloyl-CoA, while *Ech* progressively catalyses the conversion of feruloyl-CoA into vanillin (2-step process). *VpVAN* catalyses the conversion of ferulic acid into vanillin in a single step. The occurrence of downstream conversions of vanillin to vanillin glucoside, vanillylamine (subsequently to capsaicin), and/or vanillic acid is debatable, as shown by question marks (?).

7.4 RECOMMENDATIONS AND FUTURE PERSPECTIVES

Looking at the phenylpropanoid pathway for capsaicin biosynthesis, vanillin accumulation could possibly be achieved with the knockdown of genes

involved downstream conversion(s) of vanillin into other compounds, such as the *pAMT* gene. The upregulation of endogenous genes involved in upstream conversion(s) leading to vanillin production, such as the *HCHL* gene, and/or exogenous genes, such as *fcs*, *ech* and *VpVAN*, would be an added advantage. Having said that, it would be fundamental to examine the kinetics of vanillin accumulation and its compartmentalization, as well as the concentration benchmark of vanillin and other associated compounds that may pose negative effects on plant cells.

Recent breakthroughs in the CRISPR/Cas technology have opened a new frontier in genetic engineering. The application of an appropriate cloning technology for the cloning of vectors that are compatible with the CRISPR/Cas system can enable transfer of exogenous genes into very specific regions of the plant genome (Nødvig *et al.*, 2015; Sakuma *et al.*, 2014; Vad-Nielsen *et al.*, 2016). In addition, the inhibition or activation of a gene can be regulated with the binding of a broken Cas9 enzyme to the gene to prevent transcription by RNA polymerase (inhibition) or the attachment of an activator protein to the broken Cas9 to stimulate the gene expression (activation) (Ledford, 2016). Hence, the adoption of CRISPR/Cas technology is recommended as a prospective improvement to be explored in future studies.

Considerable debates have been raised concerning human health with regards to plant genetic engineering. These include the negative effects of selectable markers for the selection of transformed cells, the transfer of extraneous genetic materials other than the target DNA into the plant genome, and the higher possibility of mutations in transformed plants than their wild-type counterparts (Key *et al.*, 2008). To address these issues, the above-mentioned concerns are discussed and possible remediations are recommended. Antibiotic resistance genes are normally

used as selectable markers that are co-integrated with transgenes of interest to enable the differentiation between transformed and untransformed cells. It is claimed that there is a possibility of antibiotic resistance being transferred to microorganisms in the environment or the human body by various means. Putting aside the fact that many of the antibiotic resistance genes were originally isolated from microorganisms themselves, many of the antibiotics are generally regarded as safe and have been in use for many years (Key *et al.*, 2008). Besides that, it has been established that the horizontal transfer of non-mobile DNA may occur only at very low frequencies due to mechanistic challenges in such transfer of genetic materials (Kay *et al.*, 2002; Midtvedt, 2014). Hence, events of horizontal transfer of antibiotic resistance genes would happen rarely in the overall microorganism population. Alternatively, other selection strategies, such as the mannose-based selection using phosphomannose isomerase gene, may be used (Hu *et al.*, 2016; Negrotto *et al.*, 2000). Other than that, site-specific recombinases, such as XerC/XerD from *E. coli*, RipX/CodV from *Bacillus subtilis* and Cre/Lox from P1 bacteriophage, can be employed for the excision of selectable marker genes when their expressions are no longer required (Bloor and Cranenburgh, 2006; Hare and Chua, 2002; Ledbetter *et al.*, 2014).

The next issue of concern in the plant genetic engineering is the transfer of miscellaneous DNA other than the gene of interest into the plant genome. DNA alone should not be harmful as it is present in most food consumed by humans. Furthermore, many of the purified compounds would have had DNA and other cellular matrix components removed to the minimal extent during the purification process. Nevertheless, the design of minimal expression cassettes could be a solution, as successfully demonstrated by Fu and co-workers (2000) in their transformation of rice

using only a plasmid carrying the *bar* gene and a linear DNA fragment containing a promoter, an open reading frame and a terminator.

Tissue culture and plant transformation procedures may cause genome-wide mutations known as somaclonal variations, or DNA rearrangements around the integrated transgene. These phenomena may produce plants with elevated levels of allergens or toxins, and/or on the contrary, with the expression of desirable traits (Jain, 2001). Considering these possibilities, it is recommended to analyse the transgenic plants or the purified compounds by testing the samples against an array of allergens and toxic compounds to determine the presence of the undesirable substances.

It is good to note that rigorous regulatory frameworks are in place to govern genetic engineering works and to ensure that the products are tested for any possible risks to health and safety prior to their release into the environment or for consumption. Nevertheless, this study only serves as a proof-of-concept and is still a long way to commercialisation. Much effort is needed to ensure that the expression system and the vanillin production and accumulation systems are sustainable in larger scales. Nevertheless, the approach in this research is proven to be promising with the potential that the vanillin yield of the production system becomes comparable to those of vanilla pods and microbial fermentation systems, which are currently the more common systems for the “natural” vanillin production.

APPENDIX

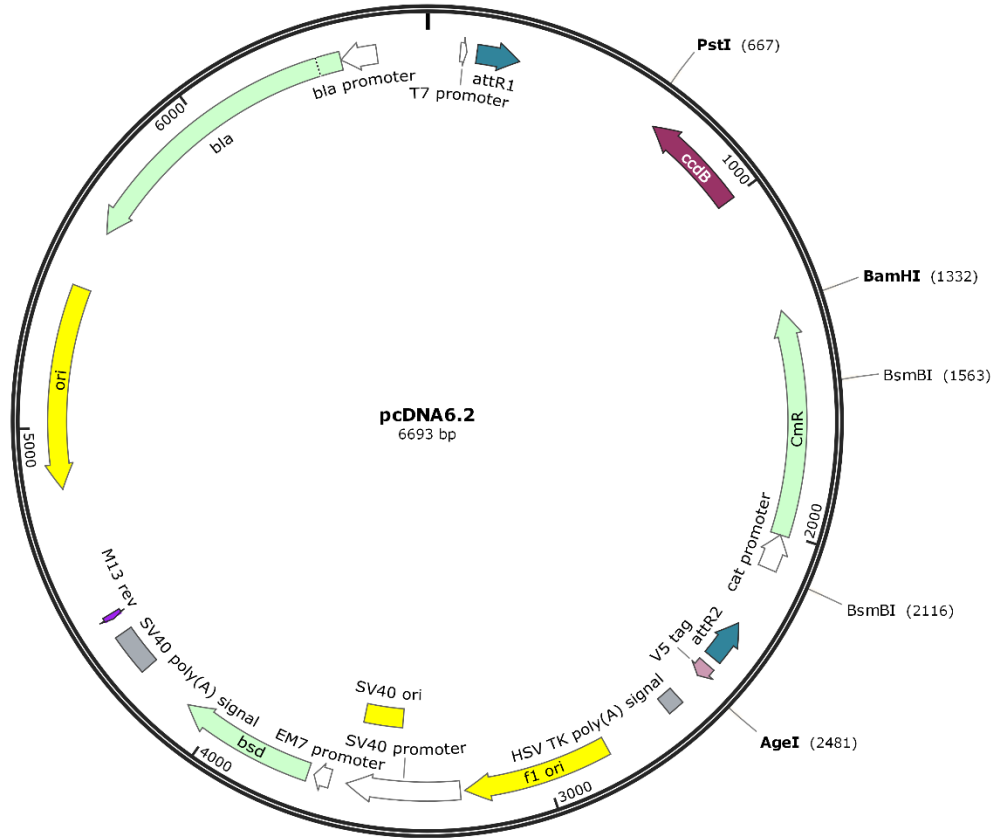
A. Formulation of MS basal salt and vitamins

Formula	Content (mg/l)
Ammonium nitrate	1650.0
Boric acid	6.2
Calcium chloride, anhydrous	332.2
Cobalt chloride·6H ₂ O	0.025
Copper sulphate·5H ₂ O	0.025
Na ₂ EDTA·2H ₂ O	37.26
Ferrous sulphate·7H ₂ O	27.8
Magnesium sulphate, anhydrous	180.7
Manganese sulphate·H ₂ O	16.9
Molybdc acid (sodium salt) ·2H ₂ O	0.25
Potassium iodide	0.83
Potassium nitrate	1900.0
Potassium phosphate, monobasic	170.0
Zinc sulphate·7H ₂ O	8.6
Glycine (free base)	2.0
myo-Inositol	100.0
Nicotinic acid (free acid)	0.5
Pyridoxine·HCl	0.5
Thiamine·HCl	0.1

B. Maps of transformation vectors

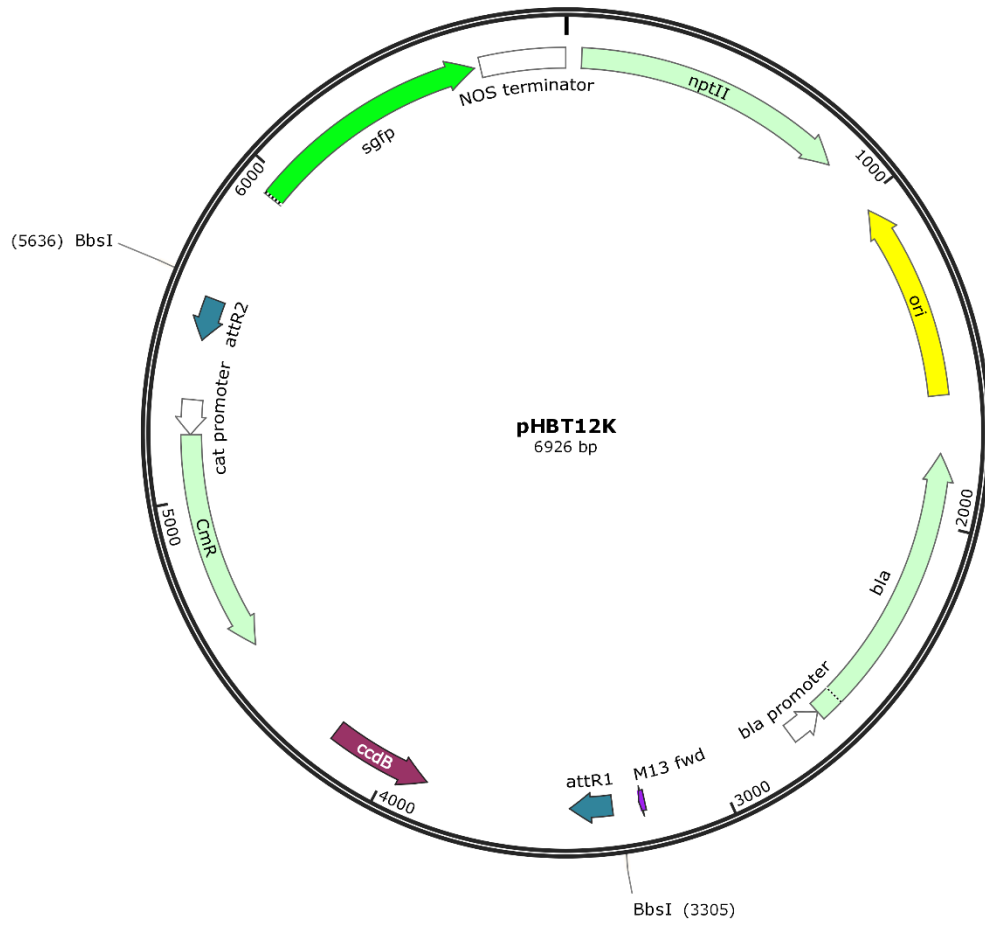
(i) pcDNA6.2

Created with SnapGene®



Created with SnapGene® Viewer v3.1.2

(ii) pHBT12K



Created with SnapGene® Viewer v3.1.2

C. Primer sequences

Primer name	Sequence (5' -3')	Annealing temperature (°C)	Amplicon size (bp)
PF/ <i>Pst</i> I-35Sp- <i>sgfp</i>	GGCTATCTGCAGGGGTACTCCAAGA ATATCAAAGATACA	64	1303
PR/35Sp- <i>sgfp</i> - <i>Age</i> I	TCGGACCGGTGGGTTACTTGTACAG CTCGTCCATGCC		
PF/ <i>att</i> B1-35Sp	GGGGACAAGTTTGTACAAAAAAGCA GGCTCCAGCTTACTCCAAGAATATC AAAGA	52	407
PR/35Sp- <i>att</i> B5r	GGGGACAACCTTTTGTATACAAAGTT GTCGAAGGATAGTGGGATTGTGCGT C		
PF/ <i>fcs</i>	ATGAGGAATCAAGGATTAGG	56	1473
PR/ <i>fcs</i>	CTAACCGAATCTCCTACGAA		
PF/NOSp	GACAAGCCGTTTTACGTTTG	53	233
PR/NOSp	GATTGAGAGTGAATATGAGA		
PF/ <i>ech</i>	TTTTTCAGGATCGAAAGCAC	56	861
PR/ <i>ech</i>	ATGTCAACGGCTGTTGGGAA		
PF/ <i>att</i> B5- <i>fcs</i> (2)	GGGGACAACCTTTGTATACAAAAGTT GCCATGAGGAATCAAGGATTAGGAT CA	54.5	1576
PR/ <i>fcs</i> - <i>att</i> B2(2)	GGGGACCACTTTGTACAAGAAAGCT GGGTAATAAGTAGAATCAAGTCCAA GAAGTGGATTTGGAATTGGCTTTCC ACCGAATCTCCTACGAACTTCGCCC TTCAA		
PF/ <i>Bsm</i> BI-NOSp	CGTCTCATGGCAAGCTTACGCGGGA CAAGCCGTTTTACGTT	71	273
PR/NOSp- <i>Bsm</i> BI	CGTCTCTTATTGGATCCGATTGAGAG TGAATATGAGACTCT		
PF/ <i>Bsm</i> BI- <i>ech</i>	CGTCTCGAATAGGATCCATGTCAAC GGCTGTTGGGAACGGG	81	922
PR/ <i>ech</i> - <i>Bsm</i> BI	CGTCTCCAAAATACCGGTGCTAGTG ATGGTGGTGGTGTATGTTTTTCAGGA TCGAAAGCACTAAGGCC		
PF/ <i>Bbs</i> I-35Sp- <i>VpVAN</i>	CGAGGAAGACCAAAGGCTCGAGTAC TCCAAGAATATCAAAGAT	60	1505
PR/35Sp- <i>VpVAN</i> - <i>Bbs</i> I	TGCCGAAGACGTGGTTGAGCTCGCA GTAGAATCAAGTCCAAGAAG		
SCREEN <i>gfp</i> -F	ATGGTGAGCAAGGGCGAGGAG	53	720
SCREEN <i>gfp</i> -R	TTACTTGTACAGCTCGTCCAT		
PF/ <i>VpVAN</i>	AGGACGTCTCGTACACCATGGATGG CAGCTAAGCTCCTCTTC	63	1068
PR/ <i>VpVAN</i>	GGTCAAAATGAGACGGGGATCCGCT AGTGATGGTGGTGGTGTATGCACAGC CACAATGGGATAAGATGC		

D. Sequences of synthesised DNA fragments

(i) Codon optimised *fcs*

ATGAGGAATCAAGGATTAGGATCATGGCCAGTCAGAAGAGCTAGGATGTCTCCTCATGCC
ACCGCTGTGCGGCATGGCGGAACAGCCCTGACTTATGCAGAGCTCAGCAGGGCAGTTGCA
CGGCTTGCAAATGGCCTCCGAGCTGCTGGGGTGAGACCTGGGGATCGGGTGGCTTATCTG
GGACCTAATCACCCAGCATATCTAGAGACACTATTTGCTTGCGGACAGGCTGGAGCTGTGT
TTGTACCGCTAAACTTCCGTCTGGGAGTCCCTGAGCTCGATCACGCCTTGGCTGACTCAGG
CGTAGCGTACTTATCCATACTCCGGAACATGCAGAAACTGTCGCAGCATTGGCAGCTGG
GAGATTGCTACGAGTTCGCCCGGAGAGTTAGACGCAGCAGATGATGAGCCGCCAGATCT
CCCCGTTGGACTTGACGATGTCTGCTTGTCTTATGTACACTTCTGGAAGTACAGGAAGGCCT
AAGGGCGCTATGTTGACTCATGGAAATTTGACTTGGAAATTGCGTTAATGTACTTGTGGAGA
CGGACTTGGCATCTGATGAGAGGGCACTAGTTGCTGCTCCCCTTTTTCACGCCGCAGCTCT
TGGAAATGGTTTGCCTTCCGACACTTCTCAAAGGAGGGACAGTTATACTTCATTACAGCATT
GATCCTGGGGCCGTTCTTAGTGCTGTGCGAGCAAGAAAGGGTTACGCTCGTCTTTGGAGTA
CCAATATGTATCAGGCAATAGCTGCTCATCCACGATGGAGAAGTGCTGACCTTTCAAGTT
TAAGGACTCTGTTGTGTGGCGGCGCACCAGTTCCTGCTGACCTAGCATCCCGATACCTCGA
TAGAGGTTTGGCATTGTGCAAGGATATGGCATGACCGAGGCAGCTCCTGGTGTCTAGT
GCTAGATAGAGCTCACGTCGCAGAGAAAATAGGGAGCGCTGGGGTCCCTTCTTTACT
GATGTACGGCTGGCAGGACCATCTGGGGAGCCGTTCTCCCGAGAGAAAAGGCGAGAT
AGTCGTCAGTGGACCTAATGTTATGAAAGGTTATTGGGGACGTCCAGAAGCAACTGCTGAA
GTTCTGAGGGATGGTTGGTTCCATAGTGGAGACGTTGCCACAGTTGATGGTGACGGTTATT
TTCACGTTGTGGATAGGCTTAAAGATATGATCATTAGTGGCGGAGAAAATATTTATCCTGCT
GAGGTCGAAAACGAACTATATGGTTACCCTGGAGTTGAAGCATGTGCAGTGATTGGAGTTC
CTGATCCTAGATGGGGTGAAGTAGGAAAGGCAGTCGTGGTTCCTGCAGATGGTTCTCGGA
TCGATGGGGATGAATTACTTGCCTGGCTGCGTACCCGATTGGCTGGATACAAAGTTCCAAA
GTCTGTGGAATTTACGGATAGGTTGCCACAACAGGCTCAGGAAAAATATTGAAGGGCGA
AGTTCGTAGGAGATTCCGGT

(ii) Codon optimised *ech*

ATGTCAACGGCTGTTGGGAACGGGAGAGTTAGAACAGAGCCTTGGGGTGAGACTGTTCTG
GTGGAGTTTGACGAAGGCATCGCATGGGTTATGCTTAACAGACCTGATAAACGAAATGCTA
TGAATCCAACCTTTAAATGATGAAATGGTCAGGGTGCTAGATCATCTCGAGGGAGATGATCG
TTGCAGGGTGCTTGTCTGACAGGGGCTGGAGAATCATTTTCCGCCGTATGGATCTAAAG
GAGTACTTCAGAGAAGTGGATGCTACTGGAAGTACTGCCGTTCAAATTAAGGTGCGGAGA
GCTAGCGCAGAGTGGCAGTGGAAAGCGGTTAGCCAACTGGAGCAAACCAACAATCGCTATG
GTTAATGGTTGGTGTTCGGGGGTGCATTTACTCCACTGGTTGCCTGCGACCTTGCCTTTG
CTGATGAGGATGCAAGGTTTGGTTTGAGCGAGGTGAATTGGGGAATTCCTCCCGGTGGCG
TAGTGTACGGGCACTGGCCGCAACTGTTCTCAGAGGGACGCTTTATACTATATTATGAC
TGCGGAACCTTTGACGGTCGACGAGCTGCTGAGATGAGGCTTGTGAACGAAGCTCTGCC
GGCTGACAGACTTCGGGAACGAACCCGAGAGGTTGCTTTGAAACTAGCTTCTATGAATCAA
GTGGTACTTCATGCAGCTAAGACAGGATATAAGATTGCTCAAGAAATGCCATGGGAGCAA
GCTGAGGACTATCTGTACGAAAACCTGGATCAGTCCCAGTTCGCTGATAAGGCTGGTGCA
CGAGCTAAAGGGTTAACACAGTTCCTTGATCAAAAATCCTATCGGCCAGGCCTTAGTGCTT
TCGATCCTGAAAAA

(iii) Codon optimised *VpVAN*

ATGGCAGCTAAGCTCCTCTTCTTCTACTTCTCCTGGTCTCCGCCCTCTCCGTCGCGCTCGC
CGGTTTCGAAGAAGACAATCCAATCCGGTCCGTTACACAAAGGCCTGACTCGATTGAGCCT
GCCATCCTCGGCCTCCTTGGCAGTTGCCGCCACGCCTTCCACTTCGCACGGTTCGCCCGC
AGGTACGGGAAGAGCTACGGATCGGAGGAGGAGATCAAGAAGAGGTTCCGGGATCTTCGT
GGAGAATCTAGCGTTTATCCGGTCCACTAATCGGAAGGATCTGTCGTATACCCTAGGAATC
AACCAATTCGCCGACCTGACCTGGGAGGAATCCGGACCAATCGCCTTGGTGCGGCGCAG
AACTGCTCGGCGACTGCGCATGGAAACCACCGGTTTGTGATGGCGTGCTTCTGTAAACG
AGGGATTGGAGGGAGCAAGGGATAGTGAGCCCTGTAAAGGACCAAGGAAGCTGTGGATC
TTGCTGGACTTTCAGTACTACTGGAGCACTAGAGGCTGCATATACACAGCTAACTGGAAAG
AGCACATCATTATCTGAACAGCAACTTGTGGACTGTGCCTCAGCATTCAATAACTTTGGATG
CAATGGAGGTTTGCCTTCCAAGCCTTTGAATACGTTAAGTACAATGGAGGCATCGACACA
GAACAGACTTATCCATACCTTGGTGTCAATGGTATCTGCAACTTCAAGCAGGAGAATGTTG
GTGTCAAGGTCATTGATTGATAAACATCACCTGGGTGCTGAGGATGAGTTGAAGCATGC
AGTGGGCTTGGTGCCTCAGTTAGCGTTGCATTTGAGGTTGTGAAAGGTTTCAATCTGTAC
AAGAAAGGTGTATACAGCAGTGACACCTGTGGAAGAGATCCAATGGATGTGAACCACGCA
GTTCTTGCCGTCGGTTATGGAGTCGAGGACGGGATTCTTATTGGCTCATCAAGAACTCAT
GGGGTACAAATTGGGGTGACAATGGCTACTTTAAGATGGAACCTCGGCAAGAACATGTGTG
GTGTTGCAACTTGCGCATCTTATCCATTGTGGCTGTG

E. DNA sequencing results

(i) *pcDNA6.2::35Sp-sgfp (35Sp + sgfp cassette)*

GGGTACTCCAAGAATATCAAAGATACAGTCTCAGAAGACCAAAGGGCTATTGAGACTTTTTCAA
CAAAGGGTAATATCGGGAAACCTCCTCGGATTCCATTGCCAGCTATCTGTCACTTCATCAAA
AGGACAGTAGAAAAGGAAGGTGGCACCTACAAATGCCATCATTGCGATAAAGGAAAGGCTATC
GTTCAAGATGCCTCTGCCGACAGTGGTCCCAAAGATGGACCCCAACCACAAGGAGCATCGTG
GAAAAGAAGACGTTCCAACCACGTCTTCAAAGCAAGTGGATTGATGTGATATCTCCACTGAC
GTAAGGGATGACGCACAATCCCCTATCCTTCGCCCAAGCTTGGGCCCCAAGCTTGGGTGCGG
CCCCACGGATGGTATAAGAATAAAGGCATTCCGCGTGCAGGATTCACCCGTTTCGCTCTCACC
TTTTCGCTGTACTCTCTCGCCACACACACCCCTCTCCAGCTCCGTTGGAGCTCCGGACAGCA
GCAGGCGCGGGGCGGTACGTTAGTAAGCAGCTCTCGGCTCCCTCTCCCTTGTCCGTTGGATC
CATGGTGAGCAAGGGCGAGGAGCTGTTACCGGGGTGGTGCCCATCCTGGTTCGAGCTGGACGG
CGACGTAAACGGCCACAAGTTTACGCGTGTCCGGCGAGGGCGAGGGCGATGCCACCTACGGCAA
GCTGACCCTGAAGTTTCACTCTGCACCACCGGCAAGCTGCCCGTGCCTGGCCACCCCTCGTGAC
CACCTTACCTACGGCGTGCAGTGCTTACGCCGCTACCCCGACCACATGAAGCAGCAGCACTT
CTTCAAGTCCGCCATGCCCGAAGGCTACGTCCAGGAGCGCACCATCTTCTTCAAGGACGACGG
CAACTACAAGACCCGCGCCGAGGTGAAGTTTCGAGGGCGACACCCTGGTGAACCGCATCGAGCT
GAAGGGCATCGACTTCAAGGAGGACGGCAACATCCTGGGGCACAAGCTGGAGTACAACCTACAA
CAGCCACAACGTCTATATCATGGCCGACAAGCAGAAGAACGGCATCAAGGTGAACCTTCAAGAT
CCGCCACAACATCGAGGACGGCAGCGTGCAGCTCGCCGACCACTACCAGCAGAACACCCCAT
CGGCGACGGCCCCGTGCTGCTGCCCGACAACCACTACCTGAGCACCCAGTCCGCCCTGAGCAA
AGACCCCAACGAGAAGCGGATCACATGGTCTGCTGGAGTTTCGTGACCGCCCGGGGATCAC
TCACGGCATGGACGAGCTGTACAAGTAACCC

(ii) pcDNA6.2::35Sp-*fcs*-NOSp-*ech* (35Sp + *fcs* + NOSp + *ech* cassette)

ACAAGTTTGTACAAAAAGCAGGCTCCAGCTTACTCCAAGAATATCAAAGATACAGTCTCAGA
AGACCAAAGGGCTATTGAGACTTTTCAACAAAGGGTAATATCGGGAAACCTCCTCGGATTCCA
TTGCCAGCTATCTGTCACTTCATCAAAGGACAGTAGAAAAGGAAGGTGGCACCTACAAATG
CCATCATGCGATAAAGGAAAGGCTATCGTTCAAGATGCCTCTGCCGACAGTGGTCCCAAAGAT
GGACCCCAACCACAAGGAGCATCGTGGAAAAAGAAGACGTTCCAACCACGTCTTCAAAGCAA
GTGGATTGATGTGATATCTCCACTGACGTAAGGGATGACGCACAATCCCCTATCCTTCGACA
ACTTTGTATACAAAAGTTGCCATGAGGAATCAAGGATTAGGATCATGGCCAGTCAGAAGAGCT
AGGATGTCTCCTCATGCCACCGCTGTGCGGCATGGCGGAACAGCCCTGACTTATGCAGAGCTC
AGCAGGCGAGTTGCACGGCTTGCAAATGGCCTCCGAGCTGCTGGGGTGAGACCTGGGGATCGG
GTGGCTTATCTGGGACCTAATCACCCAGCATATCTAGAGACACTATTTGCTTGCGGACAGGCT
GGAGCTGTGTTTGTACCGCTAAACTTCCGTCTGGGAGTCCCTGAGCTCGATCACGCCTTGGCT
GACTCAGGCGCTAGCGTACTTATCCATACTCCGGAACATGCAGAACTGTGCGAGCATTGGCA
GCTGGGAGATTGCTACGAGTTCCCGCCGGAGAGTTAGACGCAGCAGATGATGAGCCGCCAGAT
CTCCCGGTTGGACTTGACGATGTCTGCTTGGCTTATGTACACTTCTGGAAGTACAGGAAGGCC
AAGGGCGCTATGTTGACTCATGGAAATTTGACTTGGAAATTGCGTTAATGTACTTGTGGAGACG
GACTTGGCATCTGATGAGAGGGCACTAGTTGCTGCTCCCTTTTTTACGCCCGAGCTCTTGGA
ATGGTTTGCCTTCCGACACTTCTCAAAGGAGGGACAGTTATACTTCATTACAGCATTTCGATCCT
GGGGCCGTTCTTAGTGCTGTGAGCAAGAAAGGGTTACGCTCGTCTTTGGAGTACCAACTATG
TATCAGGCAATAGCTGCTCATCCACGATGGAGAAGTGCTGACCTTTCAAGTTAAGGACTCTG
TTGTGTGGCGGCGCACCAGTTCCTGCTGACCTAGCATCCCGATACCTCGATAGAGGTTTGGCA
TTTGTGCAAGGATATGGCATGACCGAGGCAGCTCCTGGTGTCTAGTGCTAGATAGAGCTCAC
GTCGCAGAGAAAATAGGGAGCGCTGGGGTCCCTTCTTTACTGATGTACGGCTGGCAGGA
CCATCTGGGGAGCCGGTTCCTCCCGGAGAGAAAAGGCGAGATAGTCGTAGTGGACCTAATGTT
ATGAAAGGTTATTGGGGACGTCCAGAAGCAACTGCTGAAGTTCTGAGGATGGTGGTTCCAT
AGTGGAGACGTTGCCACAGTTGATGGTGACGGTTATTTTTACGTTTGTGGATAGGCTTAAAGAT
ATGATCATTAGTGGCGGAGAAAATATTTATCCTGCTGAGGTCGAAAACGAACTATATGGTTAC
CCTGGAGTTGAAGCATGTGCAGTGATTGGAGTTCCTGATCCTAGATGGGGTGAAGTAGGAAAG
GCAGTCGTGGTTCCTGCAGATGGTTCCTCGGATCGATGGGGATGAATTACTTGCTGGCTGCGT
ACCCGATTGGCTGGATACAAAGTTCCAAAGTCTGTGGAATTTACGGATAGGTTGCCACAACA
GGCTCAGGAAAATATTGAAGGGCGAAGTTCGTAGGAGATTCCGGTAGCATCACCACCACCAT
CACACCCAACCTTTTCTATACAAAGTTGCCACGCGGGACAAGCCGTTTTACGTTTGGAACTGAC
AGAACCACAACGATTGAAGGAGCCACTCAGCCGCGGGTTTTCTGGAGTTAATGAGCTAAGCAC
ATACGTCAGAAACCATTATTGCGCGTTCAAAGTTCGCTAAGGTCACTATCAGCTAGCAAATA
TTTCTTGTCAAAAATGCTCCACTGACGTTCCATAAATTTCCCTCGGTATCCAATTAGAGTCTC
ATATTCCTCTCAATCACAACCTTTGTATAATAAAGTTGGTATGTCAACGGCTGTTGGGAACGG
GAGAGTTAGAACAGAGCCTTGGGGTGAGACTGTTCTGGTGGAGTTTGCAGAAAGGCATCGCATG
GGTTATGCTTAACAGACCTGATAAACGAAATGCTATGAATCCAACCTTAAATGATGAAATGGT
CAGGGTGTAGATCATCTCGAGGGAGATGATCGTTGCAGGGTGTGTTCTGACAGGGGCTGG
AGAATCATTTTTCCGCCGGTATGGATCTAAAGGAGTACTTCAGAGAAGTGGATGCTACTGGAAG
TACTGCCGTTCAAATTAAGGTGCGGAGAGCTAGCGCAGAGTGGCAGTGGAAAGCGGTTAGCCAA
CTGGAGCAAACCAACAATCGCTATGGTTAATGGTTGGTGTTCGGGGGTGCATTTACTCCACT
GGTTGCCTGCGACCTTGCCTTTGCTGATGAGGATGCAAGGTTTGGTTTGGAGGTTGAATTG
GGGAATTCCTCCCGGTGGCGTAGTGTACGGGCACTGGCCGCAACTGTTCCCTCAGAGGGACGC
TTTATACTATATTGACTGGCGAACCTTTTCGACGGTGCACGAGCTGCTGAGATGAGGCTTGT
GAACGAAGCTCTGCCGGCTGACAGACTTCGGGAACGAACCCGAGAGGTTGCTTTGAAACTAGC
TTCTATGAATCAAGTGGTACTTTCATGCAGCTAAGACAGGATATAAGATTGCTCAAGAAATGCC
ATGGGAGCAAGCTGAGGACTATCTGTACGCAAACTGGATCAGTCCCAGTTCCGTGATAAGGC
TGGTGCACGAGCTAAAGGGTTAACACAGTTCCTTGTATCAAAAATCCTATCGGCCAGGCCTTAG
TGCTTCGATCCTGAAAATACCCAGCTTTCTTGTACAAAGTGGT

(iii) pcDNA6.2::35Sp-fcs (35Sp + fcs cassette)

ACAAGTTTGTACAAAAAGCAGGCTCCAGCTTACTCCAAGAATATCAAAGATACAGTCTCAGA
AGACCAAAGGGCTATTGAGACTTTTCAACAAAGGGTAATATCGGGAAAACCTCCTCGGATTCCA
TTGCCAGCTATCTGTCACTTCATCAAAGGACAGTAGAAAAGGAAGGTGGCACCTACAAATG
CCATCATGCGATAAAGGAAAGGCTATCGTTCAAGATGCCTCTGCCGACAGTGGTCCCAAAGAT
GGACCCCAACCCACAAGGAGCATCGTGGAAAAAGAAGACGTTCCAACCACGTCTTCAAAGCAA
GTGGATTGATGTGATATCTCCACTGACGTAAGGGATGACGCACAATCCCACTATCCTTCGACA
ACTTTGTATACAAAAGTTGCCATGAGGAATCAAGGATTAGGATCATGGCCAGTCAGAAGAGAT
AGGATGTCTCCTCATGCCACCGCTGTGCGGCATGGCGGAACAGCCCTGACTTATGCAGAGCTC
AGCAGGCGAGTTGCACGGCTTGCAAATGGCCTCCGAGCTGCTGGGGTGAGACCTGGGGATCGG
GTGGCTTATCTGGGACCTAATCACCCAGCATATCTAGAGACACTATTTGCTTGCGGACAGGCT
GGAGCTGTGTTTGTACCGCTAACTTCCGTCTGGGAGTCCCTGAGCTCGATCACGCCTTGGCT
GACTCAGGCGCTAGCGTACTTATCCATACTCCGGAACATGCAGAACTGTGCGAGCATTGGCA
GCTGGGAGATTGCTACGAGTTCCCGCCGGAGAGTTAGACGCAGCAGATGATGAGCCGCCAGAT
CTCCCGTTGGACTTGACGATGTCTGCTTGCTTATGTACACTTCTGGAAGTACAGGAAGGCCCT
AAGGGCGCTATGTTGACTCATGGAAATTTGACTTGGAAATTGCGTTAATGTACTTGTGGAGACG
GACTTGGCATCTGATGAGAGGGCACTAGTTGCTGCTCCCTTTTTTACGCCCGCAGCTCTTGGA
ATGGTTTGCCTTCCGACACTTCTCAAAGGAGGGACAGTTATACTTCATTCAGCATTTCGATCCT
GGGGCCGTTCTTAGTGCTGTGCGAGCAAGAAAGGGTTACGCTCGTCTTTGGAGTACCAACTATG
TATCAGGCAATAGCTGCTCATCCACGATGGAGAAGTGCTGACCTTTCAAGTTAAGGACTCTG
TTGTGTGGCGGCGCACCAGTTCCTGCTGACCTAGCATCCCAGATACCTCGATAGAGGTTTGGCA
TTTGTGCAAGGATATGGCATGACCGAGGCAGCTCCTGGTGTCTAGTGCTAGATAGAGCTCAC
GTCGCAGAGAAAATAGGGAGCGCTGGGGTCCCTTCTTCTTACTGATGTACGGCTGGCAGGA
CCATCTGGGGAGCCGGTTCCTCCCGGAGAGAAAGGCGAGATAGTCGTAGTGGACCTAATGTT
ATGAAAGTTATTGGGGACGTCAGAAGCAACTGCTGAAGTTCTGAGGATGTTGGTTCCAT
AGTGGAGACGTTGCCACAGTTGATGGTGACGGTTATTTTACGTTGTGGATAGGCTTAAAGAT
ATGATCATTAGTGGCGGAGAAAATATTTATCCTGCTGAGGTCGAAAACGAACTATATGGTTAC
CCTGGAGTTGAAGCATGTGCAGTGATTGGAGTTCCTGATCCTAGATGGGGTGAAGTAGGAAAAG
GCAGTCGTGGTTCCTGCAGATGGTTCTCGGATCGATGGGGATGAATTACTTGCTGGCTGCGT
ACCCGATTGGCTGGATACAAAGTTCCAAAGTCTGTGGAATTTACGGATAGGTTGCCACAACA
GGCTCAGGAAAATATTGAAGGGCGAAGTTCGTAGGAGATTCCGGTTAGCATCACCACCACCAT
CACTACCCAGCTTTCTTGTACAAAGTGGT

(iv) pcDNA6.2::NOSp-ech (NOSp + ech cassette)

ACGCGGGACAAGCCGTTTTACGTTTGGAACTGACAGAACC GCAACGATTGAAGGAGCCACTCA
GCCGCGGGTTTTCTGGAGTTTAAATGAGCTAAGCACATACGTCAGAAACCATTATTGCGCGTTCA
AAAGTCGCCTAAGGTCATATCAGCTAGCAAATATTTCTTGTCAA AAAATGCTCCACTGACGTT
CCATAAATTCCCCTCGGTATCCAATTAGAGTCTCATATTCACTCTCAATCGGATCCAATAGGA
TCCATGTCAACGGCTGTTGGGAACGGGAGAGTTAGAACAGAGCCTTGGGGTGAGACTGTTCTG
GTGGAGTTTGACGAAGGCATCGCATGGGTTATGCTTAAACAGACCTGATAAACGAAATGCTATG
AATCCAAC TTTAAATGATGAAATGGTCAGGGTGCTAGATCATCTCGAGGGAGATGATCGTTGC
AGGGTGCTTGTCTGACAGGGGCTGGAGAATCATTTTCCGCCGGTATGGATCTAAAGGAGTAC
TTCAGAGAAGTGGATGCTACTGGAAGTACTGCCGTTCAAATTAAGGTGCGGAGAGCTAGCGCA
GAGTGGCAGTGAAGCGGTTAGCCA ACTGGAGCAAACCAACAATCGCTATGGTTAATGGTTGG
TGTTTTCGGGGGTGCATTTACTCCACTGGTTGCCTGCGACCTTGCCTTTGCTGATGAGGATGCA
AGGTTTGGTTT GAGCGAGGTGAATTGGGGAATTCCTCCCGGTGGCGTAGTGTCACGGGCACTG
GCCGCAACTGTTCTCAGAGGGACGCTTTATACTATATTATGACTGGCGAACCTTTTCGACGGT
CGACGAGCTGCTGAGATGAGGCTTGTGAACGAAGCTCTGCCGGCTGACAGACTTCGGGAACGA
ACCCGAGAGGTTGCTTTGAAACTAGCTTCTATGAATCAAGTGGTACTTTCATGCAGCTAAGACA
GGATATAAGATTGCTCAAGAAATGCCATGGGAGCAAGCTGAGGACTATCTGTACGCAAAA ACTG
GATCAGTCCCAGTTCGCTGATAAGGCTGGTGCACGAGCTAAAGGGTTAACACAGTTCCTTGAT
CAAAAATCCTATCGGCCAGGCCTTAGTGCTTTTCGATCCTGAAAACATCACCACCACCATCAC
TAGCACC GGTCGGTCTCA

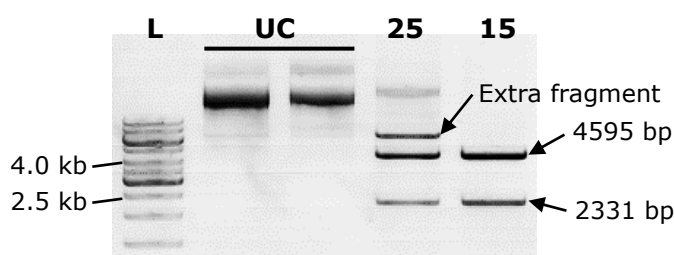
(v) pcDNA6.2::35Sp-VpVAN (35Sp + VpVAN cassette)

CTGCAGTACTCCAAGAATATCAAAGATACAGTCTCAGAAGACCAAAGGGCTATTGAGACTTTT
CAACAAAGGGTAATATCGGGAAACCTCCTCGGATTCCATTGCCCAGCTATCTGTCACTTCATC
AAAAGGACAGTAGAAAAGGAAGGTGGCACCTACAAATGCCATCATTGCGATAAAGGAAAGGCT
ATCGTTCAAGATGCCTCTGCCGACAGTGGTCCCAAAGATGGACCCCCACCCACAAGGAGCATC
GTGGAAAAGAAGACGTTCCAACCACGTCTTCAAAGCAAGTGGATTGATGTGATATCTCCACT
GACGTAAGGGATGACGCACAATCCCACTATCCTTCGATGGCAGCTAAGCTCCTCTTCTCCTA
CTCTTCCTGGTCTCCGCCCTCTCCGTCGCGCTCGCCGGTTTCGAAGAAGACAATCCAATCCGG
TCCGTTACACAAAGGCCTGACTCGATTGAGCCTGCCATCCTCGGCGTCCTTGGCAGTTGCCGC
CACGCCTTCCACTTCGCACGGTTCGCCCCGAGGTACGGGAAGAGCTACGGATCGGAGGAGGAG
ATCAAGAAGAGGTTCCGGATCTTCGTGGAGAATCTAGCGTTTATCCGGTCCACTAATCGGAAG
GATCTGTTCGTATACCCTAGGAATCAACCAATTCGCCGACCTGACCTGGGAGGAATTCGGACC
AATCGCCTTGGTGC GGCGCAGA ACTGCTCGGCGACTGCGCATGGAAACCACCGGTTTGTTCGAT
GGCGTGCTTCCTGTAACGAGGGATTGGAGGGAGCAAGGGATAGTGAGCCCTGTAAAGGACCAA
GGAAGCTGTGGATCTTGCTGGACTTTTCAGTACTACTGGAGCACTAGAGGCTGCATATACACAG
CTAACTGGAAAGAGCACATCATTATCTGAACAGCAACTTGTGGACTGTGCCTCAGCATTCAAT
AACTTTGGATGCAATGGAGGTTTGCCTTCCCAAGCCTTTGAATACGTTAAGTACAATGGAGGC
ATCGACACAGAACAGACTTATCCATACCTTGGTGTCAATGGTATCTGCAACTTCAAGCAGGAG
AATGTTGGTGTCAAGGTCATTGATTTCGATAAACATCACCCCTGGGTGCTGAGGATGAGTTGAAG
CATGCAGTGGGCTTGGTGCCTCCAGTTAGCGTTGCATTTGAGGTTGTGAAAGGTTTCAATCTG
TACAAGAAAGGTGTATACAGCAGTGACACCTGTGGAAGAGATCCAATGGATGTGAACCACGCA
GTTCTTGCCGTCGGTTATGGAGTCGAGGACGGGATTCCTTATTGGCTCATCAAGA ACTCATGG
GGTACAAATTGGGGTGACAATGGCTACTTTAAGATGGA ACTCGGCAAGA ACATGTGTGGTGT
GCAACTTGCGCATCTTATCCCATTGTGGCTGTGGGAAAGCCAATTCCAATCCACTTCTTGGA
CTTGATTCTACTGGATCC

(vi) pHBT12K::35Sp-VpVAN (35Sp + VpVAN cassette)

```
AAGGCTCGAGTACTCCAAGAATATCAAAGATACAGTCTCAGAAGACCAAAGGGCTATTGAGAC
TTTTCAACAAAGGGTAATATCGGGAAACCTCCTCGGATTCCATTGCCAGCTATCTGTCACTT
CATCAAAAGGACAGTAGAAAAGGAAGGTGGCACCTACAAATGCCATCATTGCGATAAAGGAAA
GGCTATCGTTCAAGATGCCTCTGCCGACAGTGGTCCCAAAGATGGACCCCCACCCACAAGGAG
CATCGTGGAAAAAGAAGACGTTCCAACCACGTCTTCAAAGCAAGTGGATTGATGTGATATCTC
CACTGACGTAAGGGATGACGCACAATCCCACACTATCCTTCGATGGCAGCTAAGCTCCTTCTT
CCTACTCTTCCCTGGTCTCCGCCCTCTCCGTCGCGCTCGCCGGTTTTCAAGAAGACAATCCAAT
CCGGTCCGTTACACAAAGGCCTGACTCGATTGAGCCTGCCATCCTCGGCGTCTTTGGCAGTTG
CCGCCACGCTTCCACTTCGCACGGTTCGCCCAGGTACGGGAAGAGCTACGGATCGGAGGA
GGAGATCAAGAAGAGGTTCCGGATCTTCGTGGAGAATCTAGCGTTTATCCGGTCCACTAATCG
GAAGGATCTGTCTATACCCTAGGAATCAACCAATTCGCCGACCTGACCTGGGAGGAATTCCG
GACCAATCGCCTTGGTGCGGCGCAGAACTGCTCGGCGACTGCGCATGGAAACCACCGGTTTGT
CGATGGCGTGCTTCCCTGTAACGAGGGATTGGAGGGAGCAAGGGATAGTGAGCCCTGTAAAGGA
CCAAGGAAGCTGTGGATCTTGCTGGACTTTCAGTACTACTGGAGCACTAGAGGCTGCATATAC
ACAGCTAACTGGAAAGAGCACATCATTATCTGAACAGCAACTTGTGGACTGTGCCTCAGCATT
CAATAACTTTGGATGCAATGGAGGTTTGCCTTCCCAAGCCTTTGAATACGTTAAGTACAATGG
AGGCATCGACACAGAACAGACTTATCCATACCTTGGTGTCAATGGTATCTGCAACTTCAAGCA
GGAGAATGTTGGTGTCAAGGTCATTGATTGATAAACATCACCCCTGGGTGCTGAGGATGAGTT
GAAGCATGCAGTGGGCTTGGTGCCTCCAGTTAGCGTTGCATTTGAGGTTGTGAAAGGTTTCAA
TCTGTACAAGAAAGGTGTATACAGCAGTGACACCTGTGGAAGAGATCCAATGGATGTGAACCA
CGCAGTTCTTGCCGTCGGTTATGGAGTCGAGGACGGGATTCCTTATTGGCTCATCAAGAACTC
ATGGGGTACAAATTGGGGTGACAATGGCTACTTTAAGATGGAACCTCGGCAAGAACATGTGTGG
TGTTGCAACTTGCGCATCTTATCCCATTGTGGCTGTGTAGGGAAAGCCAATTCCAAATCCACT
TCTTGGACTTGATTCTACTGCGAGCTCAACC
```

F. Gel electrophoresis diagram showing an extra band resulting from the star activity of *BbsI*



The occurrence of star activity in 25-cycle RE digestion of pHBT12K with *BbsI*, giving an extra fragment in the digestion product. Star activity did not occur at 15-cycle digestion with *BbsI* and the expected fragments of 4595 bp and 2331 bp were observed. L: GeneRuler 1kb DNA ladder, UC: Undigested pHBT12K, 25: pHBT12K after 25-cycle digestion. 15: pHBT12K after 15-cycle digestion.

G. Biolistic optimisation results

(i) Number of transformants obtained and the highest achievable GFP intensities across the parameters tested

Microcarrier size (μm)	Target distance (cm)	He pressure (psi)	Replicate 1		Replicate 2		Replicate 3	
			No. of transformant	GFP intensity	No. of transformant	GFP intensity	No. of transformant	GFP intensity
0.6	3	900	0	-	0	-	0	-
		1100	0	-	0	-	0	-
		1350	0	-	0	-	0	-
	6	900	0	-	0	-	0	-
		1100	0	-	1	10.11	1	9.57
		1350	1	17.54	0	-	1	13.42
	9	900	0	-	0	-	0	-
		1100	0	-	0	-	0	-
		1350	1	13.04	0	-	0	-
1.0	3	900	0	-	0	-	0	-
		1100	0	-	0	-	0	-
		1350	0	-	0	-	0	-
	6	900	0	-	0	-	0	-
		1100	1	18.89	0	-	1	15.73
		1350	4	39.15	2	44.67	1	25.25
	9	900	0	-	0	-	0	-
		1100	0	-	1	19.77	1	21.38
		1350	2	10.90	2	12.34	0	-
1.6	3	900	0	-	0	-	0	-
		1100	0	-	0	-	0	-
		1350	0	-	0	-	0	-
	6	900	0	-	0	-	0	-
		1100	3	42.51	1	36.42	2	30.11
		1350	8	87.63	5	91.43	7	74.78
	9	900	0	-	0	-	0	-
		1100	3	14.78	0	-	3	10.03
		1350	5	17.62	3	14.59	1	15.57

(ii) Accumulated analysis of deviance by logistic regression within groups and between groups of microcarrier size, target distance and He pressure.

Comparison of parameters	Mean number of transformants	Accumulated analysis of deviance		
		Degree of freedom	Mean deviance	F probability
<i>Within groups</i>				
Microcarrier size (μm)		2	17.466	<0.001
0.6	0.185 ^b			
1.0	0.556 ^{a,b}			
1.6	1.519 ^a			
Target distance (cm)		2	27.636	<0.001
3	0.00 ^b			
6	1.444 ^a			
9	0.815 ^{a,b}			
He pressure (psi)		2	31.029	<0.001
900	0.000 ^b			
1100	0.667 ^{a,b}			
1350	1.593 ^a			
<i>Between groups</i>				
Microcarrier size and target distance	0.753	4	0.174	0.816
Microcarrier size and He pressure	0.753	4	0.087	0.941
Target distance and He pressure	0.753	4	0.259	0.681
Microcarrier size, target distance and He pressure	0.753	8	0.236	0.830

Mean values with the same superscript letters are not significantly different at $p=0.05$ within their respective groups, where F probability <0.001

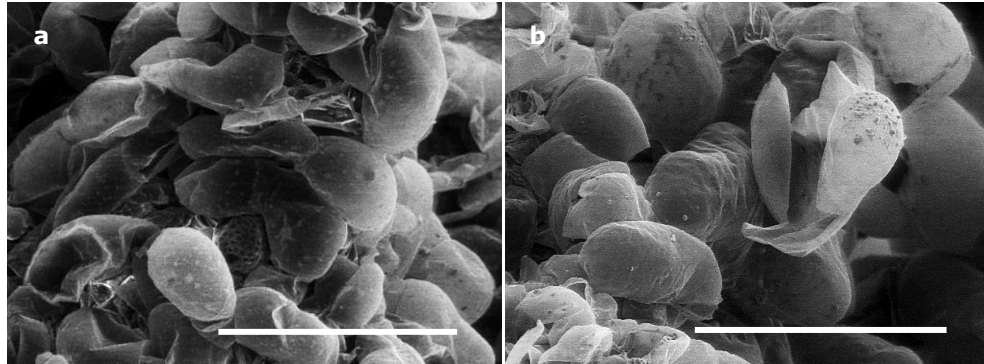
H. qPCR primer sequences

Gene symbol	Primer sequence (5' – 3' length)	Amplicon length (bp)
Reference genes		
<i>ACT</i>	For TGTTATGGTAGGGATGGGTC (20) Rev TTCTCTCTATTTGCCTTGGG (20)	228
<i>UBI-1</i>	For AAGGAAATGTGTGTCTCAAC (20) Rev TCCAAATGCCAAACTTCTAG (20)	278
<i>GAPDH</i>	For ATGATGATGTGAAAGCAGCG (20) Rev TTTCAACTGGTGGCTGCTAC (20)	276
<i>B-TUB</i>	For GAGGGTGAGTGAGCAGTTC (19) Rev CTCATCGTCATCTGCTGTC (20)	167
Adapted from: Wan <i>et al.</i> (2011). Identification of reference genes for reverse transcription quantitative real-time PCR normalization in pepper (<i>Capsicum annuum</i> L.). <i>Biochemical and Biophysical Research Communications</i> . 416: 24–30.		
Target genes		
<i>VpVAN</i>	For AGTTCTTGCCGTCGGTTATG (20) Rev CACAGCCACAATGGGATAAGA (21)	160
<i>fcs</i>	For GGACCTAATCACCCAGCATATC (22) Rev GCATGTTCCGGAGTATGGATAA (22)	155
<i>ech</i>	For TTGGGAACGGGAGAGTTAGA (20) Rev GATCTAGCACCTGACCATTTC (22)	150
Designed using: IDT PrimerQuest Tool http://sg.idtdna.com/PrimerQuest/Home/Index?Display=AdvancedParams . qPCR setting: amplicon size min 100, opt 150, max 200		

I. Mean Cq values and calculations of ΔCq , $\Delta\Delta Cq$ and $2^{-\Delta\Delta Cq}$ for the quantification of relative expression levels

Sample	Target / Reference gene	Cq mean	ΔCq	$\Delta\Delta Cq$	$2^{-\Delta\Delta Cq}$
FcsEch	<u>Target genes</u>				
	<i>fcs</i>	13.54	-7.77	1.25	0.42
	<i>ech</i>	7.54	-14.03	-5.02	32.37
	<u>Reference genes</u>				
	<i>ACT*UBI-1</i> (normalise <i>fcs</i>)	21.30			
	<i>ACT*UBI-1</i> (normalise <i>ech</i>)	21.58			
Fcs	<u>Target genes</u>				
	<i>fcs</i>	13.28	-7.82	1.20	0.44
	<u>Reference genes</u>				
	<i>ACT*UBI-1</i>	21.10			
Ech	<u>Target genes</u>				
	<i>ech</i>	7.76	-16.05	-7.04	131.33
	<u>Reference genes</u>				
	<i>ACT*UBI-1</i>	23.81			
pcVAN	<u>Target genes</u>				
	<i>VpVAN</i>	12.91	-9.02	0.00	1.00
	<u>Reference genes</u>				
	<i>ACT*UBI-1</i>	21.93			
pHVAN	<u>Target genes</u>				
	<i>VpVAN</i>	9.29	-12.09	-3.07	8.42
	<u>Reference genes</u>				
	<i>ACT*UBI-1</i>	21.39			
Neg	<u>Target genes</u>				
	<i>fcs</i>	-	-	-	0.00
	<i>ech</i>	-	-	-	0.00
	<i>VpVAN</i>	-	-	-	0.00
	<u>Reference genes</u>				
	<i>ACT*UBI-1</i> (normalise <i>fcs</i>)	21.06			
	<i>ACT*UBI-1</i> (normalise <i>ech</i>)	21.36			
	<i>ACT*UBI-1</i> (normalise <i>VpVAN</i>)	21.47			

J. Scanning electron microscopy (SEM) images of compact and friable calli of *C. frutescens*



SEM images of (a) compact and (b) friable calli of *C. frutescens* under 500 \times magnification. Note that the parenchymatous cell surfaces of both callus types are smooth and lacking fibrillar network. Scale bar represents 200 μm (Original).

REFERENCES

- Abraham, D.J., Mehanna, A.S., Wireko, F.C., Whitney, J., Thomas, R.P. & Orringer, E.P., 1991. Vanillin, a potential agent for the treatment of sickle cell anemia. *Blood*, 77, 1334–1341.
- Abumhadi, N., Trifonova, A., Takumi, S., Nakamura, C., Todorovska, E., Getov, L., Christov, N. & Atanassov, A., 2001. Development of the particle inflow gun and optimizing the particle bombardment method for efficient genetic transformation in mature embryos of cereals. *Biotechnology and Biotechnological Equipment*, 15, 87–96.
- Achterholt, S., Priefert, H. & Steinbuchel, A., 2000. Identification of *Amycolatopsis* sp. strain HR167 genes, involved in the bioconversion of ferulic acid to vanillin. *Applied Microbiology and Biotechnology*, 54, 799–807.
- Agrawal, S., Chandra, N. & Kothari, S.L., 1989. Plant regeneration in tissue cultures of pepper (*Capsicum annuum* L. cv. Mathania). *Plant Cell, Tissue and Organ Culture*, 16, 47–55.
- Aida, M., Beis, D., Heidstra, R., Willemsen, V., Blilou, I., Galinha, C., Nussaume, L., Noh, Y., Amasino, R. & Scheres, B., 2004. The *PLETHORA* genes mediate patterning of the *Arabidopsis* root stem cell niche. *Cell*, 119, 109–120.
- Al-allaf, F.A., Tolmachov, O.E., Zambetti, L.P., Tchetchelnitski, V. & Mehmet, H., 2013. Remarkable stability of an instability-prone lentiviral vector plasmid in *Escherichia coli* Stbl3. *3 Biotech*, 3, 61–70.
- Aloni, R., Aloni, E., Langhans, M. & Ullrich, C.I., 2006. Role of cytokinin and auxin in shaping root architecture: regulating vascular differentiation, lateral root initiation, root apical dominance and root gravitropism. *Annals of Botany*, 97, 883–893.
- American Type Culture Collection (ATCC), 2012. *Amycolatopsis* sp. (ATCC® 39116™). Available at: <http://www.atcc.org/products/all/39116.aspx>.
- Amersham Biosciences, 1999. Reversed phase chromatography: Principles and methods. *Note 18-1134-16*, Edition AA.
- An, G., Costa, M.A. & Ha, S.-B., 1990. Nopaline synthase promoter is wound inducible and auxin inducible. *The Plant Cell*, 2, 225–233.
- Anandalakshmi, R., Pruss, G.J., Ge, X., Marathe, R., Mallory, A.C., Smith, T.H. & Vance, V.B., 1998. A viral suppressor of gene silencing in plants. *Proceedings of the National Academy of Sciences of the United States of America*, 95, 13079–13084.
- Antai, S.P., Crawford, D.L. & Crawford, D.O.N.L., 1981. Degradation of softwood, hardwood, and grass lignocelluloses by two *Streptomyces* strains. *Applied and Environmental Microbiology*, 42, 378–380.
- Aoyama, T. & Oka, A., 2003. Cytokinin signal transduction in plant cells. *Journal of Plant Research*, 116, 221–231.
- Armbruster, D.A. & Pry, T., 2008. Limit of blank, limit of detection and limit of quantitation. *The Clinical Biochemistry Reviews*, 29, S49–52.

- von Arnold, S., Sabala, I., Bozhkov, P., Dyachok, J. & Filonova, L., 2002. Developmental pathways of somatic embryogenesis. *Plant Cell, Tissue and Organ Culture*, 69, 233–249.
- Asma, B.M., 2008. Determination of pollen viability, germination ratios and morphology of eight apricot genotypes. *African Journal of Biotechnology*, 7, 4269–4273.
- Aulinger, I.E., Peter, S.O., Schmid, J.E. & Stamp, P., 2003. Gametic embryos of maize as a target for biolistic transformation: comparison to immature zygotic embryos. *Plant Cell Reports*, 21, 585–591.
- Azeez, S., 2008. Vanilla. In V. A. Parthasarathy, B. Chempakam, & T. J. Zachariah, eds. *Chemistry of Spices*. Oxfordshire: CAB International, pp. 287–311.
- Baldwin, I.T. & Callahan, P., 1993. Autotoxicity and chemical defense: nicotine accumulation and carbon gain in solanaceous plants. *Oecologia*, 94, 534–541.
- Ball, E., 1946. Development in sterile culture of stem tips and subjacent regions of *Trapaecolum majus* L. and of *Lupinus albus* L. *American Journal of Botany*, 33, 301–318.
- Banerjee, A.K., Agrawal, D.C., Nalawade, S.M., Hazra, S. & Krishnamurthy, K. V., 2003. Multiple shoot induction and plant regeneration from embryo axes of six cultivars of *Gossypium hirsutum*. *Biologia Plantarum*, 47, 433–436.
- Banno, H., Ikeda, Y., Niu, Q.-W. & Chua, N.-H., 2001. Overexpression of *Arabidopsis ESR1* induces initiation of shoot regeneration. *The Plant Cell*, 13, 2609–2618.
- Bardini, M., Labra, M., Winfield, M., Sala, F., Celoria, V., Biologia, D. & Generale, B., 2003. Antibiotic-induced DNA methylation changes in calluses of *Arabidopsis thaliana*. *Plant Cell, Tissue and Organ Culture*, 72, 157–162.
- Barghini, P., Di Gioia, D., Fava, F. & Ruzzi, M., 2007. Vanillin production using metabolically engineered *Escherichia coli* under non-growing conditions. *Microbial Cell Factories*, 6, 13.
- Barile, M.F., 1973. Mycoplasmal contamination of cell cultures: Mycoplasma-virus-cell culture interactions. In J. Fogh, ed. *Contamination in Tissue Culture*. New York: Academic Press, pp. 131–171.
- Barkovich, M., 2017. High performance liquid chromatography. *LibreTexts: Chemistry*. Available at: https://chem.libretexts.org/Core/Analytical_Chemistry/Instrumental_Analysis/Chromatography/High_performance_liquid_chromatography.
- Baumann, H. & Pigman, W., 1957. Naturally occurring glycosides and glycosidases. In W. Pigman, ed. *The Carbohydrates: Chemistry and Biochemistry Physiology*. New York: Academic Press, pp. 536–601.

- Becerra-Herrera, M., Sánchez-Astudillo, M., Beltrán, R. & Sayago, A., 2014. Determination of phenolic compounds in olive oil: New method based on liquid-liquid micro extraction and ultra high performance liquid chromatography-triple-quadrupole mass spectrometry. *Food Science and Technology*, 57, 49–57.
- Begas, E., Papandreou, C., Tsakalof, A., Daliani, D., Papatsibas, G. & Asproдини, E., 2014. Simple and reliable HPLC method for the monitoring of methotrexate in osteosarcoma patients. *Journal of Chromatographic Science*, 52, 590–595.
- Beltrán, J., Jaimes, H., Echeverry, M., Ladino, Y., López, D., Duque, M.C., Chavarriaga, P. & Tohme, J., 2009. Quantitative analysis of transgenes in cassava plants using real-time PCR technology. *In Vitro Cellular and Developmental Biology - Plant*, 45, 48–56.
- Bernard, P. & Couturier, M., 1992. Cell killing by the F plasmid CcdB protein involved poisoning of DNA-topoisomerase II complexes. *Journal of Molecular Biology*, 226, 735–745.
- Best, K., Oakes, T., Heather, J.M., Shawe-Taylor, J. & Chain, B., 2015. Computational analysis of stochastic heterogeneity in PCR amplification efficiency revealed by single molecule barcoding. *Scientific Reports*, 5, 14629.
- Betekhtin, A., Rojek, M., Milewska-Hendel, A., Gawecki, R., Karcz, J., Kurczynska, E. & Hasterok, R., 2016. Spatial distribution of selected chemical cell wall components in the embryogenic callus of *Brachypodium distachyon*. *PLoS ONE*, 11, e0167426.
- Betz, J.M., Brown, P.N. & Roman, M.C., 2011. Accuracy, precision, and reliability of chemical measurements in natural products research. *Fitoterapia*, 82, 44–52.
- Bhojwani, S.S. & Razdan, M.K., 1983. *Plant Tissue Culture: Theory and Practice*, Amsterdam: Elsevier B.V.
- Billinton, N. & Knight, A.W., 2001. Seeing the wood through the trees: A review of techniques for distinguishing green fluorescent protein from endogenous autofluorescence. *Analytical Biochemistry*, 197, 175–197.
- Bio-Rad, Biolistic Delivery Systems, Bulletin 5443.
- Bird, I.M., 1989. High performance liquid chromatography: principles and clinical applications. *BMJ*, 299, 783–787.
- Blechl, A.E. & Jones, H.D., 2009. Transgenic applications in wheat improvement. In B. F. Carver, ed. *Wheat: Science and Trade*. Iowa: Wiley-Blackwell, pp. 397–436.
- Bloor, A.E. & Cranenburgh, R.M., 2006. An efficient method of selectable marker gene excision by Xer recombination for gene replacement in bacterial chromosomes. *Applied and Environmental Microbiology*, 72, 2520–2525.
- Böhmer, P., Meyer, B. & Jacobsen, H.-J., 1995. Thidiazuron-induced high frequency of shoot induction and plant regeneration in protoplast derived pea callus. *Plant Cell Reports*, 15, 26–29.

- Bois, J.F., Winkel, T., P, L.J., Raffailac, J.P. & Rocheteau, A., 2006. Response of some Andean cultivars of quinoa (*Chenopodium quinoa* Willd.) to temperature: Effects on germination, phenology, growth and freezing. *European Journal of Agronomy*, 25, 299–308.
- Borlaug, N.E., 1983. Contributions of conventional plant breeding to food production. *Science*, 219, 689–693.
- Boudolf, V., Lammens, T., Boruc, J., Van Leene, J., Van Den Daele, H., Maes, S., Van Isterdael, G., Russinova, E., Kondorosi, E., Witters, E., De Jaeger, G., De Veylder, L. & Inz, D., 2009. CDKB1;1 forms a functional complex with CYCA2;3 to suppress endocycle onset. *Plant Physiology*, 150, 1482–1493.
- Brand, U., Grünewald, M., Hobe, M. & Simon, R., 2002. Regulation of *CLV3* expression by two homeobox genes in *Arabidopsis*. *Plant Physiology*, 129, 565–575.
- Brochado, A.R., Matos, C., Møller, B.L., Hansen, J., Mortensen, U.H. & Patil, K.R., 2010. Improved vanillin production in baker's yeast through in silico design. *Microbial Cell Factories*, 9, 84.
- Brown, D.C.W., Finstad, K.I. & Watson, E.M., 1995. Somatic embryogenesis in herbaceous dicots. In T. A. Thorpe, ed. *In Vitro Embryogenesis in Plants*. Dordrecht: Springer Netherlands, pp. 345–415.
- Buj, R., Iglesias, N., Planas, A.M. & Santalucía, T., 2013. A plasmid toolkit for cloning chimeric cDNAs encoding customized fusion proteins into any Gateway destination expression vector. *BMC Molecular Biology*, 14, 18.
- Burri, J., Graf, M., Lambelet, P. & Loliger, J., 1989. Vanillin: more than a flavoring agent - a potent antioxidant. *Journal of the Science of Food and Agriculture*, 48, 49–56.
- Burt, J., 2005. Farmnote: Growing capsicums and chillies, No. 64/99, ISSN 0726-934X.
- Bustin, S.A., Beaulieu, J.-F., Huggett, J., Jaggi, R., Kibenge, F.S.B., Olsvik, P.A., Penning, L.C. & Toegel, S., 2010. MIQE précis: Practical implementation of minimum standard guidelines for fluorescence-based quantitative real-time PCR experiments. *BMC Molecular Biology*, 11, 74–78.
- Bustin, S.A., Benes, V., Garson, J.A., Hellemans, J., Huggett, J., Kubista, M., Mueller, R., Nolan, T., Pfaffl, M.W. & Shipley, G.L., 2009. The MIQE Guidelines: Minimum information for publication of quantitative real-time PCR. *Clinical Chemistry*, 55, 611–622.
- Campbell, T.N. & Choy, F.Y.M., 2001. The effect of pH on green fluorescent protein: a brief review. *Molecular Biology Today*, 2, 1–4.
- Cankar, K., Stebih, D., Dreo, T., Zel, J. & Gruden, K., 2006. Critical points of DNA quantification by real-time PCR - effects of DNA extraction method and sample matrix on quantification of genetically modified organisms. *BMC Biotechnology*, 6, 37.

- Cao, D., Hussain, A., Cheng, H. & Peng, J., 2005. Loss of function of four *DELLA* genes leads to light- and gibberellin-independent seed germination in *Arabidopsis*. *Planta*, 223, 105–113.
- Carlson, A., Letarte, J., Chen, J. & Kasha, K., 2001. Visual screening of microspore-derived transgenic barley (*Hordeum vulgare* L.) with green-fluorescent protein. *Plant Cell Reports*, 20, 331–337.
- Carsono, N. & Yoshida, T., 2008. Transient expression of green fluorescent protein in rice calluses: optimization of parameters for Helios gene gun device. *Plant Production Science*, 11, 88–95.
- Cassells, A.C., 2012. Pathogen and biological contamination management in plant tissue culture: Phytopathogens, vitro pathogens, and vitro pests. *Plant Cell Culture Protocols*, 877, 57–80.
- Castillo, U.F., Strobel, G.A., Mullenberg, K., Condrón, M.M., Teplow, D.B., Folgiano, V., Gallo, M., Ferracane, R., Mannina, L., Viel, S., Robison, R., Porter, H. & Jensen, J., 2006. Munumbicins E-4 and E-5: novel broad-spectrum antibiotics from *Streptomyces* NRRL 3052. *FEMS Microbiology Letters*, 255, 296–300.
- Castro-Concha, L.A., Tuyub-Che, J., Moo-Mukul, A., Vazquez-Flota, F.A. & Miranda-Ham, M.L., 2014. Antioxidant capacity and total phenolic content in fruit tissues from accessions of *Capsicum chinense* Jacq. (Habanero pepper) at different stages of ripening. *The Scientific World Journal*, 809073.
- Cazes, J., 1997. Basic principles of HPLC and HPLC system troubleshooting. *Instrumentation Science and Technology*, 25, 367.
- Cerruti, P. & Alzamora, S.M., 1996. Inhibitory effects of vanillin on some food spoilage yeasts in laboratory media and fruit purees. *International Journal of Food Microbiology*, 29, 379–386.
- Cerruti, P., Alzamora, S.M. & Vidales, S.L., 1997. Vanillin as an antimicrobial for producing shelf-stable strawberry puree. *Journal of Food Science*, 62, 608–610.
- Chan, V., Dreolini, L.F., Flintoff, K.A., Lloyd, S.J. & Mattenley, A.A., 2002. The effect of increasing plasmid size on transformation efficiency in *Escherichia coli*. *Journal of Experimental Microbiology and Immunology*, 2, 207–223.
- Chapa-Oliver, A.M. & Mejía-Teniente, L., 2016. Capsaicin: From plants to a cancer-suppressing agent. *Molecules*, 21, 931.
- Chee, J.Y. & Chin, C.F., 2015. Gateway cloning technology: Advantages and drawbacks. *Cloning and Transgenesis*, 4, 138–140.
- Chee, M.J.Y., Lycett, G.W., Khoo, T.-J. & Chin, C.F., 2016. Bioengineering of the plant culture of *Capsicum frutescens* with vanillin synthase gene for the production of vanillin. *Molecular Biotechnology*, 59, 1–8.
- Chen, F., Dahal, P. & Bradford, K.J., 2001. Two tomato expansin genes show divergent expression and localization in embryos during seed development and germination. *Plant Physiology*, 127, 928–936.

- Chen, H., 2014. *Biotechnology of Lignocellulose: Theory and Practice*, Dordrecht: Chemical Industry Press, Springer.
- Cheng, W.-Y., Hsiang, C.-Y., Bau, D.-T., Chen, J.-C., Shen, W.-S., Li, C.-C., Lo, H.-Y., Wu, S.-L., Chiang, S.-Y. & Ho, T.-Y., 2007. Microarray analysis of vanillin-regulated gene expression profile in human hepatocarcinoma cells. *Pharmacological Research*, 56, 474–482.
- Chinn, M.S., Sharma-Shivappa, R.R. & Cotter, J.L., 2011. Solvent extraction and quantification of capsaicinoids from *Capsicum chinense*. *Food and Bioproducts Processing*, 89, 340–345.
- Chitravathi, K., Chauhan, O.P. & Raju, P.S., 2014. Postharvest shelf-life extension of green chillies (*Capsicum annuum* L.). *Postharvest Biology and Technology*, 92, 146–148.
- Chiu, W., Niwa, Y., Zeng, W., Hirano, T., Kobayashi, H. & Sheen, J., 1996. Engineered GFP as a vital reporter in plants. *Current Biology*, 6, 325–330.
- Choffe, K.L., Murch, S.J. & Saxena, P.K., 2000. Regeneration of *Echinacea purpurea*: Induction of root organogenesis from hypocotyl and cotyledon explants. *Plant Cell, Tissue and Organ Culture*, 62, 227–234.
- Christou, P., 1991. Genetic transformation of crop plants using microprojectile bombardment. *The Plant Journal*, 2, 275–281.
- Cocking, E.C., 1960. A method for the isolation of plant protoplasts and vacuoles. *Nature*, 187, 927–929.
- Cockroft, C.E., den Boer, B.G.W., Sandra Healy, J.M. & Murray, J.A.H., 2000. Cyclin D control of growth rate in plants. *Nature*, 405, 575–579.
- Coffman, V.C. & Wu, J.-Q., 2014. Every laboratory with a fluorescence microscope should consider counting molecules. *Molecular Biology of the Cell*, 25, 1545–1548.
- Cole, C.N. & Stacy, T.P., 1985. Identification of sequences in the herpes simplex virus thymidine kinase gene required for efficient processing and polyadenylation. *Molecular and Cellular Biology*, 5, 2104–2113.
- Cone, M.C., Yin, X., Grochowski, L.L., Parker, M.R. & Zabriskie, T.M., 2003. The blasticidin S biosynthesis gene cluster from *Streptomyces griseochromogenes*: sequence analysis, organization, and initial characterization. *ChemBioChem*, 4, 821–828.
- Conrad, U. & Fiedler, U., 1998. Compartment-specific accumulation of recombinant immunoglobulins in plant cells: an essential tool for antibody production and immunomodulation of physiological functions and pathogen activity. *Plant Molecular Biology*, 38, 101–109.
- Converti, A., Aliakbarian, B., Dominguez, J.M., Vazquez, G.B. & Perego, P., 2010. Microbial production of biovanillin. *Brazilian Journal of Microbiology*, 41, 519–530.
- Cresswell, R.C., Fowler, M.W., Stafford, A. & Stephan-Sarkissian, G., 2012. Inputs and outputs: Primary substrates and secondary metabolism. In W. G. W. Kurz, ed. *Primary and Secondary Metabolism of Plant Cell Cultures II*. Heidelberg: Springer Science & Business Media, pp. 14–26.

- Croteau, R., Kutchan, T.M. & Lewis, N.G., 2015. Natural products (secondary metabolites). In B. B. Buchanan, W. Gruissem, & R. L. Jones, eds. *Biochemistry and Molecular Biology of Plants*. West Sussex: Wiley Blackwell, pp. 1132–1206.
- Curtis, I.S., 2010. Genetic transformation - *Agrobacterium*. In M. R. Davey & P. Anthony, eds. *Plant Cell Culture: Essential Methods*. West Sussex: John Wiley & Sons, pp. 199–216.
- Dahal, P., Bradford, K.J. & Jones, R.A., 1990. Effects of priming and endosperm integrity on seed germination rates of tomato genotypes: I. Germination at suboptimal temperature. *Journal of Experimental Botany*, 41, 1431–1439.
- Daniell, H. & Dhingra, A., 2002. Multigene engineering: dawn of an exciting new era in biotechnology. *Current Opinion in Biotechnology*, 13, 136–141.
- Danielson, D.C. & Paul, J., 2013. Studying the RNA silencing pathway with the p19 protein. *FEBS Letters*, 587, 1198–1205.
- Davis, J.R., Goodwin, L. a, Woyke, T., Teshima, H., Bruce, D., Detter, C., Tapia, R., Han, S., Han, J., Pitluck, S., Nolan, M., Mikhailova, N., Land, M.L. & Sello, J.K., 2012. Genome sequence of *Amycolatopsis* sp. strain ATCC 39116, a plant biomass-degrading actinomycete. *Journal of bacteriology*, 194, 2396–7.
- Deepak, S.A., Kottapalli, K.R., Rakwal, R., Oros, G., Rangappa, K.S., Iwahashi, H., Masuo, Y. & Agrawal, G.K., 2007. Real-time PCR: Revolutionizing detection and expression analysis of genes. *Current Genomics*, 8, 234–251.
- Delis, M., Garbaczewska, G. & Niemirowicz-Szczytt, K., 2005. Differentiation of adventitious buds from *Capsicum annuum* L. hypocotyls after co-culture with *Agrobacterium tumefaciens*. *Abta Biologica Cracoviensia Series Botanica*, 47, 193–198.
- Demir, I., Ermis, S., Mavi, K. & Matthews, S., 2008. Mean germination time of pepper seed lots (*Capsicum annuum* L.) predicts size and uniformity of seedlings in germination tests and transplant modules. *Seed Science and Technology*, 36, 21–30.
- Dhaliwal, H.S., Ramesar-Fortner, N.S., Yeung, E.C. & Thorpe, T.A., 2003. Competence, determination, and meristemoid plasticity in tobacco organogenesis in vitro. *Canadian Journal of Botany*, 81, 611–621.
- Dickson, R.M., Cubitt, A.B., Tsien, R.Y. & Moerner, W.E., 1997. On/off blinking and switching behavior of single molecules of green fluorescent protein. *Nature*, 388, 355–358.
- Dobberstein, D. & Bunzel, M., 2010. Separation and detection of cell wall-bound ferulic acid dehydrodimers and dehydrotrimers in cereals and other plant materials by reversed phase high-performance liquid chromatography with ultraviolet detection. *Journal of Agriculture and Food Chemistry*, 58, 8927–8935.
- Dong, J.-Z. & Jia, S.-R., 1991. High efficiency plant regeneration from cotyledons of watermelon (*Citrullus vulgaris* Schrad). *Plant Cell Reports*, 9, 559–562.

- Dong, M.W. & Zhang, K., 2014. Ultra-high-pressure liquid chromatography (UHPLC) in method development. *Trends in Analytical Chemistry*, 63, 21–30.
- Dörnenberg, H. & Knorr, D., 1997. Challenges and opportunities for metabolite production from plant cell and tissue cultures. *Food Technology*, 51, 47–54.
- Dotto, G.P., Horiuchi, K. & Zinder, N.D., 1984. The functional origin of bacteriophage f1 DNA replication. Its signals and domains. *Journal of Molecular Biology*, 172, 507–521.
- Ebert, P.R., Ha, S.B. & An, G., 1987. Identification of an essential upstream element in the nopaline synthase promoter by stable and transient assays. *Proceedings of the National Academy of Sciences of the United States of America*, 84, 5745–5749.
- Ekong, C.S., Okon, O.G. & Akpan, G.U., 2014. Effect of different treatment on seed germination and breaking of seed dormancy in *Capsicum annuum* Linn., *Aframomum melegueta* K. Schum. and *Capsicum chinense* Jacq. *International Journal of Research*, 1, 1339–1345.
- Elghabi, Z., Ruf, S. & Bock, R., 2011. Biolistic co-transformation of the nuclear and plastid genomes. *The Plant Journal*, 67, 941–948.
- Engler, C., Kandzia, R. & Marillonnet, S., 2008. A one pot, one step, precision cloning method with high throughput capability. *PLoS ONE*, 3, e3647.
- van den Ent, F. & Lowe, J., 2006. Short note RF cloning: A restriction-free method for inserting target genes into plasmids. *Journal of Biochemical and Biophysical Methods*, 67, 67–74.
- Esposito, L.J., Formanek, K., Kientz, G., Mauger, F., Maureaux, V., Robert, G. & Truchet, F., 1997. Vanillin. *Kirk-Othmer Encyclopedia of Chemical Technology*, 4th Edition, pp.812–825.
- Estrela, C., Estrela, C.R.A., Barbin, E.L., Spanó, J.C.E., Marchesan, M.A. & Pécora, J.D., 2002. Mechanism of action of sodium hypochlorite. *Brazilian Dental Journal*, 13, 113–117.
- Fan, M., Xu, C., Xu, K. & Hu, Y., 2012. LATERAL ORGAN BOUNDARIES DOMAIN transcription factors direct callus formation in *Arabidopsis* regeneration. *Cell Research*, 22, 1169–1180.
- Ferenc, M., 2015. Common lab *E. coli* strains. In Addgene, ed. *Plasmids 101: A Desktop Resource*. Cambridge: Addgene, pp. 27–31. Available at: http://cdn2.hubspot.net/hubfs/306096/Addgene-Plasmids-101-eBook-Second-Edition_Final.pdf?hsCtaTracking=71186a5f-f907-4f26-afd9-df20b881d517%7C21df67f2-0ba5-4750-894f-a439cecc8357&__hstc=246494683.9fea903e7b229259e7cfff49ad734296.1489481781302.148948178130 [Accessed December 18, 2016].
- Finer, J.J., Vain, P., Jones, M.W. & McMullen, M.D., 1992. Development of the particle inflow gun for DNA delivery to plant cells. *Plant Cell Reports*, 11, 323–328.

- Fitch, M.M.M. & Manshardt, R.M., 1990. Somatic embryogenesis and plant regeneration from immature zygotic embryos of papaya (*Carica papaya* L.). *Plant Cell Reports*, 9, 320–324.
- Fleige, C., Hansen, G., Kroll, J. & Steinbüchel, A., 2013. Investigation of the *Amycolatopsis* sp. strain ATCC 39116 vanillin dehydrogenase and its impact on the biotechnical production of vanillin. *Applied and environmental microbiology*, 79, 81–90.
- Fleige, C. & Meyer, F., 2016. Metabolic engineering of the actinomycete *Amycolatopsis* sp. strain ATCC 39116 towards enhanced production of natural vanillin. *Applied and Environmental Microbiology*, 82, 3410–3419.
- Fletcher, S.J., 2014. qPCR for quantification of transgene expression and determination of transgene copy number. In D. Fleury & R. Whitford, eds. *Crop Breeding*. New York: Springer, pp. 213–237.
- Fogh, J., Holmgren, N.B. & Ludovici, P.P., 1971. A review of cell culture contaminations. *In Vitro*, 7, 26–41.
- Food and Agriculture Organization of the United Nations, 2013. Food and Agricultural commodities production / Countries by commodity. *FAOSTAT*. Available at: http://faostat3.fao.org/browse/rankings/countries_by_commodity/E [Accessed December 28, 2015].
- Fouché, J.G. & Jouve, L., 1999. Vanilla planifolia: history, botany and culture in Reunion island. *Agronomie*, 19(8), pp.689–703.
- Frary, A. & Hamilton, C.M., 2001. Efficiency and stability of high molecular weight DNA transformation: An analysis in tomato. *Transgenic Research*, 10, 121–132.
- Friehs, K., 2004. Plasmid copy number and plasmid stability. In T. Scheper, ed. *New Trends and Developments in Biochemical Engineering*. Heidelberg: Springer-Verlag, pp. 47–82.
- Fu, X., Duc, L.T., Fontana, S., Bong, B.B., Tinjuangjun, P., Sudhakar, D., Twyman, R.M. & Kohli, A., 2000. Linear transgene constructs lacking vector backbone sequences generate low-copy-number transgenic plants with simple integration patterns. *Transgenic Research*, 9, 11–19.
- Funk, C. & Brodelius, P., 1990. Phenylpropanoid metabolism in suspension cultures of *Vanilla planifolia* Andr. III. *Plant Physiology*, 94, 95–101.
- Furutani, N. & Hidaka, S., 2004. Efficient production of transgenic soybean using a co-transformation method. *Breeding Science*, 54, 91–98.
- Galinha, C., Hofhuis, H., Luijten, M., Willemsen, V., Blilou, I., Heidstra, R. & Scheres, B., 2007. PLETHORA proteins as dose-dependent master regulators of *Arabidopsis* root development. *Nature*, 449, 1053–1057.
- Gallage, N.J., Hansen, E.H., Kannangara, R., Olsen, C.E., Motawia, M.S., Jørgensen, K., Holme, I., Hebelstrup, K., Grisoni, M. & Møller, B.L., 2014. Vanillin formation from ferulic acid in *Vanilla planifolia* is catalysed by a single enzyme. *Nature Communications*, 5, 4037.

- Gallage, N.J. & Møller, B.L., 2015. Vanillin–Bioconversion and Bioengineering of the Most Popular Plant Flavor and Its De Novo Biosynthesis in the Vanilla Orchid. *Molecular Plant*, 8, 40–57.
- Gamborg, O.L., Murashige, T., Thorpe, T.A. & Vasil, I.K., 1976. Plant tissue culture media. *In Vitro*, 12, 473–478.
- Gayathri, N., Gopalakrishnan, M. & Sekar, T., 2016. Phytochemical screening and antimicrobial activity of *Capsicum chinense* Jacq. *International Journal of Advances in Pharmaceutics*, 5, 12–20.
- Gelvin, S.B., 2000. Agrobacterium and plant genes involved in T-DNA transfer and integration. *Annual Review of Plant Physiology and Plant Molecular Biology*, 51, 223–256.
- Gerson, R. & Homna, S., 1978. Emergence response of the pepper at low soil temperature. *Euphytica*, 27, 151–156.
- Gilardi, P., García-Luque, I. & Serra, M.T., 1998. Pepper mild mottle virus coat protein alone can elicit the *Capsicum* spp. L3 gene-mediated resistance. *Molecular Plant-Microbe Interactions*, 11, 1253–1257.
- Gilardi, P., García-Luque, I. & Serra, M.T., 2004. The coat protein of tobamovirus acts as elicitor of both L2 and L4 gene-mediated resistance in *Capsicum*. *Journal of General Virology*, 85, 2077–2085.
- Glaeser, A. & Heermann, R., 2015. A novel tool for stable genomic reporter gene integration to analyze heterogeneity in *Photobacterium luminescens* at the single-cell level. *BioTechniques*, 59, 74–81.
- Gondo, T., Tsuruta, S., Akashi, R., Kawamura, O. & Hoffmann, F., 2005. Green, herbicide-resistant plants by particle inflow gun-mediated gene transfer to diploid bahiagrass (*Paspalum notatum*). *Journal of Plant Physiology*, 162, 1367–1375.
- Goodwin, J.L., Pastori, G.M., Davey, M.R. & Jones, H.D., 2005. Selectable markers: antibiotic and herbicide resistance. *Methods in Molecular Biology*, 286, 191–202.
- Gotfred-Rasmussen, H., Lund, M., Enemark, H.L., Erlandsen, M. & Petersen, E., 2016. Comparison of sensitivity and specificity of 4 methods for detection of *Giardia duodenalis* in feces: immunofluorescence and PCR are superior to microscopy of concentrated iodine-stained samples. *Diagnostic Microbiology and Infectious Disease*, 84, 187–190.
- Graf, N. & Altenbuchner, J., 2014. Genetic engineering of *Pseudomonas putida* KT2440 for rapid and high-yield production of vanillin from ferulic acid. *Applied Microbiology and Biotechnology*, 98, 137–149.
- Greenbaum, L., Rothmann, C., Lavie, R. & Malik, Z., 2000. Green fluorescent protein photobleaching: a model for protein damage by endogenous and exogenous singlet oxygen. *Biological Chemistry*, 381, 1251–1258.
- Grieneisen, V.A., Xu, J., Marée, A.F., Hogeweg, P. & Scheres, B., 2007. Auxin transport is sufficient to generate a maximum and gradient guiding root growth. *Nature*, 449, 1008–1013.

- Grosser, J.W. & Omer, A.A., 2011. Protoplasts-An increasingly valuable tool in plant research. In R. N. Trigiano & D. J. Gray, eds. *Plant Tissue Culture, Development, and Biotechnology*. Boca Raton: CRC Press, pp. 349–364.
- Grozeva, S., Rodeva, V. & Todorova, V., 2012. In vitro shoot organogenesis in Bulgarian sweet pepper (*Capsicum annuum* L.) varieties. *Electronic Journal of Biology*, 8, 39–44.
- Gualberti, G., Papi, M., Bellucci, L., Ricci, I., Bouchez, D., Camilleri, C., Costantino, P. & Vittorioso, P., 2002. Mutations in the Dof zinc finger genes *DAG2* and *DAG1* influence with opposite effects the germination of *Arabidopsis* seeds. *The Plant Cell*, 14, 1253–1263.
- Gunatilaka, A.L., 2012. Plant natural products. In N. Civjan, ed. *Natural Products in Chemical Biology*. New Jersey: John Wiley & Sons, pp. 3–29.
- Gupta, R. & Chakrabarty, S.K., 2013. Gibberellic acid in plant: Still a mystery unresolved. *Plant Signaling and Behaviour*, 8, e25504.
- Gururaj, H.B., Padma, M.N., Giridhar, P. & Ravishankar, G.A., 2012. Functional validation of *Capsicum frutescens* aminotransferase gene involved in vanillylamine biosynthesis using *Agrobacterium* mediated genetic transformation studies in *Nicotiana tabacum* and *Capsicum frutescens* calli cultures. *Plant Science*, 195, 96–105.
- Hansen, E.H., Møller, B.L., Kock, G.R., Bünner, C.M., Kristensen, C., Jensen, O.R., Okkels, F.T., Olsen, C.E., Motawia, M.S. & Hansen, J., 2009. De novo biosynthesis of vanillin in fission yeast (*Schizosaccharomyces pombe*) and baker's yeast (*Saccharomyces cerevisiae*). *Applied and environmental microbiology*, 75, 2765–2774.
- Hanson, M.R. & Köhler, R.H., 2001. GFP imaging: methodology and application to investigate cellular compartmentation in plants. *Journal of Experimental Botany*, 52, 529–539.
- Hare, P.D. & Chua, N.-H., 2002. Excision of selectable marker genes from transgenic plants. *Nature Biotechnology*, 20, 575–580.
- Harpster, M.H., Townsend, J.A., Jones, J.D.G., Bedbrook, J. & Dunsmuir, P., 1988. Relative strengths of the 35S califlower mosaic virus, 1', 2', and nopaline synthase promoters in transformed tobacco sugarbeet and oilseed rape callus tissue. *Molecular Genetics and Genomics*, 212, 182–190.
- Harris, P.J., 2006. Primary and secondary plant cell walls: A comparative overview. *New Zealand Journal of Forestry Science*, 36, 36–53.
- Harris, P.J. & Trethewey, J.A.K., 2010. The distribution of ester-linked ferulic acid in the cell walls of angiosperms. *Phytochemistry Reviews*, 9, 19–33.
- Hartley, J.L., Temple, G.F. & Brasch, M.A., 2000. DNA cloning using in vitro site-specific recombination. *Genome Research*, 10, 1788–1795.
- Hasnat, R., Abbasi, N.A., Ahmad, T. & Hafiz, I.A., 2007. Induction and regeneration of hypocotyl derived calli in hot chilli (*Capsicum frutescens* L.) varieties. *Pakistan Journal of Botany*, 39, 1787–1795.

- Hasnat, R., Abbasi, N.A., Hafiz, I.A., Ahmad, T. & Chudhary, Z., 2008. Effect of different bacterial dilutions on transformation efficiency of hot chilli (*Capsicum frutescens* L.) Varieties. *Pakistan Journal of Botany*, 40, 2655–2662.
- Havkin-Frenkel, D. & Belanger, F.C., 2008. Biotechnological production of vanillin. In D. Havkin-Frenkel & F. C. Belanger, eds. *Biotechnology in Flavor Production*. Oxford: Blackwell Publishing, pp. 83–103.
- Heid, C., Stevens, J., Livak, K.J. & Williams, P.M., 1996. Real time quantitative PCR. *Genome Research*, 6, 986–994.
- Heinrich, S., Geissen, E.M., Kamenz, J., Trautmann, S., Widmer, C., Drewe, P., Knop, M., Radde, N., Hasenauer, J. & Hauf, S., 2013. Determinants of robustness in spindle assembly checkpoint signalling. *Nature Cell Biology*, 15, 1328–1339.
- Heiser, W., Optimization of biolistic transformation using the helium-driven PDS-1000/He system, EG Bulletin 1688.
- Helenius, E., Boije, M., Niklander-Teeri, V., Palva, E.T. & Teeri, T.H., 2000. Gene delivery into intact plants using the Helios™ gene gun. *Plant Molecular Biology Reporter*, 18, 287–288.
- Hemstrom, P. & Irgum, K., 2006. Hydrophilic interaction chromatography. *Journal of Separation Science*, 29, 1784–1821.
- Hernandez-Hernandez, J., 2010. Mexican vanilla production. In D. Havkin-Frenkel & F. Belanger, eds. *Handbook of Vanilla Science and Technology*. Hoboken: Wiley-Blackwell, pp. 3–25.
- Hernandez-Hernandez, J. & Lubinsky, P., 2010. Cultivation systems. In E. Odoux & M. Grisoni, eds. *Vanilla*. Boca Raton: CRC Press, pp. 75–96.
- van den Heuvel, R.H., Fraaije, M.W., Laane, C. & van Berkel, W.J., 2001. Enzymatic synthesis of vanillin. *Journal of agricultural and food chemistry*, 49, 2954–8.
- Hiei, Y., Ohta, S. & Komari, T., 1994. Efficient transformation of rice (*Oryza sativa* L.) mediated by *Agrobacterium* and sequence analysis of the boundaries of the T-DNA. *The Plant Journal*, 6, 271–282.
- Hill, K. & Schaller, G.E., 2013. Enhancing plant regeneration in tissue culture: A molecular approach through manipulation of cytokinin sensitivity. *Plant Signaling and Behaviour*, 8, e25709.
- Hocking, M.B., 1997. Vanillin: Synthetic flavoring from spent sulfite liquor. *Journal of Chemical Education*, 74, 1055–1059.
- Hofmann, N., 2014. Getting to the root of regeneration: Adventitious rooting and callus formation. *The Plant Cell*, 26, 845.
- Hu, L., Li, H., Qin, R., Xu, R., Li, J., Li, L., Wei, P. & Yang, J., 2016. Plant phosphomannose isomerase as a selectable marker for rice transformation. *Scientific Reports*, 6, 25921.

- Huang, X., Bao, Y.N., Wang, B., Liu, L.J., Chen, J., Dai, L.J. & Peng, D.X., 2016. Identification and expression of Aux/IAA, ARF, and LBD family transcription factors in *Boehmeria nivea*. *Biologia Plantarum*, 60, 244–250.
- Husaini, A.M., Abdin, M.Z., Parray, G.A., Sanghera, G.S., Murtaza, I., Alam, T., Srivastava, D.K., Farooqi, H. & Khan, H.N., 2010. Vehicles and ways for efficient nuclear transformation in plants. *GM Crops*, 1, 276–287.
- Hussain, M., 2015. A direct qPCR method for residual DNA quantification in monoclonal antibody drugs produced in CHO cells. *Journal of Pharmaceutical and Biomedical Analysis*, 115, 603–606.
- Hwang, I. & Sheen, J., 2001. Two-component circuitry in *Arabidopsis* cytokinin signal transduction. *Nature*, 413, 383–389.
- Ibrahim, E.R., Hossain, M.A. & Roslan, H.A., 2014. Genetic transformation of Metroxylon sagu (Rottb.) cultures via *Agrobacterium*-mediated and particle bombardment. *BioMed Research International*, 348140.
- Ikeda, Y., Banno, H., Niu, Q., Howell, S.H. & Chua, N.-H., 2006. The *ENHANCER OF SHOOT REGENERATION 2* gene in *Arabidopsis* regulates *CUP-SHAPED COTYLEDON 1* at the transcriptional level and controls cotyledon development. *Plant Cell Physiology*, 47, 1443–1456.
- Ikeuchi, M., Sugimoto, K. & Iwase, A., 2013. Plant callus: Mechanisms of induction and repression. *The Plant Cell*, 25, 3159–3173.
- Ingelbrencht, I., Breyne, P., Vancompernelle, K., Jacobs, A., van Montagu, M. & Depicker, A., 1991. Transcriptional interference in transgenic plants. *Gene*, 109, 239–242.
- Inzé, D. & De Veylder, L., 2006. Cell cycle regulation in plant development. *Annual Review of Genetics*, 40, 77–105.
- Ishida, Y., Saito, H., Ohta, S., Hiei, Y., Komari, T. & Kumashiro, T., 1996. High efficiency transformation of maize (*Zea mays* L.) mediated by *Agrobacterium tumefaciens*. *Nature Biotechnology*, 14, 745–750.
- ITC Market Insider, 2016. Frightening ride forecast for vanilla. *International Trade Centre*. Available at: <http://www.intracen.org/itc/blogs/market-insider/Frightening-ride-forecast-for-vanilla/> [Accessed September 19, 2016].
- Ivics, Z., Garrels, W., Mátés, L., Yau, T.Y., Bashir, S., Zidek, V., Landa, V., Geurts, A., Pravenec, M., Rüllicke, T., Kues, W.A. & Izsvák, Z., 2014. Germline transgenesis in pigs by cytoplasmic microinjection of Sleeping Beauty transposons. *Nature Protocols*, 9, 810–827.
- Izumi, M., Miyazawa, H., Kamakura, T., Yamaguchi, I., Endo, T. & Hanaoka, F., 1991. Blasticidin S-resistance gene (*bsr*): a novel selectable marker for mammalian cells. *Experimental Cell Research*, 197, 229–233.
- Jadhav, D., Rekha, B.N., Gogate, P.R. & Rathod, V.K., 2009. Extraction of vanillin from vanilla pods: A comparison study of conventional soxhlet and ultrasound assisted extraction. *Journal of Food Engineering*, 93, 421–426.

- Jain, R.K., Jain, S., Wang, B. & Wu, R., 1996. Optimization of biolistic method for transient gene expression and production of agronomically useful transgenic Basmati rice plants. *Plant Cell Reports*, 15, 963–968.
- Jain, S.M., 2001. Tissue culture-derived variation in crop improvement. *Euphytica*, 118, pp.153–166.
- Janna, O.A., Maziah, M., Ahmad Parvees, G.K.A. & K, S., 2006. Factors affecting delivery and transient expression of b-glucuronidase gene in *Dendrobium sonia* protocorm-like body. *African Journal of Biotechnology*, 5, 88–94.
- Jenkins, T., Bovi, A. & Edwards, R., 2011. Plants: biofactories for a sustainable future? *Philosophical Transactions of the Royal Societies A*, 369, 1826–1839.
- Jobling, M.G. & Holmes, R.K., 1990. Construction of vectors with the p15a replicon, kanamycin resistance, inducible lacZa and pUC18 or pUC19 multiple cloning sites. *Nucleic Acids Research*, 18, 5315–5316.
- Johnson, T.S., Ravishankar, G.A. & Venkataraman, L. V., 1996. Biotransformation of ferulic acid and vanillylamine to capsaicin and vanillin in immobilized cell cultures of *Capsicum frutescens*. *Plant Cell, Tissue and Organ Culture*, 44, 117–121.
- Jones, A.R., Kramer, E.M., Knox, K., Swarup, R., Bennett, M.J., Lazarus, C.M., Leyser, H.M.O. & Grierson, C.S., 2009. Auxin transport through non-hair cells sustains root-hair development. *Nature Cell Biology*, 11, 78–84.
- Jones, H.D. & Sparks, C.A., 2009. Selection of transformed plants. *Methods in Molecular Biology*, 478, 23–37.
- Juangsamoot, J., Ruangviriyachai, C., Techawongstien, S. & Chanthai, S., 2012. Determination of capsaicin and dihydrocapsaicin in some hot chilli varieties by RP-HPLC-PDA after magnetic stirring extraction and clean up with C18 cartridge. *International Food Research Journal*, 19, 1217–1226.
- Julie R Kikkert, José R Vidal, B.I.R., Kikkert, J.R., Vidal, J.R. & Reisch, B.I., 2004. Stable transformation of plant cells by particle bombardment / biolistics. In L. Pena, ed. *Transgenic Plants*. New Jersey: Humana Press, pp. 61–78.
- Kaeppler, S.M., Kaeppler, H.F. & Rhee, Y., 2000. Epigenetic aspects of somaclonal variation in plants. *Plant Molecular Biology*, 43, 179–188.
- Kalantidis, K., Tsagris, M. & Tabler, M., 2006. Spontaneous short-range silencing of a GFP transgene in *Nicotiana benthamiana* is possibly mediated by small quantities of siRNA that do not trigger systemic silencing. *The Plant Cell*, 45, 1006–1016.
- Kamakura, T., Yoneyama, K. & Yamaguchi, I., 1990. Expression of the blasticidin S deaminase gene (*bsr*) in tobacco: fungicide tolerance and a new selective marker for transgenic plants. *Molecular and General Genetics*, 223, 332–334.

- Kang, S.-M., Jung, H.-Y., Kang, Y.-M., Min, J.-Y., Karigar, C.S., Yang, J., Kim, S.-W., Ha, Y.-R., Lee, S.-H. & Choi, M.-S., 2005. Biotransformation and impact of ferulic acid on phenylpropanoid and capsaicin levels in *Capsicum annuum* L. cv. P1482 cell suspension cultures. *Journal of Agricultural and Food Chemistry*, 53, 3449–3453.
- Kanta, K., Rangaswamy, N.S. & Maheshwari, P., 1962. Test tube fertilization in a flowering plant. *Nature*, 194, 1214–1217.
- Karuppusamy, S., 2009. A review on trends in production of secondary metabolites from higher plants by in vitro tissue, organ and cell cultures. *Journal of Medicinal Plants Research*, 3, 1222–1239.
- Kay, E., Vogel, T.M., Bertolla, F., Nalin, R. & Simonet, P., 2002. In situ transfer of antibiotic resistance genes from transgenic (transplastomic) tobacco plants to bacteria. *Applied and Environmental Microbiology*, 68, 3345–3351.
- Kelley, K.D., Olive, L.Q., Hadziselimovic, A. & Sanders, C.R., 2010. Look and see if it is time to induce protein expression in *Escherichia coli* cultures. *Biochemistry*, 49, 5405–5407.
- Kemper, E.L., da Silva, M.-J. & Arruda, P., 1996. Effect of microprojectile bombardment parameters and osmotic treatment on particle penetration and tissue damage in transiently transformed cultured immature maize (*Zea mays* L.) embryos. *Plant Science*, 121, 85–93.
- Kern, K.A., Pergo, E.M., Kagami, F.L., Arraes, L.S., Sert, M.A. & Ishii-Iwamoto, E.L., 2009. The phytotoxic effect of exogenous ethanol on *Euphorbia heterophylla* L. *Plant Physiology and Biochemistry*, 47, 1095–1101.
- Key, S., Ma, J.K.-C. & Drake, P.M.W., 2008. Genetically modified plants and human health. *Journal of the Royal Society of Medicine*, 101, 290–298.
- Khah, E.M. & Passam, H.C., 1992. Sodium hypochlorite concentration, temperature, and seed age influence germination of sweet pepper. *HortScience*, 27, 821–823.
- Khoddami, A., Wilkes, M.A. & Roberts, T.H., 2013. Techniques for analysis of plant phenolic compounds. *Molecules*, 18, 2328–2375.
- Kim, S.H., Mok, H., Jeong, J.H., Kim, S.W. & Park, T.G., 2006. Comparative evaluation of target-specific GFP gene silencing efficiencies for antisense ODN, synthetic siRNA, and siRNA plasmid complexed with PEI-PEG-FOL conjugate. *Bioconjugate Chemistry*, 17, 241–244.
- Kim, S.J. & Martinson, H.G., 2003. Poly(A)-dependent transcription termination. *The Journal of Biological Chemistry*, 278, 41691–41701.
- Kimura, M., Takatsuki, A. & Yamaguchi, I., 1994. Blastocidin S deaminase gene from *Aspergillus terreus* (BSD): a new drug resistance gene for transfection of mammalian cells. *Biochimica et Biophysica Acta*, 1219, 653–659.

- Kindle, K.L., 1998. Nuclear transformation: Technology and applications. In J.-D. Rochaix, M. Goldschmidt-Clermont, & S. Merchant, eds. *The Molecular Biology of Chloroplasts and Mitochondria in Chlamydomonas*, Vol 7. Dordrecht: Springer Netherlands, pp. 41–61.
- Kivilompolo, M. & Hyötyläinen, T., 2008. Comparison of separation power of ultra performance liquid chromatography and comprehensive two-dimensional liquid chromatography in the separation of phenolic compounds in beverages. *Journal of Separation Science*, 31, 3466–3472.
- Klein, T.M., Fromm, M. & Weissinger, A., 1988. Transfer of foreign genes into intact maize cells with high-velocity microprojectiles. *Proceedings of the National Academy of Sciences of the United States of America*, 85, 4305–4309.
- Klein, T.M., Fromm, M., Weissinger, A., Tomes, D., Schaaf, S., Sletten, M. & Sanford, J.C., 1987. High velocity microprojectiles for delivering nucleic acids into living cells. *Nature*, 327, 70–73.
- Klein, T.M., Knowlton, S. & Arentzen, R., 1991. Gene transfer by particle bombardment. In K. Lindsey, ed. *Plant Tissue Culture Manual*. The Netherlands: Kluwer Academic Publishers, p. D1: 1-12.
- De Klerk, G.J., Arnholdt-Schmitt, B., Lieberei, R. & Neumann, K.H., 1997. Regeneration of roots, shoots and embryos: Physiological, biochemical and molecular aspects. *Biologia Plantarum*, 39, 53–66.
- Kometani, T., Tanimoto, H., Nishimura, T. & Okada, S., 2014. Glucosylation of vanillin by cultured plant cells. *Bioscience, Biotechnology and Biochemistry*, 57, 1290–1293.
- Komori, T., Imayama, T., Kato, N., Ishida, Y., Ueki, J. & Komari, T., 2007. Current status of binary vectors and superbinary vectors. *Plant Physiology*, 145, 1155–1160.
- Koornneel, M., Bentsink, L. & Hilhorst, H., 2002. Seed dormancy and germination. *Current Opinion in Plant Biology*, 5, 33–36.
- Korthou, H. & Verpoorte, R., 2004. Vanilla. In R. Berger, ed. *Flavours and Fragrances: Chemistry, Bioprocessing and Sustainability*. Heidelberg: Springer-Verlag, pp. 203–218.
- Kothari, S.L., Joshi, A., Kachhwaha, S. & Ochoa-Alejo, N., 2010. Chilli peppers — A review on tissue culture and transgenesis. *Biotechnology Advances*, 28, 35–48.
- Kovalchuk, N., Jia, W., Eini, O., Morran, S., Pyvovarenko, T., Fletcher, S., Bazanova, N., Harris, J., Beck-Oldach, K., Shavrukov, Y., Langridge, P. & Lopato, S., 2013. Optimization of TaDREB3 gene expression in transgenic barley using cold-inducible promoters. *Plant Biotechnology Journal*, 11, 659–670.
- Krishnaraj, S. & Vasil, I.K., 1995. Somatic embryogenesis in herbaceous monocots. In T. A. Thorpe, ed. *In Vitro Embryogenesis in Plants*. Dordrecht: Springer Netherlands, pp. 417–470.

- Kumar, A.M., Reddy, K.N., Manjulatha, M., Arellano, E.S., Sreevathsa, R. & Ganesham, G., 2011. A rapid, novel and high-throughput identification of putative bell pepper transformants generated through in planta transformation approach. *Scientia Horticulturae*, 129, 898–903.
- Kumar, M., Campbell, L. & Turner, S., 2016. Secondary cell walls: biosynthesis and manipulation. *Journal of Experimental Botany*, 67, 515–531.
- Kumar, N. & Pruthi, V., 2014. Potential applications of ferulic acid from natural sources. *Biotechnology Reports*, 4, 86–93.
- Kumar, P.K.R., Maschke, H.-E., Friehs, K. & Schugerl, K., 1991. Strategies for improving plasmid stability in genetically modified bacteria in bioreactors. *Trends in Biotechnology*, 9, 279–284.
- Kumar, R., Sharma, P.K. & Mishra, P.S., 2012. A review on the vanillin derivatives showing various biological activities. *International Journal of PharmTech Research*, 4, 266–279.
- Kung, S.H., Retchless, A.C., Kwan, J.Y. & Almeida, R.P.P., 2013. Effects of DNA size on transformation and recombination efficiencies in *Xylella fastidiosa*. *Applied and Environmental Microbiology*, 79, 1712–1717.
- Lakatos, L., Szittyá, G., Silhavy, D. & Burgyán, J., 2004. Molecular mechanism of RNA silencing suppression mediated by p19 protein. *The EMBO Journal*, 23, 876–884.
- Lakshmanan, M., Yoshizumi, T., Sudesh, K., Kodama, Y. & Numata, K., 2015. Double-stranded DNA introduction into intact plants using peptide-DNA complexes. *Plant Biotechnology*, 32, 39–45.
- Langbecker, C.L., Ye, G.-N., Broyles, D.L., Duggan, L.L., Xu, C.W., Hajdukiewicz, P.T.J., Armstrong, C.L. & Staub, J.M., 2004. High-frequency transformation of undeveloped plastids in tobacco suspension cells. *Plant Physiology*, 135, 39–46.
- Laplaze, L., Benkova, E., Casimiro, I., Maes, L., Vanneste, S., Swarup, R., Weijers, D., Calvo, V., Parizot, B., Herrera-Rodriguez, M.B., Offringa, R., Graham, N., Doumas, P., Friml, J., Bogusz, D., Beeckman, T. & Bennett, M., 2007. Cytokinins act directly on lateral root founder cells to inhibit root initiation. *The Plant Cell*, 19, 3889–3900.
- LaRue, C.D., 1942. The rooting of flowers in culture. *Bulletin of the Torrey Botany Club*, 69, 332–341.
- Latham, J.R., Wilson, A.K. & Steinbrecher, R.A., 2006. The mutational consequences of plant transformation. *Journal of Biomedicine and Biotechnology*, 25376, 1–7.
- Laxmi, A., Gupta, A., Mishra, B.S., Singh, M., Jamsheer, K.M. & Kushwah, S., 2013. Signal integration, auxin homeostasis, and plant development. In R. Chen & F. Baluška, eds. *Polar Auxin Transport*. Heidelberg: Springer-Verlag, pp. 45–79.
- Ledbetter, D.J., Thomson, J.G., Piedrahita, J.A. & Rucker III, E.B., 2014. 5 – Gene Targeting in Embryonic Stem Cells, II: Conditional Technologies. In C. A. Pinkert, ed. *Transgenic Animal Technology*. Oxford: Elsevier, pp. 141–165.

- Lee, E.-G., Yoon, S.-H., Das, A., Lee, S.-H., Li, C., Kim, J.-Y., Choi, M.-S., Oh, D.-K. & Kim, S.-W., 2009. Directing vanillin production from ferulic acid by increased acetyl-CoA consumption in recombinant *Escherichia coli*. *Biotechnology and bioengineering*, 102, 200–8.
- Lee, S.K. & Kader, A.A., 2000. Preharvest and postharvest factors influencing vitamin C content of horticultural crops. *Postharvest Biology and Technology*, 20, 207–220.
- Leifert, C. & Cassells, A.C., 2001. Microbial hazards in plant tissue and cell cultures. *In Vitro Cellular & Developmental Biology - Plant*, 37, 133–138.
- Leifert, C., Ritchie, J.Y. & Waites, W.M., 1991. Contaminants of plant-tissue and cell cultures. *World Journal of Microbiology and Biotechnology*, 7, 452–469.
- Leong, C.C. (2015). *An Investigation of Insertion of Recombination Cloning Site and Plant Selectable Marker into a Nuclear Transformation Vector*. BSc Dissertation, University of Nottingham.
- Li, D., Zhao, K., Xie, B., Zhang, B. & Luo, K., 2003a. Establishment of a highly efficient transformation system for pepper (*Capsicum annuum* L.). *Plant Cell Reports*, 21, 785–788.
- Li, X. & Gallagher, J.L., 1996. Expression of foreign genes, GUS and hygromycin resistance, in the halophyte *Kosteletzkya virginica* in response to bombardment with the Particle Inflow Gun. *Journal of Experimental Botany*, 47, 1437–1447.
- Liang, X., Peng, L., Baek, C.-H. & Katzen, F., 2013. Single step BP/LR combined Gateway reactions. *BioTechniques*, 55, 265–267.
- Lico, C., Desiderio, A., Banchieri, S. & Benvenuto, E., 2005. Plants as biofactories: Production of pharmaceutical recombinant proteins. In R. Tuberosa, R. L. Philips, & M. Gale, eds. *Proceedings of the International Congress "In the Wake of the Double Helix: From the Green Revolution to the Gene Revolution."* Bologna: Avenue Media, pp. 577–593.
- Lila, M.A., 2005. Valuable secondary products from in vitro culture. In R. N. Trigiano & D. J. Gray, eds. *Plant Development and Biotechnology*. Boca Raton: CRC Press, pp. 285–290.
- Lin, L.-Z., Lu, S. & Harnly, J.M., 2007. Detection and quantification of glycosylated flavonoid malonates in celery, chinese celery, and celery seed by LC-DAD-ESI/MS. *Journal of Agricultural and Food Chemistry*, 55, 1321–1326.
- Liu, J.Y., 2014. Direct qPCR quantification of unprocessed forensic casework samples. *Forensic Science International: Genetics*, 11, 96–104.
- Livak, K.J. & Schmittgen, T.D., 2001. Analysis of relative gene expression data using real-time quantitative PCR and the 2-ddCT method. *Methods*, 25, 402–408.
- Lockey, C., Otto, E. & Long, Z., 1998. Real-time fluorescence detection of a single DNA molecule. *BioTechniques*, 24, 744–746.

- Longo, M.A. & Sanromán, M.A., 2006. Production of Food Aroma Compounds: Microbial and Enzymatic Methodologies. *Food Technology and Biotechnology*, 44, 335–353.
- Lonsdale, D.M., Lindup, S., Moisan, L.J. & Harvey, A.J., 1998. Using firefly luciferase to identify the transition from transient to stable expression in bombarded wheat scutellar tissue. *Physiologia Plantarum*, 102, 447–453.
- Lopez-Malo, A., Alzamora, S.M. & Argai, A., 1995. Effect of natural vanillin on germination and radical growth on moulds in fruit-based agar systems. *Food Microbiology*, 12, 213–219.
- Lubinsky, P., Bory, S., Hernández Hernández, J., Kim, S.C. & Gómez-Pompa, A., 2008. Origins and dispersal of cultivated vanilla (*Vanilla planifolia* Jacks. [Orchidaceae]). *Economic Botany*, 62, 127–138.
- Luo, D. & Saltzman, W.M., 2000. Synthetic DNA delivery systems. *Nature Biotechnology*, 18, 33–37.
- Maguire, J.D., Kropf, J.P. & Steen, K.M., 1973. Pea seed viability in relation to bleaching. *Proceedings of the Association of Official Seed Analysts*, 63, 51–58.
- Mancuso, C. & Santangelo, R., 2014. Ferulic acid: Pharmacological and toxicological aspects. *Food and Chemical Toxicology*, 65, 185–195.
- Manoharan, M., Vidya, C.S.S. & Sita, G.L., 1998. *Agrobacterium*-mediated genetic transformation in hot chilli (*Capsicum annuum* L. var. Pusa Jwala). *Plant Science*, 131, 77–83.
- Manuselis, G., 2011. Use of colonial morphology for the presumptive identification of microorganisms. In C. R. Mahon, D. C. Lehman, & G. Manuselis Jr., eds. *Textbook of Diagnostic Microbiology*. Missouri: Saunders Elsevier, pp. 170–185.
- Marx, V., 2013. PCR: living life amplified and standardized. *Nature Methods*, 10, 391–395.
- Matthew, S. & Abraham, T.E., 2004. Ferulic acid: An antioxidant found naturally in plant cell walls and feruloyl esterases involved in its release and their applications. *Critical Reviews in Biotechnology*, 24, 59–83.
- Matzke, A.J.M., Neuhuber, F., Park, Y.D., Ambros, P.F. & Matzke, M.A., 1994. Homology-dependent gene silencing in transgenic plants: epistatic silencing loci contain multiple copies of methylated transgenes. *Molecular Genetics and Genomics*, 244, 219–229.
- Maxwell, B.B. & Kieber, J.J., 2010. Cytokinin signal transduction. In P. J. Davies, ed. *Plant Hormones*. Dordrecht: Springer Netherlands, pp. 329–357.
- Mazourek, M., Pujar, A., Borovsky, Y., Paran, I., Mueller, L. & Jahn, M.M., 2009. A dynamic interface for capsaicinoid systems biology. *Plant Physiology*, 150, 1806–21.

- de Melo, J., Olarreaga, M. & Takacs, W., 2015. Pricing Policy Under Double Market Power: Madagascar and the International Vanilla Market. In J. de Melo, ed. *Developing Countries in the World Economy*. Geneva: World Scientific Press, pp. 199–218.
- Men, S., Ming, X., Wang, Y., Liu, R., Wei, C. & Li, Y., 2003. Genetic transformation of two species of orchid by biolistic bombardment. *Plant Cell Reports*, 21, 592–598.
- de Mesa, M.C., Jiménez-Bermúdez, S., Pliego-Alfaro, F., Quesada, M.A. & Mercado, J.A., 2000. *Agrobacterium* cells as microprojectile coating: a novel approach to enhance stable transformation rates in strawberry. *Australian Journal of Plant Physiology*, 27, 1093–1100.
- Miché, L. & Balandreau, J., 2001. Effects of rice seed surface sterilization with hypochlorite on inoculated *Burkholderia vietnamiensis*. *Applied*, 67, 3046–3052.
- Midtvedt, T., 2014. Antibiotic resistance and genetically modified plants. *Microbial Ecology in Health and Disease*, 25, 25918.
- Misato, T., Ko, K. & Yamaguchi, I., 1977. Use of antibiotics in agriculture. In D. Perlman, ed. *Advances in Applied Microbiology: Volume 21*. New York: Academic Press, pp. 53–88.
- Misawa, M., 1985. Production of useful plant metabolites. In A. Fiechter, ed. *Advances in Biochemical/Biotechnology*. Heidelberg: Springer-Verlag, pp. 59–88.
- Mok, S.H. & Norzulaani, K., 2007. Trouble shooting for recalcitrant bud formation in *Capsicum annuum* var. Kulai. *Asia Pacific Journal of Molecular Biology and Biotechnology*, 15, 33–38.
- Morel, G., 1960. Producing virus-free cymbidium. *American Orchid Society Bulletin*, 29, 495–497.
- Morre, J.L., Permingeat, H.R., Romagnoli, M. V, Heisterborg, C.M. & Vallejos, R.H., 1998. Multiple shoot induction and plant regeneration from embryonic axes of cotton. *Plant Cell, Tissue and Organ Culture*, 54, 131.
- Mradu, G., Saumyakanti, S., Sohini, M. & Arup, M., 2012. HPLC profiles of standard phenolic compounds present in medicinal plants. *International Journal of Pharmacognosy and Phytochemical Research*, 4, 162–167.
- Müller, D. & Leyser, O., 2011. Auxin, cytokinin and the control of shoot branching. *Annals of Botany*, 107, 1203–1212.
- Murashige, T. & Skoog, F., 1962. A revised medium for rapid growth and bioassays with tobacco tissue cultures. *Physiologia Plantarum*, 15, 473–497.
- Narbad, A. & Gasson, M.J., 1998. Metabolism of ferulic acid via vanillin using a novel CoA-dependent pathway in a newly- isolated strain of *Pseudomonas fluorescens*. *Microbiology*, 144, 1397–1405.

- Negrotto, D., Jolley, M., Beer, S., Wenck, A.R. & Hansen, G., 2000. The use of phosphomannose-isomerase as a selectable marker to recover transgenic maize plants (*Zea mays* L.) via *Agrobacterium* transformation. *Plant Cell Reports*, 18, 798–803.
- Newell, C.A., 2000. Plant transformation technology: Developments and advances. *Molecular Biotechnology*, 16, 53–65.
- Ni, J., Tao, F., Du, H. & Xu, P., 2015. Mimicking a natural pathway for de novo biosynthesis : natural vanillin production from accessible carbon sources. *Scientific Reports*, 5, 13670.
- Nianiou, I., Karavangeli, M., Zambounis, A. & Tsaftaris, A., 2002. Development of pepper transgenic plants via *Agrobacterium* and biolistic transformation. *Acta Horticulturae*, 579,83–87.
- Nitsch, J.P. & Nitsch, C., 1956. Auxin-dependent growth of excised *Helianthus tuberosus* tissues. *American Journal of Botany*, 43, 839–851.
- Niwa, Y., 2003. A synthetic GFP for plant biotechnology. *Plant Biotechnology*, 20, 1–11.
- Nødvig, C.S., Nielsen, J.B., Kogle, M.E. & Mortensen, U.H., 2015. A CRISPR-Cas9 system for genetic engineering of filamentous fungi. *PLoS ONE*, 10, e0133085.
- Nybo, K., 2011. qPCR efficiency calculations. *BioTechniques*, 51, 401–402.
- O'Brien, J.A. & Lummis, S.C.R., 2011. Nano-biolistics: a method of biolistic transfection of cells and tissues using a gene gun with novel nanometer-sized projectiles. *BMC Biotechnology*, 11, 2–7.
- Ochoa-Alejo, N. & Gómez-Peralta, J.E., 1993. Activity of enzymes involved in capsaicin biosynthesis in callus tissue and fruits of chili pepper (*Capsicum annum* L.). *Journal of Plant Physiology*, 141, 147–152.
- Ochoa-Alejo, N. & Ramírez-Malagón, R., 2001. In vitro chili pepper biotechnology. *In Vitro Cellular & Developmental Biology*, 37, 701–729.
- Ogawa, K., Murota, K., Shimura, H., Furuya, M., Togawa, Y., Matsumura, T. & Masuta, C., 2015. Evidence of capsaicin synthase activity of the Pun1-encoded protein and its role as a determinant of capsaicinoid accumulation in pepper. *BMC Plant Biology*, 15, 93–102.
- Ogawa, M., Hanada, A., Yamauchi, Y., Kuwahara, A., Kamiya, Y. & Yamaguchi, S., 2003. Gibberellin biosynthesis and response during *Arabidopsis* seed germination. *The Plant Cell*, 15, 1591–1604.
- Oh, E., Kang, H., Yamaguchi, S., Park, J., Lee, D., Kamiya, Y. & Choi, G., 2009. Genome-wide analysis of genes targeted by PHYTOCHROME INTERACTING FACTOR 3-LIKE5 during seed germination in *Arabidopsis*. *The Plant Cell*, 21, 403–419.
- Ohse, M., Takahashi, K., Kadowaki, Y. & Kusaoke, H., 1995. Effects of plasmid DNA sizes and several other factors on transformation of *Bacillus subtilis* ISW1214 with plasmid DNA by electroporation. *Bioscience, Biotechnology, and Biochemistry*, 59, 1433–1437.

- Okonkwo, S.N.C. & Nwoke, F.I.O., 1975. Bleach-induced germination and breakage of dormancy of seeds of *Alectra vogelii*. *Physiologia Plantarum*, 35, 175–180.
- Ormo, M., Cubitt, A.B., Kallio, K., Gross, L.A., Tsien, R.Y. & Remington, S.J., 1996. Crystal structure of the *Aequorea victoria* green fluorescent protein. *Science*, 273, 1392–1395.
- Ou, S. & Kwok, K.-C., 2004. Ferulic acid: pharmaceutical functions, preparation and applications in foods. *Journal of the Science of Food and Agriculture*, 84, 1261–1269.
- Overvoorde, P., Fukaki, H. & Beeckman, T., 2010. Auxin Control of Root Development. *Cold Spring Harbor Perspectives in Biology*, 2, a001537.
- Park, Y.D., Papp, I., Moscone, E.A., Iglesias, V.A., Vaucheret, H., Matzke, A.J. & Matzke, M.A., 1996. Gene silencing mediated by promoter homology occurs at the level of transcription and results in meiotically heritable alterations in methylation and gene activity. *The Plant Journal*, 9, 183–194.
- Parveez, G.K., Chowdhury, M.K.U. & Saleh, N.M., 1998. Biological parameters affecting transient GUS gene expression in oil palm (*Elaeis guineensis* Jacq.) embryogenic calli via microprojectile bombardment. *Industrial Crops and Products*, 8, 17–27.
- Patrick, M., 2015. Antibiotic resistance genes. In Addgene, ed. *Plasmids 101: A Desktop Resource*. Cambridge: Addgene, pp. 11–13. Available at: http://cdn2.hubspot.net/hubfs/306096/Addgene-Plasmids-101-eBook-Second-Edition_Final.pdf?hsCtaTracking=71186a5f-f907-4f26-afd9-df20b881d517%7C21df67f2-0ba5-4750-894f-a439cecc8357&__hstc=246494683.9fea903e7b229259e7cfff49ad734273.1489481781302.148948178130 [Accessed December 15, 2016].
- Patron, N.J., 2013. Type IIS assembly protocol. *TheSainsburyLaboratory (TSL) Plasmids & Molecular Tools*. Available at: <http://synbio.tsl.ac.uk/golden-gate-assembly-protocol/> [Accessed November 29, 2016].
- Pena, L., 2004. *Transgenic Plants*, New Jersey: Humana Press.
- Peng, A., Ye, H., Li, X. & Chen, L., 2009. Preparative separation of capsaicin and dihydrocapsaicin from *Capsicum frutescens* by high-speed counter-current chromatography. *Journal of Separation Science*, 32, 2967–73.
- Pérez-Barranco, G., Mercado, J.A., Pliego-Alfaro, F. & Sánchez-Romero, C., 2007. Genetic transformation of olive somatic embryos through biolistics. *Acta Horticulturae*, 739, 473–477.
- Pérez-González, J.A., Ruiz, D., Esteban, J.A. & Jiménez, A., 1990. Cloning and characterization of the gene encoding a blasticidin S acetyltransferase from *Streptoverticillum* sp. *Gene*, 86, 129–134.
- Perrot-Rechenmann, C., 2010. Cellular responses to auxin: Division versus expansion. *Cold Spring Harbor Perspectives in Biology*, 2, a001446.
- Peter, K. V., 2004. *Handbook of Herbs and Spices Volume 2*, Boca Raton: CRC Press.

- Peterson, G. & Smith, R., 1991. Effect of abscisic acid and callus size on regeneration of american and international rice varieties. *Plant Cell Reports*, 10, 35–38.
- Petropoulos, A.D., Xaplanteri, M.A., Dinos, G.P., Wilson, D.N. & Kalpaxis, D.L., 2004. Polyamines affect diversely the antibiotic potency: Insight gained from kinetic studies of the blasticidin S and spiramycin interactions with functional ribosomes. *The Journal of Biological Chemistry*, 279, 26518–26525.
- Pfaffl, M.W., 2001. A new mathematical model for relative quantification in real-time RT-PCR. *Nucleic Acids Research*, 29, e45.
- Pfaffl, M.W., 2010. The ongoing evolution of qPCR. *Methods*, 50, pp.215–336.
- Piechaczek, C., Fetzner, C., Baiker, A., Bode, J. & Lipps, H.J., 1999. A vector based on the SV40 origin of replication and chromosomal S/MARs replicates episomally in CHO cells. *Nucleic Acids Research*, 27, 426–428.
- Pilate, G., Dejardin, A. & Leple, J.-C., 2010. Field trials with lignin-modified transgenic trees. In L. Jouanin & C. Lapierre, eds. *Lignings: Biosynthesis, Biodegradation and Bioengineering*. Massachusetts: Academic Press, pp. 2–36.
- Pluhar, S.A., Erickson, L. & Pauls, K.P., 2001. Effects of tissue culture on a highly repetitive DNA sequence (E180 satellite) in *Medicago sativa*. *Plant Cell, Tissue and Organ Culture*, 67, 195–199.
- Polisetty, R., Paul, V., Deveshwar, J.J., Khetarpal, S., Suresh, K. & Chandra, R., 1997. Multiple shoot induction by benzyladenine and complete plant regeneration from seed explants of chickpea (*Cicer arietinum* L.). *Plant Cell Reports*, 16, 565–571.
- Pometto, A.L.I. & Crawford, D.L., 1983. Whole-cell bioconversion of vanillin to vanillic acid by *Streptomyces viridosporus*. *Applied and Environmental Microbiology*, 45, 1582–1585.
- Priefert, H., Rabenhorst, J. & Steinbüchel, A., 2001. Biotechnological production of vanillin. *Applied Microbiology and Biotechnology*, 56, 296–314.
- Proudfoot, N.J., 2011. Ending the message: poly(A) signals then and now. *Genes and Development*, 25, 1770–1782.
- Pryor, R.J. & Wittwer, C.T., 2006. Real-time polymerase chain reaction and melting curve analysis. *Methods in Molecular Biology*, 336, 19–32.
- Qin, J.B., Wang, Y. & Zhu, C.Q., 2014. Biolistic transformation of wheat using the HMW-GS 1Dx5 gene without selectable markers. *Genetics and Molecular Research*, 13, 4361–4371.
- Radonic, A., Thulke, S., Mackay, I.M., Landt, O., Siegert, W. & Nitsche, A., 2004. Guideline to reference gene selection for quantitative real-time PCR. *Biochemical and Biophysical Research Communications*, 313, 856–862.

- Ramachandra, R. & Ravishankar, G., 2000a. Biotransformation of protocatechuic aldehyde and caffeic acid to vanillin and capsaicin in freely suspended and immobilized cell cultures of *Capsicum frutescens*. *Journal of Biotechnology*, 76, 137–146.
- Ramachandra, R. & Ravishankar, G., 2000b. Vanilla flavour: production by conventional and biotechnological routes. *Journal of the Science of Food and Agriculture*, 80, pp.289–304.
- Rana, R., Mathur, A., Jain, C.K., Sharma, S.K. & Mathur, G., 2013. Microbial production of vanillin. *International Journal of Biotechnology and Bioengineering Research*, 4, pp.227–234.
- Ranadive, A.S., 2010. Quality control of vanilla beans and extracts. In D. Havkin-Frenkel & F. C. Belanger, eds. *Handbook of Vanilla Science and Technology*. Hoboken: Wiley-Blackwell, pp. 141–161.
- Ranal, M.A. & De Santana, D.G., 2006. How and why to measure the germination process? *Revista Brasileira de Botanica*, 29, 1–11.
- Randle, W.M. & Homna, S., 1981. Dormancy in peppers. *Scientia Horticulturae*, 14, 19–25.
- Rao, A.Q., Bakhsh, A., Kiani, A., Shahzad, K., Shahid, A.A., Husnain, T. & Riazuddin, S., 2009. The myth of plant transformation. *Biotechnology Advances*, 27, 753–763.
- Rao, S.R. & Ravishankar, G.A., 2000. Biotransformation of protocatechuic aldehyde and caffeic acid to vanillin and capsaicin in freely suspended and immobilized cell cultures of *Capsicum frutescens*. *Journal of Biotechnology*, 76, 137–146.
- Rao, S.R. & Ravishankar, G.A., 2002. Plant cell cultures: Chemical factories of secondary metabolites. *Biotechnology Advances*, 20, 101–153.
- Ravishankar, G.A., Suresh, B., Giridhar, P., Rao, S.R. & Johnson, T.S., 2003. Biotechnological studies on *Capsicum* for metabolite production and plant improvement. In A. K. De, ed. *Capsicum: The genus Capsicum*. Reading: Harwood Academic Publishers, pp. 96–128.
- Rech, E.L., Vianna, Giovanni, R. & Aragão, F.J.L., 2008. High-efficiency transformation by biolistics of soybean, common bean and cotton transgenic plants. *Nature Protocols*, 3, 410–418.
- Reddy, D.S., Bhatnagar-Mathur, P., Cindhuri, K.S. & Sharma, K.K., 2013. Evaluation and validation of reference genes for normalization of quantitative real-time PCR based gene expression studies in peanut. *PLoS ONE*, 8, e78555.
- Reed, B.M. & Tanprasert, P., 1995. Detection and control of bacterial contaminants of plant tissue cultures. A review of recent literature. *Plant Tissue Culture and Biotechnology*, 3, 137–142.
- Reed, R.C., Brady, S.R. & Muday, G.K., 1998. Inhibition of auxin movement from the shoot into the root inhibits lateral root development in *Arabidopsis*. *Plant Physiology*, 118, pp.1369–1378.
- Reineccius, G., 1994. *Source Book of Flavors* 2nd ed., Dordrecht: Springer.

- Rizwan, M., Sharma, R., Soni, P. & Singh, G., 2014. Protocol for direct transformation through gene gun in *Capsicum annuum* L. cv. Mathania. *Biocatalysis and Biotransformation*, 3, 1.
- Robertson, D., Weissinger, A.K., Ackley, R., Glover, S. & Sederoff, R.R., 1992. Genetic transformation of Norway spruce (*Picea abies* (L.) Karst) using somatic embryo explants by microprojectile bombardment. *Plant Molecular Biology*, 19, 925–935.
- Rochange, F., Serrano, L., Marque, C., Teulières, C. & Boudet, A.-M., 1995. DNA delivery into *Eucalyptus globulus* zygotic embryos through biolistics: optimization of the biological and physical parameters of bombardment for two different particle guns. *Plant Cell Reports*, 14, 674–678.
- Rodolphe, G., Severine, B., Michel, G. & Pascale, B., 2011. Biodiversity and evolution in the *Vanilla* genus. In O. Grillo & G. Venora, eds. *The Dynamical Processes of Biodiversity – Case Studies of Evolution and Spatial Distribution*. Rijeka: InTech, pp. 1–27.
- Ruduś, I., Kępczyński, J. & Kępczyńska, E., 2001. The influence of the jasmonates and abscisic acid on callus growth and somatic embryogenesis in *Medicago sativa* L. tissue culture. *Acta Physiologiae Plantarum*, 23, 103.
- Ruijter, J.M., Ramakers, C., Hoogaars, W.M.H., Karlen, Y., Bakker, O., van den hoff, M.J.B. & Moorman, A.F.M., 2009. Amplification efficiency: Linking baseline and bias in the analysis of quantitative PCR data. *Nucleic Acids Research*, 37, e45.
- Ruma, D., Dhaliwal, M.S., Kaur, A. & Gosal, S.S., 2009. Transformation of tomato using biolistic gun for transient expression of the β -glucuronidase gene. *Indian Journal of Biotechnology*, 8, 363–369.
- Russell, J.A., Roy, M.K. & Sanford, J.C., 1992. Major improvements in Biolistic transformation of suspension cultured tobacco cells. *In Vitro Cellular & Developmental Biology*, 28P, 97–105.
- Sabisch, M. & Smith, D., 2014. The complex regulatory landscape for natural flavor ingredients. *Sigma-Aldrich*. Available at: <http://www.sigmaaldrich.com/technical-documents/articles/white-papers/flavors-and-fragrances/natural-flavor-ingredients-regulations.html#definitions> [Accessed December 1, 2015].
- Saidi, Y., Schaefer, D.G., Goloubinoff, P., Zryd, J. & Finka, A., 2009. The CaMV 35S promoter has a weak expression activity in dark grown tissues of moss *Physcomitrella patens*. *Plant Signaling and Behaviour*, 4, 457–459.
- Saini, S., Sharma, I., Kaur, N. & Pati, P.K., 2013. Auxin: a master regulator in plant root development. *Plant Cell Reports*, 32, 741–757.
- Sainsbury, P.D., Hardiman, E.M., Ahmad, M., Otani, H., Seghezzi, N., Eltis, L.D. & Bugg, T.D.H., 2013. Breaking down lignin to high-value chemicals: The conversion of lignocellulose to vanillin in a gene deletion mutant of *Rhodococcus jostii* RHA1. *ACS Chemical Biology*, 8, 2151–2156.

- Sakuma, T., Nishikawa, A., Kume, S., Chayama, K. & Yamamoto, T., 2014. Multiplex genome engineering in human cells using all-in-one CRISPR/Cas9 vector system. *Scientific Reports*, 4, 5400.
- Sanatombi, K. & Sharma, G.J., 2007. Micropropagation of *Capsicum annuum* L. *Notulae Botanicae Horti Agrobotanici Cluj-Napoca*, 35, 57–64.
- Sandal, I., Koul, R., Saini, U., Mehta, M., Dhiman, N., Kumar, N., Ahuja, P.S. & Bhattacharya, A., 2015. Development of transgenic tea plants from leaf explants by the biolistic gun method and their evaluation. *Plant Cell, Tissue and Organ Culture*, 123, 245–255.
- Sanders, P.R., Winter, J.A., Barnason, A.R., Rogers, S.G. & Fraley, R.T., 1987. Comparison of cauliflower mosaic virus 35S and nopaline synthase promoters in transgenic plants. *Nucleic Acids Research*, 15, 1543–1558.
- Sanford, J.C., Klein, T.M., Wolf, E.D. & Allen, N., 1987. Delivery of substances into cells and tissues using a particle bombardment process. *Journal of Particulate Science and Technology*, 5, 27–37.
- Sanford, J.C., Smith, F.D. & Russell, J.A., 1993. Optimizing the Biolistic process for different biological applications. *Methods in Enzymology*, 217, 483–509.
- Santana-Buzzy, N., Canto-flick, A., Barahona-pérez, F., Montalvo-peniche, M.C., Zapata-castillo, P.Y., Solís-ruiz, A., Zaldívar-collí, A. & Gutiérrez-alonso, O., 2005. Regeneration of Habanero pepper (*Capsicum chinense* Jacq.) via organogenesis. *HortScience*, 40, 1829–1831.
- Sari Gorla, M., Ottaviano, E. & Faini, D., 1975. Genetic variability of gametophyte growth rate in maize. *Theoretical and Applied Genetics*, 46, 289–294.
- Sato, D., Eshita, Y., Katsuragi, H., Hamada, H., Shimoda, K. & Kubota, N., 2012. Glycosylation of vanillin and 8-nordihydrocapsaicin by cultured *Eucalyptus perriniana* cells. *Molecules*, 17, 5013–5020.
- Sauer, D.B. & Burroughs, R., 1986. Disinfection of seed surfaces with sodium hypochlorite. *Phytopathology*, 76, 745–749.
- Schomburg, D., Schomburg, I. & Chang, A., 2010. Vanillin synthase. In *Class 4-6 Lyases, Isomerases, Ligases*. Heidelberg: Springer-Verlag, pp. 39–41.
- Seternes, T., Tonheim, T.C., Myhr, A.I. & Dalmo, R.A., 2016. A plant 35S CaMV promoter induces long-term expression of luciferase in Atlantic salmon. *Scientific Reports*, 6, 25096.
- Sezonov, G., Joseleau-Petit, D. & D'Ari, R., 2007. *Escherichia coli* physiology in Luria-Bertani broth. *Journal of Bacteriology*, 189, 8746–8749.
- Sharma, A., Kumar, V., Giridhar, P. & Ravishankar, G.A., 2008. Induction of *in vitro* flowering in *Capsicum frutescens* under the influence of silver nitrate and cobalt chloride and pollen transformation. *Electronic Journal of Biotechnology*, 11, 1–7.

- Sharma, N. & Chandel, K.P.S., 1992. Effects of ascorbic acid on axillary shoot induction in *Tylophora indica* (Burm. f.) Merrill. *Plant Cell, Tissue and Organ Culture*, 29, 109–113.
- Shetty, K., Asano, Y. & Oosawa, K., 1992. Stimulation of in vitro shoot organogenesis in *Glycine max* (Merrill.) by allantoin and amides. *Plant Science*, 81, 245–251.
- Shim, Y.S. & Kasha, K.J., 2003. Barley microspore transformation protocol by biolistic gun. In M. Maluszynski et al., eds. *Doubled Haploid Production in Crop Plants*. Dordrecht: Springer Netherlands, pp. 363–366.
- Shrivastava, A. & Gupta, V., 2011. Methods for the determination of limit of detection and limit of quantitation of the analytical methods. *Chronicles of Young Scientists*, 2, 21–25.
- Sidorov, V.A., Kasten, D., Pang, S.Z., Hajdukiewicz, P.T.J., Staub, J.M. & Nehra, N.S., 1999. Stable plastid transformation in potato: Use of green fluorescent protein as a plastid marker. *The Plant Journal*, 19, 209–216.
- Sigma-Aldrich. *Quantitative PCR and Digital PCR Detection Methods: A Technical Guide to PCR Technologies*. Available at: <http://www.sigmaaldrich.com/technical-documents/articles/biology/quantitative-pcr-and-digital-pcr-detection-methods.html> [Accessed January 5, 2017].
- Singh, A.K., Verma, S.S. & Bansal, K.C., 2010. Plastid transformation in eggplant (*Solanum melongena* L.). *Transgenic Research*, 19, 113–119.
- Singh, U., Suman, A., Sharma, M., Singh, J., Singh, A. & Maurya, S., 2007. HPLC analysis of the phenolic profiles in different parts of chilli (*Capsicum annuum*) and okra (*Abelmoschus esculentus* L. Moench). *The Internet Journal of Alternative Medicine*, 5, 1–6.
- Sinha, A.K., Sharma, U.K. & Sharma, N., 2008. A comprehensive review on vanilla flavor: Extraction, isolation and quantification of vanillin and others constituents. *International Journal of Food Sciences and Nutrition*, 59, 299–326.
- Skiryecz, A., Radziejwoski, A., Busch, W., Hannah, M.A., Czeszejko, J., Kwaśniewski, M., Zantor, M.-I., Lohmann, J.U., De Veylder, L., Witt, I. & Mueller-Roeber, B., 2008. The DOF transcription factor OBP1 is involved in cell cycle regulation in *Arabidopsis thaliana*. *The Plant Journal*, 56, 779–792.
- Skoog, D.A., Holler, F.J. & Crouch, S.R., 2007. *Principles of Instrumental Analysis* 6th edition. Australia: Thomson Brooks/Cole.
- Smith, F.D., Harpending, P.R. & Sanford, J.C., 1992. Biolistic transformation of prokaryotes: factors that affect biolistic transformation of very small cells. *Journal of General Microbiology*, 138, 239–248.
- Smith, R.H., 2013. Callus induction. In R. H. Smith, ed. *Plant Tissue Culture: Techniques and Experiments*. San Diego: Academic Press, pp. 63–79.

- Sodiende, O.A. & Kindle, K.L., 1993. Homologous recombination in the nuclear genome of *Chlamydomonas reinhardtii*. *Proceedings of the National Academy of Sciences of the United States of America*, 90, 9199–9203.
- Soitamo, A.J., Jada, B. & Lehto, K., 2011. HC-Pro silencing suppressor significantly alters the gene expression profile in tobacco leaves and flowers. *BMC Plant Biology*, 11, 68.
- De Spiegelaere, W., Dern-Wieloch, J., Weigel, R., Schumacher, V., Schorle, H., Nettersheim, D., Bergmann, M., Brehm, R., Kliesch, S., Vandekerckhove, L. & Fink, C., 2015. Reference gene validation for RT-qPCR, a note on different available software packages. *PLoS ONE*, 10, e0122515.
- Spokevicius, A. V, Van Beveren, K. & Bossinger, G., 2006. *Agrobacterium*-mediated transformation of dormant lateral buds in poplar trees reveals developmental patterns in secondary stem tissues. *Functional Plant Biology*, 33, 133–139.
- Steinitz, B., Wolf, D., Matzevitch-Josef, T. & Zelcer, A., 1999. Regeneration in vitro and genetic transformation of pepper (*Capsicum* spp.): the current state of the art. *Caosicum and Eggplant Newsletter*, 18, 9–15.
- Stentelaire, C., Lesage-Meessen, L., Oddou, J., Bernard, O., Bastin, G., Ceccaldi, B.C. & Asther, M., 2000. Design of a fungal bioprocess for vanillin production from vanillic acid at scalable level by *Pycnoporus cinnabarinus*. *Journal of Bioscience and Bioengineering*, 89, 223–230.
- Su, Y.-H., Liu, Y.-B. & Zhang, X.-S., 2011. Auxin–cytokinin interaction regulates meristem development. *Molecular Plant*, 4, 616–625.
- Sudhakar Johnson, T., Ravishankar, G.A. & Venkataraman, L. V, 1992. Separation of capsaicin from phenylpropanoid compounds by high-performance liquid chromatography to determine the biosynthetic status of cells and tissues of *Capsicum frutescens* Mill. in vivo and in vitro. *Journal of Agriculture and Food Chemistry*, 40, 2461–2463.
- Sugimoto, K., Jiao, Y. & Meyerowitz, E.M., 2010. *Arabidopsis* regeneration from multiple tissues occurs via a root development pathway. *Developmental Cell*, 18, 463–471.
- Sujalmi, S. & Supriyanto, R., 2005. Determination of vanillin from vanilla (*Vanilla planifolia* Andrews) from Lampung Indonesia by high performance liquid chromatography. *Indonesian Journal of Chemistry*, 5, 7–10.
- Sukrasno, N. & Yeoman, M.M., 1993. Phenylpropanoid metabolism during growth and development of *Capsicum frutescens* fruits. *Phytochemistry*, 32, 839–844.
- Suriyamongkol, P., Weselake, R., Narine, S., Moloney, M. & Shah, S., 2007. Biotechnological approaches for the production of polyhydroxyalkanoates in microorganisms and plants. *Biotechnology Advances*, 25, 148–175.
- Sutherland, J.B., 1986. Demethylation of veratrole by cytochrome P-450 in *Streptomyces setonii*. *Applied and Environmental Microbiology*, 52, 98–100.

- Svec, D., Tichopad, A., Novosadova, V., Pfaffl, M.W. & Kubista, M., 2015. How good is a PCR efficiency estimate: Recommendations for precise and robust qPCR efficiency assessments. *Biomolecular Detection and Quantification*, 3, 9–16.
- Swarup, R., Friml, J., Marchant, A., Ljung, K., Sandberg, G., Palme, K. & Bennett, M., 2001. Localization of the auxin permease AUX1 suggests two functionally distinct hormone transport pathways operate in the *Arabidopsis* root apex. *Genes and Development*, 15, 2648–2653.
- Tamura, K., Kimura, M. & Yamaguchi, I., 1995. Blastocidin S deaminase gene (*BSD*): a new selection marker gene for transformation of *Arabidopsis thaliana* and *Nicotiana tabacum*. *Bioscience, Biotechnology, and Biochemistry*, 59, 2336–2338.
- Tanaka, M., Takei, K., Kojima, M., Sakakibara, H. & Mori, H., 2006. Auxin controls local cytokinin biosynthesis in the nodal stem in apical dominance. *The Plant Journal*, 45, 1028–1036.
- Tang, W., Newton, R.J. & Weidner, D.A., 2007. Genetic transformation and gene silencing mediated by multiple copies of a transgene in eastern white pine. *Journal of Experimental Botany*, 58, 545–554.
- Taylor, S., Wakem, M., Dijkman, G., Alsarraj, M. & Nguyen, M., 2010. A practical approach to RT-qPCR—Publishing data that conform to the MIQE guidelines. *Methods*, 50, S1–S5.
- Tee, C.S. & Maziah, M., 2005. Optimization of biolistic bombardment parameters for *Dendrobium sonia* 17 calluses using GFP and GUS as the reporter system. *Plant Cell, Tissue and Organ Culture*, 80, 77–89.
- Terouchi, N., Kato, C. & Hosoya, N., 2010. Characterization of *Arabidopsis* response regulator genes with regard to bisphenol A signaling. *Plant Biotechnology*, 27, 115–118.
- Thermo Fisher Scientific, 2016. Blastocidin. Available at: <https://www.thermofisher.com/my/en/home/life-science/cell-culture/transfection/selection/blastocidin.html> [Accessed December 9, 2016].
- Thomas, T.D., 2003. Thidiazuron induced multiple shoot induction and plant regeneration from cotyledonary explants of mulberry. *Biologia Plantarum*, 46, 529–533.
- Thorpe, T.A., 2013. History of plant cell culture. In R. H. Smith, ed. *Plant Tissue Culture: Techniques and Experiments*. pp. 1–22.
- To, J.P.C., Deruère, J., Maxwell, B.B., Morris, V.F., Hutchison, C.E., Ferreira, F.J., Schaller, G.E. & Kieber, J.J., 2007. Cytokinin regulates type-A *Arabidopsis* response regulator activity and protein stability via two-component phosphorelay. *Plant Cell*, 19, 3901–3914.
- Toivonen, P.M.A. & Bowen, P.A., 1999. The effect of preharvest foliar sprays of calcium on quality and shelf life of two cultivars of sweet bell peppers (*Capsicum annuum* L.) grown in plasticulture. *Canadian Journal of Plant Science*, 79, 411–416.

- Toplak, N., Okršlar, V., Stanič-Racman, D., Gruden, K. & Žel, J., 2004. A high-throughput method for quantifying transgene expression in transformed plants with real-time PCR analysis. *Plant Molecular Biology Reporter*, 22, 237–250.
- Torre, P., Faveri, D.D.E., Perego, P., Ruzzi, M. & Barghini, P., 2004. Bioconversion of ferulate into vanillin by *Escherichia coli* strain JM109 / pBB1 in an immobilized-cell reactor. *Annals of Microbiology*, 54, 517–527.
- Trinh, T., Jessee, J. & Bloom, F.R., 1994. STBL2: An *Escherichia coli* strain for the stable propagation of retroviral clones and direct repeat sequences. *FOCUS*, 16, 78–80.
- Tulecke, W. & Nickell, L.G., 1959. Production of large amounts of plant tissue by submerged culture. *Science*, 130, 863–864.
- Umamaheswari, A. & Lalitha, V., 2007. *In vitro* effect of various growth hormones in *Capsicum annum* L. on the callus induction and production of capsaicin. *Journal of Plant Sciences*, 2, 545–551.
- Urreta, I. & Castañón, S., 2012. Transgenic plants as biofactories for the production of biopharmaceuticals: A case study of human placental lactogen. In Y. O. Çiftçi, ed. *Transgenic Plants - Advances and Limitations*. Rijeka: InTech, pp. 305–328.
- Vad-Nielsen, J., Lin, L., Bolund, L., Nielsen, A.L. & Luo, Y., 2016. Golden Gate Assembly of CRISPR gRNA expression array for simultaneously targeting multiple genes. *Cellular and Molecular Life Sciences*, 73, 4315–4325.
- Vain, P., Keen, N., Murillo, J., Rathus, C., Nemes, C. & Finer, J.J., 1993. Development of the Particle Inflow Gun. *Plant Cell, Tissue and Organ Culture*, 33, 237–246.
- Valadez-Bustos, M.G., Aguado-Santacruz, G.A., Carrillo-Castañeda, G., Aguilar-Rincón, V.H., Espitia-Rangel, E., Montes-Hernández, S. & Robledo-Paz, A., 2009. *In vitro* propagation and agronomic performance of regenerated chili pepper (*Capsicum* spp.) plants from commercially important genotypes. *In Vitro Cellular and Developmental Biology - Plant*, 45, 650.
- Valera-Montero, L.L. & Ochoa-Alejo, N., 1992. A novel approach for chili pepper (*Capsicum annum* L.) plant regeneration: shoot induction in rooted hypocotyls. *Plant Science*, 84, 215–219.
- Vandesompele, J., De Preter, K., Poppe, B., Van Roy, N. & De Paepe, A., 2002. Accurate normalization of real-time quantitative RT-PCR data by geometric averaging of multiple internal control genes. *Genome Biology*, 3, research0034.1-0034.11.
- Vasanthakumari, R., 2007. *Textbook of Microbiology*, New Delhi: BI Publications.
- Vaucheret, H., Béclin, C., Elmayan, T., Feuerbach, F., Godon, C., Morel, J.-B., Mourrain, P., Palauqui, J.-C. & Vernhettes, S., 1998. Transgene-induced gene silencing in plants. *The Plant Journal*, 16, 651–659.

- Verdaasdonk, J.S., Lawrimore, J. & Bloom, K., 2014. Determining absolute protein numbers by quantitative fluorescence microscopy. *Methods in Cell Biology*, 123, 347–365.
- De Veylder, L., Beeckman, T. & Inzé, D., 2007. The ins and outs of the plant cell cycle. *Nature Reviews Molecular Cell Biology*, 8, 655–665.
- Vidal, J.R., Kikkert, J.R., Donzelli, B.D., Wallace, P.G. & Reisch, B.I., 2006. Biolistic transformation of grapevine using minimal gene cassette technology. *Plant Cell Reports*, 25, 807–814.
- Vidal, J.R., Kikkert, J.R., Wallace, P.G. & Reisch, B.I., 2003. High-efficiency biolistic co-transformation and regeneration of “Chardonnay” (*Vitis vinifera* L.) containing npt-II and antimicrobial peptide genes. *Plant Cell Reports*, 22, 252–260.
- Vinoth Kumar, R., Sharma, V.K., Chattopadhyay, B. & Chakraborty, S., 2012. An improved plant regeneration and *Agrobacterium* - mediated transformation of red pepper (*Capsicum annuum* L.). *Physiology and Molecular Biology of Plants*, 18, 357–364.
- Voinnet, O. & Baulcombe, D.C., 1997. Systemic signaling in gene silencing. *Nature*, 389, 553.
- Vos, P. De, Ludwig, W., Schleifer, K.-H. & Whitman, W.B., 2011. Family IV. Paenicibacillaceae fam. nov. In P. Vos et al., eds. *Bergey's Manual of Systematic Bacteriology: Volume 3: The Firmicutes*. Dordrecht: Springer, pp. 269–327.
- de Vries, J. & Wackernagel, W., 1998. Detection of *nptII* (kanamycin resistance) genes in genomes of transgenic plants by marker-rescue transformation. *Molecular and General Genetics*, 257, 606–613.
- Waliszewski, K.N., Pardo, V.T. & Ovando, S.L., 2006. A simple and rapid HPLC technique for vanillin determination in alcohol extract. *Food Chemistry*, 101, 1059–1062.
- Walton, N., Narbad, A., Faulds, C. & Williamson, G., 2000. Novel approaches to the biosynthesis of vanillin. *Current Opinion in Biotechnology*, 11, 490–496.
- Wan, H., Yuan, W., Ruan, M., Ye, Q., Wang, R., Li, Z., Zhou, G., Yao, Z., Zhao, J., Liu, S. & Yang, Y., 2011. Identification of reference genes for reverse transcription quantitative real-time PCR normalization in pepper (*Capsicum annuum* L.). *Biochemical and Biophysical Research Communications*, 416, 24–30.
- Wang, D. & Bosland, P.W., 2006. The genes of capsicum. *HortScience*, 41, 1169–1187.
- Wang, X., Ryu, D., Houtkooper, R.H. & Auwerx, J., 2015. Antibiotic use and abuse: A threat to mitochondria and chloroplasts with impact on research, health, and environment. *Bioessays*, 37, 1045–1053.
- Wang, Y., Yang, M., Pan, N. & Chen, Z., 1991. Plant regeneration and transformation of sweet pepper (*Capsicum frutescens*). *Acta Botanica Sinica*, 33, 780–786.

- Wang, Z., Jin, L., Yuan, Z., Wegrzyn, G. & Wegrzyn, A., 2009. Plasmid Classification of plasmid vectors using replication origin, selection marker and promoter as criteria. *Plasmid*, 61, 47–51.
- Wani, S.H., Haider, N., Kumar, H. & Singh, N.B., 2010. Plant plastid engineering. *Current Genomics*, 11, 500–512.
- Waters, 2014. HPLC separation modes. Available at: http://www.waters.com/waters/en_US/HPLC-Separation-Modes/nav.htm?cid=10049076&locale=en_US [Accessed May 17, 2014].
- Waters, J.C., 2009. Accuracy and precision in quantitative fluorescence microscopy. *The Journal of Cell Biology*, 185, 1135–1148.
- Waters, M.T. & Langdale, J. a, 2009. The making of a chloroplast. *The EMBO Journal*, 28, 2861–2873.
- Weiss, E.A., 2002. *Spice Crops*, Oxon: CAB International.
- Werner, T. & Schmülling, T., 2009. Cytokinin action in plant development. *Current Opinion in Plant Biology*, 12, 527–538.
- Westcott, R., Cheetham, P. & Barraclough, A., 1994. Use of organised viable vanilla plant aerial roots for the production of natural vanillin. *Phytochemistry*, 35, 135–138.
- White, J.W. & Montes-R, C., 1993. The influence of temperature on seed germination in cultivars of common bean. *Journal of Experimental Botany*, 44, 1795–1800.
- White, P.R., 1963. *The cultivation of animal and plant cells* 2nd ed., New York: Ronald Press.
- Wilkinson, J.E., Twell, D. & Lindsey, K., 1997. Activities of CaMV 35S and nos promoters in pollen: implications for field release of transgenic plants. *Journal of Experimental Botany*, 48, 265–275.
- Willenborg, C.J., Wildeman, J.C., Miller, A.K., Rossnagel, B.G. & Shirtliffe, S.J., 2005. Oat germination characteristics differ among genotypes, seed sizes, and osmotic potentials. *Crop Science*, 45, 2023–2029.
- Wong, M.L. & Medrano, J.F., 2005. Real-time PCR for mRNA quantitation. *BioTechniques*, 39, 1–11.
- Wright, M., Dawson, J., Dunder, E., Suttie, J., Reed, J., Kramer, C., Chang, Y., Novitzky, R., Wang, H. & Artim-Moore, L., 2001. Efficient biolistic transformation of maize (*Zea mays* L.) and wheat (*Triticum aestivum* L.) using the phosphomannose isomerase gene, *pmi*, as the selectable marker. *Plant Cell Reports*, 20, 429–436.
- Wu, N., Welch, C.J., Natishan, T.K., Gao, H., Chandrasekaran, T. & Li, Z., 2013. Practical aspects of ultrahigh performance liquid chromatography. In Q. A. Xu, ed. *Ultra-High Performance Liquid Chromatography and Its Applications*. New Jersey: John Wiley & Sons, pp. 55–94.

- Yadav, R.K., Perales, M., Gruel, J., Girke, T., Jönsson, H. & Reddy, G.V., 2011. WUSCHEL protein movement mediates stem cell homeostasis in the *Arabidopsis* shoot apex. *Genes and Development*, 25, 2025–2030.
- Yahiaoui, N., Marque, C., Myton, K.E., Negrel, J. & Boudet, A.M., 1998. Impact of different levels of cinnamyl alcohol dehydrogenase down-regulation on lignins of transgenic tobacco plants. *Planta*, 204, 8–15.
- Yamada, M., Okada, Y., Yoshida, T. & Nagasawa, T., 2007. Biotransformation of isoeugenol to vanillin by *Pseudomonas putida* IE27 cells. *Applied microbiology and biotechnology*, 73, 1025–30.
- Yamamoto, S., Misumi, M. & Nawata, E., 2007. Effects of various photoperiods on flowering in *Capsicum frutescens* and *C. annuum*. *Environmental Control in Biology*, 45, 133–142.
- Yang, W., Tang, H., Ni, J., Wu, Q., Hua, D., Tao, F. & Xu, P., 2013. Characterization of two *Streptomyces* enzymes that convert ferulic acid to vanillin. *PLoS ONE*, 8, e67339.
- Yao, Q.A., Simion, E., William, M., Krochko, J. & Kasha, K.J., 1997. Biolistic transformation of haploid isolated microspores of barley (*Hordeum vulgare* L.). *Genome*, 40, 570–581.
- Yeoman, M.M., 1973. Tissue (callus) cultures - techniques. In H. E. Street, ed. *Plant Tissue and Cell Culture*. Berkeley: University of California Press, pp. 31–58.
- Yeoman, M.M., Dyer, A.F. & Robertson, A.I., 1965. Growth and differentiation of plant tissue cultures: I. Changes accompanying the growth of explants from *Helianthus tuberosus* tubers. *Annals of Botany*, 29, 276.
- Yoon, S.-H., Lee, E.-G., Das, A., Lee, S.-H., Li, C., Ryu, H.-K., Choi, M.-S., Seo, W.-T. & Kim, S.-W., 2007. Enhanced vanillin production from recombinant *E. coli* using NTG mutagenesis and adsorbent resin. *Biotechnology progress*, 23, 1143–1148.
- Yoon, S.-H., Li, C., Kim, J.-Y.J.-E., Lee, S.-H., Yoon, J.-Y., Choi, M.-S., Seo, W.-T., Yang, J.-K. & Kim, S.-W., 2005. Production of vanillin by metabolically engineered *Escherichia coli*. *Biotechnology Letters*, 27, 1829–1832.
- Young, M., Cogbill, S., Jones, G., Faulcon, T., Green, K., Mcdaniel, M., Harmon, G. & Blackmon, R., 2008. Optimization of biolistics parameters in explants of rapid-cycling fast plants (*Brassica rapa* L.). *Journal of the North Carolina Academy of Science*, 124, 58–60.
- Yuan, J.S., Reed, A., Chen, F. & Stewart Jr, C.N., 2006. Statistical analysis of real-time PCR data. *BMC Bioinformatics*, 7, 85.
- Zampieri, M., Enke, T., Chubukov, V., Ricci, V., Piddock, L. & Sauer, U., 2017. Metabolic constraints on the evolution of antibiotic resistance. *Molecular Systems Biology*, 13, 917–930.

- Zenk, M.H., El-Shagi, H., Arens, H., Stockigt, J., Weiler, E.W. & Deus, B., 1977. Formation of indole alkaloids serpentine and ajmalicine in cell suspension cultures of *Catharanthus roseus*. In W. Barz, E. Reinhard, & M. H. Zenk, eds. *Plant Tissue Culture and Its Bio-technological Application*. Heidelberg: Springer-Verlag, pp. 27–43.
- Zhang, W., Swarup, R., Bennett, M., Schaller, G.E. & Kieber, J.J., 2013. Cytokinin induces cell division in the quiescent center of the *Arabidopsis* root apical meristem. *Current Biology*, 23, 1979–1989.
- Zhang, X., Tang, Q., Wang, X. & Wang, Z., 2016. Structure of exogenous gene integration and event-specific detection in the glyphosate-tolerant transgenic cotton line BG2-7. *PLoS ONE*, 11, e0158384.
- Zhang, Z., Mitra, A. & Coyne, D.P., 1996. Optimization of parameters influencing biolistic DNA transformation of common bean (*Phaseolus vulgaris* L.). *HortScience*, 31, 616.
- Zheng, X., Deng, W., Luo, K., Duan, H., Chen, Y., McAvoy, R., Song, S., Pei, Y. & Li, Y., 2007. The cauliflower mosaic virus (CaMV) 35S promoter sequence alters the level and patterns of activity of adjacent tissue- and organ-specific gene promoters. *Plant Cell Reports*, 26, 1195–1203.
- Zhong, C., Xu, H., Ye, S., Li, L., Zhang, S. & Wang, X., 2015. Gibberellic acid-stimulated *Arabidopsis6* serves as an integrator of gibberellin, abscisic acid, and glucose signaling during seed germination in *Arabidopsis*. *Plant Physiology*, 169, 2283–2303.
- Zhu, Y.-X., Ou-Yang, W.-J., Zhang, Y.-F. & Chen, Z.-L., 1996. Transgenic sweet pepper plants from *Agrobacterium* mediated transformation. *Plant Cell Reports*, 16, 71–75.
- Ziv, M., 1999. Developmental and structural patterns of in vitro plants. In W.-Y. Soh & S. S. Bhojwani, eds. *Morphogenesis in Plant Tissue Cultures*. Dordrecht: Springer Netherlands, pp. 135–153.
- Zuker, A., Ahroni, A., Tzfira, T., Ben-Meir, H. & Vainstein, A., 1999. Wounding by bombardment yields highly efficient *Agrobacterium*-mediated transformation of carnation (*Dianthus caryophyllus* L.). *Molecular Breeding*, 5, 367–375.
- Zupan, J., Muth, T.R., Draper, O. & Zambryski, P., 2000. The transfer of DNA from *Agrobacterium tumefaciens* into plants: a feast of fundamental insights. *The Plant Journal*, 23, 11–28.

